ACTIVE CONTROL OF AIRCRAFT USING SPOILERS

by

SUN XIAO-DONG
B.Sc. Eng. (Control), M.Sc. Eng. (Control)

Thesis submitted for the degree of
Doctor of Philosophy of the University of London
and for the
Diploma of Imperial College

March 1993

Department of Aeronautics
Department of Electrical and Electronic Engineering
Imperial College of Science, Technology and Medicine
London SW7 2BY

ABSTRACT

Recent studies on spoiler aerodynamics have suggested that it might be possible to improve the current use of spoilers for advanced flight control. This study appears to be the first attempt at using spoilers as active control devices for augmenting the control of aircraft. Based on recent experimental data, both linear and nonlinear generic control-coefficient models for the most typical aft-mounted spoilers were generated and included in complete nonlinear aircraft models.

Linear range space theory was applied to the controllability analysis of the aircraft for predicting the manoeuvres benefiting most from use of spoilers. Nonlinear open-loop optimal control techniques were used for two-point descent manoeuvring of a nonlinear aircraft. A series of nonlinear flight simulations were conducted, based on the development of a multi-functional flight simulation code. The studies showed the potential advantages of spoiler control and suggested that it should be worthwhile to attack the harder problem of closed-loop spoiler control.

The most appropriate feedback control technique seems to be that provided by the nonlinear inverse dynamics (NID) methodology. This was applied to the complete nonlinear aircraft system, giving an advanced flight control system which exploited spoilers and enhanced aircraft manoeuvring ability, safety and stability levels. The contributions made in this area include:

(1) Study and development of a systematic design procedure and package for the synthesis of feedback-decoupled model-following control systems for aircraft using the NID approach.

(2) Design of a multi-mode longitudinal flight control system for an aircraft (BAe HAWK) using spoilers as an active control device.

(3) Development of active control using spoilers for various mission objectives, including manoeuvring enhancement, fast deceleration and alleviation of the effects of gusts, turbulence and microbursts.

Finally, some parameter-adaptive control studies are presented, based on NID techniques and aimed at the robust enhancement of aircraft control using approximate models. The results are encouraging.

For Pan Hua and Qiao-Qiao

ACKNOWLEDGMENTS

I wish to express my gratitude to my supervisors, Professor J.M.R. Graham (Aeronautical Engineering), Dr J.C. Allwright (Electrical and Electronic Engineering) and Dr D.J. Doorly (Aeronautical Engineering) for their guidance, advice and support throughout the course of the research work. Gratitude is also due to Dr K.G. Woodgate of the Department of Aeronautics for his many helpful advice and suggestions. Working with them has left with me a happy and unforgettable experience.

I acknowledge the TCT department of the British Council and the state education committee of P.R. China for funding the PhD research fellowship and for their efficient and logistical administration of the project. I am appreciative of the joint efforts and help from the British Council and my supervisors in funding my attendance of several conferences to present my research papers.

Warmest thanks go to all the academic staff who helped me during my years in the Departments of Aeronautics and Electrical & Electronic Engineering, and in particular, to Professor Peter Bearman, Professor Mark Davis, Mr Ken Sage, Mr Ernie Turner, Mr John O'Learn, Mrs Roslie Fairhurst and Mrs Doris Abeysekara. Special thanks are due to the IRC for Process System Engineering of Imperial College for letting me use their computer facilities and for providing me with a very pleasant research environment.

I am very grateful to many friends and colleagues whose friendship and help has made my study and stay in Britain happy and enjoyable. I would particularly like to mention: Ellen Haigh, Andrew Courly, Shuji Tanaka, Egon Long, Zhou Yu Hong, Koo Yen and Ho Quan Wai.

Last, but not least, I would like to express my sincere appreciation to my wife Pan Hua and my little Qiao-Qiao, for their persistent patience, support and encouragement, and for their willingness to share my every sadness, happiness and success.

NOMENCLATURE

AC	= Aircraft
ACSS	= Aircraft Static Stability
ACT	= Active Control Technology
FCC	= Flight Control Command
FCS	= Flight Control System
HAWK	= British Aerospace Single-engined Jet Trainer/Flight Aircraft
IPVCA	= Integrated Pitch and Velocity Control Augmentation
IPTCA	= Integrated Pitch and Trajectory Control Augmentation
LIDFCS	= Longitudinal Inverse Dynamics Flight Control System
MB	= Most Beneficial
NID	= Nonlinear Inverse Dynamics
PACL	= Parameter Adaptive Control Logic
SP	= Spoiler
ρ	= Air Density
m	= Aircraft Mass
$\bar{c}$	= Wing Mean Chord
WC	= Wing/Aerofoil Chord
S	= Wing Reference Area
b	= Wing Span
H	= Flight Height above Sea Level
U_0	= Equivalent Air Speed
V	= Flight Path Velocity
M	= Mach Number
Q	= $1/2\ \rho V^2$
A_{nz}	= Normal Acceleration

α = Wing Incidence Angle (angle of attack)

γ = Flight Path Angle

θ = Pitch Angle

q = Pitch Rate

L = Lift Force

C_L = Lift Coefficient

D = Drag Force

C_D = Drag Coefficient

M = Pitching Moment

δ_e = Elevator Deflection

δ_{sp} = Spoiler Deflection

δ_{spo} = Spoiler Off-set Angle

δ_t = Thrust Setting (in ratio form)

$C_{LSP}(C_{l\delta s})$ = Spoiler Lift Coefficient (Lift Derivative)

C_{NLSP} = Generic Spoiler Lift Coefficient

$C_{DSP}(C_{d\delta s})$ = Spoiler Drag Coefficient (Drag Derivative)

C_{NDSP} = Generic Spoiler Drag Coefficient

$C_{MSP}(C_{m\delta s})$ = Spoiler Moment Coefficient (Moment Derivative)

C_{NMSP} = Generic Spoiler Moment Coefficient

$\lambda(\alpha)$ = Incidence Influence Function

$\zeta_{sp}(\zeta_p)$ = Short Period (Phugoid) Damping Ratio of Longitudinal Dynamics

$\omega_{nsp}(\omega_{np})$ = Short Period (Phugoid) Natural Frequency

$n_{z\alpha}$ = Acceleration Sensitivity of Aircraft

$L_A{}^i(*)$ = The ith Lie Derivative with respect to A (p118)

[A, B] = The Lie Bracket of A and B (p120)

ΔJR_{min} = Relative Cost Saving Function

J_E = Time-average Error Derivative Index

CONTENTS

Chapter One

INTRODUCTION

1.1 A Survey of Spoiler Research

1.1.1 General remarks

Spoilers are deflected plates, usually on the upper surface of a wing, which can be used to disturb the flow and cause separation, and thereby change the lift and drag of the aircraft. A popular and conventional arrangement of spoilers on the upper aft-surface of a wing section can be seen in **Fig. 1-1.**

The flow field generated by a deflected spoiler on a wing can be very complicated and contains the phenomena of flow separation, reattachment and vortex shedding. When the spoiler is deployed on the aerofoil which is at an angle of attack below the stall, flow separates from the upper aerofoil surface ahead of the spoiler due to the adverse pressure gradient from the spoiler, and then reattaches on the spoiler surface. It separates again from the spoiler tip and sheds a free shear layer into the wake. These separating shear layers form a large reverse flow bubble from the spoiler to just downstream of the trailing edge. The mixing of vortices shed from the spoiler tip and the trailing edge make the wake highly turbulent and oscillatory. (**Fig. 1-2**)

As effective aerodynamic control surfaces, spoilers have been traditionally and widely used in aircraft control as speed brakes and/or as lift dumpers at touch down, they are also used as effective lateral control devices when asymmetrically deflected. A special feature of spoilers as far as control is concerned is that the variable δ_{sp}, the deflection angle between spoiler and the wing, can not change sign within the working authority. (**Fig. 1-1**)

Recent experimental and computational studies in spoiler aerodynamics have suggested their potential usefulness for the active control of future aircraft, owing to their effectiveness at providing rapid force variation, the absence of large changes in pitch moment and their flexibility in use. Much effort has been devoted to the description of the flowfield structures of spoilers and the related aerodynamic features.

1.1.2 Brief review of spoiler research history

The study and application of spoilers originated from the 1930's, when interest in spoilers was mainly to use them as lateral control devices (WEICK & SHORT, 1932;

FRANKS, 1954). Most of the early works were confined to steady parameters, such as static surface pressure, lift, drag and moment.

Until recently, due to the complex nature of the spoiler flowfield, the aerodynamic data for spoilers were only the global mean quantities and they guided the theoretical analysis in a limited way.

Recent efforts made to obtain complete flowfield and parameter modelling information may be classified as:

Experimental: using various means of testing or visualization to determine the characteristic flows around airfoils fitted with different spoilers. The measurements include partial and whole pressure distribution, lift, drag and moment, from both the steady and unsteady tests concerned with spoiler motions.

Computational: developing finite difference Navier-Stokes and inviscid discrete vortex computer codes which can predict the characteristics of flow fields for arbitrary airfoils and spoiler geometries, to complement the experimental results and to further reveal the mechanism of the spoiling flows.

Applications: generating spoiler models for effective system design and applying them to more active uses for advanced control of aircraft.

Complete measurements of spoiler flowfields, including boundary-layer development and associated wake characteristics, were conducted by SEETHARAM & WENTZ (1977), and WENTZ & OSTOWARI (1981), at the Wichita State University.

A series of experiments were also carried out by the Joint Institute for Aeronautics and Acoustics of Stanford University and the Aerodynamics Research Group of Boeing Airplane Company. Works from BODAPATI et al (1982), MCLACHLAN et al (1983), AYOUB et al (1982) and LEE & BODAPATI (1985) centred on the issues of the flow visualization of spoiler flow, measurements of the steady and unsteady surface pressures, and mean velocities of the flowfield. The experiments based on a two-dimensional ATR (Advanced Transport Research) aerofoil fitted with a conventional aft-mounted spoiler design also gave a series of measurements on the spoiler coefficients of C_{LSP}, C_{DSP} and C_{MSP}.

There has recently been an increased interest in the unsteady aerodynamics of spoilers and their potential usefulness. This is concerned with the unsteady and transient flow phenomena caused by fast moving spoilers. The very rapid deployment of a spoiler results in a momentary increase of lift and a subsequent time delay before the final decrease in wing lift is attained. A thorough understanding of the phenomena and the mechanisms involved is essential for future applications.

Notable works in this area include a series of experiments by MABEY et al (1982, 1988) at RAE on the unsteady features of moving spoilers, revealing the 'adverse' lift effect and presenting the analysis of the delay time τ and the force and moment variation patterns resulting from the spoiler motion.

Experimental programmes have also been conducted by KALLIGAS & BIRDSALL (1987) and MYERS & BIRDSALL (1989) at Bristol University to look into various features of the adverse lift effect caused by rapidly acting spoilers, with emphases on the effects of the spoiler designs (shape and location) and their motion patterns.

Numerical methods have played an increasingly important part in spoiler studies. Although facing the difficulties of little theoretical information about spoiler characteristics (especially for the unsteady cases), and complicated and expensive computation, many efforts have been made to analyse and predict the spoiler performance numerically. This is mainly because a numerical method has some advantages of demonstrating the physics involved in producing spoiler effectiveness, and providing a flexible way of analysing aerofoil/spoiler combinations, thereby reducing the experimental efforts needed.

Early works in this area included that of WOODS (1956) and BARNES (1965) who applied a linear perturbation free streamline potential theory to an aerofoil/spoiler combination in subsonic flow for the prediction of the increment pressure, lift, drag and pitching moment.

A wake source model together with conformal transformation methods was used by PARKINSON et al (1974, 1987) to analyse the flow structure, the pressure distribution and the lift coefficient due to spoiler deployment on aerofoils at arbitrary incidence. The effects of the camber and thickness of the aerofoils, and the spoiler location, height and inclination were considered.

TOU & HANCOCK (1985) developed an inviscid panel method for the solution of the inviscid separated flow past a 2-D aerofoil/spoiler/flap combination at low speeds. Similar studies prior to these can be found in HENDERSON's work (1978) and in that by Boeing's Aerodynamics Research Group.

The discrete vortex method has also become an increasingly important tool in the study of the vortex shedding mechanism of a rapidly moving spoiler. KALKANIS (1988) used this method for the simulation of the separated flow generated by both fixed and moving spoilers fitted on the upper surface of an aerofoil. In this study, the case of a rapidly moving spoiler was modelled using a distribution of singularities along its surface, and the lift and drag coefficients of the aerofoil/spoiler combination were obtained using both pressure integration and a momentum method. The results for the delay times to maximum adverse lift were presented.

1.1.3 On evaluation of spoiler effectiveness

Effects of spoilers are normally measured by integrated parameters such as the lift, drag and moment which present the effects on aircraft dynamics. Pressure and velocity distributions are also used to show the characteristics of the spoiler flow field. The measurements of these parameters provide the understanding of spoiler flow mechanism and form the basis for the mathematical modelling of spoilers.

As far as the use of spoilers for control of aircraft is concerned, for the precise modelling and the introduction of spoilers into the control systems, comprehensive measurements of spoiler coefficients, C_{LSP}, C_{DSP} and C_{MSP}, and/or their derivatives $C_{l\delta s}$, $C_{d\delta s}$ and $C_{m\delta s}$, are of great importance.

There have been many studies and efforts made on this. In particular, **Table 1-1** summarizes some recent wing-spoiler/aerofoil-spoiler experiments and their outcomes, with the focus on the measurements of the coefficients for two-dimensional aerofoils and conventional spoiler designs and locations. Summarizing these studies yields the following conclusions concerning the basic features of spoilers.

On the conventional use of spoilers and their effect on mean loads

1. Aft- and upper-wing mounted design for spoilers has been widely adopted for the conventional use of most spoilers, owing to the capability of providing a large range of effectiveness, particularly at negative wing incidence.

2. Due to possible spoiler flow reattachment on the trailing section of a wing, there usually exists a small control-insensitive region which is incidence-dependent and deployed within which a spoiler has little or nearly no control effectiveness.

3. Generally speaking, for an aft-mounted spoiler, when incidence α varies within the normal region and the spoiler deflection angle δ_{sp} is beyond the insensitive region, nearly linear coefficient functions $C_{LSP}(\delta_{sp})$, $C_{DSP}(\delta_{sp})$ and $C_{MSP}(\delta_{sp})$ are obtained. There is also a strong indication from the experimental data (WENTZ, *et al* 1981) that a linear description of spoiler effectiveness vs the spoiler project height (δ_{hsp}= $\sin(\delta_{sp})$) may be even better for the modelling.

4. There is an increasing dependence of the spoiler effectiveness on the incidence α as it approaches the stall regions (positive or negative).

5. An aft-mounted spoiler has an effect on the pitching moment of an aircraft, the extent of which depends much on the location of the spoiler. This effect may have a considerable influence on the longitudinal handling and control.

6. Under some circumstances and assumptions, two-dimensional aerofoil/spoiler data may be applied to three-dimensional cases (WENTZ). This provides the possibility that we may initially design and tailor suitable spoilers for a wing by referring to relevant two-dimensional test data.

On the unsteady properties of spoilers:

1. There is an adverse lift effect and a time lag associated with the rapid movement of a spoiler, which are caused by an initial vortex, formed immediately after the activation of the spoiler and its development .**(Fig. 1-3)**

2. The deployment rate and the location of spoilers on an aerofoil are among the important factors determining the degree of adverse lift.

3. As in the steady cases, there is an increasing dependence of the dynamic lift on incidence α, the lift is much smaller when the spoiler is activated at high α then when α=0.

4. The adverse lift effect has potential usage in future aircraft for enhancing the performance levels relating to manoeuvring enhancement and air superiority, provided the complicated and transient flow phenomena involved can be thoroughly understood

and effectively controlled. Preliminary studies from FRANCIS et al (1979), CONSIGNY et al (1984) and SIDDALINGAPPA & HANCOCK (1980) have shown that an oscillating form of spoiler motion is capable of manipulating the unsteady separation flow by introducing unsteady vorticity, suggesting a way to control adverse lift.

1.2 On Active Control Technology (ACT)

The idea of ACT is closely connected with the active control of aircraft. It originated in middle 60's owing to the demand of improving the manoeuvrability and the aerial combat performance of fighters. Great progress has been made in both the technology and its applications during the last two decades, following developments in aerodynamics, modern control theory, flight control systems, computer and micro-processors, actuator mechanics and systems, information, and system simulation and development. The successful applications can now be found in many modern aircraft including the F-16, F-15B, F/A-18A, JAGUAR, TORNADO, Boeing-747 and Boeing-767 etc.

There have been so far a large number of studies and publications in this area, bringing a variety of definitions of ACT. A summary of many previous definitions on ACT gives the following one which is believed to cover the principal features of ACT:

> **Active control technology** is a design technique which may be concerned with the introduction of advanced control at the very beginning of an aircraft design in order to gain the most from control systems. It may involve the use of a multivariable flight control system and sophisticated control law design to improve the quality and performance levels of an aircraft. That might be done by simultaneously driving an appropriate number of control surfaces and auxiliary force or moment generators in such a fashion that either the unexpected loads and motion modes which the aircraft would have experienced without using ACT are much reduced, or such that the aircraft being able to perform a degree of manoeuvring well beyond the capability of a conventional aircraft.

Fig. 1-4 shows the difference between the design of an ACT aircraft and that of a conventional aircraft. A proposed ACT aircraft configuration is illustrated in **Fig. 1-5**.

Most of recent ACT aircraft have adopted so called fly-by-wire (**FBW**) systems for the handling and control augmentation. Such a FBW control system is featured by the

use of redundant electrical circuits and cables, rather than traditional hydraulic linkages, between the pilot output to the actuator input, hence substantially reducing the weight, size and costs of the handling systems and bringing the improvement in aircraft handling and the easier realization of advanced and sophisticated control laws. Also, along with the development and the use of powerful on-board digital processors and electronics, digital fly-by-wire (**DFBW**) control has become a progressively more popular choice for modern aircraft.

The most significant and beneficial control functions resulting from ACT are generally considered to be the following:

Relaxed Static Stability (RSS): RSS is closely connected with the design of an aircraft. It can be achieved by reducing the static stability margin (NELSON, p64, 1989), by either moving the aircraft's centre of gravity backwards to (or even beyond) the lift (aerodynamic) centre, or moving the lift centre forward to the centre of gravity, through which reduced structure weight and higher lift/drag ratio, therefore the manoeuvrability enhancement of the aircraft, can be gained. It is necessary while doing this to maintain the dynamic stability and handling quality by using an effective feedback augmentation system. RSS is often used in conjunction with FBW systems.

Direct force control (DFC): DFC refers to the control of an aircraft using the additional lift or side force from appropriate control and control devices for the fast and direct changes of the trajectory while keeping the attitude as constant. In longitudinal flight, direct lift control may be achieved by appropriate control of a number of extra and unconventional control surfaces including horizontal canards, leading and trailing edge flaps and spoilers. DFC has a range of beneficial applications in mission objectives such as air-superiority, formation and precise landing.

Manoeuvre load control (MLC): MLC is a technique for redistributing the aerodynamic loads over the wing of an aircraft during a manoeuvre, by controlling surfaces such as leading edge slats, trailing edge ailerons and flaps, to gain a beneficial lift distribution for reducing drag and controlling the flow departure (for combat aircraft), thus enhancing the manoeuvrability, or for reducing the bending moment at the wing root (for transport aircraft), thus reducing the wing structure weight and improving the performance levels of the aircraft.

Gust alleviation control (GAC): GAC aims to improve ride quality for the crew and passages, and to suppresses the unexpected bending modes in aircraft structure during a gust/turbulence encounter. This is done by making measurements of the gust-induced acceleration at positions of interest and then making use of appropriate control to reduce the unexpected acceleration. Moreover, a successful GAC system will normally contribute to the reduction in structure loading so that MLC and GAC are quite likely to be used in conjunction with each other.

Flutter mode control (FMC): FMC is used to actively reduce aircraft body flutter, which is caused by the unsteady aerodynamic coupling and may result in hazard damage to the aircraft structure. This is realized by sensing the distributed accelerations and by properly controlling the deflection of certain auxiliary control surfaces for damping the flutter modes of an aircraft, thus bring the advantages of improved safety level, reduction in structure weight and increase in the flight envelop of mission objectives.

Also, ACT covers such integrated control concepts as integrated flight/thrust control (**IFTC**) and the integrated flight/fire control (**IFFC**) which bring further benefits to aircraft through the integration of flight control, navigation, instrumentation, fire control and thrust control.

1.3 Introduction to Nonlinear Flight Control

1.3.1 General remarks

Future aircraft will be expected to meet higher performance and mission superiority requirements and, therefore, will employ more and more advanced techniques like ACT. The aerodynamic characteristics and operational requirements of such aircraft present the control system design with problems that are increasingly difficult to solve with standard or conventional control system design approaches. Among these problems, the nonlinearity of an aircraft is an essential feature.

Aircraft nonlinearity arises from the following sources:

* The nonlinearity existing in the force and moment generation processes of an aircraft, with strong, multi-axis, highly coupled features.

* The nonlinearity connected with the operation of an aircraft: some anticipated operation capabilities, i.e. supermanoeuvreability (HERBST, 1983), require that aircraft be precisely controlled over a substantial portion of the flight envelope that encompasses strong nonlinear aerodynamics and loss of control effectiveness. (LANG & FRANCIS, 1985)

1.3.2 Current/Traditional design approaches

For a long time, aircraft control design has relied on the the use of linear control techniques. The so-called 'gain-schedulling' method is based on the local linearization and control, around a series of selected operating points, of a nonlinear system, and has been widely used for the design of flight control systems.

The basic design procedures involved in this method can be summarized as:

1) Select a set of operating points to adequately cover the entire operational envelope of the nonlinear system:

$$\dot{x} = f(x,u), \qquad y = c(x) \tag{1-1}$$

2) Apply the small-perturbation analysis for each operating condition x_o, with

$$\dot{x}_o = f(x_o,u_o), \qquad y_o = c(x_o) \tag{1-2}$$

and put the perturbation equation in a linear form:

$$\dot{\delta x} = \left.\frac{\partial f}{\partial x}\right|_o \delta x + \left.\frac{\partial f}{\partial u}\right|_o \delta u \quad \delta y = \left.\frac{\partial c}{\partial x}\right|_o \delta x \tag{1-3}$$

3) Apply linear design approaches to (1-3) for linear controllers.

4) Design a scheduling algorithm that ties all the individual designs into a total control for the nonlinear system (1-1).

Fig. 1-6 shows the principal configuration of the control system.

Two commonly used methods in conjunction with the linearization approach for keeping desired system properties are:

Robust Control: Designing the control system by synthesizing some constant gain feedback so that the closed-loop system is insensitive to undesirable disturbance and parameter variations.

Adaptive Control: Designing adaptive schemes that adjust the open-loop and closed-loop gains so as to adapt to variations in the perturbation model (1-3) and disturbance.

Both the methods have proven effective in flight control for the enhancement of the system robustness to disturbance and for handling, in some extents, the nonlinearities from the modelling of (1-3).

The gain-scheduling based linear approaches have been widely accepted as an effective way for the preliminary synthesis of an aircraft control system, and have had many successful applications in modern aircraft. There are, however, disadvantages in using the linear methods. Notably when the nonlinearities of an aircraft become important:

* It is hard for linear methods to deal with the strong nonlinearities which are encountered in flight control and will increasingly occur in future aircraft.

* A large number of operating points have to be selected to cover the increasingly enlarged flight envelope of an aircraft. Hypothetically, the equilibrium points may not exist or even can not be defined under certain circumstances or in some part of the envelope. (HUANG & KNOWLES, 1990)

* The control algorithm becomes complicated when feedback logic and scheduling algorithms are taken into account.

* Performance degradation may occur owing to the conservative nature of the robust controllers.

1.3.3 Nonlinear control strategies for advanced flight control

Clearly, nonlinear control strategies are required which are based directly on the nonlinear model $\dot{x} = f(x,u), y = c(x)$ and which explicitly take into account the nonlinearities during the system synthesis process. In the design of flight control systems, these are expected to provide more effective control and the efficient utilisation of control resources.

The following are the summary of recent studies and achievements in this area, with a particular interest in their applications to advanced flight control.

Feedback Linearization

The basic definition and theory of this methodology can be found in ISIDORI's 'Nonlinear Control Systems' (1990). Generally speaking, the method uses nonlinear coordinate transformation for converting a nonlinear system in the form (1-4) to an equivalent linear system. A linear control is then designed upon the linear system and applied to the nonlinear system through the transformation.

$$\dot{x} = f(x) + \sum_{i=1}^{m} g_i(x)u_i \qquad y = c(x) \qquad (1\text{-}4)$$

Necessary and sufficient conditions for the existence of local and global transformation were obtained in the studies of SU (1982) and HUNT et al (1983). The basic design logic in the contrast to the conventional flight control design (**Fig. 1-6**) can be seen in **Fig. 1-7**. **Fig. 1-8** outlines the design concept.

The method was successfully applied to the flight control of a V/STOL aircraft by MEYER & CICOLANI (1975, 1981), where the nonlinear aircraft system with complex characteristics and operational requirements was put in the form of (1-4), and the concept of 'block triangular' systems was proposed and applied for the nonlinear transformation. A 6-degree of freedom flight control system was developed and various tests and simulations were carried out. It was concluded that the method was effective for a large class of dynamic systems requiring multi-axis control which have highly coupled nonlinearities, redundant controls, and complex multidimensional operational envelopes.

During the same period, SMITH & MEYER (1980) applied the approach to a system development for the carrier landing control of an A-7. WEHREND & MEYER (1980) used the method for the automatic control of a DHC-6. Flight tests were made over a large portion of the flight envelope during which the nonlinear control performed well despite disturbance and aircraft plant modelling errors.

Later, in 1984, MEYER et al applied this method to the design of a helicopter (UH-1H) autopilot. The details of systematic construction of the transformation from the nonlinear system to the linear system was given and in particular, the necessary and sufficient conditions for the transformability were presented and evaluated with the system configuration. The performance of the designed automatic control system was simulated in flight on an on-board computer.

Nonlinear Inverse Dynamics (NID)

This is an alternative transformation approach similar to the above method, with the emphasis on the input-output linearization of nonlinear systems. Generally, the method is based on the construction of the inverse dynamics (SINGH & RUGH (1972), FREUND (1973)) by differentiating the m (number of control) elements of the output y such that the nonlinear system can be decoupled and the outputs can be individually and linearly controlled. **Fig. 1-9** shows the principal structure of a NID system.

The interrelation between these two methods, as SASTRY & ISIDORI (1989) summarized, is that the former design technique is often referred as exact state space linearization, while the later one as exact input-output linearization. The bridge between the two techniques lies in the fact that the design of a state-space linearization control is equivalent to the design of some 'output' functions for which input-output linearization is possible.

A remarkable study using the NID methodology for flight control was made by LANE and STENGEL in 1988, in which they applied the NID to the development of a flight control system for a 12-state nonlinear aircraft model. The system was designed to be valid over the entire flight envelope and the major efforts were put on the analysis and control of the severe nonlinear effects from extreme flight conditions, such as high incidence angle and high angle rates. Simulation results suggested the effectiveness of NID control in providing improved levels of performance over conventional flight control designs, especially in the extreme flight conditions.

Early studies relating to the NID were mainly on system decoupling and separation of control modes. Among them, ASSEO (1973) showed how the flight path angle and heading angle commands of a simplified aircraft model could be decoupled, leading to the control of single-axis manoeuvres. SINGH & SCHY (1980) applied the method to the manoeuvre control of an aircraft and demonstrated how the nonlinear roll coupling divergences associated with rapid open-loop manoeuvres could be eliminated.

Similar works can also been found in FALB & WOLOVICH (1967), SINGH & RUGH (1972), and FREUND (1975).

Other relevant methods

These include the work by HAUSER et al (1989) where an approximate feedback linearization was applied to a non-minimum-phase nonlinear aircraft system (a V/STOL Harrier), giving a system design with desirable properties of bounded tracking and asymptotic stability, and the work by MENON et al (1985) where the calculations of the linearizing transformations were simplified by the use of singular perturbation theory.

The extended linearization methodology (RUGH, 1984; BAUMANN & RUGH, 1986) forms another important line of research which may be potentially used for nonlinear flight control (WANG & RUGH, 1987). This method is based on the family of linearizations of a nonlinear system in the form $\dot{x} = f(x,u)$. Nonlinear state feedback control laws to be designed have the form $u=w-k(x)$, which constitute an overall, nonlinear state feedback controller, and bring the closed-loop system the property that its linearizations are equal to the desired linearly-controlled systems.

The direct dynamic inversion (DDI) method was presented by BUGAJSKI et al (1990) where application was made to the control of a NASA high incidence research aircraft. During the same period, ENNS (1990) studied the robustness issue of the DDI method and showed its application to a lateral-directional flight control.

Recent studies on nonlinear flight control other than feedback linearization are represented by the following: SINGH and COELHO (1984) and STAFORD (1987) studied nonlinear aircraft control based on the feedback of separate terms derived from the linear model and a Lyapunov equation. Later in 1989, SINGH and INNOCENTI reported application of variable structure control to aircraft control, where the feedback gains were derived from Lyapunov-based equations and switched on hyper-surfaces corresponding to different system dynamics.

Studies on nonlinear flight control based on the approximation of nonlinearities as power series were made by GARRARD et al (1989), where the feedback control for a supermanoeuvreable aircraft was generated using nonlinear optimization of a quadratic function. ABED (1989) studied bifurcation control techniques and applied them to a nonlinear flight control system aiming to stabilize a high-alpha manoeuvring aircraft.

1.3.4 On robust nonlinear control and systems

It has been widely accepted that the robustness of of a control system has become an increasingly important issue in system development. It may become essential for a range of aircraft systems where 'rough' dynamic modelling, large disturbances and perturbations in system parameters are inevitable.

Although the feedback linearization methodology has received considerable attention in the literature and has found many applications in nonlinear flight control, few works on the robustness aspect of the nonlinear control systems have been documented. However, the chief drawback of these methods is also apparent: they rely heavily on the modelling of nonlinear dynamic system and an exact cancellation of nonlinear terms in order to get linear input-output behaviour. Consequently, no robustness is guaranteed in the presence of parameter uncertainty or unmodeled dynamics, which may result in illogical control and decayed (even unacceptable) system performance. (SASTRY & ISIDORI, 1989)

Robustness analysis with respect to infinitesimal perturbation in the state model of nonlinear systems can be found in the works of SU et al (1983), GILBERT& HA (1984), and KRAVARIS & CHUNG (1987), where a variety of linearization methods were used.

SU et al studied the robustness relating to feedback linearization designs. They showed a way of constructing the Lyapunov functions for nonlinear systems using transformation methods and proved that the feedback linearization control was robust in the sense that all systems close (in the topology defined) to the mathematical model are asymptotatically stabilized about corresponding equilibrium points, and the stability holds for any trajectory starting in some fixed compact set in state space.

From a practical viewpoint, robustness design is of even more importance. It can be generally expressed as: given upper bounds on the modelling error, design a feedback control to guarantee certain stability and specifications for all perturbations within the given bounds. The salient feature of the problem is the fact that it is a deterministic treatment of uncertainty in that one requires certain performance in the presence of uncertainties.

The typical structure of a robust controller u can be put in the form: $u=k_1+k_2$, where k_1 is to give desired control in the absence of modelling error while k_2 is an additional term to provide robustness corrections to cope with modelling inaccuracies. The design procedure therefore consists of the following two steps:

1) Under the assumption of a perfect model, do a nominal controller design (e.g. a feedback linearizing or inverse control law) to meet the appropriate closed-loop linearity requirements and some design criterias.

2) Introduce robustness corrections for guaranteeing uniform ultimate boundedness of the states and the output.

The approaches to robust nonlinear design originated from that for linear systems with bounded parameters and uncertainty. (CORLESS & LEITMAIN, 1981; GUTMAN, 1979)

CORLESS & LEITMAIN studied robust design for a dynamic system containing uncertain elements. The design of the robust feedback control was based on the assumptions that the set of possible values of these uncertainties was known. It was shown that the robust control was a set of continuous functions of the states and was able to guarantee uniform ultimate boundedness of every system response within an arbitrary small neighbourhood of the zero state.

A similar study on the uncertainty dynamics was made early by GUTMAN in which the presence of uncertainty was formulated by some contingent differential equations. Generalized dynamic systems were defined upon which asymptotic stability of the nonlinear system (in the sense of Lyapunov) was developed. Some applications to quasi-linear systems were made. These studies, also many others, formed the basis of recent studies on robust nonlinear control in conjunction with feedback linearization approaches.

HA & GILBERT (1987) studied multivariable robust tracking problems using Lyapunov functions. The controller was robust in the sense that the tracking error, which was defined as a general function of system state and the input command, was ultimately bounded in the presence of modelling errors. Restricting assumptions on the structure of the model and the modelling errors were generalized through a transformation framework.

A similar Lyapunov approach was studied by KRAVARIS & PALANKI (1988) and applied to the robust synthesis of nonlinear SISO systems. The uncertainty modelled there was in terms of a class of model perturbations that satisfied appropriate matching conditions.

In addition, there is a simple approach to robust control, the so-called sliding control methodology (UTKIN, 1977; SLOTINE & LI, 1991), which is based on a notational simplification allowing an n^{th} - order tracking problem to be replaced by an equivalent first-order stabilization problem. In practice, uncertainties in the model structure (i.e. unmodelled dynamics) lead to a trade-off between tracking performance and parametric uncertainty, corresponding to replacing a switching, chattering control law by its smooth approximation. Practical implementations of the methodology included underwater vehicles (YOERGER et al, 1986), aircraft (HERDRICK & GOPALSWAMY, 1989) and highway systems (McMAHOM et al, 1990).

The adaptive control of nonlinear systems is similar in the sense of the system robustness, but in addition the model is actually updated during the operation.

In this aspect, SASTRY & ISIDORI (1989) reported a study on the adaptive control of minimum-phase nonlinear systems which were exactly input-output linearizable by state feedback. They suggested the use of a parameter adaptive algorithm to make asymptotatically exact the cancellation of nonlinear terms when the uncertainty in the nonlinear model terms could be put into a parametric form (see **Chapter 7** for details). This study was viewed as generalizations of work pioneered by NAM & ARAPOSTATHIS (1986).

Some other attempts in this area have included that of MARINO (1985) and NICOSIA & TOMEI (1984) for robot control cases, using a combination of high gain, sliding modes, and adaptation. The adaptive control of full-state linearizable SISO systems was studied by TAYLOR *et al* (1987).

1.4 An Overview of the Thesis

As control device, a spoiler exhibits more complex behaviour than do most of the conventional aircraft control devices, such as the elevator, rudder and aileron. Consequently, modelling and control of aircraft become more difficult when spoilers are involved. Moreover, although the potential of spoilers for aircraft control has been proven through a large number of aerodynamic studies, use of spoilers for active control of an aircraft does not yet seem to have been considered before in advanced control studies.

Further, in most previous studies concerning nonlinear flight control using the feedback linearization methodology, control devices such as spoilers and flaps have been normally ignored, deleted or imposed with constraints in the control synthesis (MEYER & CICOLANI,

1981). This was mainly because during these applications, these devices were considered as only being occasionally used and/or weakly coupled devices, and the incorporation of these direct force generators might result in a system which was not explicitly block-triangular and hence not invertible. Clearly, these arguments are not really valid and may bring an improper or even illogical control to an aircraft when spoilers are actually active and in principal use.

This thesis is devoted to studying the active use of spoilers for aircraft control and in particular, it appears to be the first systematic study made in this area. The main contributions concern:

1. Spoiler control modelling --- generation of a generic spoiler model for flight control from experimental data.

2. Analysis of spoiler control effectiveness --- use of nonlinear flight simulation, linear range space theory and nonlinear optimal control.

3. Design of flight control systems utilising spoiler control --- study of the NID methodology and its application to the nonlinear flight control with spoilers functioned as a principal control device.

4. Study of spoiler applications to aircraft ACT --- typically for manoeuvring enhancement and gust/microburst alleviation.

5. Adaptive control of NID-based nonlinear flight control systems.

It is expected the study will further the understanding of the use of spoilers as an important control device in future aircraft. It provides a good example of the development of spoiler control systems following a systematic routine of modelling, simulation, open-loop and closed-loop control designs.

The major contents of the thesis are summarized next:

In **Chapter 2,** a generic spoiler control model is derived, based upon the analysis and processing of aerodynamic experimental data. The model is expressed in terms of the aerodynamic coefficients C_{LSP}, C_{MSP} and C_{DSP}, and the two major nonlinear effects involved -- the spoiler deflection δ_{sp} and the wing incidence α -- are studied and introduced into the modelling. Both linear and nonlinear forms of the generic model are

presented and a special spoiler model for the HAWK aircraft is proposed. **Chapter 3** relates to the analysis of spoiler control effectiveness using a linear method -- the linear range space theory of controllability. The work is concerned with the study of the theory and the development of a general routine for the comparison of linear systems, in controllability and control efficiency. It is applied to a linearized aircraft system with spoiler control to predict manoeuvres for which the use of the spoiler control might be most beneficial. The evaluation of the stability and handling qualities of the HAWK is also given in this chapter. **Chapter** 4 is devoted to the analysis of spoiler control effectiveness, with emphasis on nonlinear flight simulations concerning spoiler control and on design of open-loop flight control using nonlinear optimal control techniques. For these purposes, a 6 degree of freedom flight simulator is developed, and nonlinear optimal two-point boundary control, combined with the first-order gradient algorithms, is applied to the HAWK aircraft system utilising spoilers. Enhancement of control for descents is demonstrated.

As far as the design of closed-loop system is concerned, **Chapter 5** considers NID control and its application to the development of a nonlinear flight control system using spoilers. In this chapter, a sophisticated computer code for the control system synthesis based on the NID method is developed. A detailed derivation of the inverse dynamics of the HAWK is given, in which an uniform relative order is defined and used for each output control variable of interest. The outcome presents a decoupled mission-defined multi-mode control system for the HAWK aircraft. In **Chapter 6**, the work of **Chapter 5** is applied to the application studies of spoilers for aircraft active control, concerning the most promising uses of spoilers in the improvement of aircraft performance levels. Four applications cases: decoupled attitude/trajectory control, fast deceleration control, gust/turbulence alleviation and low-altitude windshear/ microburst alleviation, are presented in detail. Finally, **Chapter 7** introduces the studies in the robustness of NID control using newly developed parameter adaptive control techniques. Aiming to tackle some worst modellings in aircraft system parameters, an NID-based adaptive control algorithm is derived and applied to the HAWK flight control.

Table1-1 Summary of Aerofoil --- Spoiler Studies

Authers	Aerofoil/Wing	Spoiler	Spoiler Range (o)	α Range (o)	Test Condition
DESTUYNDER (1987)	Froude Scaled (3.5m half SPA)	L: 60%W.C. CH: 8%W.C.	$-\delta_{sp}$= 5, 10, 20	0	Re. = $12*10^6$, M = 0.5, 0.78
PARKINSON & YEUNG (1987)	Joukowsky (2.4% CB, 11% THK, 12/27 CH/SPA)	L: 70%W.C. CH: 10%W.C., 5%W.C.	$-\delta_{sp}$= 30, 45, 60	0 ~ 14.0	Re. = $0.3*10^6$ (low speed)
MABEY, et al. (1982)	NACA 64A 010 (10%THK, 2/5 CH/SPA)	L: 65%W.C. CH: 8%W.C. SPA: 1/4W. SPA	$-\delta_{sp}$= 0 ~ 38	0	Re. = 1 ~ $3*10^6$ M = .25, .5, .7, .8, .85, .9
MACK, et al. (1979)	GA(w)-2 (13% THK, with flap)	L: Trailing Edge CH: 10%W.C.	$-\delta_{sp}$= 0 ~ 60	-8.0 ~ 16.0	Re. = $2.2*10^6$, M = 0.13
WENTZ, et al. (1981)	Two-Dimensional (11.3%THK, 61cm CH)	L: 73.3%W.C. CH: 15.7%W.C.	$-\delta_{sp}$= 0 ~ 60 (4, 7, 9, 19, 39, 59)	0, 8.0, 14.0, 16.0	Re. = $2.2*10^6$, M = 0.13
McLACHLAN, et al (1983)	Two-Dimensional (11.3%THK, 20/45 CH/SPA)	L: 73.3%W.C. CH: 15.54%W.C.	$-\delta_{sp}$= 0, 15, 30, 60	-8.0 ~ 18.0	Re. = 0.28 ~ $0.52*10^6$; M = 0.06 ~ 0.13
LEE & BODAPATI (1987)	Boeing ATR (11.3%THK, 20/45 CH/SPA)	L: 73%W.C. CH: 15.5%W.C.	$-\delta_{sp}$= 0, 15, 30, 45, 60	-10.0 ~ 12.0	Re. = $0.28*10^6$, M = 0.06 (20m/s)

CONSIGNY, et al. (1984)	Supercriticial Wing (16%THK, 18cm CH)	L: 52%W.C. CH: 15%W.C.	$-\delta_{sp}$= 0 ~ 20	0	Re. = 0.3 ~ 4.7*10^6, M = 0.3, 0.6, 0.73
COSTES, et al. (1987)	Supercriticial Wing (1/2 CH/SPA)	L: 67%W.C. CH: 15%W.C.	$-\delta_{sp}$= 0 ~ 31	2.0	Re. = 1 ~ 16*10^6, M = 0.2
MYERS, et al. (1989)	NACA 0012-64 (1/2 CH/SPA)	L: 70%W.C. CH: 8%W.C.	$-\delta_{sp}$= 0 ~ 40	-20.0 ~ 20.0	Re. = 0.56 ~ 71*10^6, M = 0.06 (20m/s)
TOU & HANCOCK (1983)	Clark Y-14	L: 70%W.C. CH: 10%W.C.	$-\delta_{sp}$= 0 ~ 90	6.0	N/A
KHOO & GRAHAM (1989)	LS1 0424, 0421 NACA 23018, CHP2	L: 70%W.C. CH: 10%W.C.	$-\delta_{sp}$= 90	0 ~ 35.0	Re. = 0.67 ~ 2.0*10^6, (Low Speed)

Note: CH: chord, SPA: span, THK: thichness, L: wing surface location, Re.: Renolds number, M: Mach number.W.C.: Wing/aerofoil chord

Figure 1-1 Conventional spoiler configuration

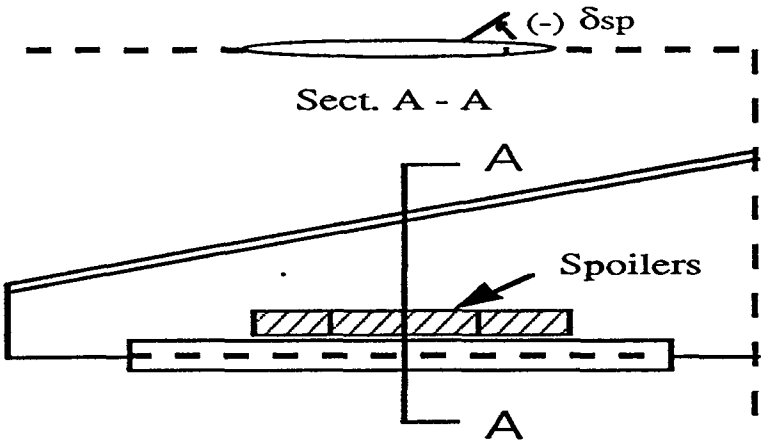

Figure 1-2 Separated flow patterns of deflected spoiler (MACK et al 1979)

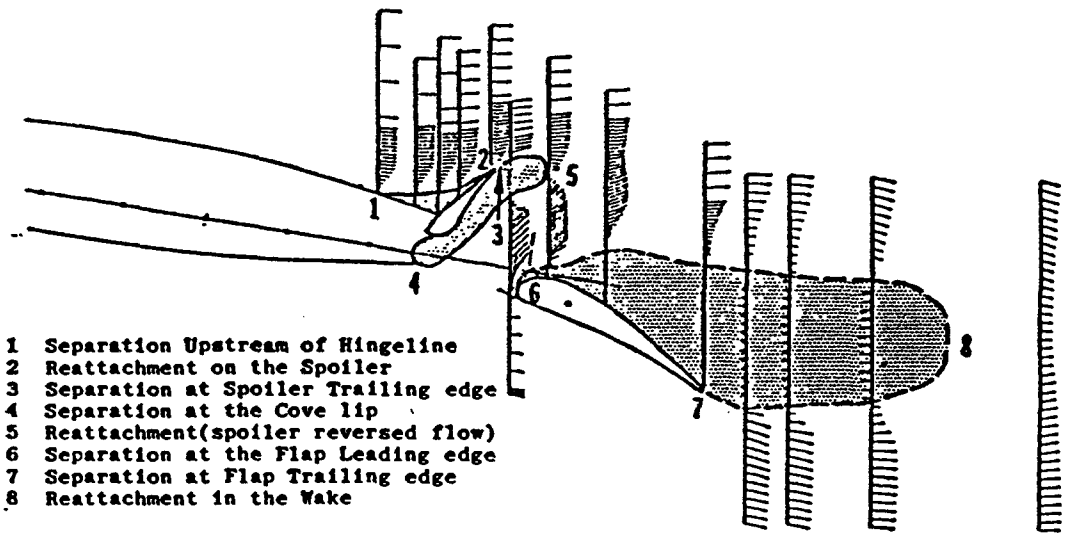

Figure 1-3 Numerical simulation of spoiler 'Adverse Lift' (KALKANIS, 1988)

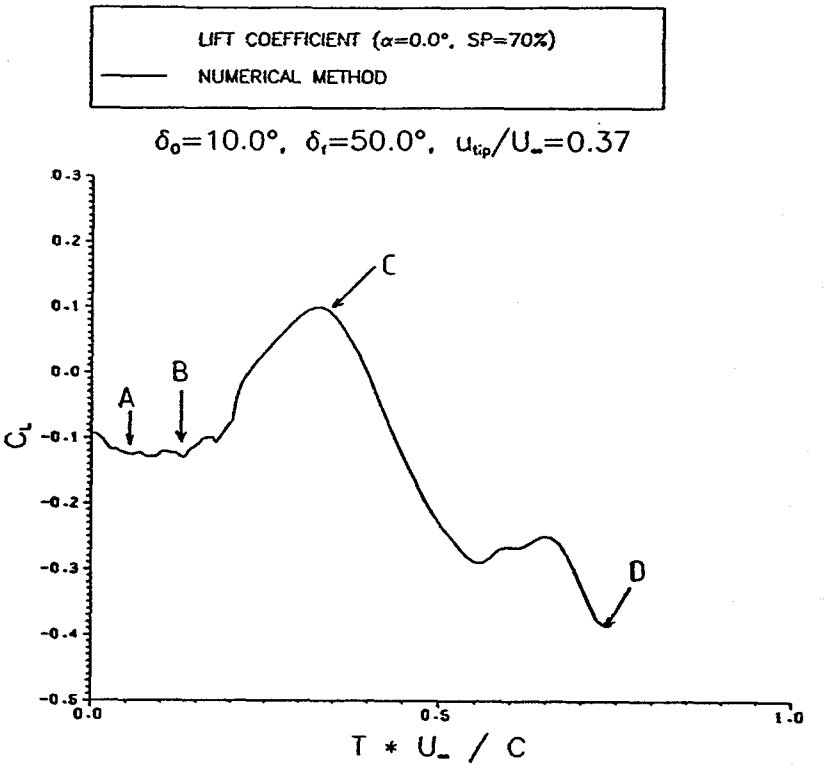

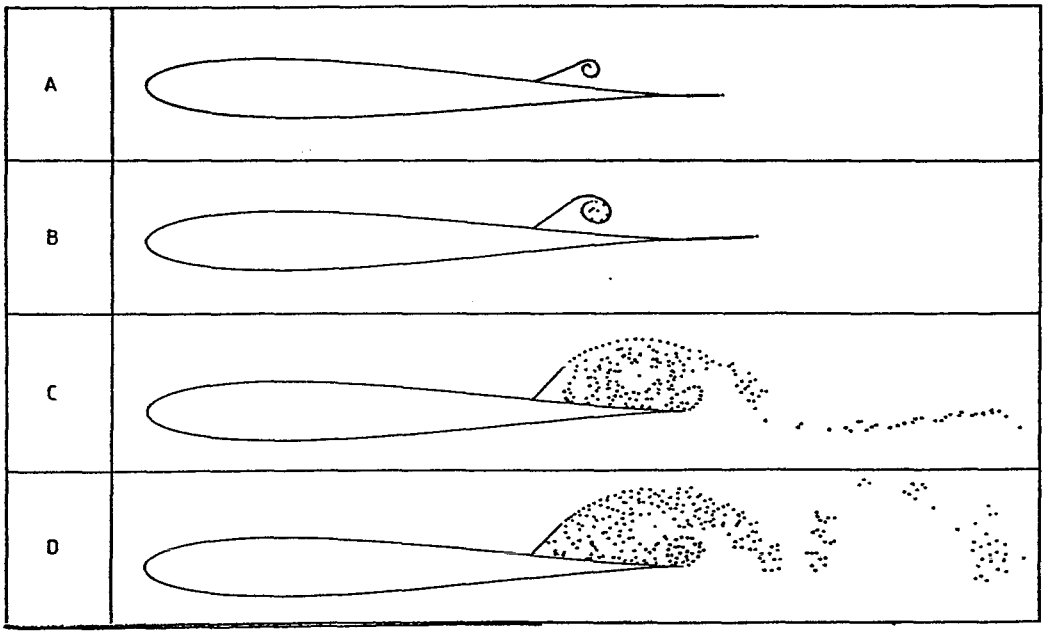

Figure 1-4 Comparison between ACT design (b) and traditional design (a)

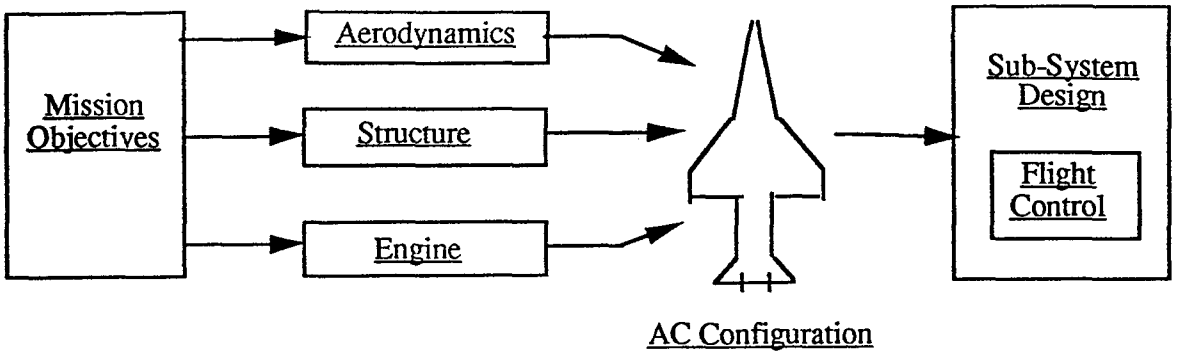

(a)

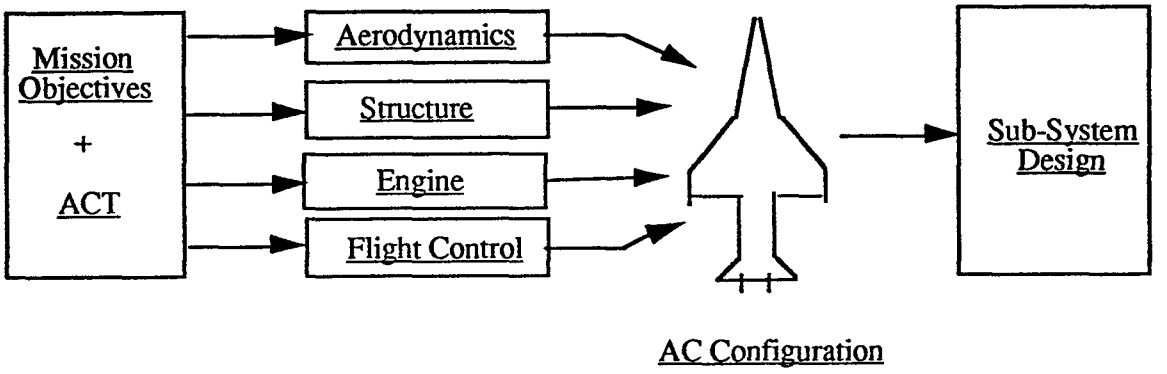

(b)

Figure 1-5 Configuration of a proposed ACT aircraft (McLEAN, 1991)

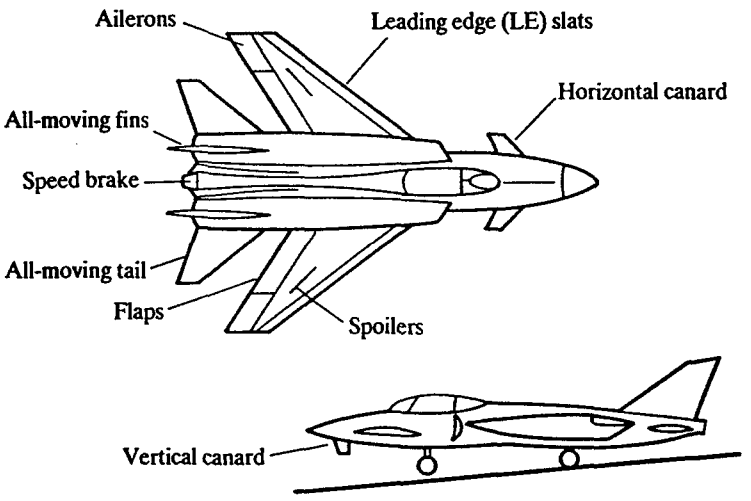

Figure 1-6 Conventional flight control configuration

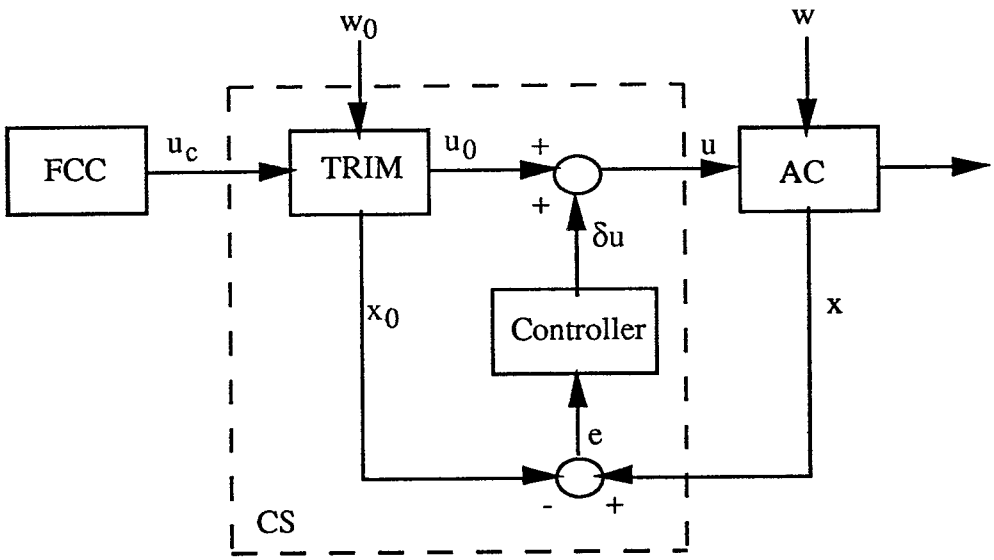

Figure 1-7 Flight control configuration with feedback closed ahead of TRIM

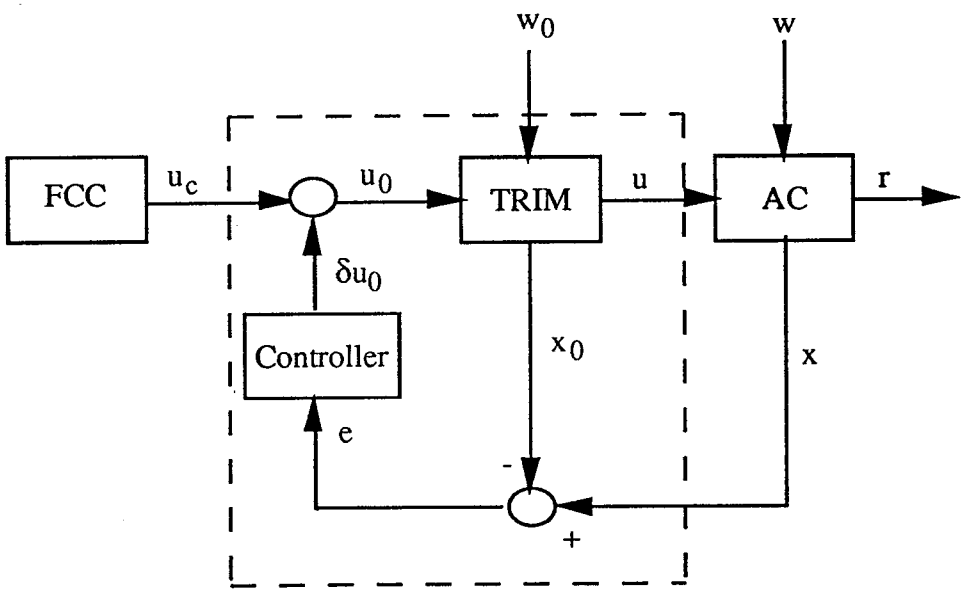

Figure 1-8 Design concept of feedback linearization

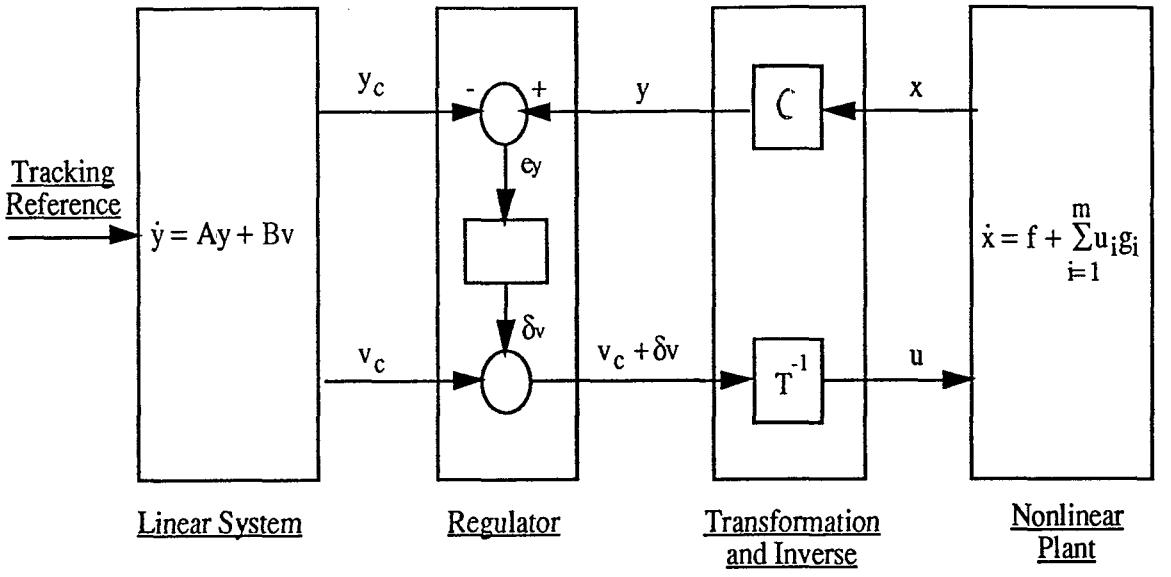

Figure 1-9 Design concept of nonlinear inverse dynamics (NID)

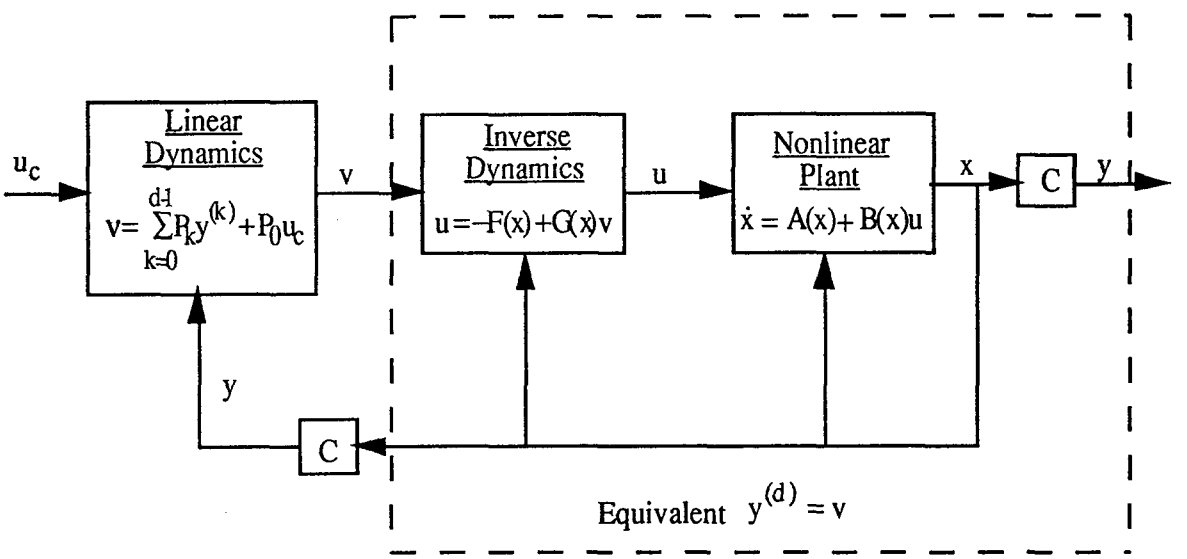

Chapter Two

SPOILER CONTROL MODELLING

2.1 General Remarks

In this chapter, a generic spoiler control model for the most typical aft-mounted spoilers is proposed. This is mainly based on the survey in **Section 1.1** and on some further discussions of the recent experimental data concerning spoiler aerodynamics.

The major objective of the work lies in the need for a generic spoiler model with a precise mathematical expression of spoiler behaviour when used as a control device. The generic model here is for a range of popular spoilers with the common features of about 70% aerofoil profile chord location, a chord of 10% aerofoil chord and a span normalized to the whole span of the aerofoil. According to the spoiler data used for the modelling, the model would be ideally used for low air-speed/Mach no. cases with spoiler motion being quasi-steady.

The model expression normally and ideally takes the form of the related aerodynamic coefficients, namely the spoiler lift coefficient C_{LSP}, the drag coefficient C_{DSP} and the moment coefficient C_{MSP}, and/or their derivatives $C_{l\delta_s}$, $C_{d\delta_s}$ and $C_{m\delta_s}$ while linear modelling is concerned. In this study, a least-square error fitting (LSEF) technique in MATLAB was applied to the spoiler data, giving algebraic expressions for the coefficients C_{LSP}, C_{DSP} and C_{MSP}. The spoiler deflection angle δ_{sp} and the wing incidence α appear as the most influential independent variables.

Based on the generic model, different forms of spoilers for HAWK aircraft were designed and applied to the control studies later.

2.2 Spoiler Modelling ------ Small Incidence Case

At first, the spoilers were modelled for the case of small wing incidence where the functional dependence of the spoiler effectiveness is mainly on its deflection angle δ_{sp}.

This view point is backed by many experiments, typically those of WENTZ et al (1981) and MCLACHLAN et al(1983), where the phenomena that the incremental lift and drag as a function of spoiler deflection angle was virtually independent of the median range change of α was reported. The underlying mechanism is that when the incidence is

small or below some critical point, there is no interaction between separated wing flow and the spoiler induced separation, hence the effectiveness of the spoilers is solely decided by the separation due to their deflection.

2.2.1 Spoiler lift coefficient C_{LSP}

This coefficient expresses the contribution of a spoiler to the lift force of an aircraft wing. The feature of negative lift force provided by deployment of most conventional spoilers has caused them to find their application in flight control as lift dumpers. The relation between the spoiler lift LSP and the coefficient CLSP is:

$$L_{SP} = \frac{\rho V^2 S}{2} C_{LSP} \qquad (2\text{-}1)$$

Fig. 2-1 presents relevant experimental data for the coefficient C_{LSP}. Data for spoilers with chords ranging from 5% WC (wing or aerofoil mean chord) to 15% WC and locations from 65% WC to 73% WC are shown. They demonstrate the general quasi-steady features of most aft-mounted upper-wing surface spoilers: the negative lift increment ($C_{LSP} \leq 0$, $L_{SP} \leq 0$) with upwards deflection of the spoilers ($\delta_{sp} \leq 0$) and the roughly linear relation between C_{LSP} and δ_{sp}.

Apparently, the data pattern shown in **Fig. 2-1** is not ideal for setting up the generic model with a fixed 10% WC. An important step to get a collapsed data distribution for this purpose is to make the assumption that the spoiler effectiveness is proportional to its chord length. Based on this, a spoiler with a chord of X% WC can therefore be normalized to the 10% WC spoiler using the following formula:

$$C_{NLSP} = \frac{10}{X} C_{LSP} \qquad (2\text{-}2)$$

Normalizing the coefficient data in **Fig. 2-1** according to (2-2) yields **Fig. 2-2.** Compared with **Fig. 2-1**, the data in **Fig. 2-2** show a much more collapsed pattern so it is more suitable for the generic model.

Applying linear interpolation to each set of data in **Fig. 2-2** brings a family of lift curves which have the range:

$$|0.6\,\delta_{sp}| < |C_{NLSP}| < |0.8\,\delta_{sp}| \qquad (2\text{-}3)$$

So initially, the generic lift coefficient model may be assumed to be:

$$C_{NLSP} = C_{l\delta_s}\,\delta_{sp} \qquad (2\text{-}4)$$

where $C_{l\delta_s}$ is the derivative (or gain) with the range: $0.6<C_{l\delta_s}<0.8$.

Further studies were made on the improvement of the model. It is easy to find while looking at **Fig. 2-1** and **Fig. 2-2** that with increase of δ_{sp}, the control effectiveness (the lift slopes) of the spoilers shows a decreasing trend, suggesting that the purely linear expression may be not accurate enough when δ_{sp} is large.

Quite naturally, this suggests that a Sine function may give a better description of the relation between C_{LSP} and δ_{sp}, as also pointed out by WENTZ from his experimental tests that "spoiler effectiveness depends primarily on projected height rather than on the deflection angle". This can be further verified by looking at **Fig. 2-3** and **Fig. 2-4**, the former showing the dependence of $C_{l\delta s}$ on δ_{sp} for all the normalized data and the latter the C_{lh} ($=C_{LSP}/\sin(\delta_{sp})$) on δ_{sp}. **Fig. 2-4** gives more uniform results for large δ_{sp} than **Fig. 2-3**.

To demonstrate this quantitatively and also to get a more general expression for the lift coefficient, an analysis was made to fit each data set in **Fig. 2-2** using three different functional expressions: namely the linear and sine function (**form a**), the linear function (**form b**) and the sine function (**form c**), respectively. The analysis was aided by the MATLAB package and gave the LESF results for the functions in the forms:

Form a: linear & sine function:

$$C_{NLSP\,(a)} = K_1\delta_{sp} + K_2 \sin(\delta_{sp}) \qquad (2\text{-}5)$$

Form b: linear function:

$$C_{NLSP\,(b)} = K_1\delta_{sp} \qquad (2\text{-}6)$$

Form c: sine function:

$$C_{NLSP\,(c)} = K_S \sin(\delta_{sp}) \qquad (2\text{-}7)$$

Table 2-1 summarizes the fittings for some of the normalized spoiler data. Comparisons between the fitting errors suggest an improvement in the accuracy using the $C_{NLSP\,(a)}$ or $C_{NLSP\,(c)}$ for the lift coefficient modelling.

The last but most important work was fitting of all the normalized spoiler data in **Fig. 2-2** using the functions (2-5), (2-6) and (2-7). This was to give an improved spoiler model with a more generic behaviour. The following results were obtained:

Form a: $C_{NLSP\,(a)} = 0.32\delta_{sp} + 0.51 \sin(\delta_{sp})$ (2-8)
(EN=0.309)

Form b: $C_{NLSP\,(b)} = 0.7\delta_{sp}$ (2-9)
(EN=0.45)

Form c: $C_{NLSP\,(c)} = 0.92 \sin(\delta_{sp})$ (2-10)
(EN=0.41)

where $\delta_{sp} \leq 0$, EN: error norm.

The lines fitted to the data are shown in **Fig. 2-5** and the errors from the fittings are shown in **Table 2-1**.

The overall data fit presents an equivalent, or 'generic', spoiler lift coefficient model with δ_{sp} as the only independent variable. Moreover, the analysis of the fitting errors shows that the combined linear and sine function (**form a**) gives the best description of the lift coefficient, and the sine function (**form c**) is better than the linear one (**form b**).

2.2.2 Spoiler drag coefficient C_{DSP}

The drag coefficient C_{DSP} represents the contribution of spoilers to the drag of an aircraft. The ability to provide fast and substantial drag force during flight is a significant feature of spoilers and has stimulated the use of them as air brakes. As the lift case, the relation between the drag and its coefficient is:

$$D_{SP} = \frac{\rho V^2 S}{2} C_{DSP} \qquad (2\text{-}11)$$

where there are $C_{DSP} \geq 0$ and $D_{SP} \geq 0$.

When attempting to model this coefficient, there was the obstacle that only a small amount of experimental data was available. **Fig. 2-6** shows the scarce distribution of the C_{DSP} data. Using the same normalizing procedure, as introduced in the C_{LSP} modelling, for the 10%WC generic spoiler, a set of normalized C_{DSP} data can be obtained and **Fig. 2-7** shows the more collapsed data distribution.

Following the same LESF procedure for C_{LSP} using the functions (2-5), (2-6) and (2-7), the drag coefficient models for all the normalized data were generated as:

Form a: $C_{NDSP\,(a)} = -0.1\delta_{sp} - 0.004 \sin(\delta_{sp})$ (2-12)
(EN=0.046)

Form b: $C_{NDSP\,(b)} = -0.1\delta_{sp}$ (2-13)
(EN=0.046)

Form c: $C_{NDSP\,(c)} = -0.15 \sin(\delta_{sp})$ (2-14)
(EN=0.071)

with $\delta_{sp} \leq 0$.

Fig. 2-8 shows the lines fitted to the data. The analysis of the fitting errors suggested the best model for the drag coefficient:

$$C_{NDSP} = -0.1\delta_{sp}. \quad (2\text{-}15)$$

2.2.3 Spoiler moment coefficient C_{MSP}

Spoiler moment coefficient C_{MSP} represents the longitudinal pitching moment increment due to spoiler deflection. For most aft-mounted upper wing surface spoilers (with the hinge line after the lift centre of the wing), C_{MSP} appears as positive, showing an increase in aircraft moment. The relation between the moment increment and its coefficient is expressed by:

$$M_{SP} = \frac{\rho V^2 Sb}{2} C_{MSP} \quad (2\text{-}16)$$

The modelling of C_{MSP} has become a controversial issue. In many previous studies, this coefficient was simply neglected because of its small size and the difficulties involved in obtaining an accurate measurement, leaving very few test data available. Also

the data, as shown in **Fig. 2-9**, seemed to be affected by various significant factors such as Mach number, scale effect, aerofoil type and, in particular, the location of spoiler hinge lines.

However, modelling and analysis of this coefficient are important for the use of spoilers in control. As MACK$_{\Lambda}^{et\,al}$(1979) and others have pointed out, the moment influence from spoilers may seriously affect aircraft handling and control. This is verified by the later analysis of this aspect while combined with the flight simulation in **Chapter Four.**

Fig. 2-10 shows the 10%WC normalized data distribution. Looking at the results from CONSIGNY (52% WC location), COSTES (67% WC) and MCLACHLAN (73% WC) and comparing the data pattern with that of C_{NLSP} and C_{NDSP}, the effect of the spoiler location is seen to be significant.

Table 2-2 lists the results of fitting some sets of the data using the three functions given above. Curve fitting for all the data from three similar locations (67%WC, 70%WC and 73%WC) using the three functions is shown in **Fig. 2-11** and yields:

Form a: $C_{NMSP\,(a)} = 0.005\delta_{sp} - 0.12 \sin(\delta_{sp})$ (2-17)
(EN=0.038)

Form b: $C_{NMSP\,(b)} = -0.1\delta_{sp}$ (2-18)
(EN=0.04)

Form c: $C_{NMSP\,(c)} = -0.114 \sin(\delta_{sp})$ (2-19)
(EN=0.038)

with $\delta_{sp} \leq 0$.

So from the fitting, a suitable model for the moment coefficient of the 70% WC spoilers appears to be:

$$C_{NMSP} = -0.1\delta_{sp}. \quad (2\text{-}20)$$

2.3 Spoiler Modelling ------ High Incidence Case

As summarized in **Chapter One**, the wing incidence α has some significant effects on the control effectiveness of most conventional spoilers. Since α also stands for

an important state variable of aircraft dynamics and its variation in most advanced high-manoeuvrable aircraft may go well beyond the small α assumption for simple modelling of spoilers, there is a need to model these effects by introducing α, as another independent variable yet related to the deflection δ_{sp}, into the coefficient functions.

Previous studies on spoiler effectiveness loss due to high incidence cases have been documented by PARKINSON et al(1987), MACK et al(1979), WENTZ et al(1981), MCLACHLAN et al(1983) and KALLIGAS et al(1987), where spoiler tests were made in various incidence regions (see **Table 1-1**). A general conclusion drawn from these and other similar studies is that the effectiveness of spoilers has an increasingly weak dependence on the deflection δ_{sp} as the wing incidence α approaches the positive or negative stall regions.

Another important conclusion regarding this aspect is obtained from MYERS's experiment in 1989 which revealed that the tendency for spoiler control effectiveness to increase or decrease with increasing incidence depends strongly on the location of the spoilers on the wing surface. A spoiler hinged forward of the mid-chord position has an increase in its effectiveness with α increase, while an aft-hinged spoiler shows the opposite tendency --- a reduction in its effectiveness.

An approach is investigated to take the incidence effect on spoiler effectiveness into account through defining an incidence influence function $\lambda(\alpha)$ and combining the function with the spoiler model previously defined:

$$\hat{C}_{NSP}(\alpha, \delta_{sp})=\lambda(\alpha)\, C_{NSP}(\delta_{sp}) \qquad (2\text{-}21)$$

where $\lambda(0)=1$ gives $\hat{C}_{NSP} = C_{NSP}$, the spoiler model described in **2.2** for small incidence cases.

$\lambda(\alpha)$ can be approximately determined using the following procedure:

1) Suppose the function $C_{NSP}(\delta_{sp})$ is linear (which is roughly true for most conventional spoilers), i.e.

$$C_{NSP}(\delta_{sp}) = C_{\delta_s}\, \delta_{sp} \qquad (2\text{-}22)$$

where C_{δ_s} is the curve slope for $\alpha \approx 0$. Then (2-21) can be written as:

$$\lambda(\alpha) = \frac{\hat{C}_{NSP}(\alpha,\delta_{sp})}{C_{NSP}(\delta_{sp})|_{\alpha\approx 0}} = \frac{\hat{C}_{NSP}(\alpha,\delta_{sp})}{C_{\delta_s}|_{\alpha\approx 0}\,\delta_{sp}} \qquad (2\text{-}23)$$

2) Given $C_{\delta_s}|_{\alpha\approx 0}$ and a family of $\hat{C}_{NSP}(\alpha,\delta_{sp})$ curves, a set of derivative data as a function of α, $C_{\delta_s}|_{\alpha=\alpha_i}$, can be obtained by linear interpolation. Then the $\lambda(a)$ can be decided by (2-23).

Applying the above procedure to some of the experimental $\hat{C}_{NLSP}$ data yields a set of points of $\lambda_L(\alpha)$ shown in **Fig. 2-12**. Based on the data, a generic formula $\lambda_{NL}(\alpha)$ is proposed as:

$$\lambda_{NL}(\alpha) = \begin{cases} 1.0 & -10^o \le \alpha < 10^o \\ 2.0 - \dfrac{\alpha}{10.0} & 10^o \le \alpha \le 20^o \end{cases} \qquad (2\text{-}24)$$

and the fit of the function to the data is shown in **Fig. 2-12.**

Similarly, the generic influence functions $\lambda_{ND}(\alpha)$ and $\lambda_{NM}(\alpha)$, for the drag and moment coefficient models, respectively, can be defined by $\lambda_D(\alpha)$ **(Fig. 2-13)** and $\lambda_M(\alpha)$ **(Fig. 2-14)** from the corresponding experimental data, and appear as:

$$\lambda_{ND}(\alpha) = 1 - \frac{\alpha}{15.0} \qquad -15^o \le \alpha \le 20^o \qquad (2\text{-}25)$$

and

$$\lambda_{NM}(\alpha) = 1 - \frac{\alpha}{30.0} \qquad -15^o \le \alpha \le 20^o \qquad (2\text{-}26)$$

The function curves are drawn in **Fig. 2-13** and **Fig. 2-14**, respectively.

Finally, it should be pointed out that because of the limited amount of experimental tests giving the spoiler data of interest over a large scope of α variation, the proposed influence functions $\lambda_{NL}(\alpha)$, $\lambda_{ND}(\alpha)$ and $\lambda_{NM}(\alpha)$ may only be a rough estimate of the incidence effect and require validation by further cases. However, the modelling process does show that the formula (2-21) could be an effective way by which the most essential features of spoiler effectiveness can be modelled and then introduced into flight control design.

2.4 A Generic Spoiler Control Model

Summarizing the work on the spoiler modelling so far, a generic spoiler control model for a range of normalized full-span, two-dimensional, 70% WC location and 10% WC spoilers, preferably working quasi-steadily under low Mach number conditions (Mach. No. < 0.2), is set up in the coefficient forms of $\hat{C}_{NLSP}$, $\hat{C}_{NDSP}$ and $\hat{C}_{NMSP}$.

2.4.1 The generic lift model $\hat{C}_{NLSP}$

In the interest of simplicity and flexibility in use, from (2-9), (2-10) and (2-24) this coefficient is modelled as:

First form: $$\hat{C}_{NLSP} = 0.92\lambda_{NL}(\alpha)\sin(\delta_{sp}) \qquad (2\text{-}27)$$

Second form: $$\hat{C}_{NLSP} = 0.7\lambda_{NL}(\alpha)\,\delta_{sp} \qquad (2\text{-}28)$$

where,

$$\lambda_{NL}(\alpha) = \begin{cases} 1.0 & -10^{o} \le \alpha < 10^{o} \\ 2.0 - \dfrac{\alpha}{10.0} & 10^{o} \le \alpha \le 20^{o} \end{cases}.$$

2.4.2 The generic drag model $\hat{C}_{NDSP}$

From (2-13) and (2-15), this coefficient is modelled as:

$$\hat{C}_{NDSP} = -0.1\lambda_{ND}(\alpha)\,\delta_{sp} \qquad (2\text{-}29)$$

where $\lambda_{ND}(\alpha) = 1 - \dfrac{\alpha}{15.0}$ $\qquad -15^{o} \le \alpha \le 20^{o}.$

2.4.3 The generic moment model $\hat{C}_{NMSP}$

From (2-18) and (2-26), the model is given as:

$$\hat{C}_{NMSP} = -0.1\lambda_{NM}(\alpha)\,\delta_{sp} \qquad (2\text{-}30)$$

where $\lambda_{NM}(\alpha) = 1 - \dfrac{\alpha}{30.0}$ $\qquad -15^{o} \le \alpha \le 20^{o}.$

2.5 An Artificial Spoiler Model for the HAWK Aircraft

Finally, upon the modelling of the generic spoiler, an attempt was made to design a spoiler for the British Aerospace Hawk aircraft. It is called 'artificial' simply because the Hawk, which has been in service for more than 20 years, has not got any spoilers in the original design, and the introduction and combination of the spoilers with the aircraft model aim to further the analysis and evaluation of spoiler control effectiveness, and to design and develop a nonlinear flight control system utilising spoiler control, making use of the Hawk as a flight testing platform.

Basic features and data concerning the Hawk can be found in HERD's report (1985) and WHITFORD's paper(1991). Detailed 3-dimensional diagrams of the HAWK 60/100 and HAWK 200 are shown in **Fig. 4-1**. The design of the spoiler used here for the Hawk 60/100 is:

Wing Data:

Ref. Area: 16.7m^2 Aspect Ratio: 5.28
Mean Chord: 1777mm Angle of Sweepback: 26^o
Thickness/Chord Ratio: 10.9% (root)

Spoiler Geometric Data:

Ref. Area: 0.9m^2 Movement about Hinge Line: 90^o
Hinge Line: 65% WC Chord: 10% WC

Spoiler Control Coefficients Models: For different application cases, the spoiler is modelled in different forms:

Spoiler Model One:

Lift: $C_{LSP} = K_l\lambda_L(\alpha)\sin(\delta_{sp})$ (2-31)

Drag: $C_{DSP} = K_d\lambda_D(\alpha)\delta_{sp}$ (2-32)

Moment: $C_{MSP} = K_m\lambda_M(\alpha)\delta_{sp}$ (2-33)

Here $\delta_{sp} \leq 0$, and $\lambda_L(\alpha)$, $\lambda_D(\alpha)$ and $\lambda_M(\alpha)$ are taken as the same as the functions defined in (2-24), (2-25) and (2-26), respectively. A nominal set of the gains K_l, K_d and K_m are $K_l = 0.46$, $K_d = -0.05$ and $K_m = -0.05$.

Spoiler Model Two:

The drag and moment models are the same as (2-32) and (2-33) yet the lift model becomes:

Lift: $C_{LSP} = K_l \lambda_L(\alpha) \delta_{sp}$ (2-34)

where $K_l = 0.35$.

Spoiler Model Three: (linear model)

Lift: $C_{LSP} = C_{l\delta_s} \delta_{sp}$ (2-35)

Drag: $C_{DSP} = C_{d\delta_s} \delta_{sp}$ (2-36)

Moment: $C_{MSP} = C_{m\delta_s} \delta_{sp}$ (2-37)

where a set of the derivatives are given as $C_{l\delta_s} = 0.35$, $C_{d\delta_s} = -0.05$ and $C_{m\delta_s} = -0.05$

Explanatory Remarks:

1. The hinge line of the spoiler is subject to its chord length and the actual hinge lines of the ailerons and flaps of the Hawk. Also, at the nominated hinge line of 65%WC, it is considered reasonable to employ a smaller gain/derivative for the moment models.

2. The spoiler coefficient data C_{LSP}, C_{DSP} and C_{MSP} are defined such that they correspond with the data of a half semi-span design of the two-dimensional generic spoiler ($\hat{C}_{NLSP}$, $\hat{C}_{NDSP}$, $\hat{C}_{NMSP}$) in **2.4**. For the Hawk wing with its relatively low swept angle, this mainly relies on WENTZ's experimental result that the control effectiveness is directly proportional to spoiler span and three-dimensional effects are negligible for unswept wings, even for spoilers of relatively low-aspect ratio. However, due to the more complex nature of 3-dimensional flow and its considerable effects on the boundary

layers, the view point on which the design is based should still be subject to the validation of further studies of spoilers on swept wings.

2.6 Concluding Remarks

Appearing as the first attempt at research in this area, the work described above has produced a generic mathematical model for a range of conventional spoilers with some common features. Its importance lies in the facts that by using the model, further analysis and evaluation of spoiler effectiveness in control are made possible, and some artificial spoilers for a specified aircraft (e.g. the HAWK) could be designed, for advanced studies of flight control utilising spoilers and for reference for a practical spoiler design.

The modelling was based on processing the spoiler coefficient data which is available. A key step involved in gaining the collapsed data distributions for the generic model was the assumption that the spoiler effectiveness is proportional to its projected height, which not only led to formula (2-2), which revealed the effect of spoiler chord length, but also gave an improved lift coefficient expression using the sine function. With respect to the influence of wing incidence angle, a formula incorporating the influence function $\lambda(\alpha)$ (2-21) was proposed, by which the most important features of spoilers are presented in a simple and flexible way.

The different forms of the spoiler models for the HAWK will be applied to the different stages of the control studies relating spoilers. Special attention should be given to the moment coefficient since, presumably due to the limited data and considerable location effect, the gain (derivative) seems somewhat beyond expectation. A special simulation analysis has therefore been devoted to its effect on the flight control effectiveness (**Chapter 4**), suggesting that use of a smaller gain K_m ($C_{m\delta_s}$, e.g., =0.01) for the most applications.

Table 2-1 Spoiler lift coefficient function modelling

	$C_{NLSP\,(a)}$	$C_{NLSP\,(b)}$	$C_{NLSP\,(c)}$
Wentz (73%WC)	K_1=-0.34, K_2=1.27 (EN=0.028)	K_1=0.76 (EN=0.097)	K_s=0.87 (EN=0.040)
McLachlan (73%WC)	K_1=-0.17, K_2=1.06 (EN=0.002)	K_1=0.75 (EN=0.074)	K_s=0.87 (EN=0.014)
Costes (67%WC)	K_1=0.67, K_2=0.14 (EN=0.026)	K_1=0.81 (EN=0.026)	K_s=0.87 (EN=0.026)
Myers (70%WC)	K_1=-2.21, K_2=3.05 (EN=0.072)	K_1=0.67 (EN=0.112)	K_s=0.71 (EN=0.098)
Tou (70%WC)	K_1=0.19, K_2=0.69 (EN=0.042)	K_1=0.71 (EN=0.212)	K_s=0.94 (EN=0.085)
Lee (73%WC)	K_1=0.67, K_2=0.06 (EN=0.034)	K_1=0.72 (EN=0.034)	K_s=0.83 (EN=0.067)
Overall Data (70%WC)	**K_1=0.32, K_2=0.51 (EN=0.309)**	**K_1=0.7 (EN=0.45)**	**K_s=0.92 (EN=0.41)**

Table 2-2 Spoiler moment coefficient function modelling

	$C_{NMSP\,(a)}$	$C_{NMSP\,(b)}$	$C_{NMSP\,(c)}$
Consigny (52%WC)	K_1=-2.02, K_2=2.01 (EN=0.007)	K_1=-0.04 (EN=0.009)	K_s=-0.04 (EN=0.009)
McLachlan (73%WC)	K_1=0.05, K_2=-0.17 (EN=0.002)	K_1=-0.10 (EN=0.012)	K_s=-0.11 (EN=0.005)
Costes (67%WC)	K_1=0.20, K_2=-0.30 (EN=0.004)	K_1=-0.09 (EN=0.005)	K_s=-0.09 (EN=0.005)
Myers (70%WC)	K_1=1.06, K_2=-1.29 (EN=0.0)	K_1=-0.13 (EN=0.024)	K_s=-0.14 (EN=0.021)
Mabey (65%WC)	K_1=-0.50, K_2=0.47 (EN=0.008)	K_1=-0.04 (EN=0.012)	K_s=-0.04 (EN=0.012)
Overall Data (70%WC)	**K_1=0.00, K_2=-0.12 (EN=0.038)**	**K_1=-0.1 (EN=0.04)**	**K_s=-0.1139 (EN=0.038)**

Figure 2-1 Summary of spoiler lift coefficient measurements

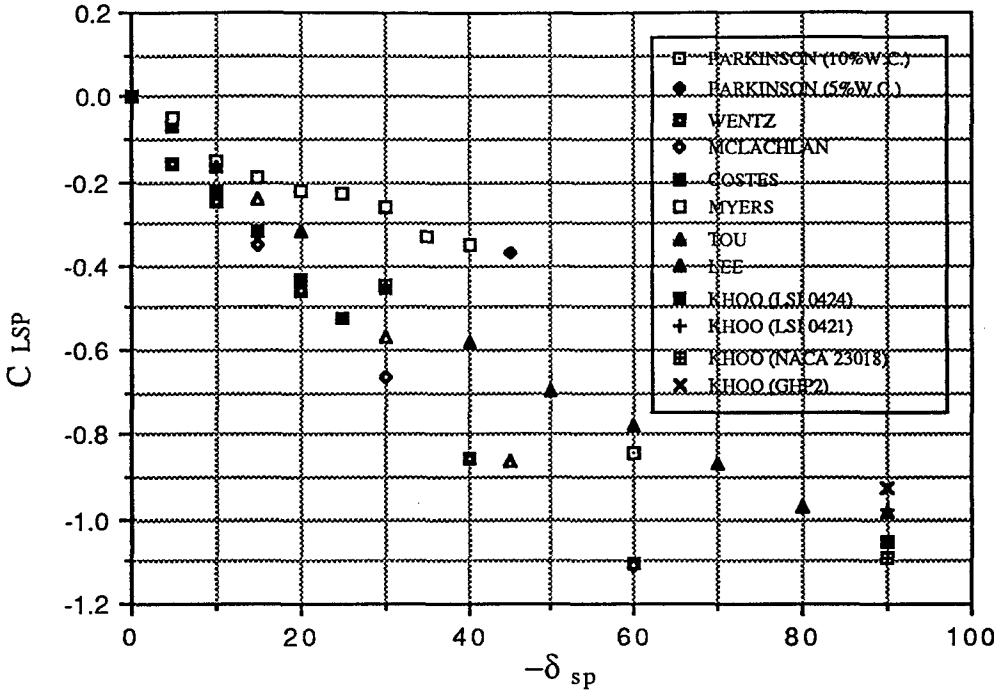

Figure 2-2 10%WC normalized spoiler lift coefficient data

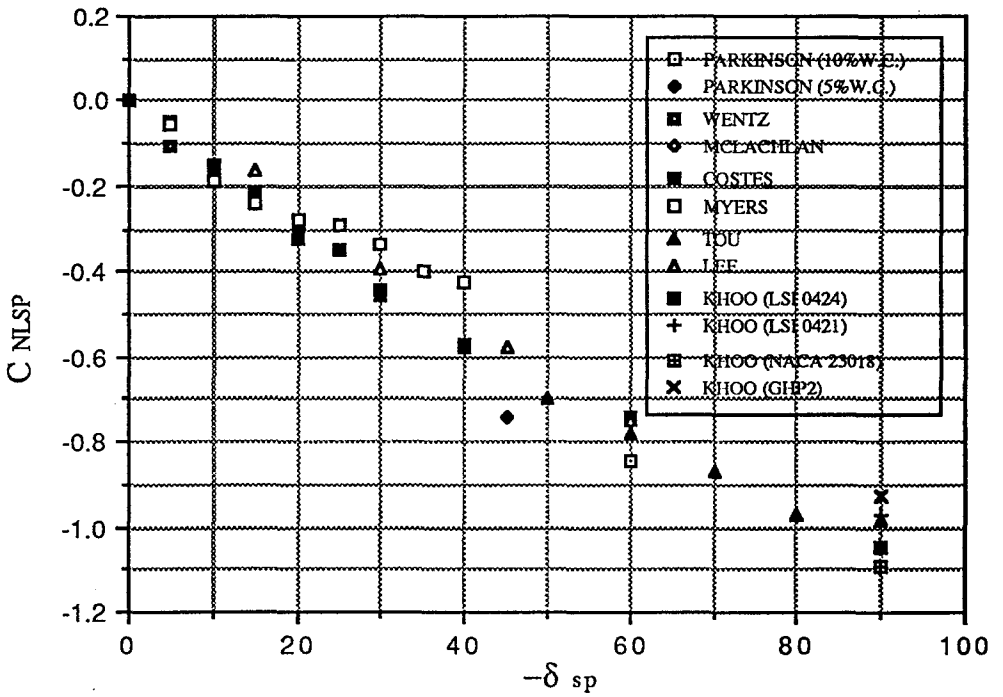

Figure 2-3 Analysis of spoiler deflection angle effect

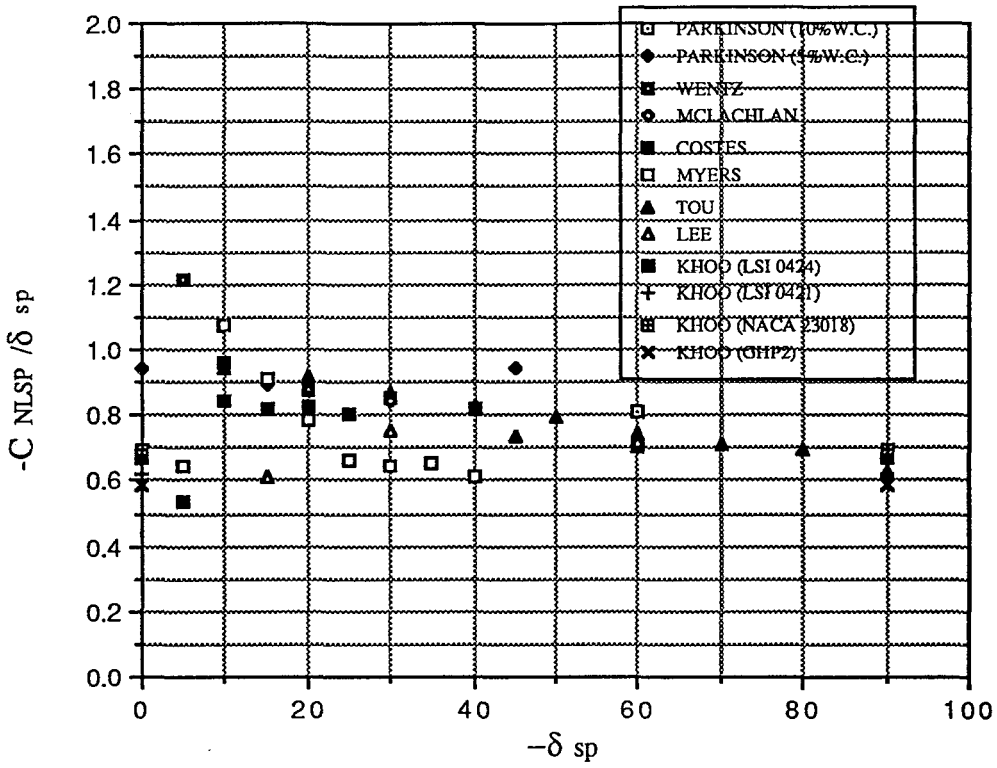

Figure 2-4 Analysis of spoiler projected height effect

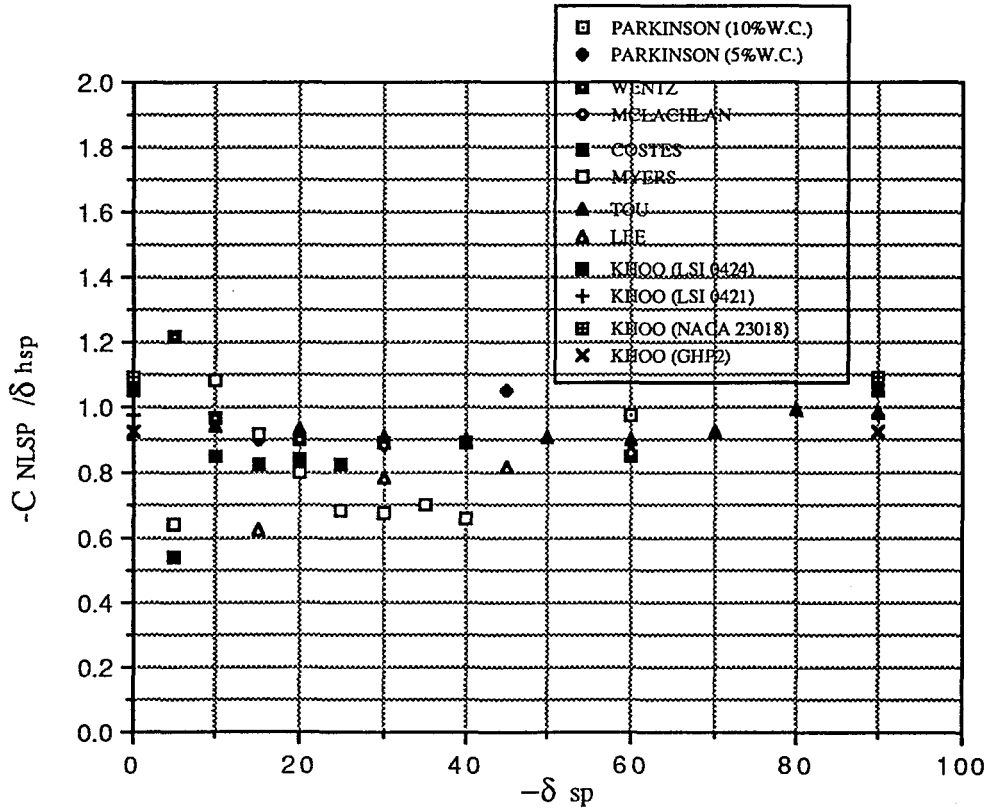

Figure 2-5 C_{NLSP} fitting using the three functions

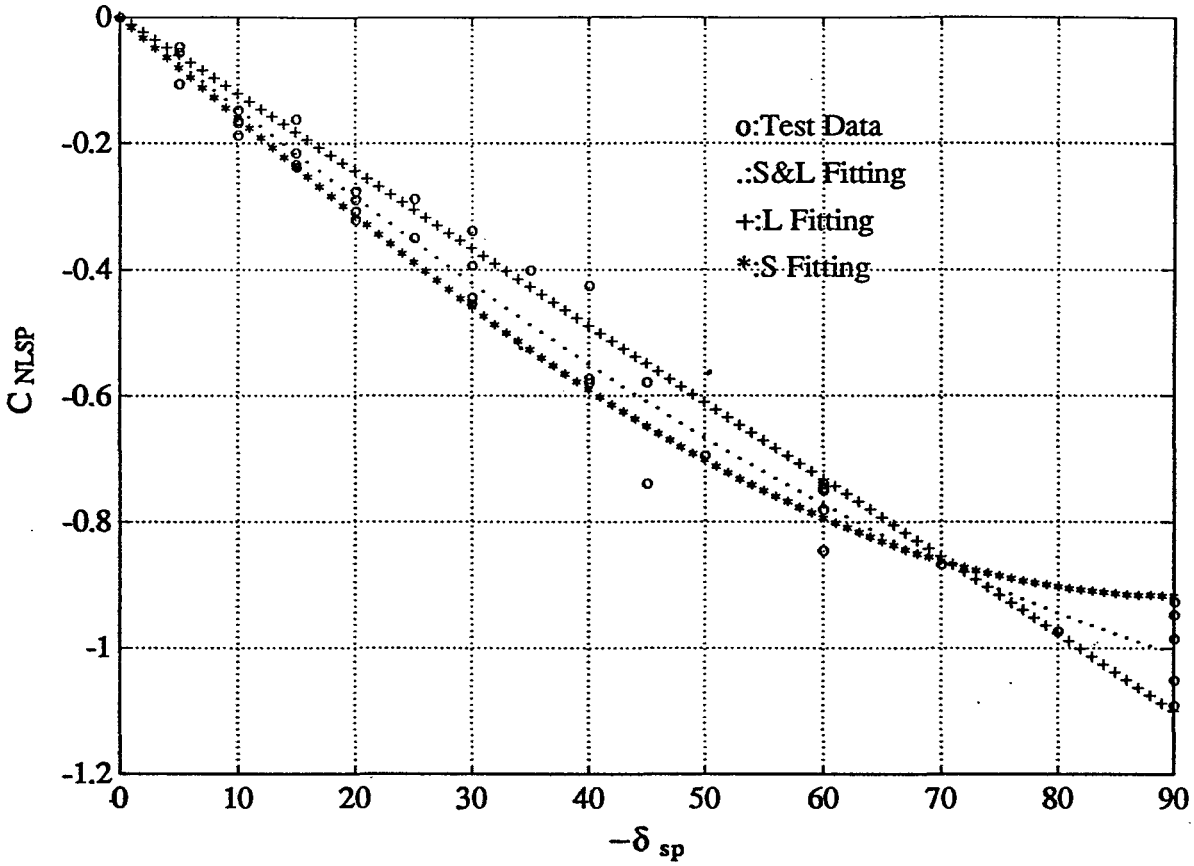

Figure 2-6 Summary of spoiler drag coefficient measurements

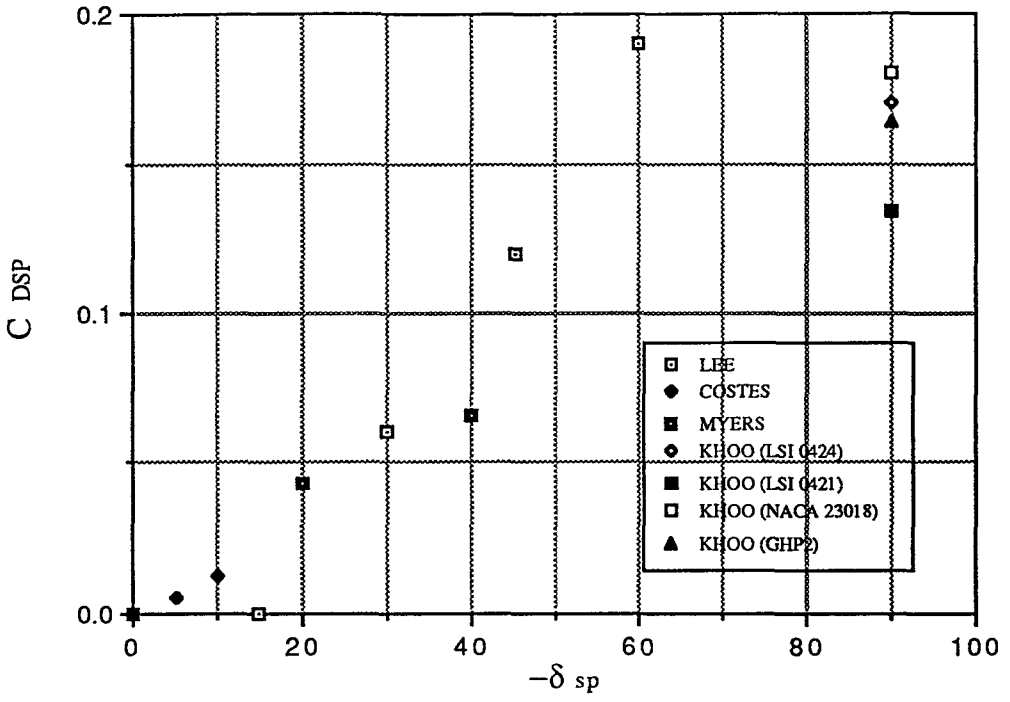

Figure 2-7 10%WC normalized spoiler drag coefficient data

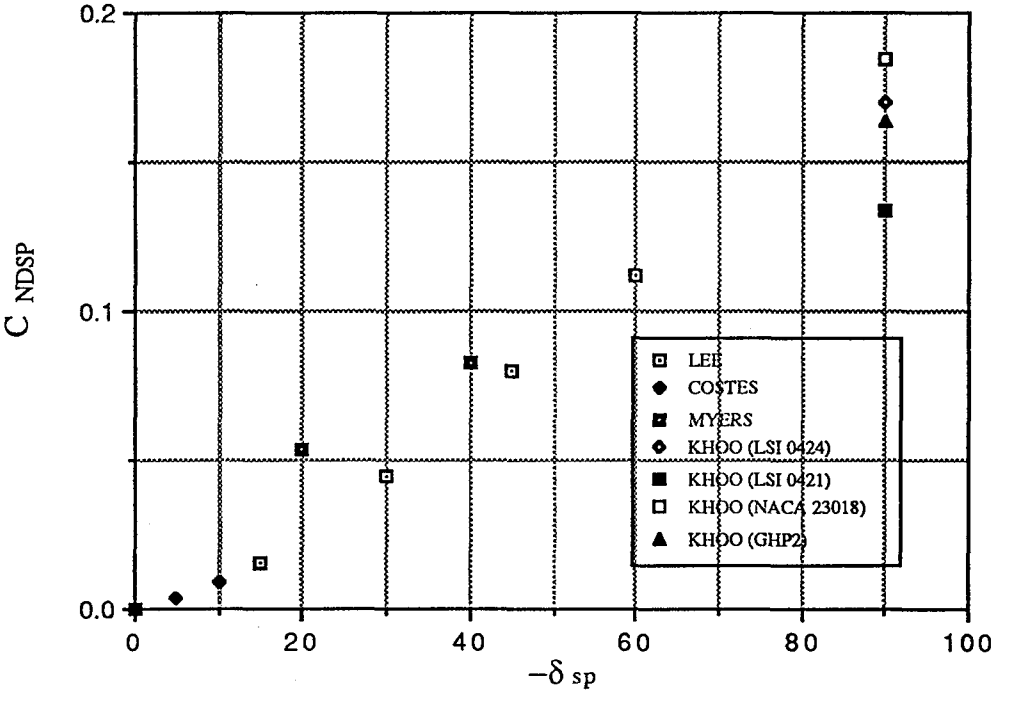

Figure 2-8 C_{NDSP} fitting using the three functions

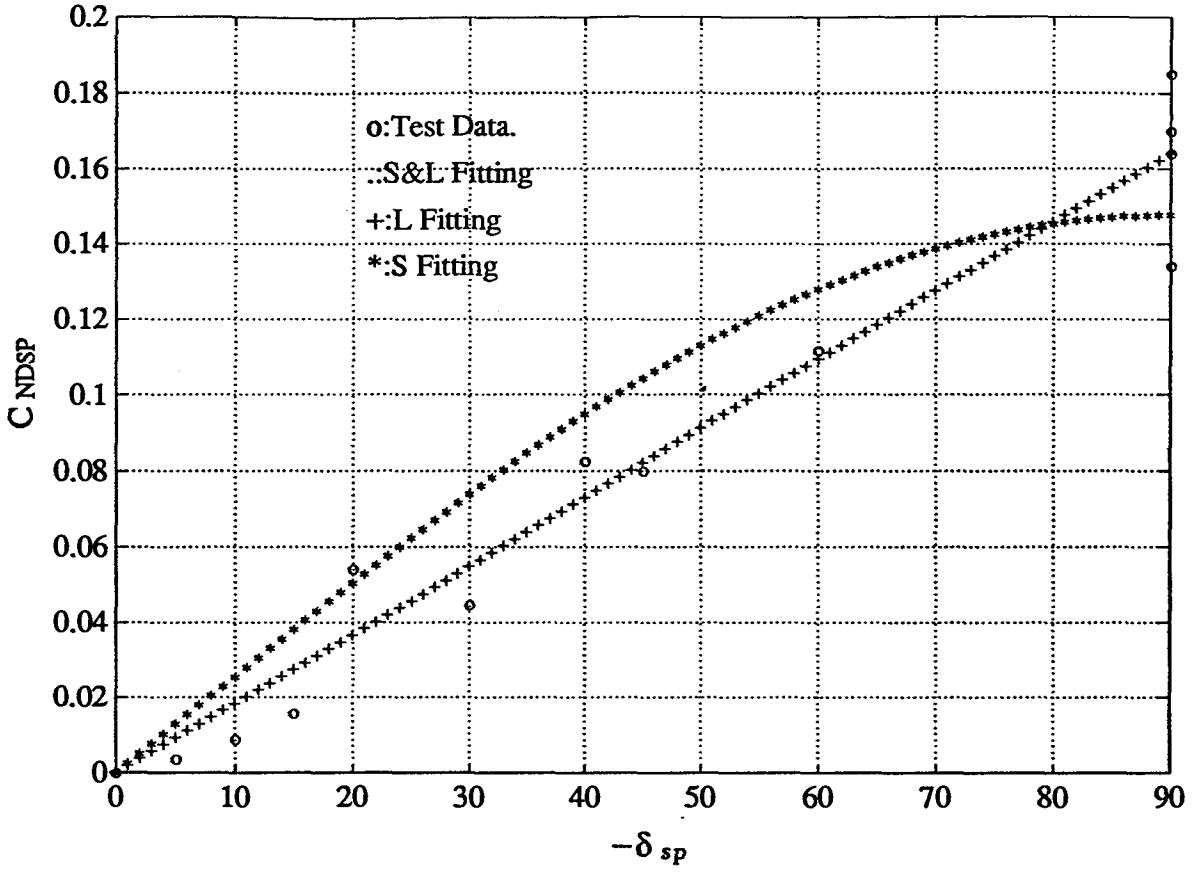

Figure 2-9 Summary of spoiler moment coefficient measurements

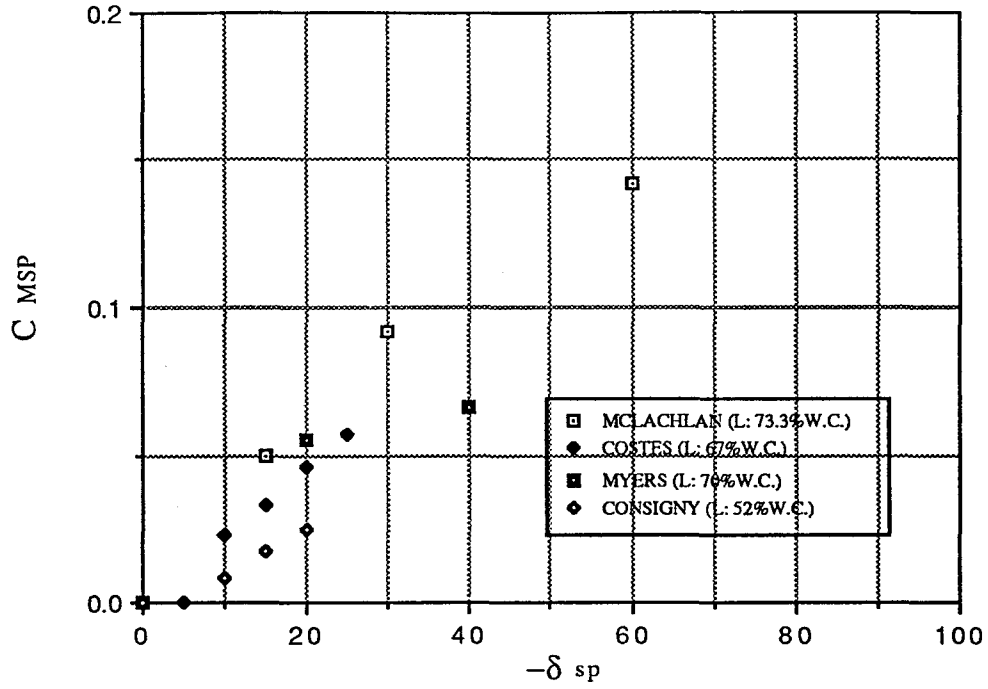

Figure 2-10 10%WC normalized spoiler moment coefficient data

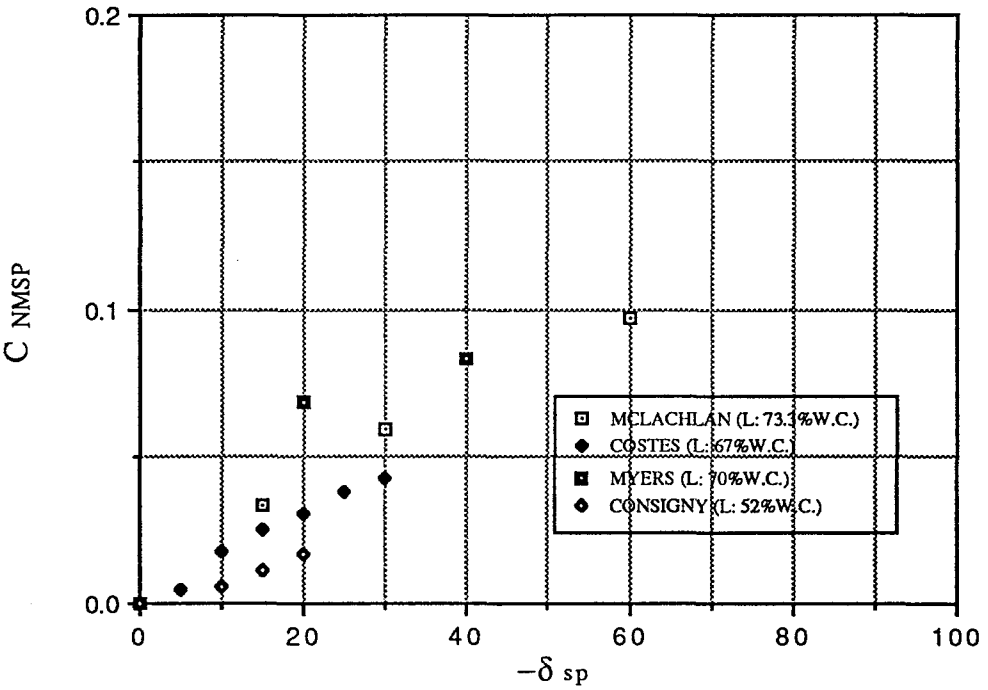

Figure 2-11 C_{NMSP} fitting using the three functions

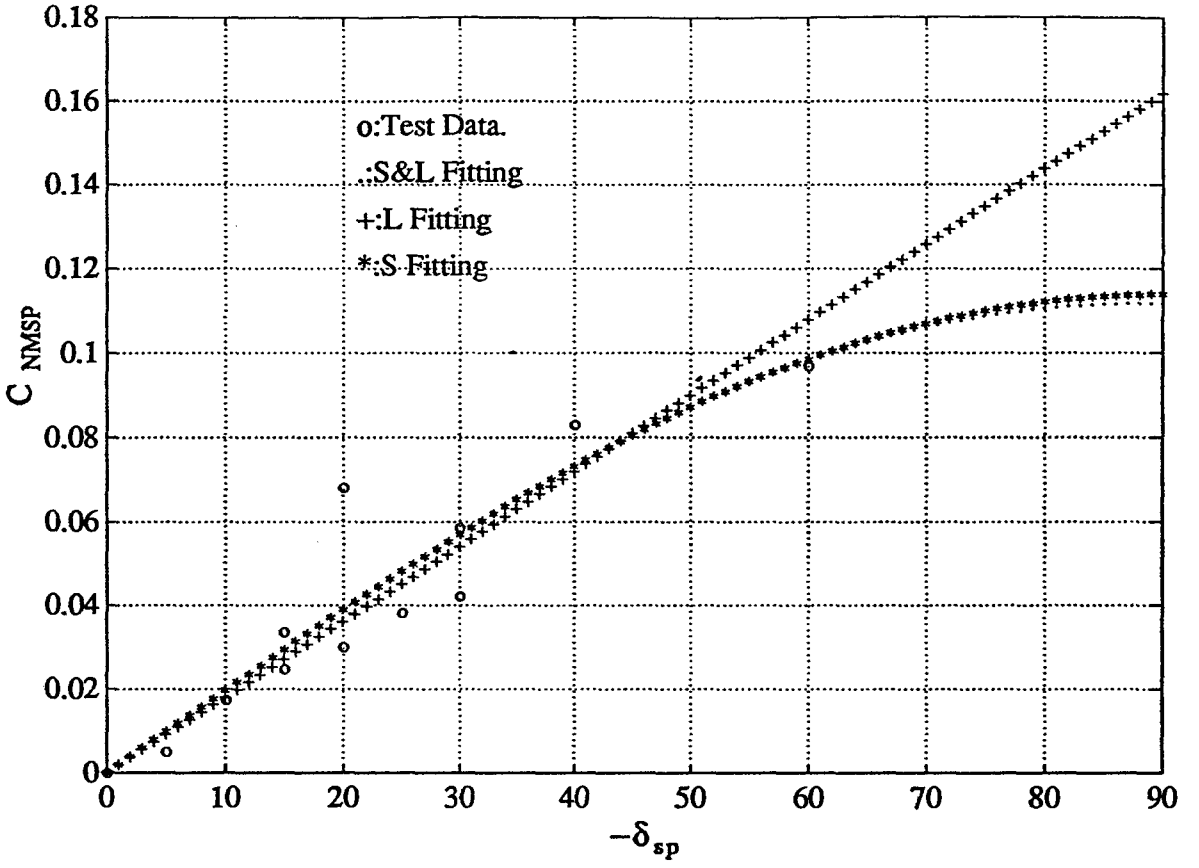

Figure 2-12 Incidence influence function of the spoiler lift coefficient

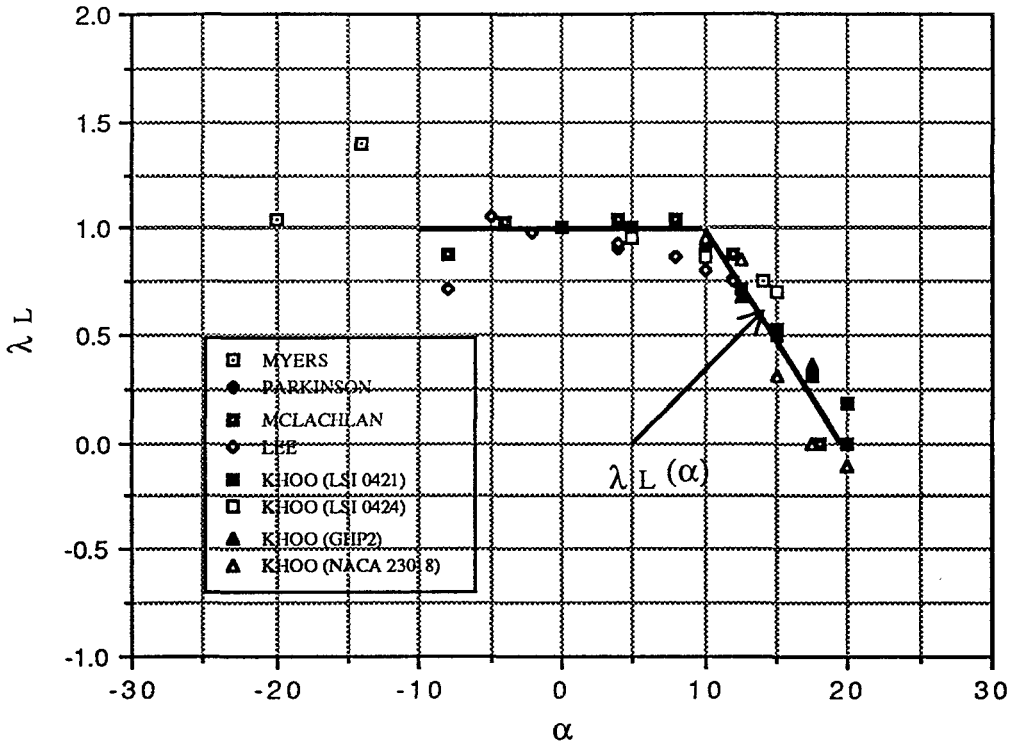

Figure 2-13 Incidence influence function of the drag coefficient

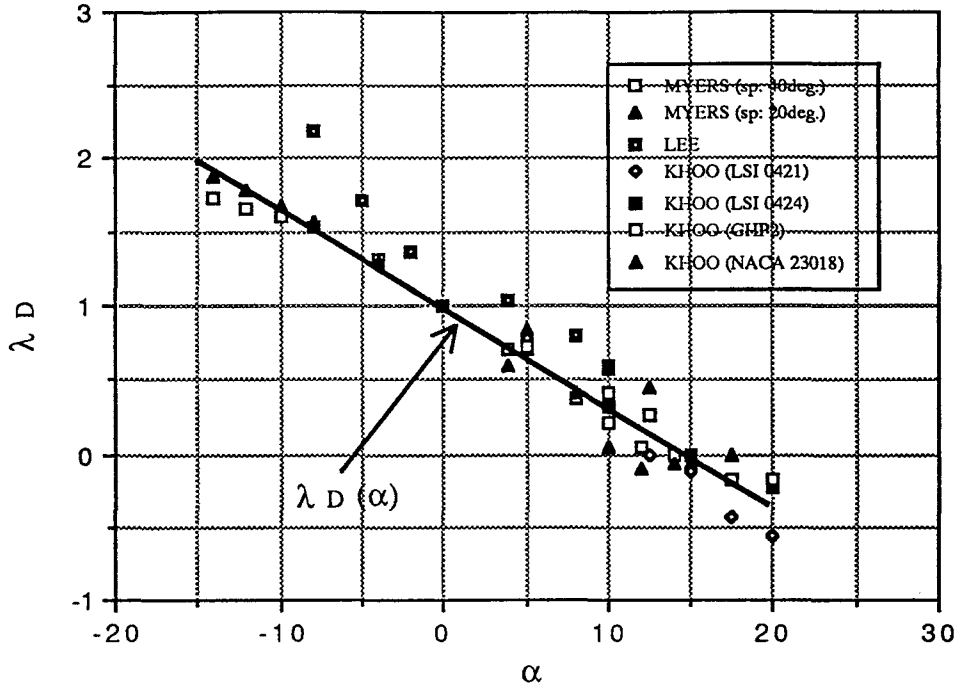

Figure 2-14 Incidence influence function of the moment coefficient

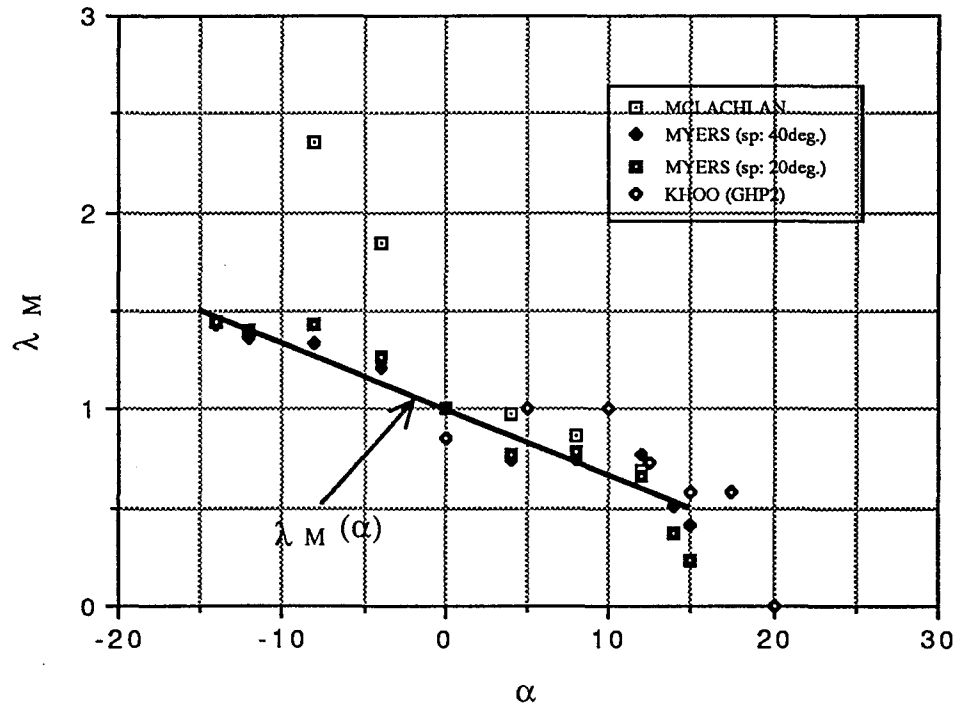

Chapter Three

RANGE SPACE THEORY AND ITS APPLICATION TO SPOILER CONTROL SYSTEMS

3.1 General Remarks

This chapter is concerned with the use of linear range space theory for the analysis of spoiler control effectiveness.

The concept of the range space of a dynamic system is closely connected with the reachability and the controllability of the system (BROCKETT, 1970). For a linear time-varying system, the analysis of its range space involves the definition of its controllability grammian, through which the optimal control with 'minimum energy cost' can be found which transfers the state between any two specified values.

Also, through the calculation of the controllability grammian, the comparison of the controllability and effectiveness of different control strategies applying to the same system can be carried out. In this chapter, a special routine for this is developed and programmed in the **MATLAB** environment, giving the results of the decomposition of a difference in minimum control cost index and the most beneficial (MB) control directions along which the most efficient control can be expected.

The theory and the analytical procedure are applied to the analysis of spoiler control. A balanced linear perturbation model of an aircraft -- a British Aerospace HAWK -- with the linear spoiler control input, is built up and the evaluation of the natural stability and handling quality of the aircraft at various flight states is given. Two control strategies, one using and the other not using spoiler control are defined and the MB control directions regarding to the most beneficial use of the spoilers are predicted using the theory. System responses to controls for those directions are simulated and improvements in the aircraft control efficiency (using a relative improvement function) are obtained, showing the potential effectiveness of spoilers in improving aircraft control.

3.2 Review of Linear Range Space Theory

Consider a general n-dimensional, time-varying linear state equation:

$$\dot{x} = A(t)x + B(t)u(t) \qquad (3\text{-}1)$$

where x is the $n\times 1$ state vector, u is the $m\times 1$ control vector, and A and B are $n\times n$ and $n\times m$ matrices, respectively, whose entries are continuous functions of t defined over (∞, ∞).

The analysis of the range space of (3-1) is based on the following theorems:

Theorem 1 (BROCKETT, 1970): There exists a control u(t) which drives the state of the system (3-1) from the value x_0 at $t=t_0$ to the value x_1 at $t=t_1$ if and only if $x_0-\Phi(t_0,t_1)x_1$ belongs to the range space of the matrix

$$w(t_0,t_1) = \int_{t_0}^{t_1} \Phi(t_0,t)B(t)B'(t)\Phi'(t_0,t)dt \qquad (3\text{-}2)$$

where $\Phi(t, t_0)$ is the transition matrix of $\dot{x} = A(t)x$, in that $x(t)=\Phi(t, t_0)x_0$, and is nonsingular for all t.

$w(t_0,t_1)$ is called the **Controllability Grammian**. In the time-invariant case, it has the same range and null space as the $n\times n$ matrix: $[B, AB, ..., A^{n-1}B][B, AB, ..., A^{n-1}B]'$.

In the case of a linear dynamic system being controllable, i.e. $\text{rank}[\Phi(t_0,\cdot)B(\cdot)]=n$, there are generally many different controls u that are able to transfer the state of the system from x_0 to x_1 during $[t_0, t_1]$. Among all these controls, there is an optimal control which is closely connected with the controllability grammian and the minimum energy consumed.

Theorem 2 (CHEN, 1970): If the state equation (3-1) is controllable at time t_0, then given any initial state x_0 at time t_0 and any desired final state x_1, there exists a finite $t_1(>t_0)$ and a control input $u^*(t)$ defined as:

$$u^*(t) = (\Phi(t_0,t)B(t))'w^{-1}(t_0,t_1)[\Phi(t_0,t_1)x_1 - x_0] \quad (3\text{-}3)$$

which is the unique optimal control minimizing the energy cost function:

$J=\int_{t_0}^{t_1}\|u(t)\|^2 dt$, i.e.

$$\int_{t_0}^{t_1}\|u^1(t)\|^2 dt \geq \int_{t_0}^{t_1}\|u^*(t)\|^2 dt \qquad (3\text{-}4)$$

where $u^1(t)$ is any control performing the transformation from (x_0, t_0) to (x_1, t_1).

Moreover, the optimal control for minimizing the general energy cost function

$$J=\int_{t_0}^{t_1} u'Rudt \tag{3-5}$$

with R a m×m positive definite matrix, can be found by the replacement of $u=R^{-1/2}v$ in (3-1), yielding:

$$\dot{x} = A(t)x + \overline{B}(t)v(t) \tag{3-6}$$

where $\overline{B}=(BR^{-1/2})$. Applying **Theorem 2** to (3-6) gives the optimal control of (3-1) for cost function (3-5):

$$u^*(t) = R^{-1/2}(\Phi(t_0,t)\overline{B}(t))'\overline{w}^{-1}(t_0,t_1)[\Phi(t_0,t_1)x_1 - x_0] \tag{3-7}$$

where $\overline{w}^{-1}(t_0,t_1) = \int_{t_0}^{t_1}\Phi(t_0,t)\overline{B}(t)\overline{B}'(t)\Phi'(t_0,t)dt$.

3.3 Control System Analysis Using the Range Space Theory

As an important application, the range space theory can be used for the evaluation and comparison of different control strategies. Typically for a linear dynamic system with two possible control structures, namely control structure one:

$$\dot{x}=A(t)x+B_1(t)u_1(t), \tag{3-8}$$

and control structure two:

$$\dot{x}=A(t)x+B_2(t)u_2(t), \tag{3-9}$$

the difference between the two control structures regarding the controllability and system performance can be analysed in the ways explained next.

3.3.1 Comparison of system controllability

This refers to the comparison between the range spaces $w_1(t_0, t_1)$ and $w_2(t_0, t_1)$, relating to structure one (3-8) and structure two (3-9), respectively. By calculating and comparing the dimensions of $\text{Rank}[\Phi(t_0,\cdot)B_1(\cdot)]$ and $\text{Rank}[\Phi(t_0,\cdot)B_2(\cdot)]$, or $\text{Rank}[B_1, AB_1, ..., A^{n-1}B_1]$ and $\text{Rank}[B_2, AB_2, ..., A^{n-1}B_2]$ for time-invariant cases, the 'structural' difference in controllability can be revealed.

3.3.2 Comparison of control efficiency

Further analysis and evaluation of the different control structures, when they result in the same range space measurement, i.e. when rank[$w_1(t_0, t_1)$] = rank[$w_2(t_0, t_1)$], can be made through the comparison between the minimum control costs needed for a certain transformation of the system state variables. The procedure is as follows:

1) Consider the control cost function $J=\int_{t_0}^{t_1} u'Rudt$.

2) Suppose systems (3-8) and (3-9) are controllable from $[x_0, t_0]$ to $[x_1, t_1]$, then the optimal controls of the systems can be found as:

$$u^*_1(t) = R^{-1/2}(\Phi(t_0,t)\overline{B}_1(t))'\overline{w}_1^{-1}(t_0,t_1)(\Phi(t_0,t_1)x_1 - x_0) \qquad (3\text{-}10)$$

and

$$u^*_2(t) = R^{-1/2}(\Phi(t_0,t)\overline{B}_2(t))'\overline{w}_2^{-1}(t_0,t_1)(\Phi(t_0,t_1)x_1 - x_0) \qquad (3\text{-}11)$$

where $\overline{B}_i = B_iR_i^{-1/2}$ and $\overline{w}_i = \int_{t_0}^{t_1}\Phi(t_0,t)\overline{B}_i\overline{B}_i'\Phi'(t_0,t)dt$ (i=1,2).

The values of the minimum cost functions are:

$$J_i = \int_{t_0}^{t_1}(u_i^*(t))'R(u_i^*(t))dt$$
$$= (\Phi(t_0,t_1)x_1 - x_0)'\overline{w}_i^{-1}(t_0,t_1)(\Phi(t_0,t_1)x_1 - x_0) \quad (i=1,2) \qquad (3\text{-}12)$$

3) The difference between the two cost functions can be evaluated as:

$$\Delta J_{21} = J_2 - J_1$$
$$= (\Phi(t_0,t_1)x_1 - x_0)'(\overline{w}_2^{-1}(t_0,t_1) - \overline{w}_1^{-1}(t_0,t_1))(\Phi(t_0,t_1)x_1 - x_0) \qquad (3\text{-}13)$$

For the time-invariant case:

$$u^*_i(t) = R^{-1/2}\overline{B}_i'e^{-A'(t-t_0)}\overline{w}_i^{-1}(e^{-A(t_1-t_0)}x_1 - x_0) \quad (i=1,2) \qquad (3\text{-}14)$$

where $\overline{w}_i = \int_{t_0}^{t_1} e^{-A(t-t_0)}\overline{B}_i\overline{B}_i'e^{-A'(t-t_0)}dt$ and

$$\Delta J_{21} = (e^{-A(t_1-t_0)}x_1 - x_0)'(\overline{w}_2^{-1} - \overline{w}_1^{-1})(e^{-A(t_1-t_0)}x_1 - x_0) \qquad (3\text{-}15)$$

Without loss of generality, let $t_0=0$, $t_1=T$ and $x_0=0$. Then from (3-15),

$$\Delta J_{21} = x_1' M_{21} x_1 \qquad (3\text{-}16)$$

where: $M_{21} = e^{-A'T}(\overline{w}_2^{-1} - \overline{w}_1^{-1})e^{-AT}$, i=1,2.

So, through the calculation and analysis of the control cost difference ΔJ_{21}, the advantage of using the second control structure over the first, or vice versa, with regard to the minimal control energy needed to reach x_1 from the origin, can be evaluated.

3.3.3 On the most beneficial (MB) control directions

In the case that the use of the second control structure is more effective in minimizing the control energy than the first one, i.e. in that $\Delta J_{21} \leq 0$, we can define the most beneficial control directions through the spectral form of the matrix M_{21}. In spectral form, $M_{21}=PQP'$, where Q is diagonal matrix with the eigenvalues of M_{21} along its diagonal, and where P is a matrix which columns are the associated normalized eigenvectors of M_{21}. Then the direction in which control structure 2 has the most advantage over control structure 1 is given by the nominal vector $\hat{x}_1$ which minimize $\frac{\hat{x}_1' M_{21} \hat{x}_1}{\|\hat{x}_1\|_2^2}$, i.e. by the eigenvector of M_{21} associated with the minimal most negative eigenvalue of M_{21}.

3.3.4 Programming using MATLAB

The above analysis procedure was programmed in the **MATLAB** environment. The key step involved is the calculation and decomposition of M_{21}, which can be deduced as:

$$\begin{aligned} M_{21} &= e^{-A'T}(\overline{w}_2^{-1} - \overline{w}_1^{-1})e^{-AT} \\ &= (\int_0^T e^{A\theta}\overline{B}_2\overline{B}_2' e^{A'\theta}d\theta)^{-1} - (\int_0^T e^{A\theta}\overline{B}_1\overline{B}_1' e^{A'\theta}d\theta)^{-1} \\ &= W_2^{-1}(T) - W_1^{-1}(T) \end{aligned} \qquad (3\text{-}17)$$

For stable system dynamics, $W_1(T)$ and $W_2(T)$ can be found by firstly solving the Lyaponuv equations:

$$AW_i(\infty) + W_i(\infty)A' = -\overline{B}_i\overline{B}_i' \qquad (i=1,2) \qquad (3\text{-}18)$$

and then:

$$W_i(T) = \int_0^T e^{A\theta}\overline{B}_i\overline{B}_i' e^{A'\theta}d\theta$$

$$= \int_0^\infty e^{A\theta}\overline{B}_i\overline{B}_i' e^{A'\theta}d\theta - \int_T^\infty e^{A\theta}\overline{B}_i\overline{B}_i' e^{A'\theta}d\theta$$

$$= W_i(\infty) - e^{AT}W_i(\infty)e^{A'T} \qquad (i=1,2) \qquad (3\text{-}19)$$

In **MATLAB**, the above calculation can be simply carried out by:

W1 = Lyap(A, $\overline{B}$1 * $\overline{B}$1′) − expm(A * T) * Lyap(A, $\overline{B}$1 * $\overline{B}$1′) * expm(A′ * T)

W2 = Lyap(A, $\overline{B}$2 * $\overline{B}$2′) − expm(A * T) * Lyap(A, $\overline{B}$2 * $\overline{B}$2′) * expm(A′ * T)

[P, Q] = eig(inv(W2)-inv(W1))

3.4 Linear Modelling of Aircraft with Spoiler Control

3.4.1 Small-perturbation modelling of aircraft

An aircraft model generally takes the nonlinear time-invariant form:

$$\dot{x} = f(x,u). \qquad (3\text{-}20)$$

Choosing an operating point (x_0, u_0), which represents balanced flight at a given height and velocity, we can locally (in the neighbourhood of x_0, u_0), define a linear perturbation state equation:

$$\delta\dot{x} = A_0\delta x + B_0\delta u \qquad (3\text{-}21)$$

where matrices A_0 and B_0 are constant and defined by $A_0 = \frac{\partial f(x_0,u_0)}{\partial x}$ and $B_0 = \frac{\partial f(x_0,u_0)}{\partial u}$.

So, the analysis of the controllability of an aircraft system in the form of (3-20) can be locally performed by applying the range space theory to the linear and time-invariant model (3-21).

Here, owing to our interest in the use of spoilers for the longitudinal control of aircraft, the matrices A_0 and B_0 are only modelled for the longitudinal body axes. The state vector is x=[U, γ, θ, q] and the control vector u=[u_e, u_t, u_{sp}].

The evaluation of spoiler control efficiency was conducted on a linear small perturbation model of the British HAWK aircraft. A linear form of the spoiler model described in **Chapter 2, Spoiler Model Three**, was combined with the linear aircraft model.

3.4.2 A new form of linear model for aircraft longitudinal dynamics

The standard equation of the small-perturbation longitudinal model by NELSON (1989, p126) can be rewritten in terms of the path angle by a coordinate transformation using the relationship: $\Delta\gamma = \Delta\theta - \Delta\alpha = \Delta\theta - \Delta W / U_0$, giving a new form of the model in (3-21) as:

$$\begin{bmatrix} \Delta\dot{U} \\ \Delta\dot{\gamma} \\ \Delta\dot{\theta} \\ \Delta\dot{q} \end{bmatrix} = \begin{bmatrix} X_u & -X_w U_0 & X_w U_0 - g & 0 \\ -Z_u / U_0 & Z_w & -Z_w & 0 \\ 0 & 0 & 0 & 1.0 \\ M_u + M_{\dot{w}} Z_u & -(M_w + M_{\dot{w}} Z_w) U_0 & (M_w + M_{\dot{w}} Z_w) U_0 & M_q + M_{\dot{w}} U_0 \end{bmatrix} \begin{bmatrix} \Delta U \\ \Delta\gamma \\ \Delta\theta \\ \Delta q \end{bmatrix}$$

$$+ \begin{bmatrix} X_e & X_t & X_{sp} \\ -Z_e / U_0 & -Z_t / U_0 & -Z_{sp} / U_0 \\ 0 & 0 & 0 \\ M_e + M_{\dot{w}} Z_e & M_t + M_{\dot{w}} Z_t & M_{sp} + M_{\dot{w}} Z_{sp} \end{bmatrix} \begin{bmatrix} u_e \\ u_t \\ u_{sp} \end{bmatrix} \qquad (3\text{-}22)$$

where $u_e = \Delta\delta_e, u_t = \Delta\delta_t, u_{sp} = \Delta\delta_{sp}$; U and W are the body-axis velocities; X_u, X_w, X_e, X_t, X_{sp}, Z_u, Z_w, Z_e, Z_t, Z_{sp}, M_u, M_w, M_q, $M_{\dot{w}}$, M_e, M_t and M_{sp} are the longitudinal stability derivatives.

3.4.3 Analysis of the stability and handling quality of the HAWK

The longitudinal stability and handling quality of HAWK aircraft were analysed upon the setting-up of its small perturbation equations at several chosen operating points ranging from low-altitude to high-altitude (500m~10000m) and from the low Mach number to the high Mach number (0.6~1.1).

Table 3-1 summarizes the analysis of the natural modes (the short period mode and the long period mode) of HAWK longitudinal dynamics at 6 chosen operating points. Here the setting time of the short period was estimated using the formula $t_s = 3.5/\zeta_{sp}\omega_{nsp}$ for the 5% convergency margin, and the half-decay time of the long period mode was calculated by $t_{1/2} = 0.693/|\eta|$.

Table 3-1 Analysis of HAWK longitudinal natural modes

Flight States	Short-period			Long-period		
	ζ_{sp}	ω_{nsp}	t_s (s)	ζ_p	ω_{np}	$t_{1/2}$ (s)
No.1 (h=500m, M=0.57)	0.83	2.78	1.52	0.13	0.063	84.46
No.2 (h=1000m, M=0.59)	0.81	2.75	1.57	0.13	0.062	86.31
No.3 (h=3000m, M=0.67)	0.75	2.69	1.74	0.16	0.058	73.82
No.4 (h=5000m, M=0.76)	0.68	2.61	1.98	0.14	0.054	88.74
No.5 (h=8000m, M=0.94)	0.56	2.50	2.50	undamped stable mode		
No.6 (h=10000m, M=1.09)	0.56	2.56	2.46	0.72	0.041	23.62

Comments: The evaluation of the natural modes of HAWK longitudinal dynamics shows a desirable natural stability of the aircraft throughout a wide flight envelope. This is illustrated by a distinguished separation of the two natural modes and by the first level (level-1, the best) of flight stability when the damping ratios (the Phugoid mode (ζ_p>0.04) and the Short mode (0.5<ζ_{sp}<1.3)) are concerned. (referring to MIL-F-8785c(ASG), MOORHOUSE, 1982)

The analysis of the longitudinal handling quality of HAWK was made through the evaluation of the **CAP** (control anticipation parameter) specification: CAP=$\omega^2_{nsp}/n_{z\alpha}$, which relates initial pitch acceleration to state normal load factor. **Table 3-2** is the summary of the analysis and the judgement of the handling quality levels at the selected operating points based on the specification of MIL-F-8785c(ASG).

Table 3-2 CAP analysis of HAWK

Flight States	$n_{z\alpha}$	ω^2_{nsp}	CAP	Quality Level (for the phase A flight)
No.1	20.43	7.71	0.377	level-1
No.2	20.06	7.58	0.378	level-1
No.3	19.87	7.23	0.364	level-1
No.4	17.52	6.80	0.388	level-1
No.5	12.39	6.27	0.506	level-1
No.6	23.95	6.55	0.274	level-1~2

Comments: The evaluation shows that the natural handling quality of HAWK (concerning the aircraft control without any control augmentation) is desirable in most of

its flight envelope, especially at low/medium altitude, and for the control missions including rapid manoeuvring and precise tracking (defined as the phase A flight).

3.5 Evaluation of Spoiler Control Using the Range Space Theory

3.5.1 Definition of the two control structures

To apply the previously designed analytical procedure to spoiler control, the two control structures for being evaluated are defined as:

control structure 1 -- conventional control using the elevator and thrust:

$$B_1 = \begin{bmatrix} X_e & X_t \\ -Z_e / U_0 & -Z_t / U_0 \\ 0 & 0 \\ M_e + M_{\dot{w}} Z_e & M_t + M_{\dot{w}} Z_t \end{bmatrix}; \quad u_1 = [u_e \quad u_t]' \qquad (3\text{-}23)$$

control structure 2 -- structure 1 plus the spoiler control:

$$B_2 = \begin{bmatrix} & X_{sp} \\ & -Z_{sp} / U_0 \\ B_1 & 0 \\ & M_{sp} + M_{\dot{w}} Z_{sp} \end{bmatrix}; \quad u_2 = [u_1 \quad u_{sp}]' \qquad (3\text{-}24)$$

A linear spoiler model in the form of $C_{SP}=C_{\delta s}\delta_{sp}$ was used. By referring to (2-35) ~ (2-37), the derivatives $C_{\delta s}$ for the lift, drag and moment coefficients were chosen as $C_{l\delta s}=0.35$, $C_{d\delta s}=-0.05$ and $C_{m\delta s}=-0.01$, so the entries regarding the spoiler control in (3-22) are given as

$$X_{sp}=-C_{d\delta s}QS/m, \quad Z_{sp}=-C_{l\delta s}QS/m, \quad M_{sp}=C_{m\delta s}QS\bar{c}/I_{yy} \qquad (3\text{-}25)$$

3.5.2 General conclusions

According to the definition and notation of **3.3**, there are some general conclusions relevant to spoiler control.

1. Controllability: The range space for the first control scheme is a subset of that for the second control ($B_2=[B_1, b_{sp}]$). Therefore rank[A AB_2 A^2B_2 .... $A^{n-1}B_2$] $\geq$ rank[A

$AB_1\ A^2B_1\ ....\ A^{n-1}B_1]$. This is also applicable for to $\bar{B}_1$&$\bar{B}_2$ of (3-10), (3-11), where

$$R_2=\begin{bmatrix} R_1 & 0 \\ 0 & r_{sp} \end{bmatrix}.$$

2. Control Efficiency: For $T > 0$ and $[A, \bar{B}_1]$ being controllable, we have $M'_{21} = M_{21} \le 0$, so

$$\Delta J_{21} = x'M_{21}x \le 0, \quad \forall x. \tag{3-26}$$

Proof: From (3-17) and using the fact for a matrix A that $(A')^{-1}=(A^{-1})'$, it is easy to verify that:

$$M_{21}' = [(\int_0^T e^{A\theta}\bar{B}_2\bar{B}_2' e^{A'\theta}d\theta)']^{-1} - [(\int_0^T e^{A\theta}\bar{B}_1\bar{B}_1' e^{A'\theta}d\theta)']^{-1}$$
$$= M_{21}$$

Let: $W_1 = \int_0^T e^{A\theta}\bar{B}_1\bar{B}_1' e^{A'\theta}d\theta$, $W_2 = \int_0^T e^{A\theta}\bar{B}_2\bar{B}_2' e^{A'\theta}d\theta$

where $\bar{B}_2 = [\bar{B}_1, \bar{b}_{sp}]$. Then:

$$W_2 = \int_0^T e^{A\theta}\bar{B}_2\bar{B}_2' e^{A'\theta}d\theta$$
$$= \int_0^T e^{A\theta}\bar{B}_1\bar{B}_1' e^{A'\theta}d\theta + \int_0^T e^{A\theta}\bar{b}_{sp}\bar{b}_{sp}' e^{A'\theta}d\theta$$
$$= W_1+\Delta W_2$$

where $\Delta W_2 = \int_0^T e^{A\theta}\bar{b}_{sp}\bar{b}_{sp}' e^{A'\theta}d\theta$.

Clearly, $\Delta W_2' = \Delta W_2 \ge 0$. Since $[A, \bar{B}_1]$ is controllable, we have $W_1'=W_1 > 0$. Thus from $W_2=W_1+\Delta W_2$, it follows that $W_2'=W_2 > 0$.

So (3-17) can be written as:

$$M_{21}=(W_1+\Delta W_2)^{-1} - W_1^{-1}$$

The Matrix Inversion Lemma (GOLUB & VANLOAN, 1989, p51) gives:

$$(A+UV')^{-1}=A^{-1} - A^{-1}U(I+V'A^{-1}U)^{-1}V'A^{-1}$$

Since $\Delta W_2' = \Delta W_2 \geq 0$, we can factorize ΔW_2 as UU' for some matrix U. Therefore:

$$W_2^{-1}=(W_1+UU')^{-1}$$
$$=W_1^{-1}-W_1^{-1}U(I+U'W_1^{-1}U)^{-1}U'W_1^{-1}$$

so

$$M_{21}=W_2^{-1}-W_1^{-1} = -W_1^{-1}U(I+U'W_1^{-1}U)^{-1}U'W_1^{-1}.$$

Since $(I+U'W_1^{-1}U) > 0$, we have $(I+U'W_1^{-1}U)^{-1} > 0$. Therefore, since $M'NM \geq 0$, if $N > 0$:

$M_{21} \leq 0$. **(End of Proof)**

In view of (3-26), the manoeuvre involving moving to x_1 at t_1 from the origin (i.e. $x_0=0$) at time 0 will exploit spoiler most control efficiency when x_1 is an eigenvector of M_{21} corresponding to the minimal eigenvalue of M_{21}. Here 'most control efficiency' refers to the minimal control energy consumption.

3.5.3 Controllability evaluation

Using **MATLAB**, the controllability grammians of the selected flight states were verified, showing that for all the evaluated operating points:

$$\text{Rank}[B_1\ AB_1\ A^2B_1\ A^3B_1] = \text{Rank}[B_2\ AB_2\ A^2B_2\ A^3B_2] = 4 \qquad (3\text{-}27)$$

i.e. there is no change in the longitudinal controllability from the structural difference due to the use of spoilers. This is also a general conclusion for an aircraft dynamics modelled as (3-22) and applicable for the whole flight envelope, while without imposing control constraints on the conventional controls -- elevator and thrust.

3.5.4 Control efficiency improvement using spoilers

This is concerned with the evaluation of spoiler control in the improvement of control efficiency of the HAWK aircraft, i.e. in the reduction of the control costs for the two-point manoeuvring of the aircraft. The evaluation employed the analytic procedure described in **3.3** and centred on the issues of the analysis of the most beneficial control directions of the spoilers and the analysis and comparison of the controls and motions of the aircraft along the MB directions.

Here is an example based on the analysis for the flight about the operating point of H_0=5000m, Mach=0.76 and with the following model matrices:

$$A_0 = \begin{bmatrix} -0.016 & -6.6533 & -3.1537 & 0.0 \\ 0.0003 & -0.0722 & 0.0722 & 0.0 \\ 0.0 & 0.0 & 0.0 & 1.0 \\ 0.005 & 4.77 & -4.77 & -2.81 \end{bmatrix}; \quad B_0 = \begin{bmatrix} 0.0 & 2.8 & 3.772 \\ 0.0 & 0.0 & 0.111 \\ 0.0 & 0.0 & 0.0 \\ -14.639 & 0.0 & -0.162 \end{bmatrix}.$$

The most beneficial control directions: Table 3-3 summarizes the most negative eigenvalues $\lambda_{min}(Q)$ and the corresponding eigenvectors $\bar{P}_{min(\lambda)}$ from the decomposition of the M_{21} in (3-17), for different time duration T, where for small perturbations, there is $\Delta V \approx u$ and P_V, P_γ, P_θ and P_q represent the respective components of the unit vector $\bar{P}_{min(\lambda)}$ in the V, γ, θ and q directions, respectively.

The weighting matrix R is defined by referring to the constraints on the deflection angles and rates of the elevator and spoilers (see **Appendix One** for the data):

$$R = \begin{bmatrix} 100.0 & & \\ & 1.0 & \\ & & 1.0 \end{bmatrix} \qquad (3\text{-}28)$$

Table 3-3 Analysis of the most beneficial control directions

T	$\lambda_{min}(Q)$	$\bar{P}_{min(\lambda)}$			
		P_V	P_γ	P_θ	P_q
0.1	-6.91×10^7	0.0000	0.9994	-0.0353	0.0006
0.5	-2.94×10^4	0.0000	0.9870	-0.1600	0.0128
1.0	-1.16×10^3	0.0042	0.9619	-0.2703	0.0400
2.0	-84.48	0.0185	0.9403	-0.3340	0.0633
5.0	-46.36	0.0152	0.9304	-0.3604	0.0682
10.0	--33.58	0.0077	0.9109	-0.4054	0.0765
50.0	-9.57	0.0002	0.7762	-0.6233	0.0953
100.	-8.49	0.0002	0.7539	-0.6500	0.0966

Since $\Delta J_{21} = (Px)'Q(Px)$, it follows that $\lambda_{min}(Q)$ represents the maximum control cost reduction allowed by using spoilers when x_1 has unit norm, i.e. $\lambda_{min}(Q) = \text{Min.}(\Delta J_{21}\big|_{\|x_1\|=1})$. By **Table 3-3**, this value is strongly dependent of the time duration T and decays sharply as T increases, indicating the time-dependant feature of the spoiler use

for the control cost saving and suggesting that, as might have been expected, the use of spoilers is most beneficial for the rapid manoeuvres. This point can be further verified through the evaluation of the relative improvement function ΔJR_{min} which is defined as:

$$\Delta JR_{min} = \frac{\Delta J_{21}}{J_1}\Big|_{x=\bar{P}min} = \frac{\lambda_{min}}{\bar{P}'_{min} w_1^{-1} \bar{P}_{min}} \qquad (3\text{-}29)$$

i.e. the ration of the maximum cost saving using the spoiler vs the cost would-be when using the conventional controls, along the most beneficial unit vector $\bar{P}_{min}$. The curve (a) in **Fig. 3-1** is ΔJR_{min} vs T for the nominal spoiler model which clearly shows a nearly 50% loss in the efficiency at T=2.5s compared with that at T=0.1s.

Table 3-3 also lists the corresponding MB directions while **Fig. 3-2** shows the variation of the MB directional vector with T in the major component γ-θ plane. It can be seen that as the state variables are equally weighted and the focus is on the short period time-domain, i.e. $T<t_s$, the vector $\bar{P}_{min}$ is dominated by the component of the vector in the γ direction, showing that the improvement using spoilers would be greatest for changing the flight path angle. Considering that the change of the path angle is closely connected with the height change of an aircraft ($\dot{H} = V \sin\gamma$), it is concluded that spoilers as modelled as (3-26) can be profitable and efficient for the longitudinal trajectory control of the aircraft. Also from the data, as T increases, the MB direction tends towards the θ direction, showing the beneficial use of the spoilers for attitude control when T is long.

A brief study on the effects of the spoiler coefficient modelling was conducted: following the above conclusion and considering that the vertical trajectory change of a balanced flight would be always associated with the lift change, it is easy to understand that the lift coefficient C_{LSP} plays a key role in the MB control usage. This can be verified by looking at the curve (b) in **Fig. 3-1** where the relative efficiency regarding the use of a higher lift coefficient gain, $C_{l\delta s}$=0.7, which was same as that of the whole-span spoiler model (2-28), is presented, showing a significant increase in the control efficiency. While the influence of the spoiler drag coefficient in the MB control can be seen by comparing the curve (c) in **Fig. 3-1** with $C_{d\delta s}$=0 (no spoiler drag effect) with the curve (a) from the nominal data, showing an increase in the control efficiency due to the drag effect. It is interesting to notice that the increase is mainly from $T > t_s$, i.e. after the short period of the aircraft, showing that while beyond the short period, the control efficiency is increasingly (with a period) associated with the thrust control saving and,

therefore, the spoiler drag coefficient could be helpful in the increase of the control efficiency through reducing the thrust control cost.

The variation of the spoiler control efficiency with the flight conditions was investigated through the evaluation of $\Delta JR_{min}(T)$ for different operating points. **Fig. 3-3** shows the comparison of the three typical curves (a), (b) and (c) for medium, high and low altitudes, respectively. It is notable that the spoiler has a higher control efficiency while acting at high altitude than at low and medium ones. **Fig. 3-4** shows the γ-θ variation pattern of the MB vector for the high altitude (h=10000m), comparing it with **Fig. 3-2** (h=5000m), it shows that the MB direction seems to be increasingly dominated by γ component as the height increases. These suggest that the use of spoilers for the trajectory control of HAWK at higher altitude could be more effective than at low/medium altitudes.

3.6 Simulations of Flight Control along MB Directions

The controls along the MB direction are given by (3-14), as follows:

Control construct one:

$$u_1=\overline{B}_1' e^{A(-t)}\overline{w}_1^{-1}e^{A(-T)}\overline{P}_{min} \qquad (3\text{-}30)$$

Control construct two:

$$u_2=\overline{B}_2' e^{A(-t)}\overline{w}_2^{-1}e^{A(-T)}\overline{P}_{min} \qquad (3\text{-}31)$$

where: $\overline{w}_i=e^{-AT}W_ie^{-A'T}$. (i=1,2)

The system (3-22) responses to the control (3-30) and (3-31), respectively, were simulated using **MATLAB** and utilised the following discrete equation:

$$x_{k+1}=Fx_k+Gu_k \qquad (3\text{-}32)$$

where F and G were the system matrices derived from the discrete of the extended matrix A_h:

$$\dot{\tilde{x}} = A_h\tilde{x} \qquad (3\text{-}33)$$

where $\tilde{x}=[x,u]'$, $A_h = \begin{bmatrix} A & B \\ 0 & 0 \end{bmatrix}$.

Simulation was made upon the selected operating point of h_0=5000(m). **Fig. 3-5** and **Fig. 3-6** compare the control u_e and u_t from the two control structures, respectively, in driving the system from the original point to the final state $x_f=\bar{P}_{min}$=[0.0015, 0.09304, -0.03604, 0.0682]' during T=5 (s). As shown in the figures, with the aid of the spoiler control in the γ-dominated MB direction, demands for the conventional controls are substantially reduced (60% reduction in the peak-peak value of u_e and 90% reduction in u_t).

Fig. 3-7, **Fig. 3-8** and **Fig. 3-9** give the time-history sketches of the state variables γ, θ and ΔV, respectively. Comparison between those with and without spoiler control in these variable transformations reveals an important aspect of spoiler control in the MB direction: the improvement in the flight stability. This is clearly shown in the figures with the advantage of the spoiler aided control in suppressing dynamic overshot (50% overshot reduction in γ, 30% in θ and 50% in ΔV) and smoothing the process of the dynamic responses.

3.7 Concluding Remarks

Following the previous chapter on the modelling of a generic spoiler, this Chapter concentrated on the analysis of spoiler control effectiveness using linear techniques based on range space theory, to give some primary and qualitative judgements and guide-lines concerning the use of spoilers.

An analytical procedure for the analysis and comparison of different control structures applied to same plant was developed. It was realized through an appropriate algorithm written in the **MATLAB** environment and was applied to spoiler control. It enabled the evaluation of the use of spoiler control for the enhancement of aircraft control efficiency concerning control cost minimization. This application has shown the success of the method in the primary analysis of control structures and suggested its further and wide use in many similar cases concerning the comparison and choice of different control strategies for cost minimization.

The evaluation of spoiler control was done with a linear model of the HAWK. It has revealed that the most beneficial control directions would be mostly dominated by the γ-component, i.e. by the trajectory angle of the aircraft, and that use of the spoilers in the

most beneficial directions for two-point manoeuvres should be within a short time duration, e.g. $T<t_s$, for most efficient control. These conclusions are closely in accord with the intuitive expectation that what spoilers are good at is the providing of rapid force variation.

Details on the evaluation of the natural stability and handling quality of the HAWK were given, and showed a desirable aircraft behaviour in most of the flight envelope. Even so, significant improvement in flight dynamic responses was achieved while spoiler control and the conventional controls were jointly applied in the most beneficial control directions. This indicated that the use of spoilers could be not only efficient in energy saving, but also effective in the control augmentation.

Of course, application of the range space theory to the spoilers is based on the linear perturbation model of the aircraft, which is valid only near the linearization point and under the assumption of no constraint on the use of the control resources. This limits the application of the theory for the further analysis of spoiler control, for which nonlinear theory and techniques are really required.

Figure 3-1 Δ JRmin vs T (state no. 4)

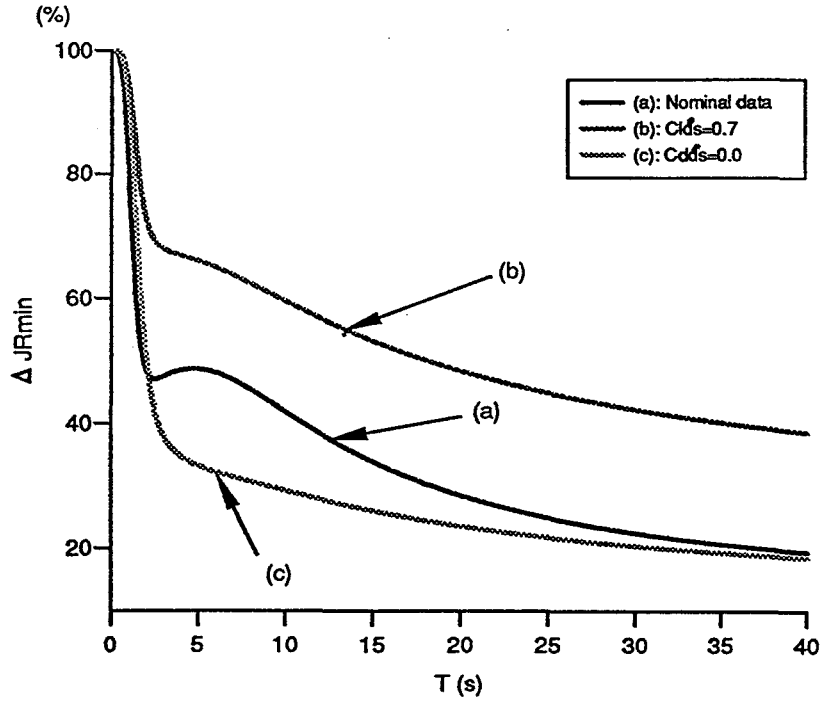

Figure 3-2 MB direction vs T (h=1000m)

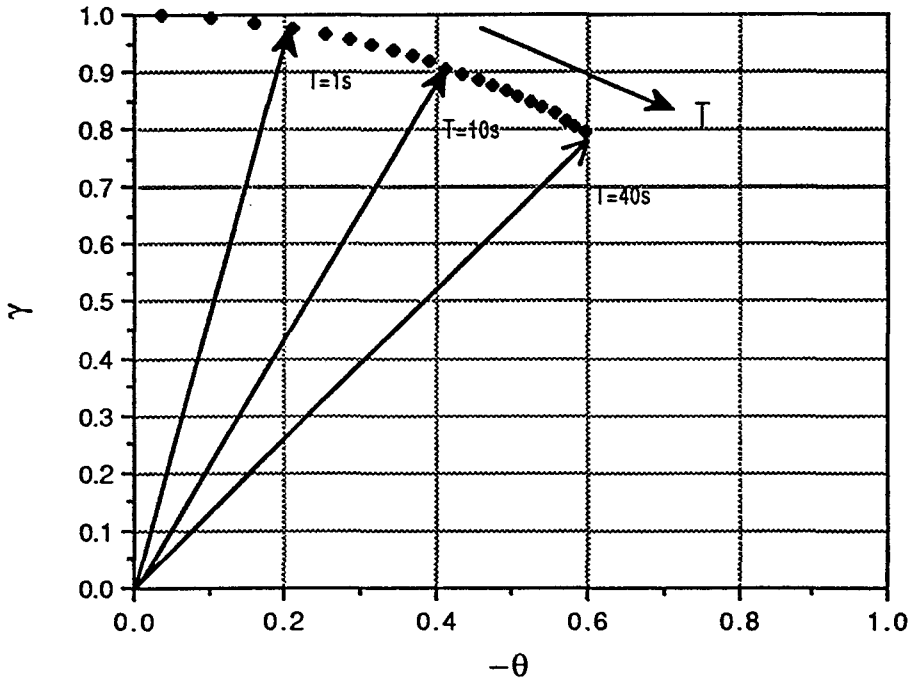

Figure 3-3 Comparison of ΔJRmin(T) at different states

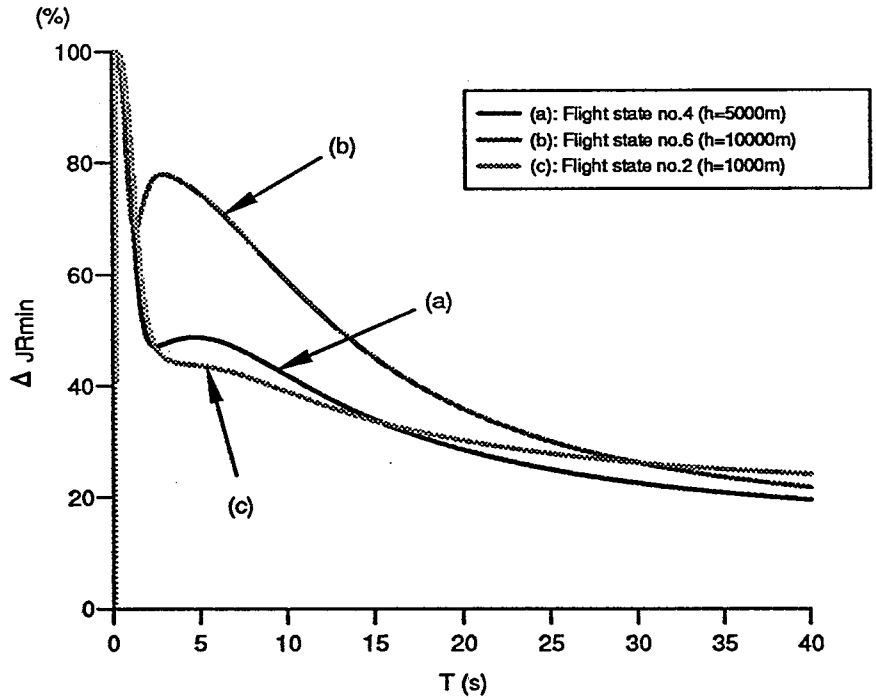

Figure 3-4 MB direction vs T (h=10000m)

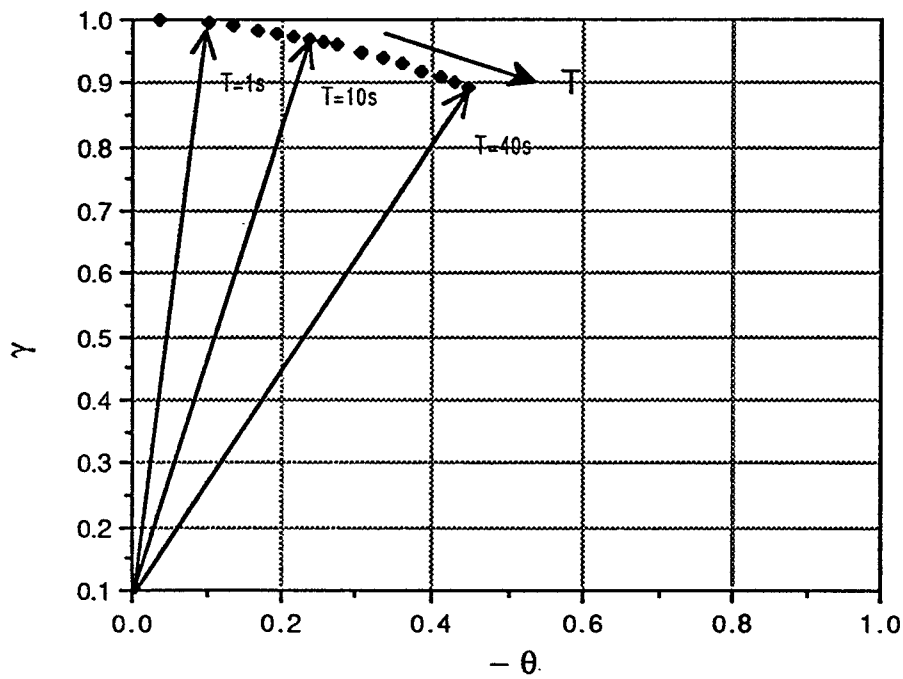

Figure 3-5 Comparison of optimal Ue in MB direction

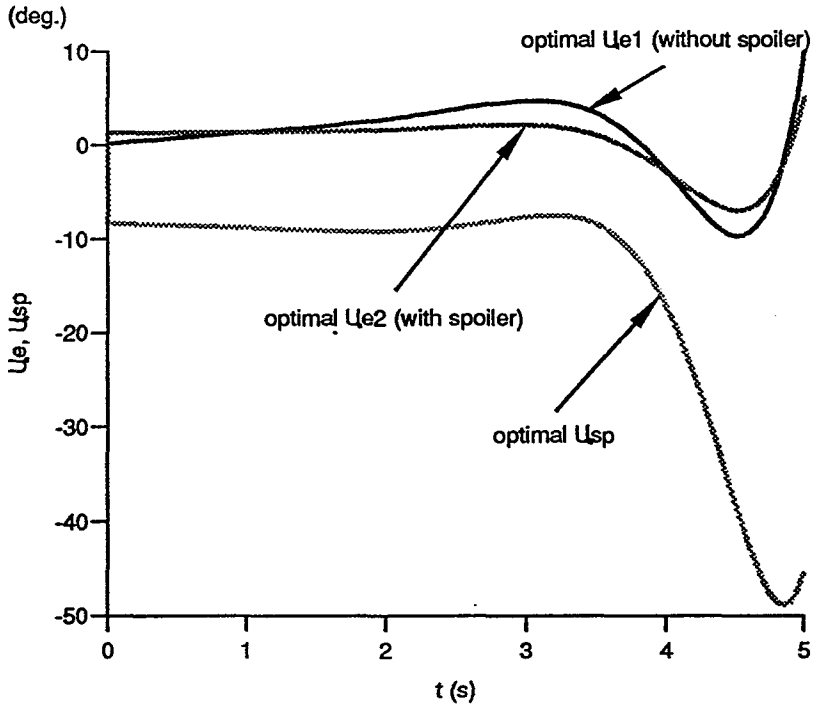

Figure 3-6 Comparison of optimal Ut in MB direction

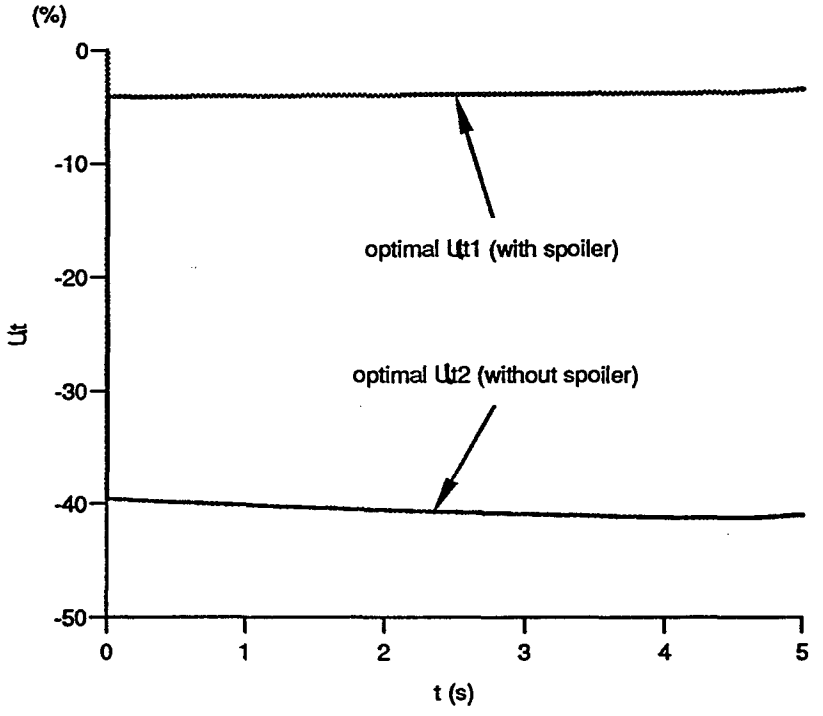

Figure 3-7 Comparison of path angle trackings in MB direction

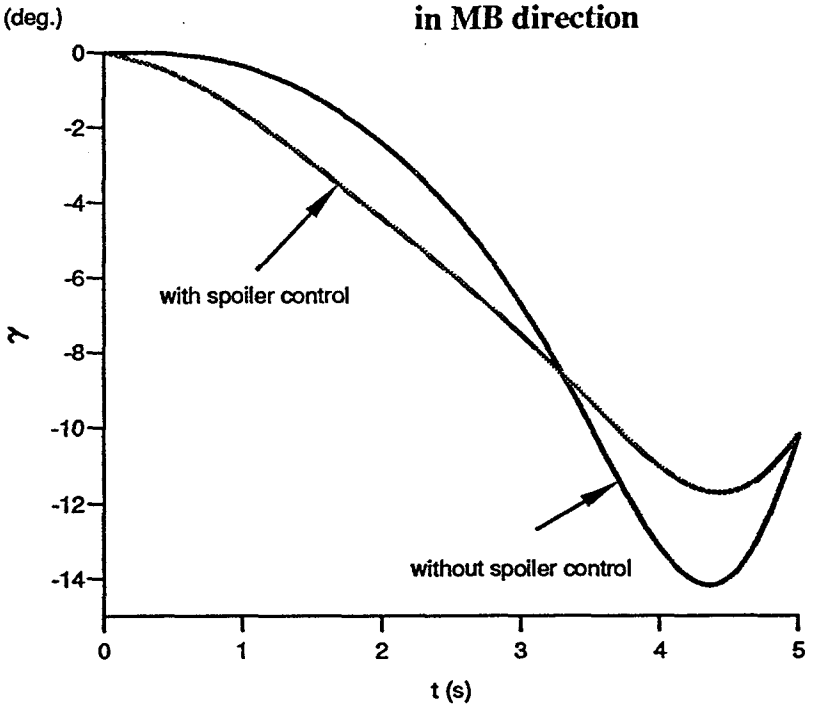

Figure 3-8 Comparison of pitch angle responses in MB direction

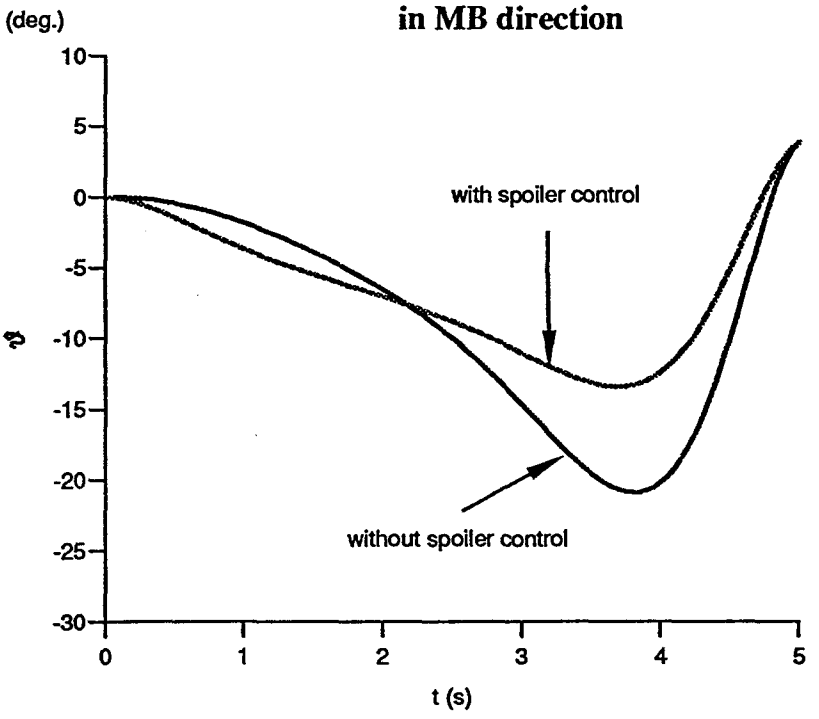

Figure 3-9 Comparison of path velocity changes in MB direction

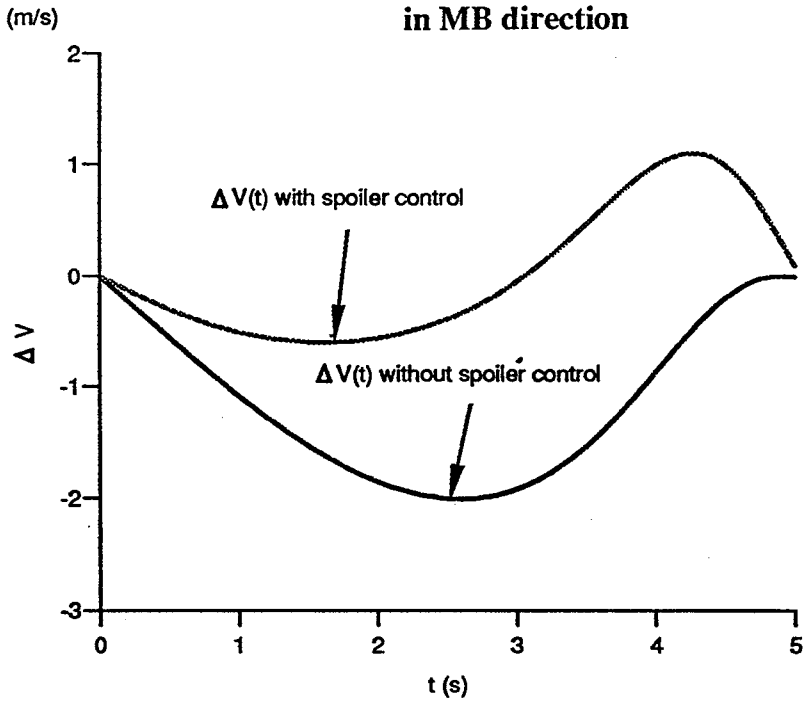

Chapter Four

SIMULATOR AND OPTIMAL CONTROL OF NONLINEAR AIRCRAFT USING SPOILERS

4.1 General Remarks

The theme of this chapter is the simulation and optimal control of nonlinear aircraft utilising spoilers. In contrast, yet also in conjunction, with the last chapter's discussions of the analysis of the linear aircraft and spoiler systems, work here is centred on the analysis and open-loop control of nonlinear aircraft and spoiler systems. These enable the evaluation and the further understandings of spoiler control and its role in the enhancement of aircraft manoeuvres.

A six-degrees of freedom flight simulator is the basis for the simulation study of aircraft nonlinear flight. In this chapter, a specified aircraft simulator (computation-based) for British Aerospace HAWK is described. The simulator is based on the previous works of HERD (1985) and PESMAJOGLOU (1989) in this area and has included many useful functions from this study for more sophisticated flight simulations and for the use of spoiler control.

For optimal control studies, the first-order gradient algorithms utilising **Armijo** iteration procedure for the solution of two-point boundary-value problems were studied. A program package based on the method was developed and applied to the design of open-loop control of the aircraft manoeuvring between two fixed points. Combining the study with the spoiler control, the effectiveness of spoilers for the enhancement of aircraft manoeuvres was further evaluated and demonstrated in a series of simulations concerning descent flight control.

4.2 The HAWK Aircraft

The British Aerospace HAWK was originally designed to an RAF requirement for a two-seat all-through jet trainer. Its first flight was in 1974 and the first type MK.1 entered service in 1976. Since then, various versions of the HAWK have been designed and put into service, signifying it as one of the most successful aircraft developed in Britain. Its latest single-seat variant, the Hawk 200 (see **Fig. 4-1(a)** for the main features) in the late 1980s promises, with the adoption of state-of-the art avionics, to extend the role of the transonic fighter into the next century.

The HAWK parameters and aerodynamic coefficients used in this study referred to the data of the Hawk 60 trainer, provided by HERD in his project report. A three-dimensional diagram of the aircraft is shown in **Fig. 4-1(b)**.

4.3 Development of Digital Flight Simulator

A digital simulator program written in standard FORTRAN was developed for the 6-degree flight simulation of the aircraft. The inputs to the system range from a given aircraft database, disturbances, programmed controls to pilot commands, and the outputs may be any system variables of interest. The basic configuration of the simulator was designed by HERD and later expanded by PESMAJOGLOU. Contributions from this study to this simulator have included:

1. Modification of the simulation configuration and the data input/output.
2. Introduction of multi-modes control simulation.
3. Introduction of spoiler control function (for linear & nonlinear spoiler models)
4. Simulation of aircraft 'pre-stall' and 'stall' flight.
5. Simulation of fly-in-atmospheric disturbance --- turbulence/gust and wind shear.

Fig. 4-2 is the major block diagram of the simulator. There are three major parts:

1. **Flight Simulation Commands**: control and simulation mode setting.
2. **Flight Control**: control modelling and the generation of airframe force and moment.
3. **Aircraft Motion Equations**: calculation of aircraft motion variables and system auxiliary variables (e.g. the direction cosines and Euler angles)

Fig. 4-3 shows the decentralized diagram of the flight control block.

Fig. 4-4 is the flow chart of the simulation package 'HAWKSIM1', which was constructed by connecting the database for the HAWK with the simulator. The major steps involved in the simulation procedure are: the initiation and trimming of the system, the definition of simulation modes and control inputs, the computation of system auxiliary variables, the computation of aircraft forces and moments, and the computation of rotation and translation motions. **Fig. 4-5** Shows the flow chart of the core subroutine 'SOLVEQ' for the solution of aircraft equations, it consists of consequent calls to other subroutines

for the calculation of aircraft equations and the update of system variables. The communication, i.e. the exchange of input and output variables and parameters, between different subroutines is by two large-scale COMMON blocks. The aircraft data is stored in nine data files.

For all the simulation cases, the aircraft is originally trimmed to follow a level, steady flight path, with all control surfaces at neutral positions. The trim-flight is provided by the balance settings of the throttle and the zero-α lift of the wing.

The simulator programs were written in standard FORTRAN 77 on the main frame (CDC-CY960/VE960) of Imperial College Computer Centre and later fitted into Sun work stations and Silicon Graphics work stations. The choice of simulation language was dictated by the possible ultimate use of parallel FORTRAN on a transputer system. (the Meiko Computing Surface)

4.4 Aircraft Handling Simulation --- without Spoilers

The simulator described above was firstly tested for various kinds of flight and control cases, based on the HAWK aircraft database, for establishing the validity of the digital representation of the system. Then, it was used for spoiler control studies.

The separation of the aircraft motions into the longitudinal and lateral groups in the simulator assumes that there are no coupling effects between the longitudinal and lateral modes. In the simulations of the longitudinal control, where spoilers are expected to be very useful, the control inputs are the elevator(δ_e), thrust(δ_t) and spoilers(δ_{sp}), and the system state variables of interest include flight height(H), flight path velocity(V), flight path angle(γ), aircraft pitch angle(θ), incidence angle(α) and the normal acceleration A_{nz}.

4.4.1 Simulation one -- small stick input

The characteristics of the short period motion of the aircraft were investigated by studying the short-time response of the aircraft to small control inputs. **Fig. 4-7** presents an example of the aircraft response to a -1.0 degree (upwards) of elevator control in 5 seconds, initiating from balanced flight at H_0=5000(m) and V_0=237(m/s). Evaluation of the time histories of the variables α and q bring the estimated setting time t_s of about 2.0(s) and a desirable damping ratio (see α, $\zeta \approx 0.7$). This is in consistent with the previous analytic results in **Chapter 3** based on small-perturbation principles. Also, in **Fig. 4-7**, a consequence change in the angular variables, from q to θ (moment), then to α and γ (force), can be clearly observed.

4.4.2 Simulation two --- manoeuvring

The nonlinearity of an aircraft exists in the dynamic equations and is closely connected with flight condition. This can be shown through the following simulation of a constant-g manoeuvre control.

The manoeuvre of the HAWK with a large and sustained control was simulated by applying a large amount of elevator control (δ_e=-6.0°) to the aircraft for 40 seconds, resulting in an oval shaped flight trace in the H-X plane (see **Fig. 4-8(a)**). **Fig. 4-8(b)** shows the time history of the path velocity V undergoing a considerable variation (up to 60% from the balanced value), caused by high-α drag and the variation in the respective gravity due to the attitude change (see **Fig. 4-8(c), (d)** for the variations in θ and α). These demonstrate the typical nonlinearity of an aircraft corresponding to large and sustained controls and manoeuvres, where the small-perturbation based linear methods (with V assumed constant and the angular variables varying within small regions) would no longer be applicable.

4.5 Aircraft Handling Simulation --- with Spoilers

The aim of spoiler control simulations is to look at the behaviour of the generic spoilers, as modelled in **Chapter 2** (2-31 ~ 2-37), while combined with the nonlinear HAWK model. The objectives include the validation of the most beneficial use of spoiler control and the evaluation of its nonlinear effects.

4.5.1 Sole spoiler control

Sole spoiler control was studied by applying a pure spoiler control to a balanced aircraft and keeping other controls constant. A simulation in this aspect is demonstrated in **Fig. 4-9** where the spoiler control was a step deflection of -60.0° (upwards) and the simulation time was 20 seconds. Both the nonlinear and linear spoiler models, based on the **Spoiler Model One** and **Spoiler Model Three** from **Chapter 2**, were applied.

The trajectories (flight height H vs distance X) of the aircraft gravity centre are in **Fig. 4-9(a)** which shows the typical motion pattern resulting from the sole open-up spoiler control to a balanced level-off flight: **descent and deceleration**. The effects of the linear and nonlinear spoiler controls are compared and the nonlinear effects are characterized by the sharper sloped descent trajectory, an increase in the final descent height ΔH_f=500(m) and a decrease in the final ground distance ΔX=400(m).

Fig. 4-9(b) shows the time histories of the angle variables α, γ and θ from the nonlinear spoiler control. Comparing the variation patterns of these variables with that previously shown in **Fig. 4-7(a)** using the conventional elevator control, it can been seen that in the spoiler control, the consequence change in the angular variables becomes: $\gamma \rightarrow \alpha \rightarrow \theta$. This therefore further verifies the conclusion of **Chapter 3** that the spoiler, due to its direct force, has a direct and effective control on the path angle γ, which, in turn, brings fast variation in the flight trajectory.

4.5.2 Effects of spoiler moment coefficient C_{MSP}

Combined with the spoiler simulation, an investigation was made into the effects of spoiler moment coefficient, C_{MSP}, on the spoiler control effectiveness. This was done through repeatedly applying a fixed sole spoiler control (δ_{sp}=-30°), with the moment coefficient adopting a different value each time, to the same balanced flight.

Fig. 4-10 shows the simulation of the descent controls corresponding to the gain of the C_{MSP}, K_m, varying from -0.05 to 0.0, with a step of 0.005. According to the analysis in **Chapter 2** on the effect of spoiler hinge line location, the variations could be seen as the results from the parallel shifting of the spoiler hinge line from a rear position on wing surface forwards to a point close to the aerodynamic centre where the moment effect becomes negligible.

The simulation reveals that, along with an increase in the spoiler moment coefficient C_{MSP} ($|K_m|\uparrow$), there is a decrease in the spoiler γ control (**Fig. 4-10(b)**) and therefore a decrease in the descent ability (**Fig. 4-10(a)**), eventually as the coefficient gain reaches a certain value (k_m=-0.045 in the HAWK case), the spoiler may entirely change its nature as a 'lift dumper' and becomes a lift-aid device instead. This is mainly owing to the fact that as C_{MSP} increases, there is an increase in the positive moment, which in turn brings a delayed positive lift that counters, and even eventually exceeds, the negative lift from the spoiler lift coefficient C_{LSP}. Clearly, this suggests that for efficient descent control of aircraft utilising spoilers, the moment coefficient should be ideally confined, by carefully adjusting the spoiler hinge location, to a small value.

4.5.3 Joint elevator-spoiler control

Finally, **Fig. 4-11** presents a simulation concerning a fast climbing-up and circling manoeuvre, under an joint elevator-spoiler control The simulation conditions were same as that of **4.4.2** except the input was joined by a -20° spoiler control. The flight trajectories in H-X plane, relating to the controls of the sole elevator, the elevator plus the linear spoiler and the elevator plus the nonlinear spoiler, respectively, are shown in **Fig. 4-11(a)**, and the

comparisons of the time histories of H and X can be found in **Fig. 4-11(b)** and **Fig. 4-11(c)** , respectively. It can be seen from these diagrams that while the whole manoeuvre is still dominated by the elevator control, the spoiler control does bring some negative effects in the climbing-up manoeuvre phase with the typical 'lag' phenomena in H and X which causes the increase of the climbing circle radius (see **Fig. 4-11(c)**), and therefore the loss of the position superiority.

The spoiler modelling effects were also shown by the simulation. **Fig. 4-11(d)** and **Fig. 4-11(e)** compare the differences between the values and variations of the coefficients C_{LSP}, and C_{DSP} and C_{MSP}, respectively, associated with the linear and nonlinear modelling cases. In particular, the effects of the high incidence angle and its variation, resulting from large and violent manoeuvres of an aircraft, on the nonlinear spoiler model can be observed (see the considerable variations in the nonlinear coefficients C_{LSP}, C_{DSP} and C_{MSP}). As demonstrated in **Fig. 4-11(a)**, the effects of the modelling differences on aircraft control can be significant.

4.6 Design of An Open-Loop Optimal Flight Control System

From previous analyses, it is clear that the most effective use of the spoiler is for trajectory control. In view of the control constraint on the spoiler's deflection (the angle can not change sign within its effective range) and for the efficient use of spoilers, there is the need to look at appropriate applications and to seek an effective nonlinear system design for spoiler control.

Among the features of conventional spoiler control, the use of spoilers for the manoeuvre enhancement for an aircraft descending from one level balanced flight to another was considered to be a good application. In this section, a Hamiltonian-based optimal control was applied to the synthesis of open-loop flight controllers aiming to enhance the control of aircraft descent using spoilers. In the aspect of the numerical solution to the problem, a modified first-order gradient algorithm was studied and applied.

4.6.1 Basic theory review of two-point boundary optimal control

A general two-point boundary optimal control problem can be described as: find the optimal control u^* for driving a dynamic system

$$\dot{x} = f(x,u,t) \qquad (4\text{-}1)$$

through a trajectory from the given initial state $x(t_0)$ to the final state $x(t_f)$ so as to minimise the index function:

$$J = \Phi[x(t_f)] + \int_{t_0}^{t_f} L[x(t), u(t), t]dt \qquad (4\text{-}2)$$

Here Φ is the weighting function for the final states which depends on the final state x_f and time t_f. L is the weighting function for the states and inputs over $[t_0, t_f]$. There is a fixed terminal time and there are no hard terminal constraints. The approach to the problem can be found through the **Hamiltonian minimisation principle** which is summarized here:

1) Define the Hamiltonian function H as:

$$H = L[x(t), u(t), t)] + \lambda'(t) f[x(t), u(t), t)] \qquad (4\text{-}3)$$

where $\lambda(t)$ is the co-state vector.

2) Apply the **calculus of variations** to (4-2) and (4-3) to yield the joint co-state equation:

$$\dot{\lambda} = \frac{\partial H}{\partial x} = -\frac{\partial f'}{\partial x}\lambda - (\frac{\partial L}{\partial x})' \qquad (4\text{-}4)$$

and the stationary condition for the optimal control u^*:

$$\frac{\partial H}{\partial u} = 0 \qquad \text{i.e.} \qquad (\frac{\partial f}{\partial u})'\lambda + (\frac{\partial L}{\partial u})' = 0 \qquad (4\text{-}5)$$

3) Substitute u^* satisfying (4-5) into (4-1) and (4-4) and use the split boundary condition $x(t_0)=x_0$ and $\lambda(t_f)=(\frac{\partial \Phi}{\partial x})'$ to give the following two-point boundary value problem which defines the optimal trajectory x^* and the optimal control u^*.

A suitable index function (4-2) for trajectory tracking control can be

$$J = \frac{1}{2}(x(t_f) - x_{tf})'QF(x(t_f) - x_{tf}) + \frac{1}{2}\int_{t_0}^{t_f}((x(t) - x_d(t))'Q(x(t) - x_d(t)) + u'(t)Ru(t))dt \qquad (4\text{-}6)$$

where R is a mxm positive definite matrix and Q and QF are nxn semi-positive definite matrices; x_{tf} are the final target states; $x_d(t)$ are the desirable state trajectories designed according to control objectives and constraints.

In general, the **Jacobians** $\frac{\partial f}{\partial x}$ and $\frac{\partial f}{\partial u}$ depend on the control u(t) so that (4-5) is an implicit equation for u(t). In the cases when $\frac{\partial f}{\partial u}$ is independent of u(t), as in some simplified aircraft systems, from (4-5) and (4-6) we have:

$$u = -R^{-1}(\frac{\partial f}{\partial u})'\lambda \tag{4-7}$$

This formula for u can be substituted in state equation (4-1) and in co-state equation (4-4), yielding a nonlinear ordinary differential equation in x(t) and λ(t) of order 2n:

$$\begin{aligned} \dot{x} &= f(x, -R^{-1}(\frac{\partial f}{\partial u})'\lambda, t) \\ \dot{\lambda} &= -(\frac{\partial f}{\partial x})'\lambda - Q(x - x_d) \end{aligned} \tag{4-8}$$

with the boundary conditions

$$x(t_0)=x_0 \qquad \text{and} \qquad \lambda_f = QF(x(t_f) - x_f) \tag{4-9}$$

However, for most flight control problems with complicated nonlinearities and dynamics, it is impossible to get unified and explicit solutions for the above nonlinear, time-variant differential equations.

4.6.2 Control modelling of the HAWK

The nonlinear longitudinal model of HAWK can be found in **Appendix One** with the state variables x are: x=[V, γ, α, q, θ, H]' and the control variables: u=[δ_e, δ_t, δ_{sp}]'. The state equation is time-invariant and takes the following form:

$$\dot{x} = A(x) + B(x)u \tag{4-10}$$

where u(t) enters linearly because the second nonlinear form of the generic spoiler model (2-32 ~ 2-24) was used. From (4-10) and (A-12):

$$\frac{\partial f}{\partial x} = \frac{\partial A(x)}{\partial x} + \frac{\partial b_e(x)}{\partial x}\delta_e + \frac{\partial b_t(x)}{\partial x}\delta_t + \frac{\partial b_{sp}(x)}{\partial x}\delta_{sp} \tag{4-11}$$

and $u = -R^{-1}B'(x)\lambda$ (4-12)

For the optimal descent control using spoilers, the control objective becomes: find the optimal control u^* for driving HAWK in (4-10) through a descent manoeuvre from one level-off state x_0 to another level-off state x_f and in the minimisation of (4-6).

To sum up, to solve the problem involves finding

1. the 6 state variables $x_i(t)$.
2. the 6 influence functions $\lambda_i(t)$.
3. the 3 control variables $u_i(t)$.

to satisfy, simultaneously,

1. the system state differential equations (4-10).
2. the influence (**Euler-Lagrange**) differential equations (4-8).
3. the optimality conditions (4-12).
4. the initial and final boundary conditions (4-9).

4.6.3 First-order gradient algorithm (Armijo method)

The direct solution of the above complex nonlinear two-point boundary-value problem demands the use of numerical methods and a number of numerical methods for the solution of such problems were summarized by BRYSON & HO (1975) which necessarily involve either flooding or iterative procedures. However, such direct solution methods do not seem appropriate here.

In this study, a modified first-order gradient algorithm was applied to the optimal flight control problem. The choice of the algorithm was dominated by the features of the control problem, the need for efficient computation and the possible analytic determination of the **Jacobians** to provide a stable numerical iteration.

The first-order gradient algorithm is outlined next.

At some iteration k, the control is $u_k(t)$, $t \in (t_0, t_f)$. The corresponding state solution is $x_k(t)$. The first-order gradient algorithm is based upon the minimisation of the first-order index increment δJ which is caused by a small change δu in $u_k(t)$. According to **calculus of variations:**

$$\delta J = \int_{t_0}^{t_f} (\lambda' \frac{\partial f}{\partial u}\Big|_{u=u_k, x=x_k} + \frac{\partial L}{\partial u}\Big|_{u=u_k, x=x_k}) \delta u dt \qquad (4\text{-}13)$$

The steepest descent direction for the minimisation of δJ is

$$S_k(t) = -[Ru + (\frac{\partial f}{\partial u})'\lambda]\Big|_{u=u_k, x=x_k, \lambda=\lambda_k} \qquad (4\text{-}14)$$

and the control increment in this direction is decided by

$$\delta u_k(t) = w_k S_k(t) \qquad (4\text{-}15)$$

which update u_k to u_{k+1}: $u_{k+1}(t)=u_k(t)+\delta u_k(t)$, $\forall t \in (t_1, t_f)$.

Where w_k is a scale chosen to minimize (at least approximately, through an inner iteration procedure), $J(u_k+du_k)$. The **Armijo** method (POLAK, 1970) was used here for the search of the best scale w_k^* at each iteration k, namely:

$$w_k = (0.8)^p (1.5)^q \qquad (4\text{-}16)$$

where p ($\geq$0) and q ($\geq$0) are the factors controlling the decrease or increase of the scale, respectively. They are decided by the iteration.

4.6.4 Iteration procedure

The iteration procedure designed for this study is summarized as:

1) Get a set of arbitrary control variable histories, $u_k(t)$.

2) Integrate (4-10) forward with $x(t_0)$ and the $u_k(t)$. Record $x_k(t)$, $u_k(t)$, J_k.

3) Determine an n-vector of influence functions $\lambda_k(t)$, by backward integration of $\lambda(t)$ equations (4-8), using (4-9) for $\lambda(t_f)$.

4) Decide the deepest direction $S_k(t)$ from (4-14).

5) Iterate for the step scalar w_k from (4-16).

6) Get an improved estimate of $u_k(t)$, where: $u_k(t)=u_k(t)+\delta u_k(t)$, with the control increment $\delta u_k(t)$ decided by (4-15).

7) Integrate (4-10) forward with $x(t_0)$ and $u_k(t)$. Record J_k.

8) Repeat steps (5) through (7), with improved estimates of the step scalar from the **Armijo** method until $J_k^* \rightarrow \text{Min}(J_k)$. Record the $\delta u_k^*(t)$ as the optimal control increment at the step k.

9) Let $u_{k+1}(t)=u_k(t)+\delta u_k^*(t)$, repeat steps (1) to (9) until obtaining the optimal control $u^*(t)$ which gives the minimisation of J: $J^* \rightarrow \text{Min}(J)$.

4.6.5 Program for optimal control synthesis: OPOPEN

A Fortran code 'OPOPEN' was developed, based on the above procedure, for the solution of the optimal control laws. It was later combined with the simulator 'HAWKSIM1' as a special subroutine for open-loop optimal control designs.

One of the core steps involved on the programming was the calculation of the Jacobians $\frac{\partial f}{\partial x}$ and $\frac{\partial f}{\partial u}$. In this study, both the numerical method introduced by LEWIS (1986) and the method based on the theoretical derivation from the aircraft equation (see **Appendix One**) were used. In the summary of computation experience, it is preferable to use the derivative formula to gain a quicker iteration and a more stable numerical configuration.

Fig. 4-6 shows the flow chart of the program 'OPOPEN'.

4.7 Optimal Control of Two-Point Descent Manoeuvres

After the development of the software package 'OPOPEN', the design of the open-loop optimal control for the nonlinear aircraft performing two-point descent manoeuvres was carried out. Three control design cases and their simulations are presented here, featuring (1) the evaluation of the program for the control objective; (2) descent optimization augmentation using spoilers; and (3) an overall comparison in the descent ability between using and not using spoilers. The results show the enhancement of the aircraft manoeuvrability obtained by using spoiler control.

4.7.1 Control objective: two-point descent manoeuving

A special control mission was defined as: controlling a HAWK aircraft in the nonlinear form of (4-10) to perform a descent manoeuvre from a balanced initial state $x_0=[V_0, \gamma_0, \alpha_0, q_0, \theta_0, H_0]'$ to a final state $x_f=[V_f, \gamma_f, \alpha_f, q_f, \theta_f, H_f]'$, within a fixed time duration T(>0). The balanced state is automatically set by 'HAWKSIM1' as $x_0=[V_0, 0, 0, 0, 0, H_0]'$ while the desirable final state is set as $x_f=[V_f, 0, 0, 0, 0, H_f]'$, so the problem is to control the aircraft to perform a two-points descent with only height and velocity changes between the start point and the final point. A manoeuvre like this can often be found in flight missions like cruise height change and approach to landing.

For the following designs, the balance condition was fixed as a balanced flight of H_0 = 5000(m) and V_0=237(m/s). The time duration was set as T=20.0(s).

4.7.2 Evaluation of the design package

The program 'OPOPEN' was developed for the synthesis of the open-loop optimal control of aircraft. It was applied to the descent control of HAWK through the connection with the simulator 'HAWKSIM1'.

Here is an example of the HAWK descent control from the initial height H_0=5000(m) to a terminal target height H_f=2500(m) while maintaining the terminal velocity V_f the same as the initial velocity, i.e. V_f=237(m/s). All three control resources (i.e. δ_e, δ_t and δ_{sp}) were supposed available. The desirable trajectory x_d in (4-6) was defined as $x_d(t)=[V_d(t)\ 0\ 0\ 0\ 0\ 0\ H_d(t)]$, with $V_d(t)=V_0$ and $H_d(t)=H_f+(H_0-H_f)e^{-t/td}$, the time constant t_d was made adjustable subject to control constraints. In this test, t_d=0.1T.

An important step involved was the choice of reasonable weighting matrices in the cost function (4-6), which were closely related to system performance and control. By trial and error, the weighting matrices for this case were defined as diagonal and are:

State weighting matrices:

$$Q=\begin{bmatrix} 0 & & & & & \\ & 0 & & & & \\ & & 0 & & & \\ & & & 0 & & \\ & & & & 70.0 & \\ & & & & & 0.000001 \end{bmatrix} \qquad QF=\begin{bmatrix} 0 & & & & & \\ & 0 & & & & \\ & & 0 & & & \\ & & & 0 & & \\ & & & & 12.0 & \\ & & & & & 0.00008 \end{bmatrix}$$

Control weighting matrix:

$$R = \begin{bmatrix} 0.25 & & \\ & 1.0 & \\ & & 0.2 \end{bmatrix}$$

It can be seen that in the state weighting matrices, major weighting effort was put on the height H and the pitch angle θ, for altitude tracking and for the limitation of the variation of the aircraft attitude during the descent process and at the final time. Due to the angular coupling relation, weighting on θ can also be expected to bring an indirect weighting effect on the trajectory angle γ, as shown in later tests. For the control weighting, however, the major work was to define the rough weighting R for scaling the control increment. The rest concerning the modification of the weighting would automatically done by the program.

The design and simulation are summarised in **Fig. 4-12**. The optimal trajectories of the height and path angle resulting from the control are shown in **Fig. 4-12(a)** and **Fig. 4-12(b)**, respectively.

The search for the optimal control was initiated with u_0 which, in this case, was given as a sole step elevator control in the descent direction, while keeping δ_t and δ_{sp} unchanged as the initial states. The time history of the initial elevator control (δ_e=1.0 (deg.)) can be seen in **Fig. 4-12(c)**, and the results (H(t) and γ(t)) from this control are compared with the optimal ones in **Fig. 4-12(a), (b)**.

It was found that in most of design cases when the initial control and the weighting matrices were properly set, one step of the outer-loop iteration, i.e. k_N=1, was sufficient to yield a satisfactory control, while keeping the search going would be costly computational and give little improvement in the performance. The optimal trajectories in **Fig. 4-12(a)** and **Fig. 4-12(b)** correspond to a computation with an outer loop iteration of k_N=2 and an inner loop **Armijo** scale of w_k=0.875 (p=3, q=0). The time histories of the controls δ_e and δ_{sp} are shown in **Fig. 4-12(c)** and **Fig. 4-12(d)**, respectively. The thrust control δ_t had met the minimum constrain(δ_{tmin}=0.0) and was in a shut-off state throughout the manoeuvre. In **Fig. 4-12(c)**, the optimal elevator control shows a significant updating from the initial given case so as to give an improved attitude control process. While the spoiler control (**Fig. 4-12(d)**), having varied within its control authority most of the time, shows a desirable pattern with a large amount of control at the beginning and little at the end, to meet both the descent and attitude requirements.

The improvement from the optimal control can be seen through the cost function evaluation: (1) relative improvement in the total cost function $\Delta JR = (J_0-J^*)/J_0) = 21\%$, (2) relative improvement in the part of the terminal state cost S $(=(x(t_f)-x_f)'QF(x(t_f)-x_f))$ $\Delta SR=99.6\%$, with $H(t_f)$ changing from 3876(m) to 2494(m), $\gamma(t_f)$ from -22.4^o to 4.8^o, $V(t_f)$ from 270(m/s) to 256(m/s).

4.7.3 Improvement of control augmentation using spoilers

The design package was further used for determining the potential benefits of spoiler control. This was done by comparing the control effects between optimal control using spoilers and that without using spoilers. First is the example showing the role of spoiler control in the improvement of the control augmentation.

Following the above design procedure, suppose the terminal target height is $H_f=2000$(m), the optimal control concerning the use of the elevator and the thrust only was found by cutting off the spoiler channel and using the following weighting matrices:

$$Q = \begin{bmatrix} 0 & & & & & \\ & 0 & & & & \\ & & 0 & & & \\ & & & 0 & & \\ & & & & 78.0 & \\ & & & & & 0.000001 \end{bmatrix} \qquad QF = \begin{bmatrix} 0 & & & & & \\ & 0 & & & & \\ & & 0 & & & \\ & & & 0 & & \\ & & & & 0 & \\ & & & & & 0.0001 \end{bmatrix}$$

$$R = \begin{bmatrix} 0.25 & \\ & 1.0 \end{bmatrix}$$

At the same time, the optimal control combined with the spoiler for the same descent objective was synthesized. The weighting matrices for this case were:

$$Q = \begin{bmatrix} 0 & & & & & \\ & 0 & & & & \\ & & 0 & & & \\ & & & 0 & & \\ & & & & 110.0 & \\ & & & & & 0.000001 \end{bmatrix} \qquad QF = \begin{bmatrix} 0 & & & & & \\ & 0 & & & & \\ & & 0 & & & \\ & & & 0 & & \\ & & & & 12.0 & \\ & & & & & 0.0001 \end{bmatrix}$$

$$R = \begin{bmatrix} 0.25 & & \\ & 1.0 & \\ & & 0.08 \end{bmatrix}$$

Fig. 4-13 presents the design results and comparison between the two cases. The time histories of the path velocity V and the path angle γ are shown in **Fig. 4-13(b), (c)**, respectively, while the H vs X trajectory can be found in **Fig. 13(a)**. **Fig. 4-13(d)** shows time histories of the optimal control variables δ_e and δ_{sp}.

It can seen from these figures that although the optimal control in the first case meets the final objective height ($H(t_f)$=2000(m)), it brings a very poor control to the other terminal states of the aircraft ($V(t_f)$=281(m/s), $\gamma(t_f)$=-41°, $\theta(t_f)$=-36°). This is mainly due to the fact that for a descent to the terminal target height like this and under the upper constraint on the elevator δ_e (3° in this case), the aircraft has nearly reached its full descent strength (H_{min}=1900(m), thus has little control potential for the augmentation of the velocity and attitude. A control like this is clearly undesirable.

The results can be much improved by the introduction of spoiler control, as shown in **Fig. 4-13**. Compared with the case without the spoiler, both the final path velocity and the final attitude were considerably improved towards the desired values ($V^*(t_f)$=237(m/s), $\gamma^*(t_f)$=-0.74°, $\theta^*(t_f)$=11°), thus bringing the preferable 'S' shaped H vs X trajectory as shown in **Fig. 4-13(a)**.

The improvement was mainly due to the aid of the spoiler control which enhanced the descent ability of the aircraft so that came the possibility of using more conventional control action (δ_e and δ_U) for the augmentation of the velocity and attitude (compare the elevator controls in **Fig. 4-13(d)**). In the design procedure, this was shown by increases in the weighting on the $\theta(t)$ and $\theta(t_f)$ of the spoiler control case to confine the attitude variation.from the elevator control.

4.7.4 Manoeuvrability enhancement using spoilers

Furthermore, there was the evaluation of spoiler control for the enhancement of the aircraft descent in a large scale. By a systematic change of the pitch angle weighting Q_θ and a series of the corresponding optimal designs, a family of the terminal states were obtained. Comparisons between the set of points from the conventional optimal control and that when spoilers were used too summarised the advantages in the use of spoilers.

Fig. 4-14 shows the graphs of groups of terminal points from the optimal control designs for both the cases. The terminal target height here was H_f=1500(m). In **Fig. 4-14(a)**, the relations between the final states of $H(t_f)$ and $\gamma(t_f)$ and its changing trend with the Q_θ variation, corresponding to the variation of γ between 0^o to -60^o, are presented, showing the inter-relation between the terminal altitude and attitude. Comparing the points obtained using spoilers and those without spoilers gives a clear picture of spoiler effectiveness in descent control: enhancing the descent ability at the same attitude (by the maximum of 1000 meters in this case), or improving the attitude during same descent height (by the maximum of 60 degrees in γ(or θ) in this case).

In **Fig. 4-14(b)**, $H(t_f)$ vs $X(t_f)$ graphs are shown. From comparison between the two cases, it can be seen that the use of the spoiler control considerably enhances the downwards manoeuvring range and provides the aircraft with superior descent ability as the further descent height and shorter distance are concerned (in this particular case, the descent in height has been increased by 1000 meters and the horizontal distance has been shortened by 2000 meters). This can be further verified by looking at **Fig. 4-14(c)** where the $H(t_f)$ vs $V(t_f)$ graphs are presented and compared, showing the advantages of spoiler control in expanding the terminal path velocity range (from $\Delta V(t_f)$=60(m/s) to $\Delta V(t_f)$=120(m/s)) along with furthering the descent ability.

4.8 Concluding Remarks

In this chapter, digital simulation and open-loop optimal control are the two key points which were studied for the analysis and synthesis of nonlinear flight control for aircraft utilising spoilers.

For simulation, a sophisticated 6-degree digital simulator based on the HAWK aircraft was developed. As an important application of the program package, it was applied to the simulation of the nonlinear aircraft model with both linear and nonlinear spoiler models. The simulations further verified the conclusion of **Chapter 3** about the spoiler's direct and effective control on the path angle γ. This enables fast control for descent manoeuvres. The simulation also revealed that the large value of the moment coefficient of the spoilers could severely affect control behaviour and should be ideally kept to a minimum, and the nonlinearity of the spoilers was heavily dependant on the aircraft manoeuvres and might bring significant variations to the control coefficients, and so to control effectiveness, during aircraft high-α manoeuvres.

For open-loop optimal control, work concentrated on the development of a software design package for open-loop control of the HAWK and for the evaluation of spoiler control in the enhancement of aircraft manoeuvrability. Aiming at the solution of the nonlinear two-point boundary-value problem, the design applied Hamiltonian minimisation principle and the **Armijo**-based first-order gradient algorithms. This has been proven to be an efficient and successful approach.

A series of designs for aircraft descent control were carried out using the design package. The advantages of the use of spoiler control were shown by the comparisons between the designs made both with and without use of the spoilers. The results reveal the effectiveness of the use of spoilers for the enhancement of descent control of aircraft in the improvement of descent range and of attitude augmentation.

However, it is clear that although open-loop optimal control provides a objective-orientated control for a class of nonlinear flight problems, its two-point boundary value nature limits its usefulness. Further, considerable effort is needed to choose suitable weighting matrices. Also in principle, it is hard to use the method for the design of a modern nonlinear flight control with qualities including desirable tracking control, robustness and flexibility. All these suggest that it should be worthwhile to attack the harder problem of feedback control of the multivariable control system, using some innovative techniques.

Figure 4-1 British Aerospace HAWK

(a) HAWK 200

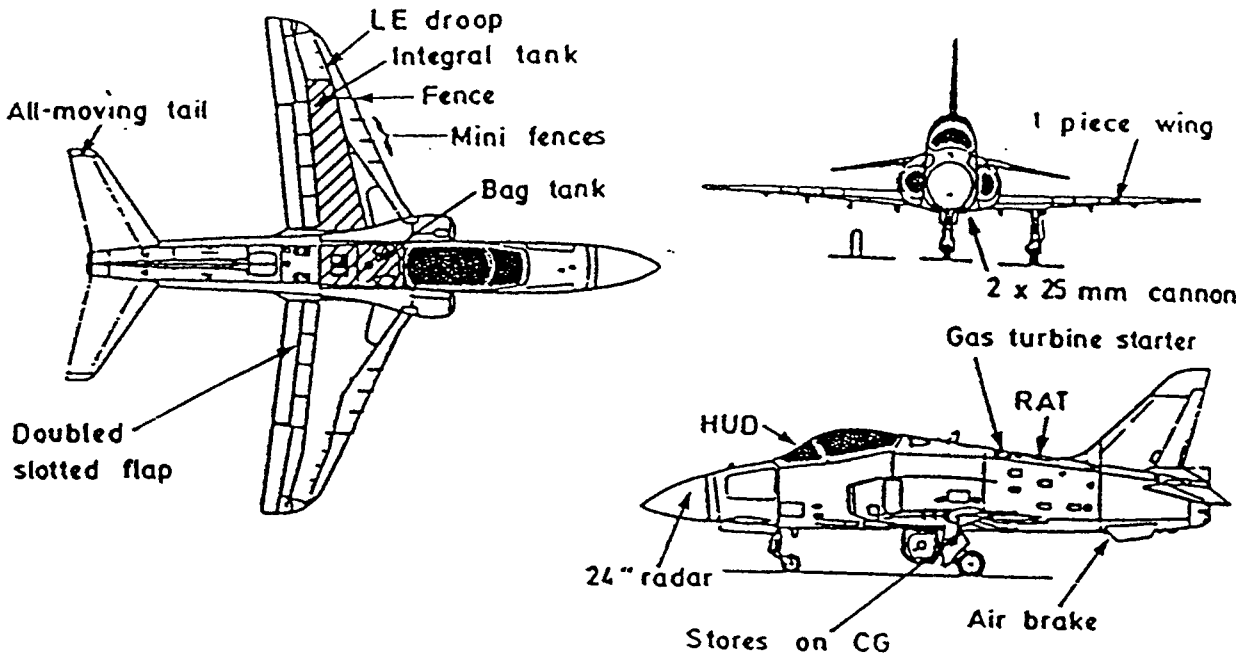

(b) HAWK 60 & HAWK 100

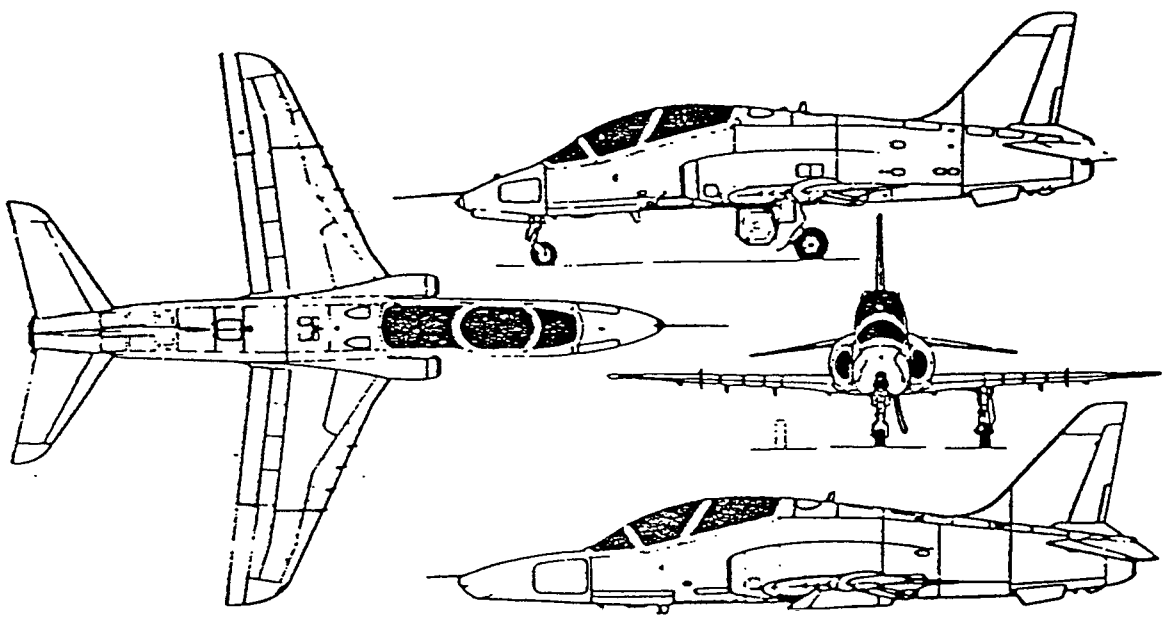

British Aerospace HAWK 60 series two-seat jet trainer, with additional side view (botton) of HAWK 100 series

Figure 4-2 Configuration of flight simulator

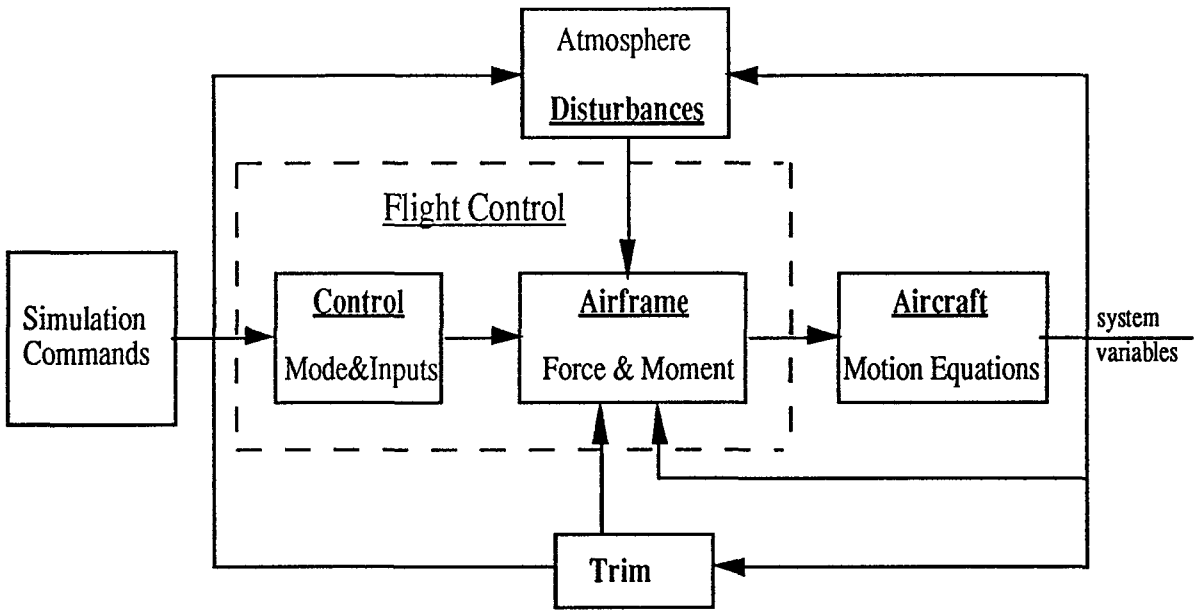

Figure 4-3 Configuration of flight control

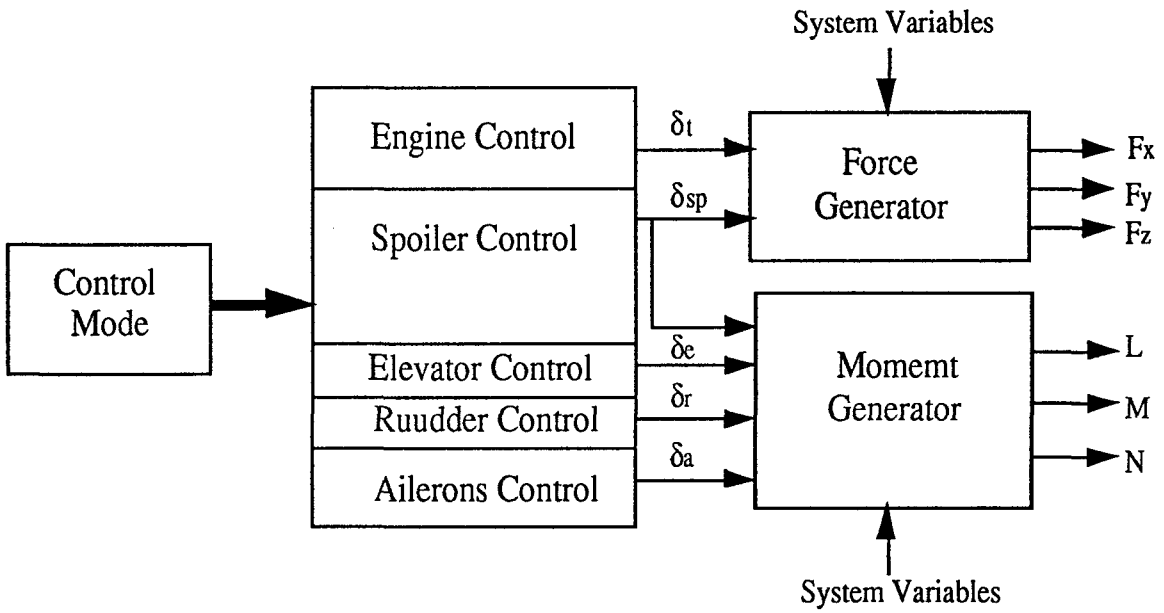

Figure 4-4 Flow chart of simulator 'HAWKSIM1'

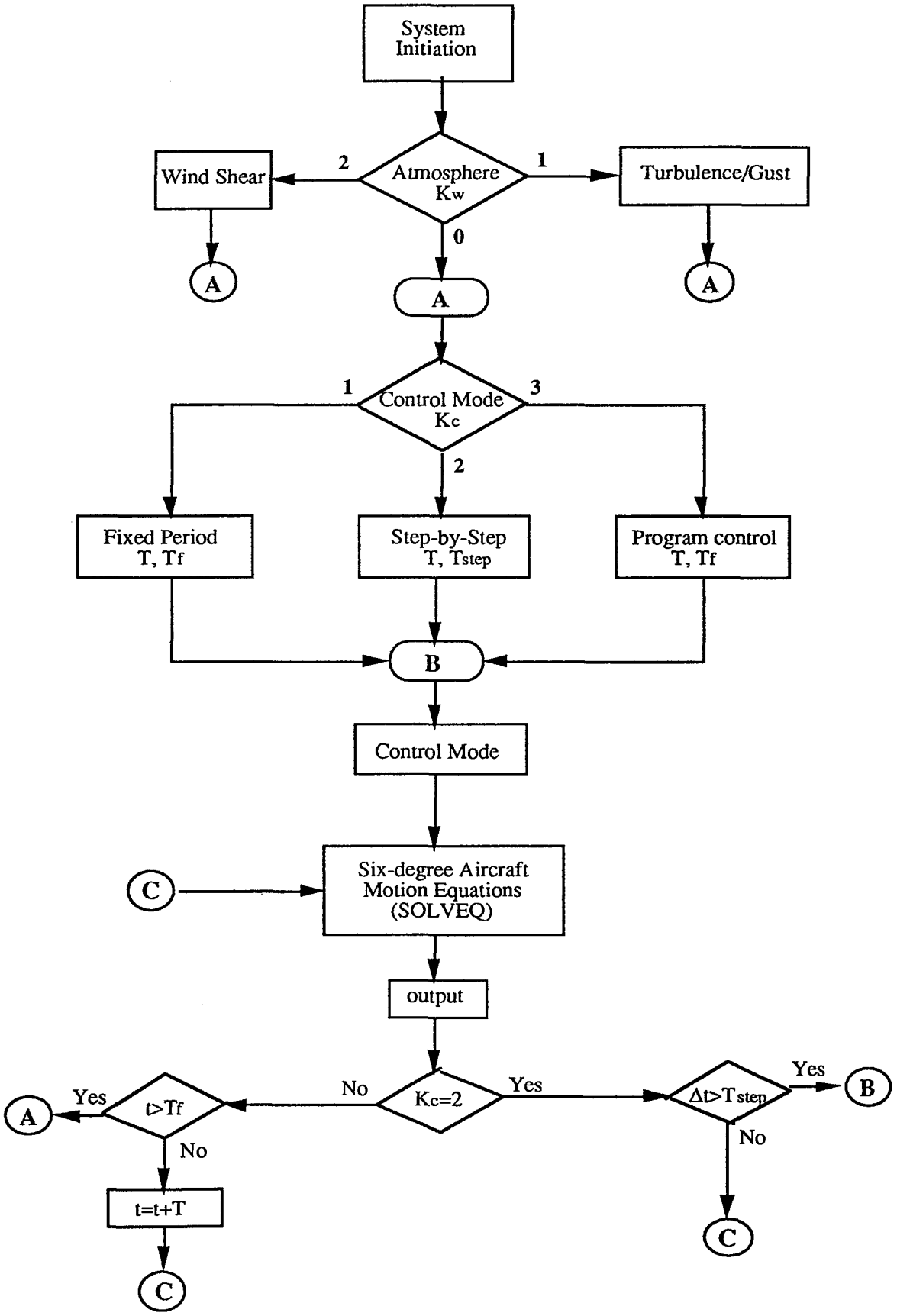

Figure 4-5 Flow chart of 'SOLVEQ'

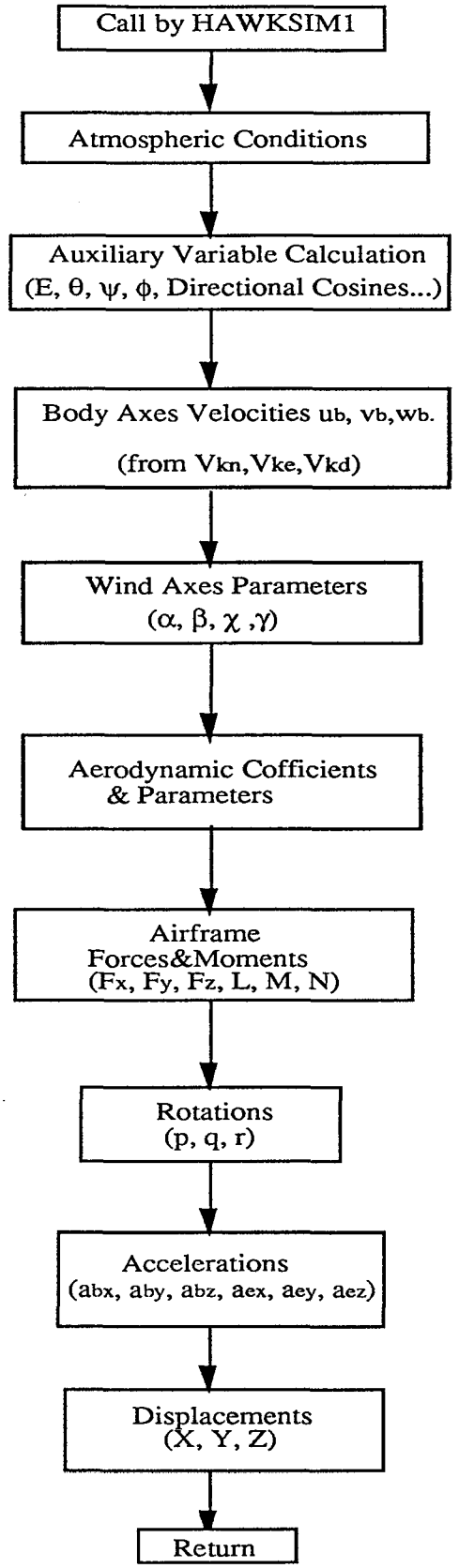

Figure 4-6 Flow chart of program 'OPOPEN'

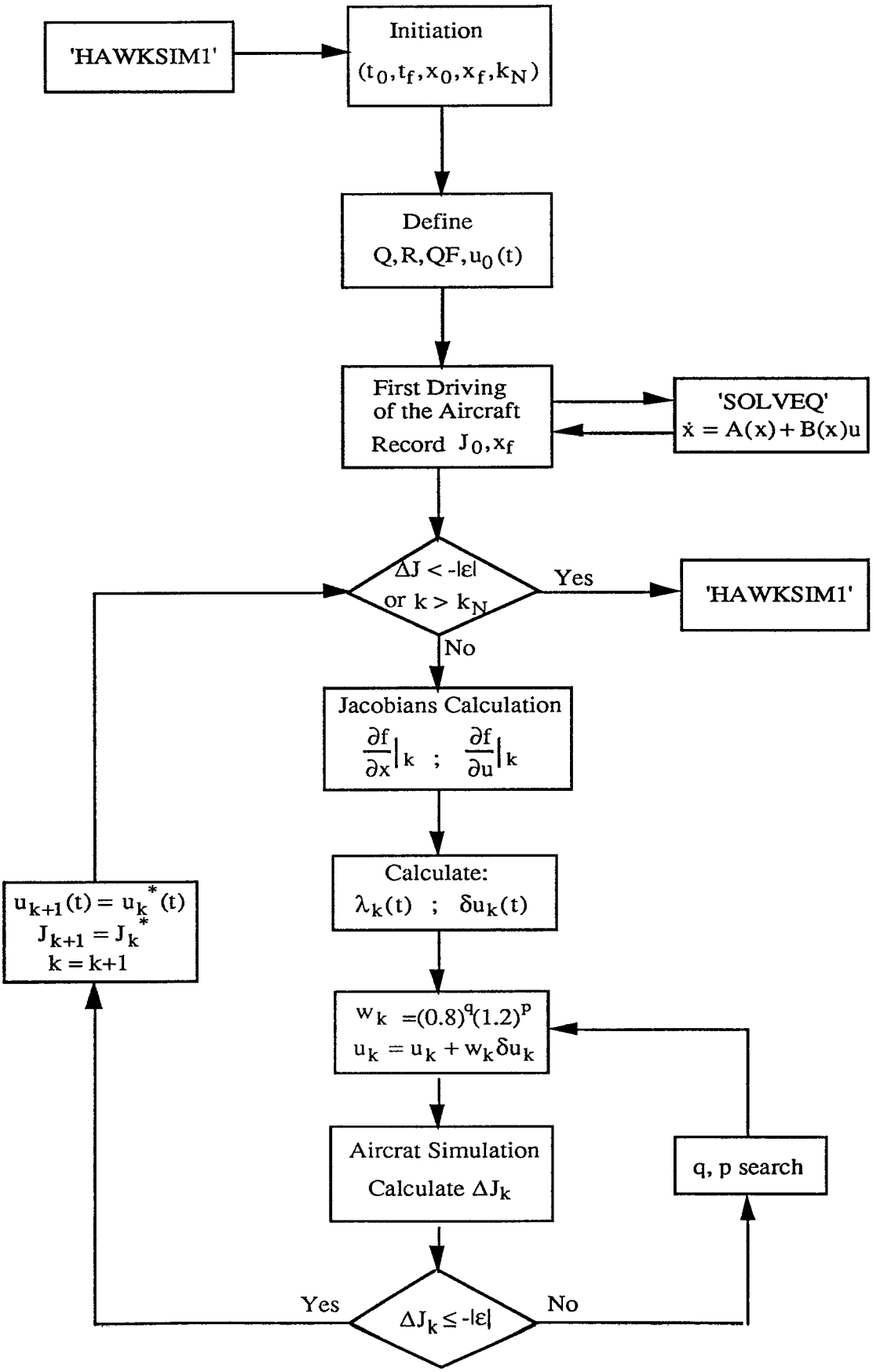

Figure 4-7 Simulation of HAWK short period dynamics
(h_0= 5000m, δ_e= -1°)

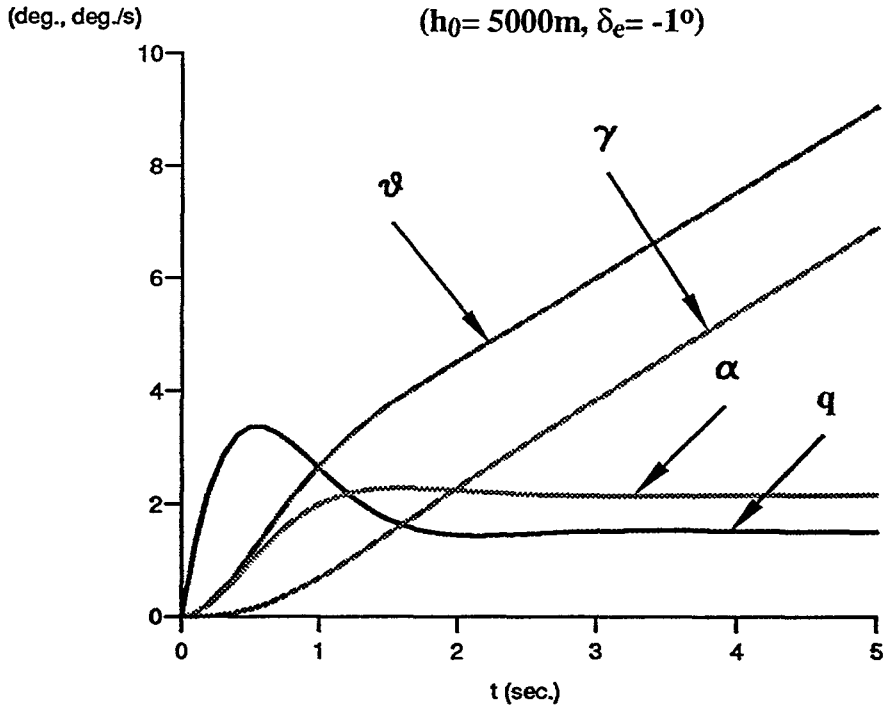

Figure 4-8(a) Flight trajectory in X-H plane
(h_0= 5000m, δ_e= -6°)

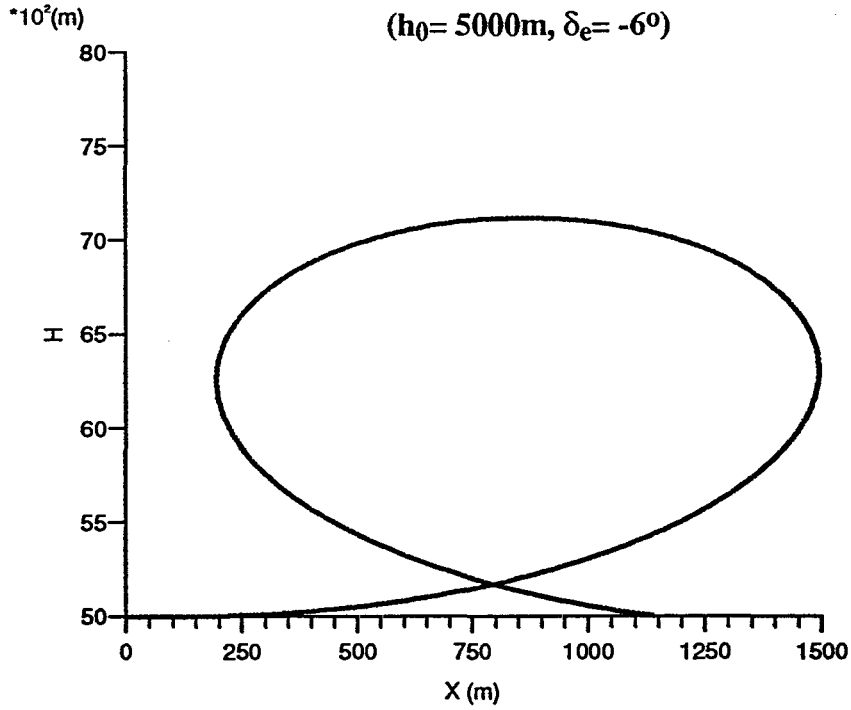

Figure 4-8(b) Path velocity response

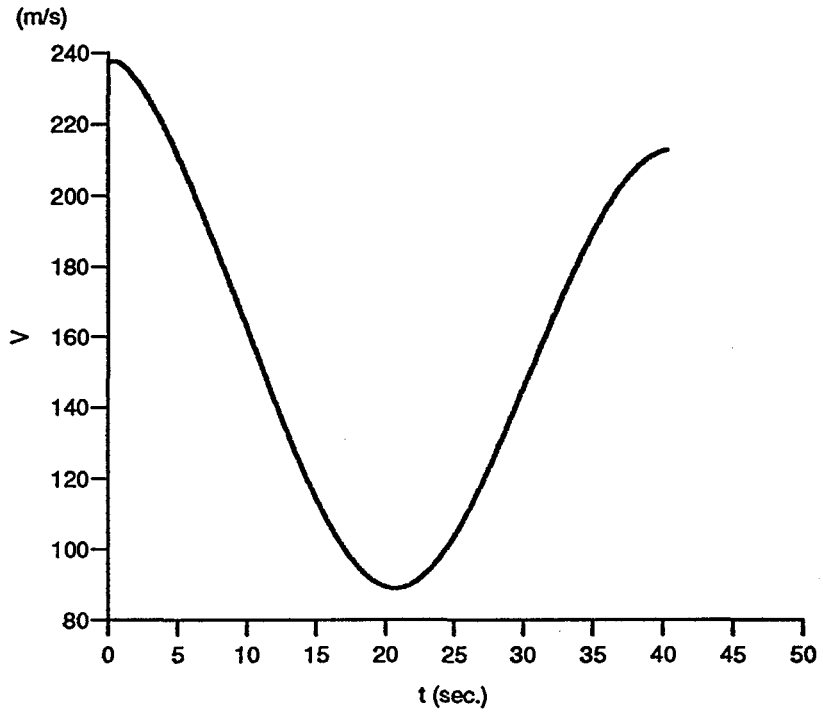

Figure 4-8(c) Pitch angle response

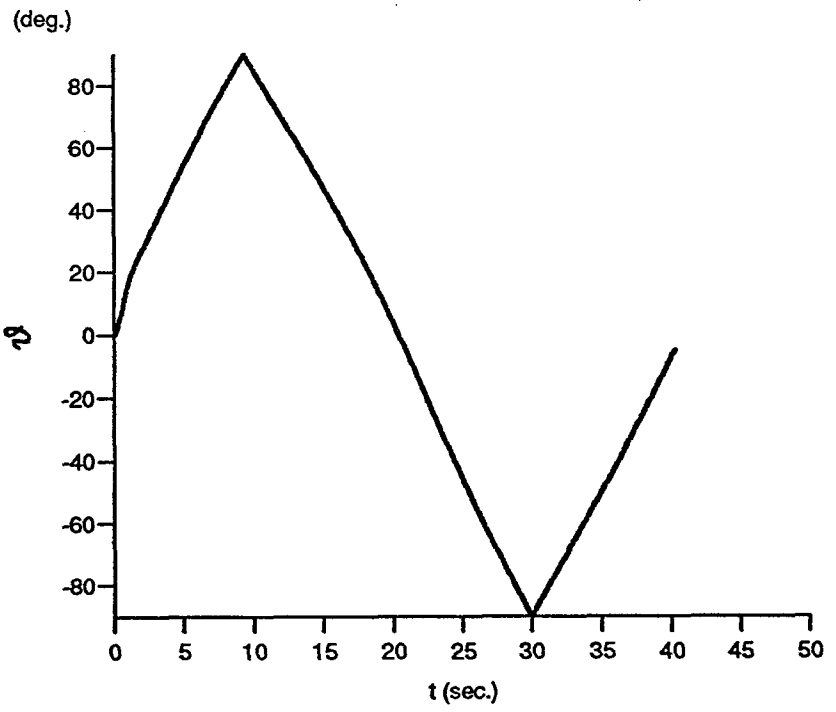

Figure 4-8(d) Incidence angle response

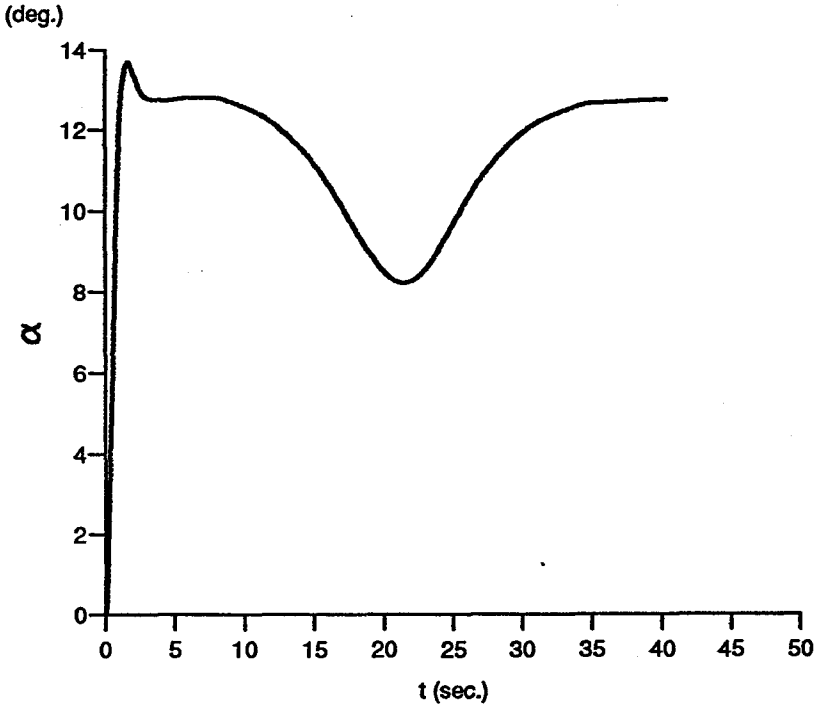

Figure 4-9(a) Flight trajectory in X-H plane
(h_0= 5000m, δ_{sp}= -60°)

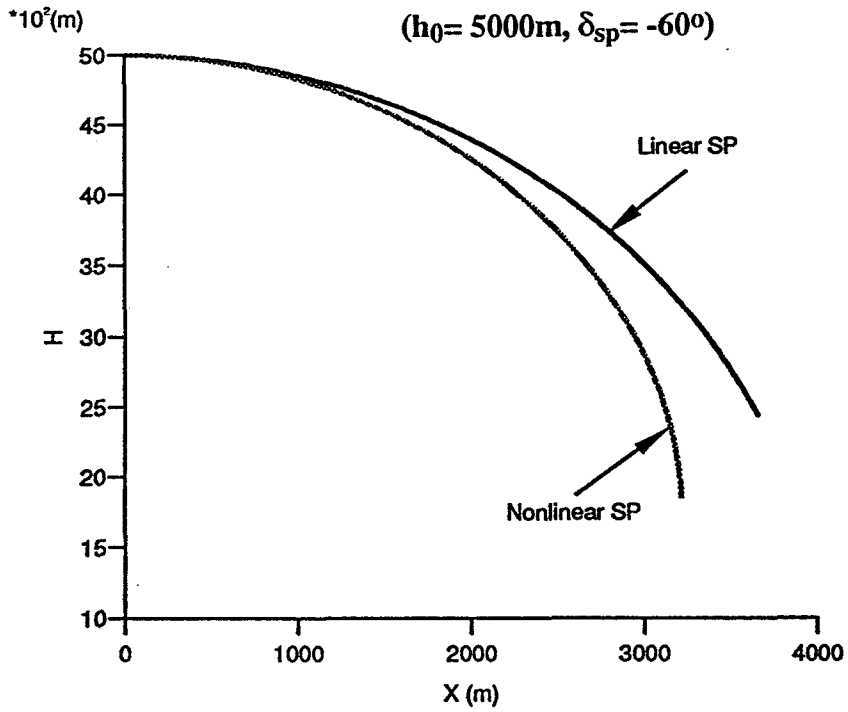

Figure 4-9(b) Responses of angular variables
(solo spoiler control)

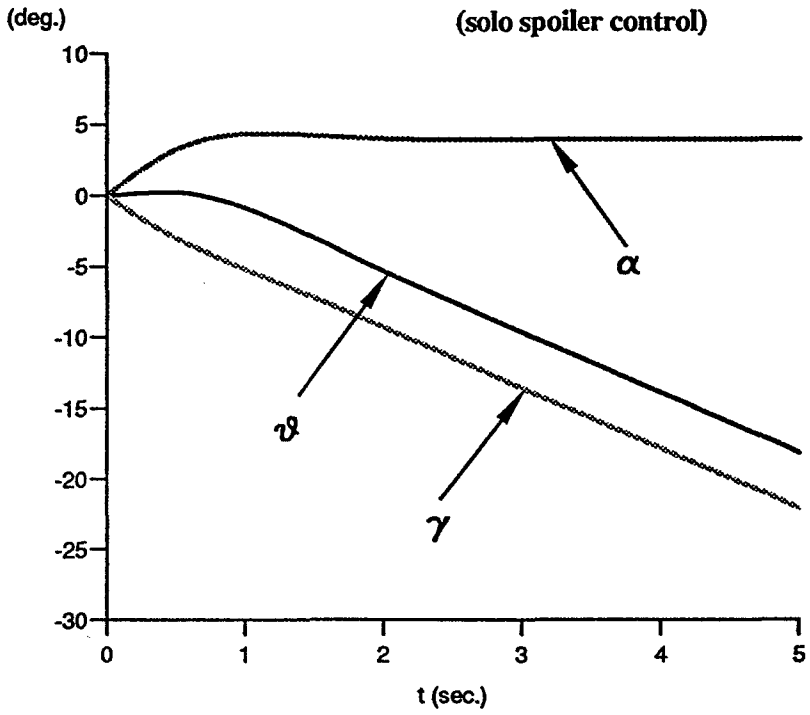

Figure 4-10(a) Effects of spoiler moment coefficient on descent height

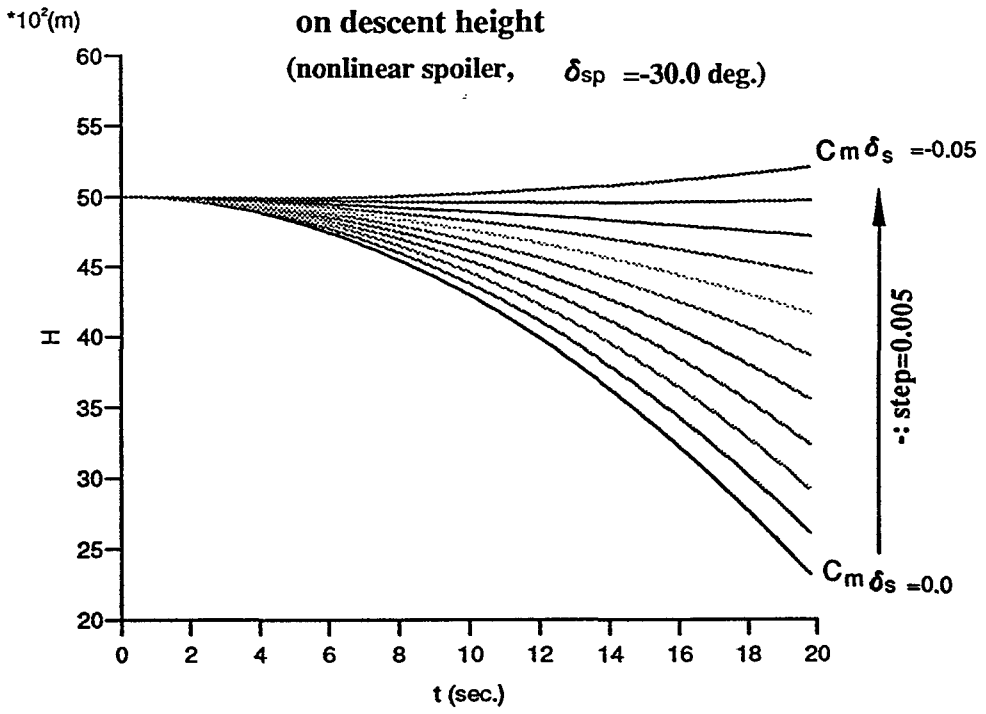

Figure 4-10(b) Effects of spoiler moment coefficient on climbing angle

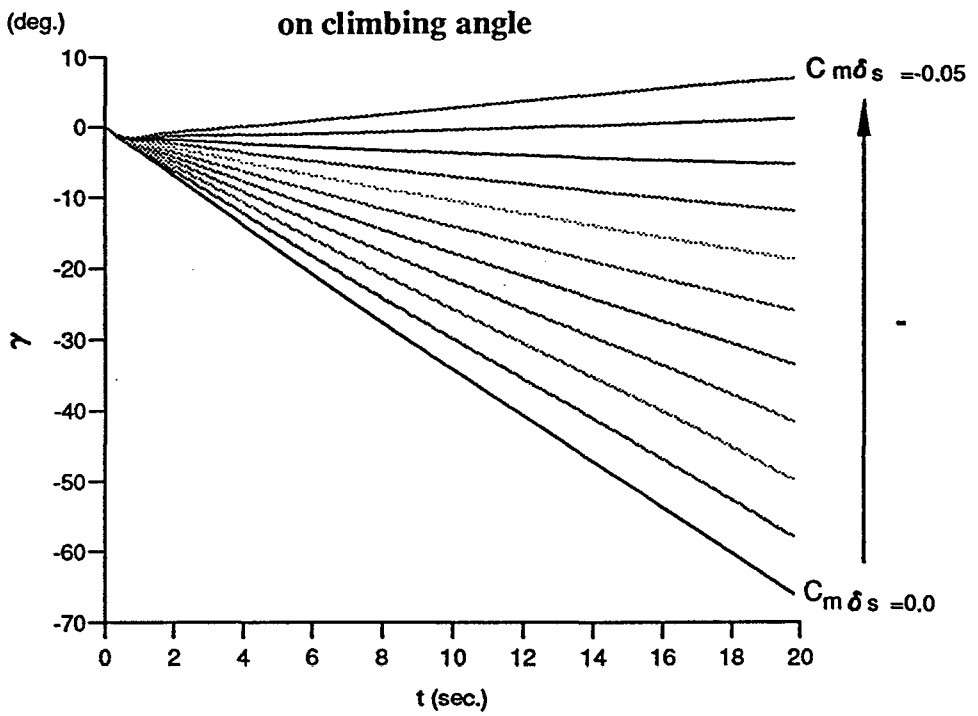

Figure 4-11(a) Comparisons of X-H trajectories
(δ_e= -6°, δ_{sp}= -20°)

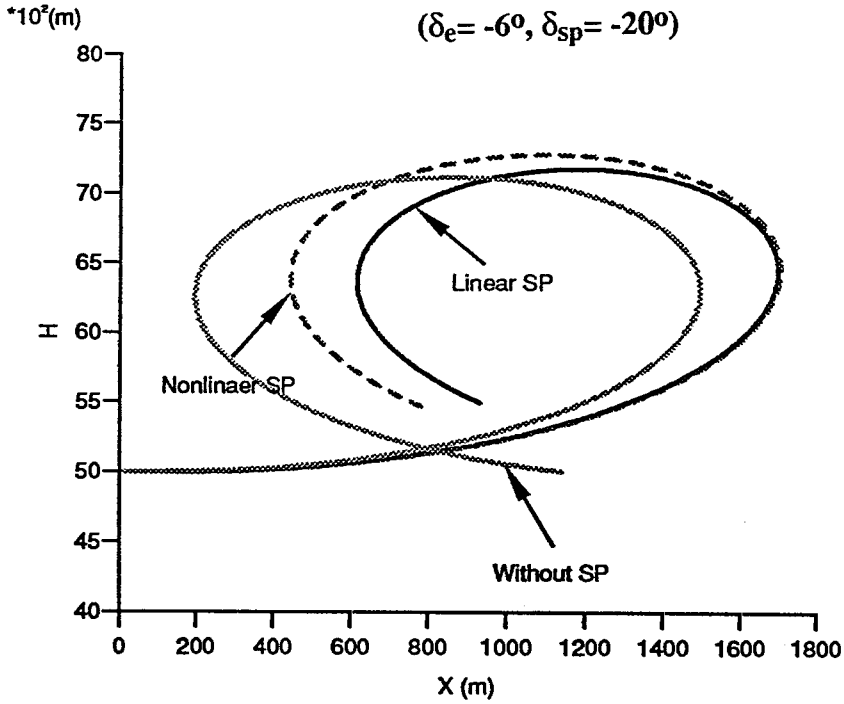

Figure 4-11(b) Comparisons of height vs time

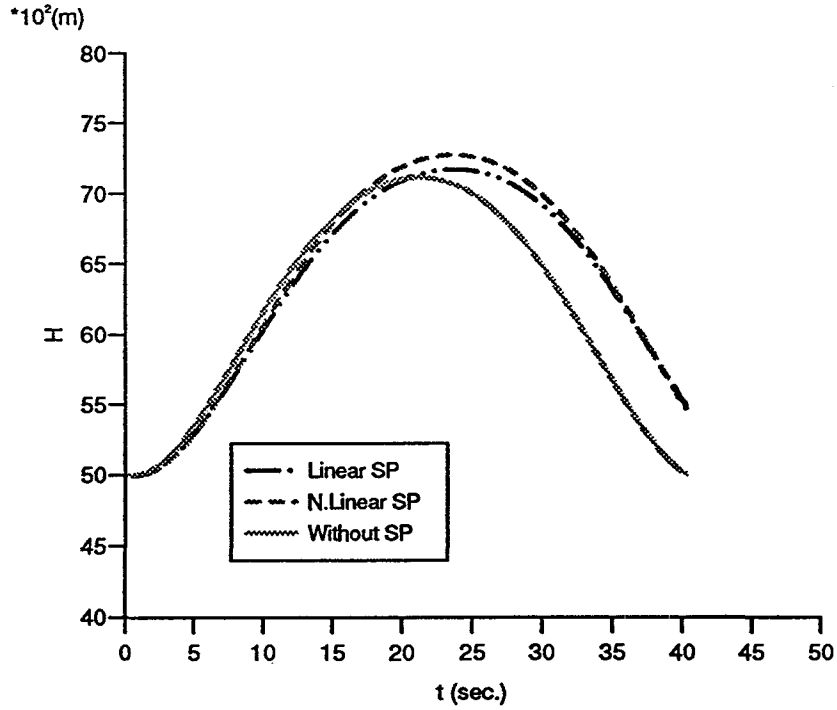

Figure 4-11(c) Comparisons of distance vs time

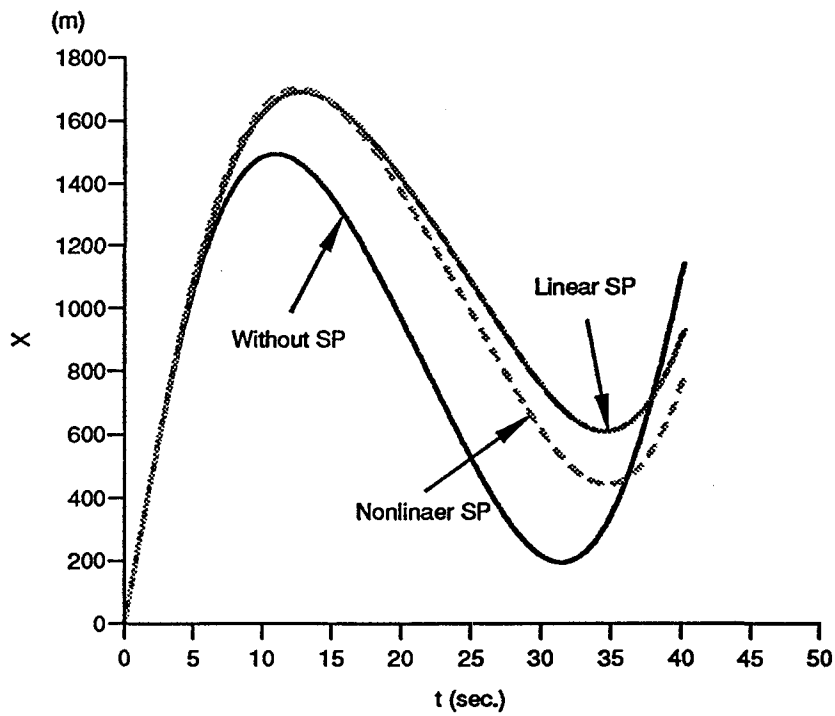

Figure 4-11(d) Comparison of spoiler coefficient C_{LSP} Variations

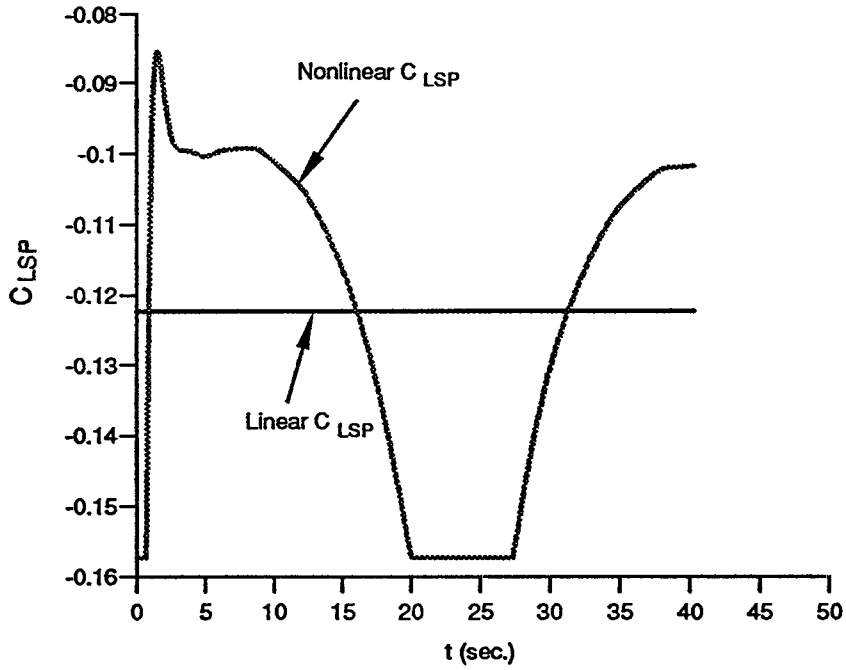

Figure 4-11(e) Comparisons of spoiler coefficient C_{DSP} and C_{MSP} variations

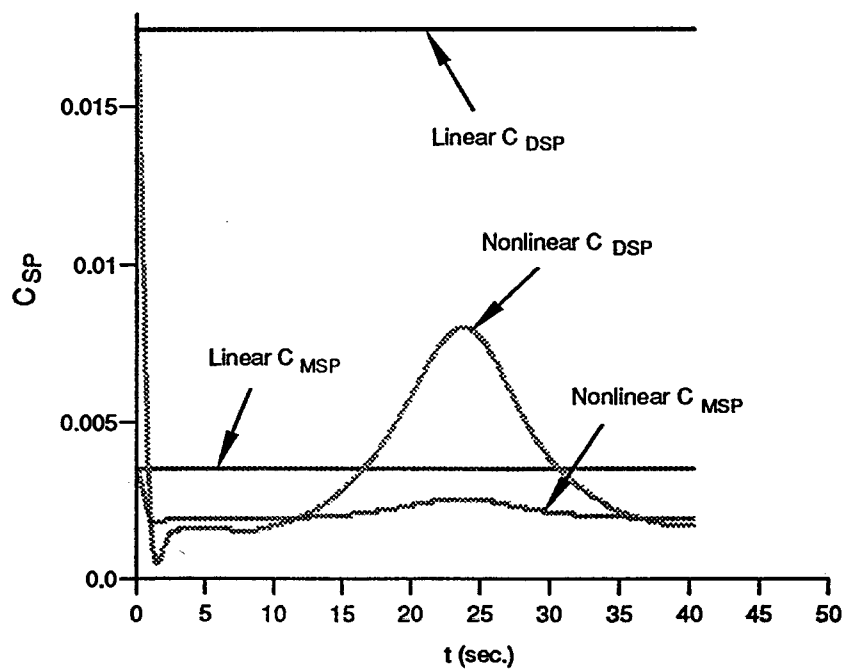

Figure 4-12(a) Optimal descent control (H_f=2500m, T_f=20s)

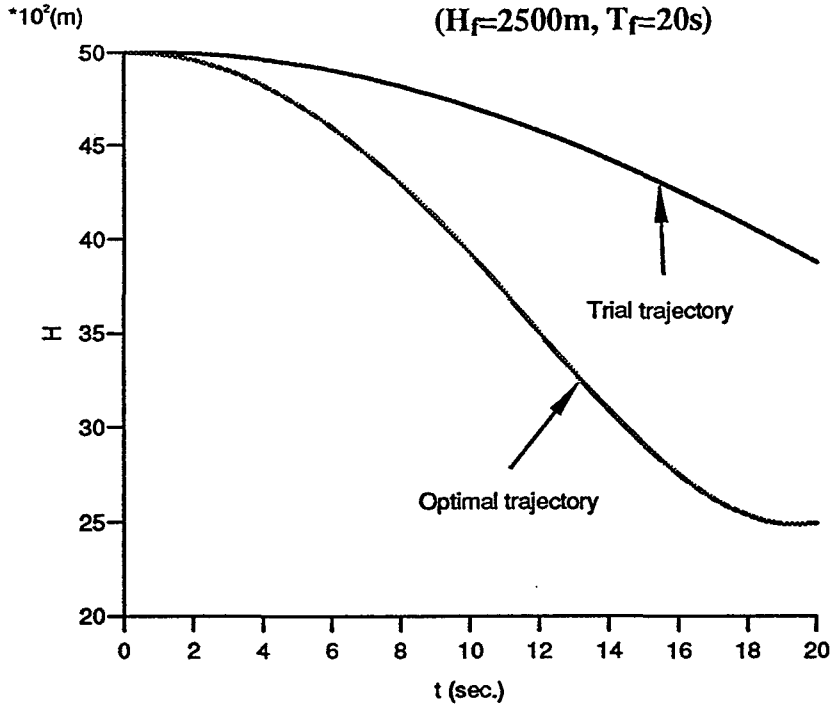

Figure 4-12(b) Optimal control of climbing angle

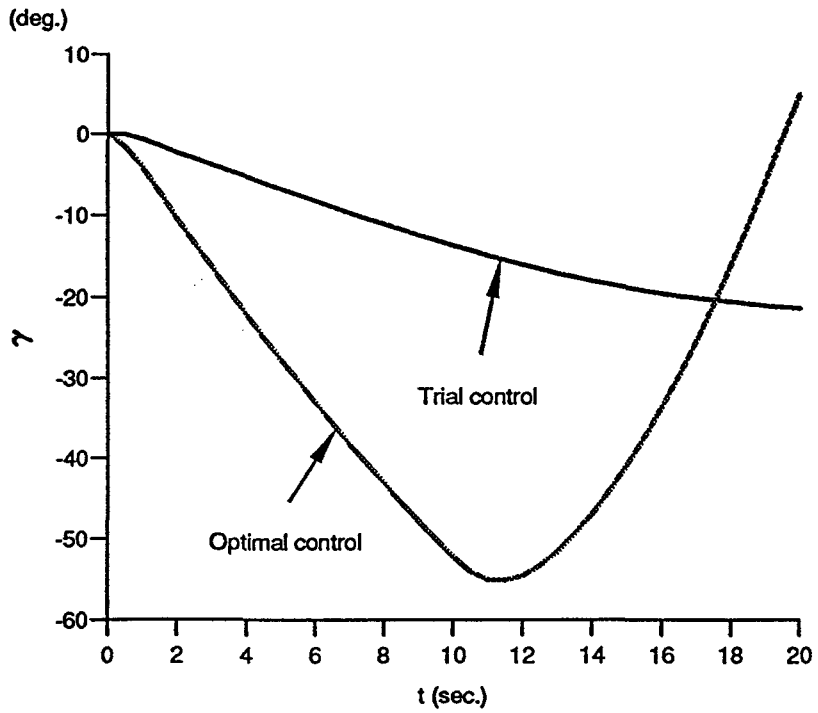

Figure 4-12(c) Optimal elevator control

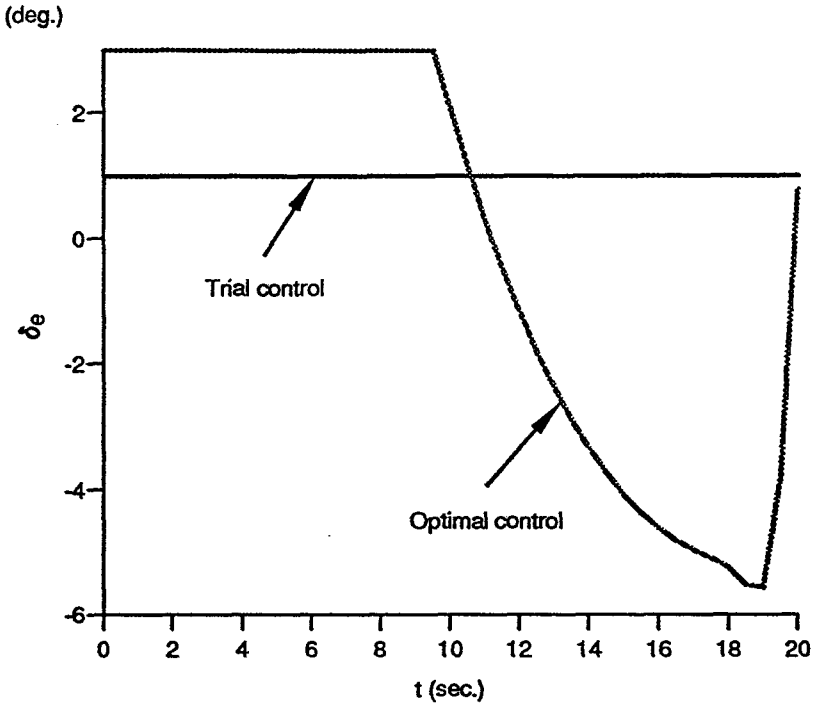

Figure 4-12(d) Optimal spoiler control

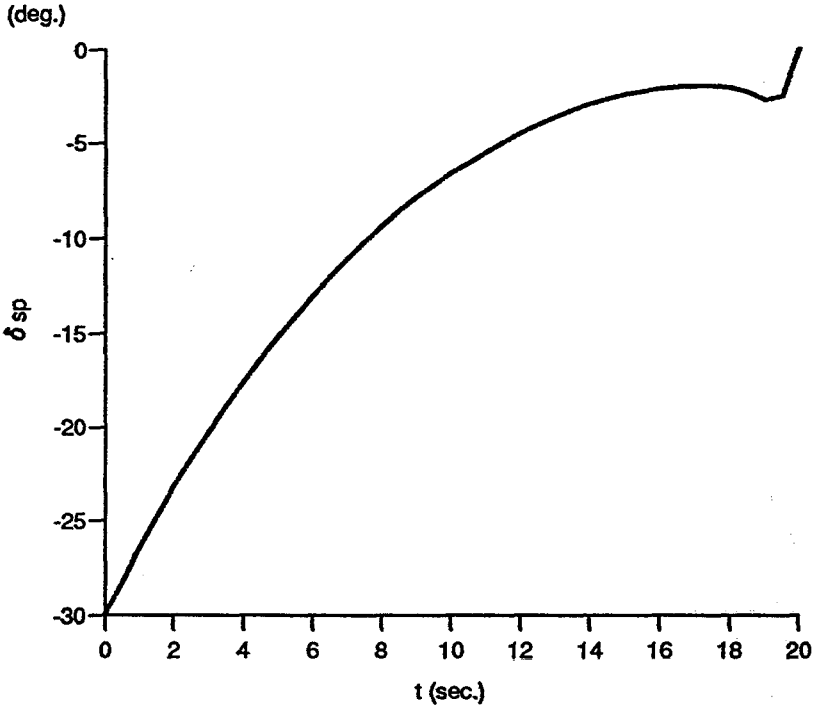

Figure 4-13(a) Comparison of H-X trajectories
(H_f=2000m, T_f=20s)

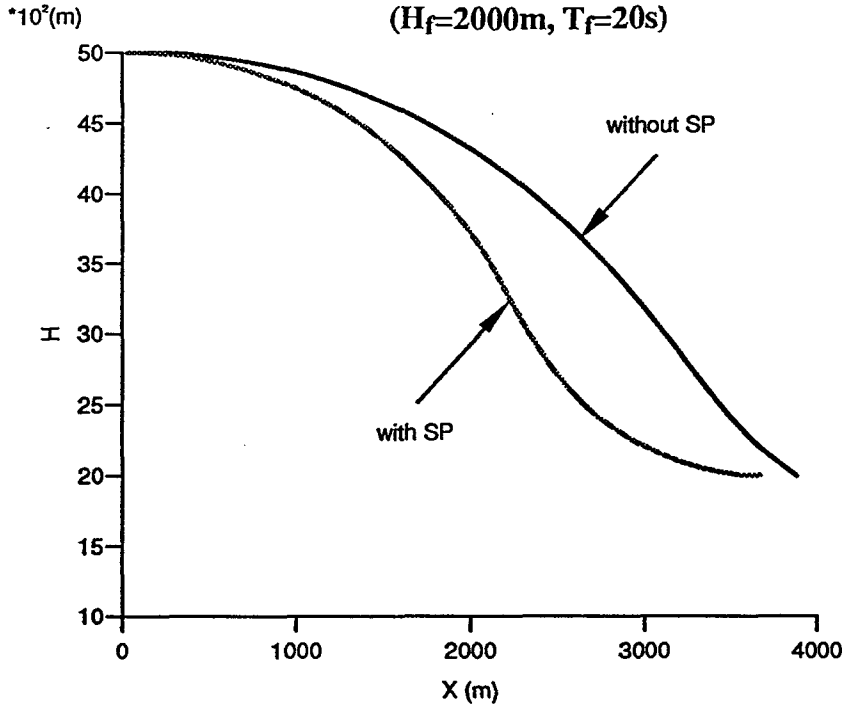

Figure 4-13(b) Comparison of path velocity

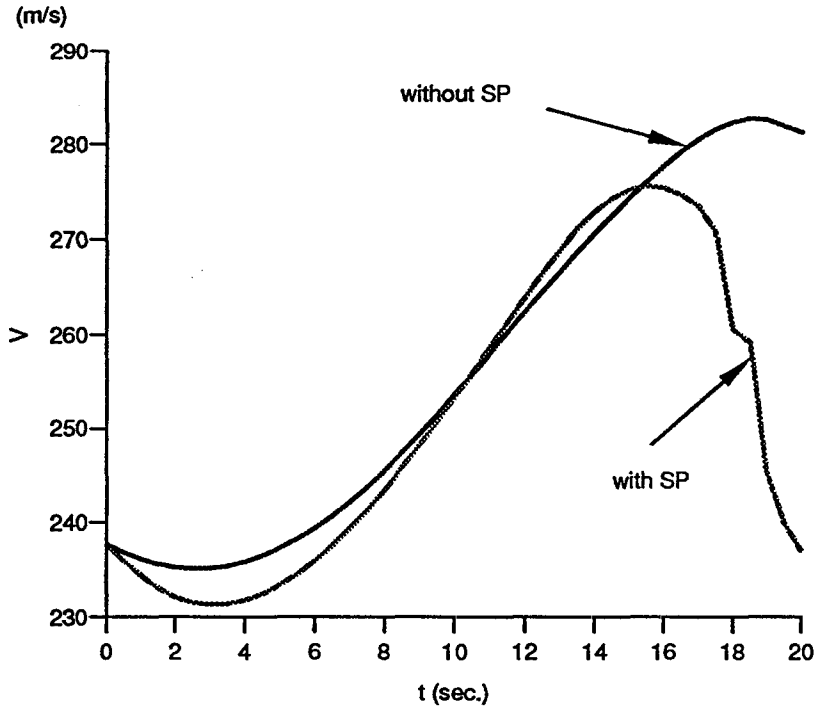

Figure 4-13(c) Comparison of climbing angle

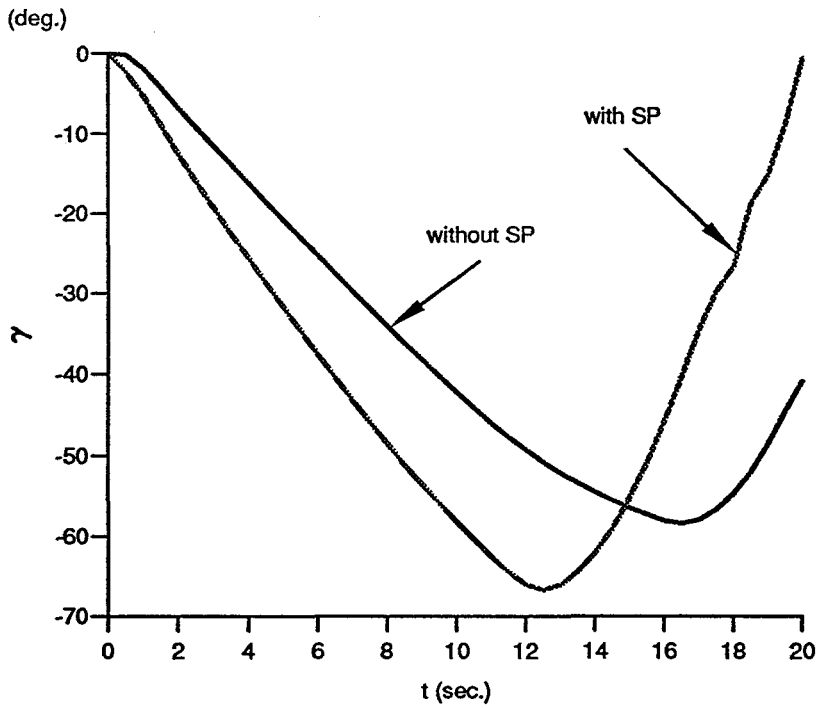

Figure 4-13(d) Elevator and spoiler control patterns

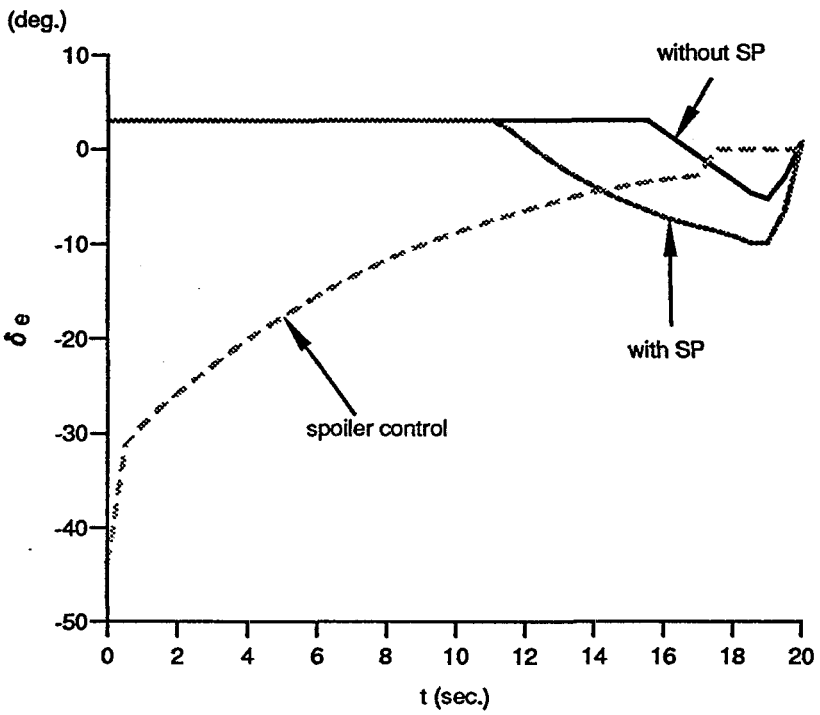

Figure 4-14(a) Comparison of the terminal height variations

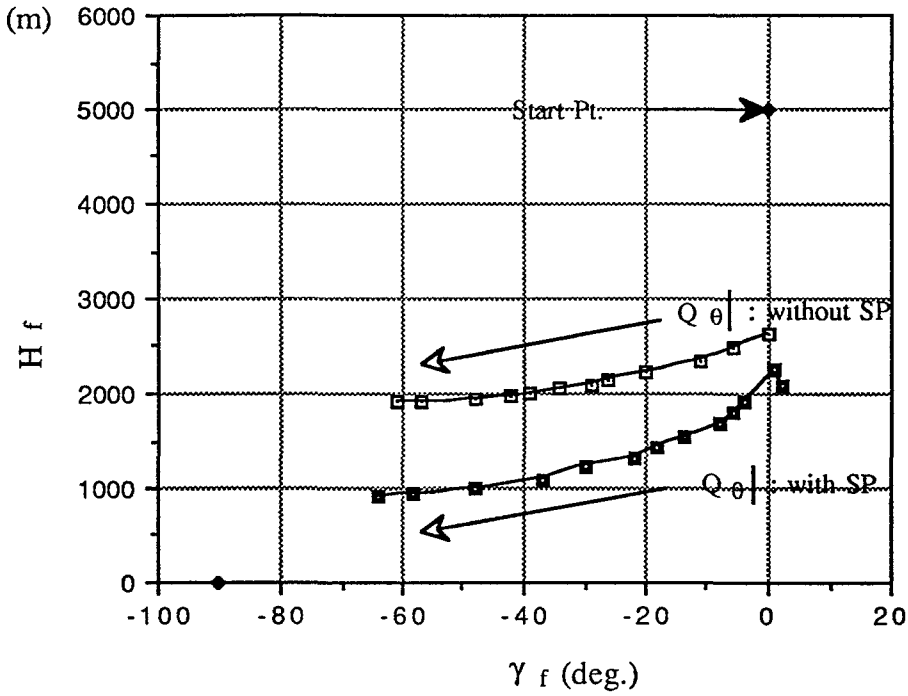

Figure 4-14(b) Comparison of H(tf) vs X(tf) graphs

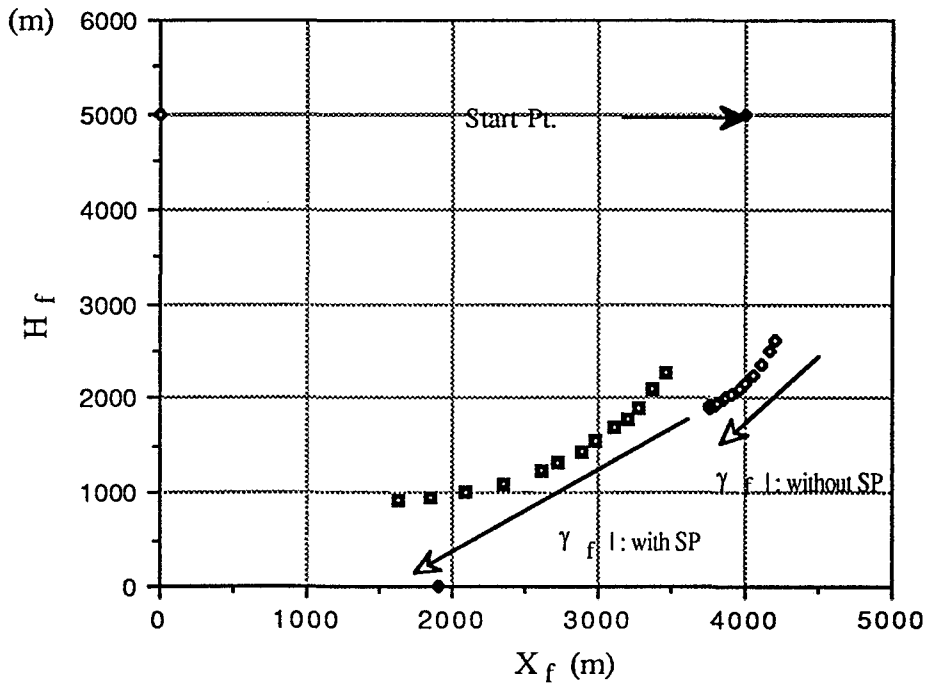

Figure 4-14(c) Comparison of H(tf) vs V(tf) contours

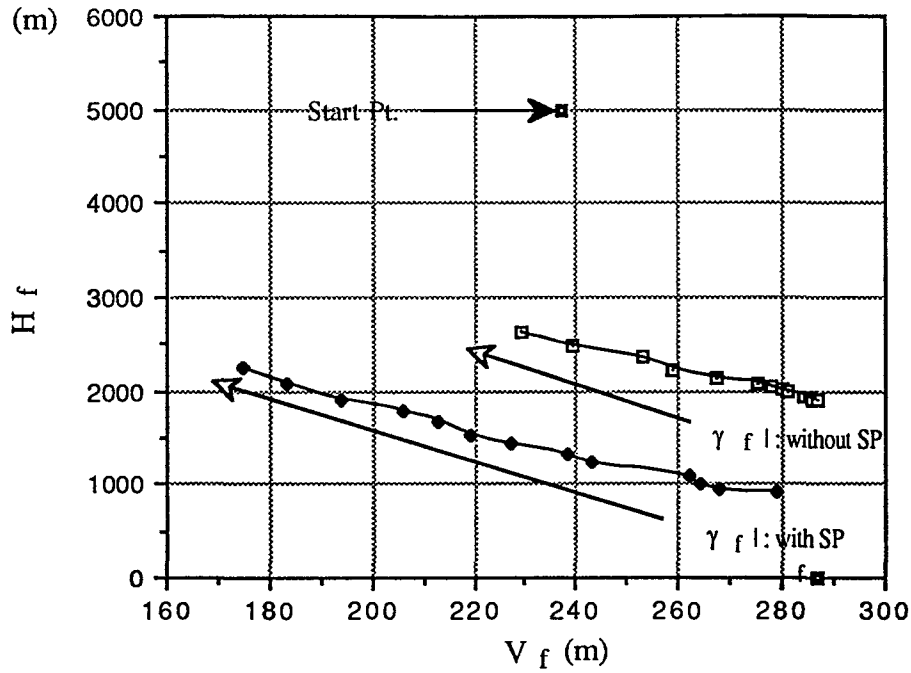

Chapter Five

INVERSE DYNAMICS METHODOLOGY AND ITS APPLICATION TO NONLINEAR FLIGHT CONTROL

5.1 General Remarks

In this chapter, a nonlinear feedback control technique, the nonlinear inverse dynamics(NID) methodology, is studied and a design procedure for the application of the technique to flight control systems is developed. As a practical application, the method is then applied to the synthesis of longitudinal controllers for the HAWK aircraft.

Generally speaking, the NID methodology yields a nonlinear control method based on input-output linearization through the construction of the inverse dynamics of nonlinear systems. It is an important part of modern differential geometrical control theory and has shown its effectiveness and success in some flight control design applications (see **Chapter One**).

To effectively use the method for the nonlinear control of aircraft with complicated dynamics and auxiliary devices like spoilers, a design procedure furnished with a sophisticated computer code was developed. It was based on the nonlinear modelling of the aircraft longitudinal dynamics and the employment of some major control objectives for actively utilising the spoiler control, giving the development of a decoupled multi-mode model-following control system which provided separated and precise control on the specific state variables that were of particular interest to the flight missions.

Here are also considered some practical problems encountered in the design of feedback linearization control systems, including the augmentation of the system to obtain stable inverse dynamics, pole-assignment of the feedback linearized system and the definition of the desired models. In particular, a detailed derivation of the inverse dynamics of the HAWK is given in which a uniform derivative order is defined and applied to each of the principal control variables by which various control modes of interest can be easily built up. The work described here contributes to the use of the NID methodology for flight control.

5.2 Summary of Basic NID Theory

5.2.1 Feedback linearization

The inverse dynamics method refers to the method of the feedback input-output linearization of a nonlinear system using its inverse dynamics. Based on the linearized system, system outputs can be decoupled and individually controlled and linear control techniques can be applied.

It is based on the following nonlinear system description in a neighbourhood of a point x_0:

$$\begin{aligned} \dot{x} &= A(x) + B(x)u \\ y &= C(x) \end{aligned} \qquad (5\text{-}1)$$

with state variable $x \in \Re^n$, control input $u \in \Re^m$, output variable $y \in \Re^m$ (here dim(y)=dim(u), so the system is a so called square system, with m outputs being independently controlled by m inputs). $A(x)(=[a_1(x),.., a_i(x),.., a_n(x)]')$, $B(x)(=[b_1(x),.., b_i(x),.., b_m(x)])$, $C(x)(=[c_1(x),.., c_i(x),.., c_m(x)]')$ are assumed smooth.

The inverse dynamics of (5-1) are constructed by differentiating the individual elements of y with respect to time a sufficient number of times, e.g.

$$y_j^{r_j} = L_A{}^{r_j} c_j + \sum_{i=1}^{m} L_{b_i}(L_A{}^{r_j-1} c_j)u_i \qquad j=1, ..., m \qquad (5\text{-}2)$$

where $L_A{}^i c_j$ stands for the ith Lie derivative of c_j with respect to A. For i=1, there is a scalar function defined by $L_A c_j = \nabla(c_j)A$, which stands for the directional derivative of c_j along the direction of the vector A.

Repeated Lie derivatives can be defined recursively:

$$\begin{aligned} &L_A{}^0 c_j = c_j; \\ &\quad \vdots \\ &L_A{}^k c_j = L_A(L_A{}^{k-1} c_j) = \nabla(L_A{}^{k-1} c_j)A \qquad \text{for } j = 1,...,m \end{aligned} \qquad (5\text{-}3)$$

and similarly,

$$L_{b_i} L_A c_j = \nabla(L_A c_j) b_i;$$
$$\vdots$$
$$L_{b_i}(L_A{}^{k-1} c_j) = \nabla(L_A{}^{k-1} c_j) b_i \qquad \text{for } i,j = 1,\ldots,m \qquad (5\text{-}4)$$

The process continues until the smallest integer r_j is found such that at least one of the control inputs u_i appears in $y_j^{r_j}$, i.e. until at least one of the $L_{b_i}(L_A{}^{r_j-1} c_j) u_i \neq 0$. The integer r_j is called the **relative order** of the output, which represents the inter-connection between the inputs and output and is decided by the definition of the output variables and of the system dynamics.

Define:

$$A^*(x) = \begin{bmatrix} L_A{}^{r_1} c_1 \\ \vdots \\ L_A{}^{r_m} c_m \end{bmatrix} \quad \text{and} \quad B^*(x) = \begin{bmatrix} L_{b_1}(L_A{}^{r_1-1} c_1) & \cdots & L_{b_m}(L_A{}^{r_1-1} c_1) \\ \vdots & \vdots & \vdots \\ L_{b_1}(L_A{}^{r_m-1} c_m) & \cdots & L_{b_m}(L_A{}^{r_m-1} c_m) \end{bmatrix} \qquad (5\text{-}5)$$

Equation (5-2) can be written as:

$$\begin{bmatrix} y_1^{r_1} \\ \vdots \\ y_m^{r_m} \end{bmatrix} = A^*(x) + B^*(x) u \qquad (5\text{-}6)$$

If $B^*(x) \in \Re^{m \times m}$ is bounded away from singularity, the state feedback control law:

$$u = -(B^*(x))^{-1} A^*(x) + (B^*(x))^{-1} v \qquad (5\text{-}7)$$

yields the closed-loop decoupled linear (input-output) system:

$$\begin{bmatrix} y_1^{r_1} \\ \vdots \\ y_m^{r_m} \end{bmatrix} = \begin{bmatrix} v_1 \\ \vdots \\ v_m \end{bmatrix} \qquad (5\text{-}8)$$

with the output y_j being solely controlled by the input v_j.

(5-7) is called a **decoupling controller**. The matrix $A^*(x)$ and the invertible matrix $B^*(x)$ are called the **transferring vector** and the **decoupling matrix** of the system , respectively. The system (5-1) is then said to have **relative order** $(r_1, ..., r_m)$ at x_0, and the scalar r $(=r_1+...+r_m)$ is called the **total relative order** of the system at x_0.

The total relative order is closely connected with the **zero dynamics** of the nonlinear system which are defined as the **internal dynamics** with the states rendered unobservable (r<n) and subject to the constraint that the outputs (and, therefore, all the derivatives of the outputs) are set to zero for all times concerned. And this in turn brings the definition of **minimum (non-minimum) phase nonlinear system** according to the stability of the zero dynamics.

An interesting case is that when the total relative order is equal to the system order n where there are no internal dynamics. In this case, a total input-state linearization of the original nonlinear system can be obtained through a control law in the form of (5-8) based on a set of output functions.

The necessary and sufficient conditions of globe input-state linearizability of the system (5-1) are: (HUNT et al, 1983)

1. the set $D=\{b_1,[A,b_1],...,ad_A^{r_1-1}(b_1),b_2,[A,b_2],...,ad_A^{r_2-1}(b_2),...,b_m,$ $[A,b_m],...,ad_A^{r_m-1}(b_m)\}$ spans an n-dimensional space.

2. the sets $D_j=\{b_1,[A,b_1],...,ad_A^{r_j-2}(b_1),b_2,[A,b_2],...,ad_A^{r_j-2}(b_2),...,b_m,$ $[A,b_m],...,ad_A^{r_j-2}(b_m)\}$ are involutive for j=1,...,m, i.e. for the vector field $\{D_1,D_2,...,D_m\}$ on $\Re^n$ there exist functions $\gamma_{ijk}(x)$ so that:

$$[D_i, D_j](x)=\sum_{k=1}^{m}\gamma_{ijk}(x)D_k(x), \quad 1\le i,j\le m, i\ne j.$$

3. the span of each D_j is equal to the span of $D_j \cap D$.

where $[A,b_j]$ is the Lie bracket of A and b_j, a third vector field defined by:

$$[A,b_j]=ad_Ab_j=\nabla b_jA-\nabla Ab_j \qquad (5\text{-}9)$$

and also where

$$ad_A^0 b_j = b_j$$
$$\vdots$$
$$ad_A^i b_j = [A, ad_A^{i-1} b_j] \qquad \text{for } i,j=1,2,... \qquad (5\text{-}10)$$

The verification for the input-state linearizability of the nonlinear system (5-1) in accordance with the above sufficient and necessary conditions has been proven a complicated and time-consuming job (MEYER et al, 1984). However, when just considering the sufficient condition, the nonlinear system in the form of (5-1) can be feedback linearizable if it can be put into **block lower triangular** form (MEYER & CICOLANI, 1981). This not only provides a much easier and more practical way of verifying linearizability but also points the way for a proper nonlinear modelling of invertible systems.

A nonlinear k-dimension block lower triangular system takes the following form:

$$\dot{x} = \begin{bmatrix} A_1(x_1,x_2) \\ A_2(x_1,x_2,x_3) \\ \vdots \\ A_{k-1}(x_1,x_2,...,x_k) \\ A_k(x_1,x_2,...,x_k) \end{bmatrix} + \begin{bmatrix} 0 \\ 0 \\ \vdots \\ 0 \\ B_k(x) \end{bmatrix} u \qquad (5\text{-}11)$$

The system is strictly m-axis in the sense that the dimension of x_j equals m for all integrator columns j from 1 to k so the system dimension is n=mxk. B_k is non-singular and m by m.

In MEYER's paper, the linearizability of the above system was proven through the existence of a discrete mapping for the system transformation. The block triangular systems are an interesting subset of the class of all systems satisfying the linearizable theorem. Yet the more interesting thing is to notice that through proper system augmentation, most aircraft can be modelled (or approximately modelled) as block triangular systems, this, therefore, considerably simplifies the verification procedure. The later design will demonstrate this.

5.2.2 Control of linearized systems

Once linearization has been achieved, many linear design methods, such as pole placement and model-tracking, can be applied.

The model-tracking problem for the linearized system (5-8) can be formulated by making use of the input:

$$v_i = {y_{mi}}^{r_i} + \alpha_{i1}({y_{mi}}^{r_i-1} - {L_A}^{r_i-1}c_i) + \cdots + \alpha_{ir_i}(y_{mi} - y_i), \quad i=1,..., m \tag{5-12}$$

where y_{mi} is the ith desired model output and the α_{ij} are the pole polynomial coefficients.

In the case of accurate system modelling, ${L_A}^{ri-1}c_i={y_i}^{ri-1}$, yielding:

$$v_i = {y_{mi}}^{r_i} + \alpha_{i1}({y_{mi}}^{r_i-1} - {y_i}^{r_i-1}) + \cdots + \alpha_{ir_i-1}(\dot{y}_{mi} - \dot{y}_i) + \alpha_{ir_i}(y_{mi} - y_i), \quad i=1,..., m \tag{5-13}$$

So the control for the linearized system, v_i, can be decomposed as:

$$v_i=v_{im}+v_{ifb} \tag{5-14}$$

where $v_{im} = {y_{mi}}^{(r_i)} + \alpha_{i1}{y_{mi}}^{(r_i-1)} + \cdots + \alpha_{ir_i-1}\dot{y}_{mi} + \alpha_{ir_i}y_{mi}$ which is defined as the output of a desired model while $v_{ifb} = -\alpha_{i1}{y_i}^{(r_i-1)} - \cdots - \alpha_{ir_i-1}\dot{y}_i - \alpha_{ir_i}y_i$ being the feedback needed for the pole-assignment of the closed-loop linearized system.

Substitution of v_i into (5-8) with (5-13) yields:

$${e_i}^{r_i} + \alpha_{i1}{e_i}^{r_i-1} + \cdots + \alpha_{ir_i}e_i = 0 \qquad \text{for } i=1,...m \tag{5-15}$$

where $e_i=y_{mi}-y_i$.

So asymptotic model-tracking can be obtained for minimum-phase systems when the desired model output and its derivatives, y_{mi}, $\dot{y}_{mi}$,....,,${y_{mi}}^{(r_i-1)}$ (i=1,..., m), are bounded and all the poles defined by $s^{ri} + \alpha_{i1}s^{ri-1} + \cdots + \alpha_{iri} = 0$, are in the left-half plane [SASTRY & BODSON, 1989].

Fig. 5-1 is an explanatory diagram showing a NID control system. The model tracking mechanism is detailed in **Fig. 5-2.**

5.3 Modelling of Nonlinear Aircraft for NID Control

As shown in **Appendix One**, the aircraft dynamics take the general nonlinear form:

$$\dot{x} = f(x,u)\ , \qquad y=C(x) \qquad (5\text{-}16)$$

with state variable $x \in \Re^n$, control input $u \in \Re^m$ and system output $y \in \Re^m$.

To get the linear form of (5-1), an appropriate transformation is required. This can be accomplished by augmenting the system dynamics with derivatives of appropriate control inputs. However, in the interest of forming a well-behaved block triangular system, special measures should be taken.

For longitudinal control, where spoilers are supposed to be in principal use, if the interesting control variables are defined as the set $Y_c=[V\ \gamma\ \alpha(\theta)]$ and the controls are the elevator, the thrust and the spoiler, where the spoiler model has the general nonlinear form $C_{sp}= K_{sp}\lambda(\alpha)\sin(\delta_{sp})$, the block triangular system based on the output set can be found by:

1) Introducing the nonlinear spoiler model in **Chapter Two** (2-31~2-33, **Spoiler Model One**) into the aircraft model by augmenting the aircraft system dynamics with the first derivative of the spoiler control input δ_{sp} so that δ_{sp} becomes a new state variable while the input from u_{sp} ($\dot{\delta}_{sp} = -a_{sp}\delta_{sp} + a_{sp}u_{sp}$) can therefore be put into the form $b_{sp}(x)u_{sp}$ (see **Fig. 5-3**), where the corresponding first-order lag represents the spoiler actuator dynamics which can be expected to have a high bandwidth (e.g. a_{sp}=40.0).

2) Defining a first-order lag model for the jet-engine dynamics (e.g. a_t=0.5) so the system dynamics are also augmented by the first derivative of the thrust control δ_t, giving $\dot{\delta}_t = -a_t\delta_t + a_t u_t$ (see **Fig. 5-3**). This is also demanded by matching the relative order of V with respect to the spoiler control.

3) Letting $u_e=\delta_e$.

So, the aircraft longitudinal dynamics can be put into the triangular form upon which the stable inverse dynamic(system linearization) can be constructed for the NID control laws:

$$\begin{bmatrix}\dot{x}_1\\ \dot{x}_2\end{bmatrix}=\begin{bmatrix}A_1(x_1,x_2)\\ A_2(x_1,x_2)\end{bmatrix}+\begin{bmatrix}0\\ B_2(x)\end{bmatrix}u \qquad (5\text{-}17)$$

which is a 2-dimensional 3-axis block lower-triangular system with

$$x=\begin{bmatrix}x_1\\ x_2\end{bmatrix},\quad x_1=\begin{bmatrix}V\\ \gamma\\ \alpha(\theta)\end{bmatrix},\quad x_2=\begin{bmatrix}q\\ \delta_t\\ \delta_{sp}\end{bmatrix}\quad \text{and}\quad u=\begin{bmatrix}u_e\\ u_t\\ u_{sp}\end{bmatrix}.$$

(refer to **Appendix One, A.4**)

5.4 A Procedure for NID Flight Control Synthesis

The NID control synthesis is applied to system model (5-1) to generate nonlinear controllers. For aircraft control, most of important output variables can be, or approximately be, expressed as:

$$y=Cx \qquad (5\text{-}18)$$

where C is a time-invariant (mxn) output matrix.

This provides some simplification for the formation of multi-mode nonlinear controls and for the development of an efficient procedure and program package for the synthesis of a variety of the mission-defined controllers. Combined with the system modelling (5-17) and the definition of output control variables, the major steps involved in the controller development are:

1) Consider the output to be y=Cx , where C is a (mxn) constant output matrix and y is chosen from the output control variable set. Here in the longitudinal control y_c= [V, γ, α, θ, q, δ_t, δ_{sp}]'.

2) Form the derivatives $L_A x,\ldots,[\frac{\partial}{\partial x}(L_A^{r_i-1}x)]A(x),[\frac{\partial}{\partial x}(L_A^{r_i-1}x)]B(x)$, where the derivative order r_i depends on the system modelling and on the control variable set. For the model of (5-17) and the selections of the group above, r_i=2 was used for x_1 while r_i=1 was for x_2.

3) Design multi-mission-defined controllers by simply assigning the output matrix C according to mission objectives and the control dimension m, and performing the following computations for the inverse dynamics matrices:

$$A(x)^*_{mxn} = C[\frac{\partial}{\partial x} L_A{}^{r_i-1} x]A(x);\ \ B(x)^*_{mxm} = C[\frac{\partial}{\partial x} L_A{}^{r_i-1} x]B(x). \tag{5-19}$$

In the case of $B(x)^*$ being non-singular, the controller is given by:

$$u = (B^*(x))^{-1}(v - A^*(x)) \tag{5-20}$$

The coefficients of the designed closed-loop pole polynomial, defined by v_{ifb} in (5-14), for each decoupled output variable are chosen by referring to the flight quality criteria Mil-F-8785C. **Table 5.1** lists the typical data for the output control variables V, γ, θ, and α.

Table 5.1 Pole Polynomial Coefficients

Output Variable Y	α_{i1}	α_{i2}
V	5.0	4.0
γ	3.0	4.0
θ	3.0	4.0
α	3.0	4.0

These coefficients assignments define the desired closed-loop systems which stability qualities meet the first-level specifications.

In the path angle γ channel, for example, the coefficient assignment gives (r_γ=2, from (5-13)):

$$v_\gamma = v_{\gamma m} - \alpha_{\gamma 1}\dot{\gamma} - \alpha_{\gamma 2}\gamma$$

then from (5-8):

$$\ddot{\gamma} = -\alpha_{\gamma 1}\dot{\gamma} - \alpha_{\gamma 2}\gamma + v_{\gamma m} \tag{5-21}$$

or, in transfer function form:

$$\gamma(s) = \frac{v_{\gamma m}}{s^2 + \alpha_{\gamma 1}s + \alpha_{\gamma 2}} \tag{5-22}$$

which corresponds to a second-order system with the natural frequency ω_n=2(1/s) and a damping ratio ζ=0.75 which give first-level flight quality as far as the short period dynamics of aircraft are concerned.

The model reference terms $v_{\gamma m}$ ($y_{m\gamma}$, $\dot{y}_{m\gamma}$ and $\ddot{y}_{m\gamma}$) are formed by a desired model generator, which has the input y_{cm} from a trajectory command generator and takes the form:

$$\ddot{y}_{m\gamma} + d_{m\gamma 1}\dot{y}_{m\gamma} + d_{m\gamma 2}y_{m\gamma} = y_{cm\gamma} \qquad (5\text{-}23)$$

So, if $d_{m\gamma 1}$ and $d_{m\gamma 2}$ are taken to be the same as $\alpha_{\gamma 1}$ and $\alpha_{\gamma 2}$, as previously illustrated, we have:

$$\gamma(s) = \frac{y_{cm\gamma}}{s^2 + \alpha_{\gamma 1}s + \alpha_{\gamma 2}} \qquad (5\text{-}24)$$

or $\gamma(s)=y_{m\gamma}(s)$, which shows the desirable model tracking in the case of precise system modelling and control.

It should be pointed out that owing to the delay in the servo-dynamics (typically in the elevator and the thrust channels) and owing to the nonlinearities caused by saturations in both the amplitude and rate of the control inputs (see **Appendix One**), appropriate and separate adjustment in the coefficients of the v_{im} (desired model) and v_{ifb} (feedback control) in (5-14) to adapt the trajectory command input is necessary and suggested.

5.5 Application of NID to the HAWK Longitudinal Flight Control

5.5.1 Definition of a set of principal control variables

The above design procedure was applied to the development of a longitudinal NID flight control system for the HAWK aircraft.

For systematic programming and efficient controller synthesis, a set of principal output control variables was defined which had the same dimension as the control inputs (m) and from the derivatives of which controllers based on other sets of output variables can be easily generated.

According to the modelling of the HAWK longitudinal dynamics (**Appendix One, A.4**), the principal control variables are chosen as the flight path velocity V, the path angle γ and the incidence α, i.e. $y_p=x_1=[V,\ \gamma,\ \alpha]'$. The nonlinear controller corresponding to this output vector was developed upon the computation of the second-order Lie derivatives.

5.5.2 The first Lie derivatives of the principal control variables

The first Lie derivatives of the principal control variables can be easily formed by referring to the aircraft dynamics equations:

$$L_A(y_p)=\dot{y}_p=A_1(x)=\begin{bmatrix}\dfrac{-(D+mg\sin\gamma)}{m}\\ \dfrac{(L-mg\cos\gamma)}{mV}\\ q-\dot{\gamma}\end{bmatrix} \qquad (5\text{-}25)$$

where from the HAWK modelling:

$$L=\frac{1}{2}\rho V^2SC_L+C_{t\max}(H,M)\delta_t\sin\alpha, D=\frac{1}{2}\rho V^2SC_D-C_{t\max}(H,M)\delta_t\cos\alpha;$$

$$C_L(M,\alpha,\delta_{sp})=C_{L0}(M)+C_{L\alpha}(M,\alpha)+C_{LSP}(\alpha,\delta_{sp}),$$

$$C_D(M,\alpha,\delta_{sp})=C_{D0}+C_{DL}(M,\alpha,\delta_{sp})+C_{DSP}(\alpha,\delta_{sp}).$$

So if the inputs are defined as those in (5-17), there is:

$$L_{b_i}(L_A{}^0y_p)=0 \qquad \text{for i=1, 2, 3.} \qquad (5\text{-}26)$$

5.5.3 The second Lie derivatives of the principal control variables

According to (5-3) and (5.4), the second-order Lie derivatives of the principal control variables can be expressed as:

$$L_A{}^2(y_p)=[\frac{\partial}{\partial x}L_A(y_p)]A(x) \quad \text{and} \quad L_BL_A(y_p)=[\frac{\partial}{\partial x}L_A(y_p)]B(x) \qquad (5\text{-}27)$$

So the key step turns out to be to find the **Jacobian**:

$$\frac{\partial L_A(y_p)}{\partial x} = \frac{\partial(\dot{y}_p)}{\partial x} \qquad (5\text{-}28)$$

Since $y_p=[V, \gamma, \alpha]'$, we need $\frac{\partial}{\partial x}(L_A(V)), \frac{\partial}{\partial x}(L_A(\gamma)), \frac{\partial}{\partial x}(L_A(\alpha))$, which are given by:

1. $$\frac{\partial}{\partial x}(L_A(V)) = \frac{\partial \dot{V}}{\partial x} = [\frac{\partial \dot{V}}{\partial V}, \frac{\partial \dot{V}}{\partial \gamma}, \frac{\partial \dot{V}}{\partial \alpha}, \frac{\partial \dot{V}}{\partial q}, \frac{\partial \dot{V}}{\partial \delta_t}, \frac{\partial \dot{V}}{\partial \delta_{sp}}], \qquad (5\text{-}29)$$

where $$\frac{\partial \dot{V}}{\partial V} = -(\rho V S C_D + \frac{1}{2}\rho V^2 S \frac{\partial C_D}{\partial V} - \frac{\partial C_{t\,max}}{\partial V}\delta_t \sin\alpha) / m$$

$$\frac{\partial \dot{V}}{\partial \gamma} = -g\cos\gamma$$

$$\frac{\partial \dot{V}}{\partial \alpha} = -[\frac{1}{2}\rho V^2 S \frac{\partial C_D}{\partial \alpha} + C_{t\,max}\delta_t \sin\alpha)] / m$$

$$\frac{\partial \dot{V}}{\partial q} = 0$$

$$\frac{\partial \dot{V}}{\partial \delta_t} = C_{t\,max}\cos\alpha / m$$

$$\frac{\partial \dot{V}}{\partial \delta_{sp}} = -(\frac{1}{2}\rho V^2 S \frac{\partial C_D}{\partial \delta_{sp}}) / m.$$

2. $$\frac{\partial}{\partial x}(L_A(\gamma)) = \frac{\partial \dot{\gamma}}{\partial x} = [\frac{\partial \dot{\gamma}}{\partial V}, \frac{\partial \dot{\gamma}}{\partial \gamma}, \frac{\partial \dot{\gamma}}{\partial \alpha}, \frac{\partial \dot{\gamma}}{\partial q}, \frac{\partial \dot{\gamma}}{\partial \delta_t}, \frac{\partial \dot{\gamma}}{\partial \delta_{sp}}], \qquad (5\text{-}30)$$

where: $$\frac{\partial \dot{\gamma}}{\partial V} = (\frac{\frac{\partial}{\partial V}(L - mg\cos\gamma)}{mV} - \frac{\dot{\gamma}}{V})$$

$$= (\rho V S C_L + \frac{1}{2}\rho V^2 S \frac{\partial C_L}{\partial V} + \frac{\partial C_{t\,max}}{\partial V}\delta_t \sin\alpha - m\dot{\gamma}) / mV$$

$$\frac{\partial \dot{\gamma}}{\partial \gamma} = g\sin\gamma / V$$

$$\frac{\partial \dot{\gamma}}{\partial \alpha} = (\frac{1}{2}\rho V^2 S \frac{\partial C_L}{\partial \alpha} + C_{t\,max}\delta_t \cos\alpha) / mV$$

$$\frac{\partial \dot{\gamma}}{\partial q} = 0$$

$$\frac{\partial \dot{\gamma}}{\partial \delta_t} = C_{t\,max}\sin\alpha / mV$$

$$\frac{\partial \dot{\gamma}}{\partial \delta_{sp}} = (\frac{1}{2}\rho V^2 S \frac{\partial C_{LSP}}{\partial \delta_{sp}}) / mV.$$

$$3.\ \frac{\partial}{\partial x}(L_A(\alpha)) = \frac{\partial \dot{\alpha}}{\partial x} = [\frac{\partial \dot{\alpha}}{\partial V}, \frac{\partial \dot{\alpha}}{\partial \gamma}, \frac{\partial \dot{\alpha}}{\partial \alpha}, \frac{\partial \dot{\alpha}}{\partial q}, \frac{\partial \dot{\alpha}}{\partial \delta_t}, \frac{\partial \dot{\alpha}}{\partial \delta_{sp}}], \qquad (5\text{-}31)$$

where in longitudinal control there is $\dot{\alpha} = q - \dot{\gamma}$, therefore:

$$\frac{\partial \dot{\alpha}}{\partial V} = -\frac{\partial \dot{\gamma}}{\partial V},\quad \frac{\partial \dot{\alpha}}{\partial \gamma} = -\frac{\partial \dot{\gamma}}{\partial \gamma},\quad \frac{\partial \dot{\alpha}}{\partial \alpha} = -\frac{\partial \dot{\gamma}}{\partial \alpha},$$

$$\frac{\partial \dot{\alpha}}{\partial q} = 1.0,\quad \frac{\partial \dot{\alpha}}{\partial \delta_t} = -\frac{\partial \dot{\gamma}}{\partial \delta_t},\quad \frac{\partial \dot{\alpha}}{\partial \delta_{sp}} = -\frac{\partial \dot{\gamma}}{\partial \delta_{sp}}.$$

5.5.4 Design of the principal controller

The transferring vector $A_p^*(x)$ and the decoupling matrix $B_p^*(x)$ for the principal output variables can therefore be defined by:

$$A_p^*(x)=[\frac{\partial}{\partial x}L_A(y_p)]A(x) \quad \text{and} \quad B_p^*(x)=[\frac{\partial}{\partial x}L_A(y_p)]B(x) \qquad (5\text{-}32)$$

where A(x) and B(x) are modelled as that in **Appendix One (A.4)**.

In the case of $B_p^*(x)$ non-singular, the feedback controller for the principal variables is given by:

$$u_p = (B_p^*(x))^{-1}(v - A_p^*(x)) \qquad (5\text{-}33)$$

Singularity Conditions:

$B_p^*(x)$ (see (5-32)) can be further expressed as

$$B_p^* = \begin{bmatrix} \frac{\partial \dot{V}}{\partial V} & \frac{\partial \dot{V}}{\partial \gamma} & \frac{\partial \dot{V}}{\partial \alpha} & 0.0 & \frac{\partial \dot{V}}{\partial \delta_t} & \frac{\partial \dot{V}}{\partial \delta_{sp}} \\ \frac{\partial \dot{\gamma}}{\partial V} & \frac{\partial \dot{\gamma}}{\partial \gamma} & \frac{\partial \dot{\gamma}}{\partial \alpha} & 0.0 & \frac{\partial \dot{\gamma}}{\partial \delta_t} & \frac{\partial \dot{\gamma}}{\partial \delta_{sp}} \\ \frac{\partial \dot{\alpha}}{\partial V} & \frac{\partial \dot{\alpha}}{\partial \gamma} & \frac{\partial \dot{\alpha}}{\partial \alpha} & 1.0 & \frac{\partial \dot{\alpha}}{\partial \delta_t} & \frac{\partial \dot{\alpha}}{\partial \delta_{sp}} \end{bmatrix} \begin{bmatrix} 0 & & \\ 0 & & \\ 0 & & \\ b_q(x) & & \\ & a_t & \\ & & a_{sp} \end{bmatrix}$$

$$= \begin{bmatrix} 0 & \frac{\partial \dot{V}}{\partial \delta_t} a_t & \frac{\partial \dot{V}}{\partial \delta_{sp}} a_{sp} \\ 0 & \frac{\partial \dot{\gamma}}{\partial \delta_t} a_t & \frac{\partial \dot{\gamma}}{\partial \delta_{sp}} a_{sp} \\ b_q(x) & \frac{\partial \dot{\alpha}}{\partial \delta_t} a_t & \frac{\partial \dot{\alpha}}{\partial \delta_{sp}} a_{sp} \end{bmatrix} \qquad (5\text{-}34)$$

This matrix will become singular when:

$$\det(B_p^*) = a_t \cdot a_{sp} \cdot b_q(x) \cdot \left(\frac{\partial \dot{V}}{\partial \delta_t} \cdot \frac{\partial \dot{\gamma}}{\partial \delta_{sp}} - \frac{\partial \dot{V}}{\partial \delta_{sp}} \cdot \frac{\partial \dot{\gamma}}{\partial \delta_t}\right) = 0 \qquad (5\text{-}35)$$

So, the inverse dynamics of the aircraft with m=3 will be unsolvable when:

(1) $a_t \cdot a_{sp} \cdot b_q(x)=0$; control device saturation or ceasing working. For individual cases (elevator or thrust or spoiler), the controller will be automatically switched to one of the reduced-dimension modes discussed next in **5.5.4**.

(2) The relation between the spoiler control and the thrust control fulfils:

$$\frac{\partial \dot{V}}{\partial \delta_t} \cdot \frac{\partial \dot{\gamma}}{\partial \delta_{sp}} = \frac{\partial \dot{V}}{\partial \delta_{sp}} \cdot \frac{\partial \dot{\gamma}}{\partial \delta_t} \qquad (5\text{-}36)$$

From (5-29) and (5-30), (5-36) can be expressed as

$$\frac{\partial C_{LSP}}{\partial \delta_{sp}} = -\frac{\partial C_D}{\partial \delta_{sp}} \tan\alpha \qquad (5\text{-}37)$$

During the synthesis of the nonlinear controller (5-33) at each time step, the above relation is checked by the program, in conjunction with the computation of (5-29) and (5-30). As it exists, the controller will be automatically switched to a basic control mode (e.g. **Controller Four** in **5.5.4**) using the conventional controls u_e and u_t.

5.5.5 Design of multi-mode controllers

After the definition of the inverse dynamics for the principal output variables, controllers in the form of (5-20) for other sets of output variables given by $y=C_{mxm}y_p$ can be easily constructed. Here are some major control modes.

Controller One: m=3, $y_1=[V, \gamma, \theta]'$

$$A_1^*=C_1A_p^*, \quad B_1^*=C_1B_p^* \qquad ; \text{with } C_1=\begin{bmatrix}1 & 0 & 0\\ 0 & 1 & 0\\ 0 & 1 & 1\end{bmatrix} \text{(for } \theta=\alpha+\gamma).$$

Controller Two: m=3, $y_2=[V, \gamma, \alpha]'$

$$A_2^*=A_p^*, \qquad B_2^*=B_p^*$$

Controller Three: m=3, $y_3=[V, \alpha, \theta]'$

$$A_3^*=C_3A_p^*, \quad B_3^*=C_3B_p^* \qquad ; \text{with } C_3=\begin{bmatrix}1 & 0 & 0\\ 0 & 0 & 1\\ 0 & 1 & 1\end{bmatrix}.$$

Also, controllers for conventional control using elevator and thrust with spoiler angle set to an arbitrary value can be synthesized as:

Controller Four: m=2, $y_4=[V, \theta]'$

$$A_4^*=C_4A_p^*, \quad B_4^*=C_4B_p^*=[B_4^*{}_{(12)} \;\; b_4^*{}_{(3)}]'; \text{ with } C_4=\begin{bmatrix}1 & 0 & 0\\ 0 & 1 & 1\end{bmatrix}.$$

In this case, the spoiler is treated as a state variable so only the (2x2) matrix $B_4^*{}_{(12)}$ will be used for the system inverse, giving the controller:

$$u_4=(B_{4(12)}^*(x))^{-1}(\nu-A_4^*(x)) \qquad (5\text{-}38)$$

Clearly, this mode can also be used as a back-up mode to which the full dimensional controller will be switched when there is a failure in spoiler control or the occurrence of the singularity relation (5-37). In the same way, controller 5 is developed.

Controller Five: m=2, $y_5=[V, \alpha]'$

$$A_5^*=C_5A_p^*, \quad B_5^*=C_5B_p^*=[B_5^*{}_{(12)} \;\; b_5^*{}_{(3)}]'; \text{ with } C_5=\begin{bmatrix}1 & 0 & 0\\ 0 & 0 & 1\end{bmatrix}.$$

While control mode 6 is specially designed for fast deceleration and pitch attitude control, using the spoiler and the elevator. This is realized through the following C_6

assignment where the actual output control variables are γ and θ and the control inputs are the elevator and the spoiler.

Controller Six: m=2, $y_6=[\gamma, \theta]'$

$$A_6^*=C_6A_p^*, \quad B_6^*=C_6B_p^*=[B_6^*(13) \ b_6^*(2)]'; \text{ with } C_6=\begin{bmatrix}0 & 1 & 0\\ 0 & 1 & 1\end{bmatrix},$$

where the decoupling matrix is $B_6^*(13)$.

Finally, reduced-dimension control mode for using the thrust and spoiler controls only is:

Controller Seven: m=2, $y_7=[V, \gamma]'$

$$A_7^*=C_7A_p^*, \quad B_7^*=C_7B_p^*=[B_7^*(23) \ b_7^*(1)]'; \text{ with } C_7=\begin{bmatrix}1 & 0 & 0\\ 0 & 1 & 0\end{bmatrix}.$$

where the decoupling matrix is $B_7^*(23)$.

5.6 Configuration of LIDFCS of the HAWK

The final configuration of the longitudinal inverse dynamics flight control system (LIDFCS) for the HAWK is shown in **Fig. 5-4**.

The design of the NID flight control was incorporated with the previous works in the flight simulator through the development of a functional subroutine' IDMFCT' and introducing it into the simulator package 'HAWKSIM1'. The major tasks of the subroutine include the definition the control modes according to mission simulation types , the synthesis of the model tracking controllers at each time step and the data exchange with the simulator using the common blocks. It is late combined with the parameter adaptive control logic (**Chapter Seven**) for the robustness of the NID control. **Fig. 5-5** shows the flow chart of the subroutine.

During the simulation, the elevator servo dynamics, which were modelled as $G_{es}(s)=\dfrac{20}{s+20}$ (see **Fig. 5-3**), and the nonlinearities due to saturations in both amplitude and rate of the control servo-dynamics were taken into account, resulting in appropriate

and mission-defined adjustment in both the parameters of the desired model generator and the closed-loop pole polynomials.

5.7 Concluding Remarks

In this chapter, a nonlinear flight control system --- LIDFCS --- for the HAWK is developed using the nonlinear inverse dynamics control techniques. The design process has demonstrated that the nonlinear inverse dynamics methodology is an effective method for synthesizing nonlinear controllers and for generating decoupled, multi-mode flight control systems for modern aircraft. The desirable qualities of the design will be further illustrated in **Chapter Six** in which are presented successful applications of the various active control schemes to the HAWK.

Combined with the system development, a number of new techniques for more efficient use of the NID method for flight control were studied, including the introduction of flight quality specifications into the desired model dynamics and into the pole polynomials, and the development of a design procedure for the formation of multi-mode controllers based on the linear output equation (5-18), the choice of a set of principal output control variables and the use of a uniform relative order. The system development work has proven these techniques to be successful.

Figure 5-1 Centralized form of a NID control system

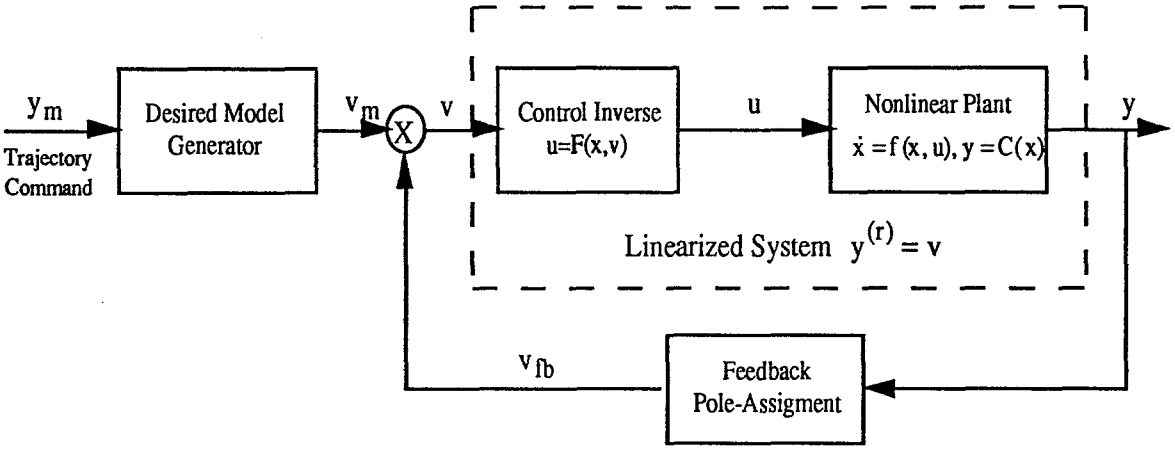

Figure 5-2 Model tracking of the linearized system

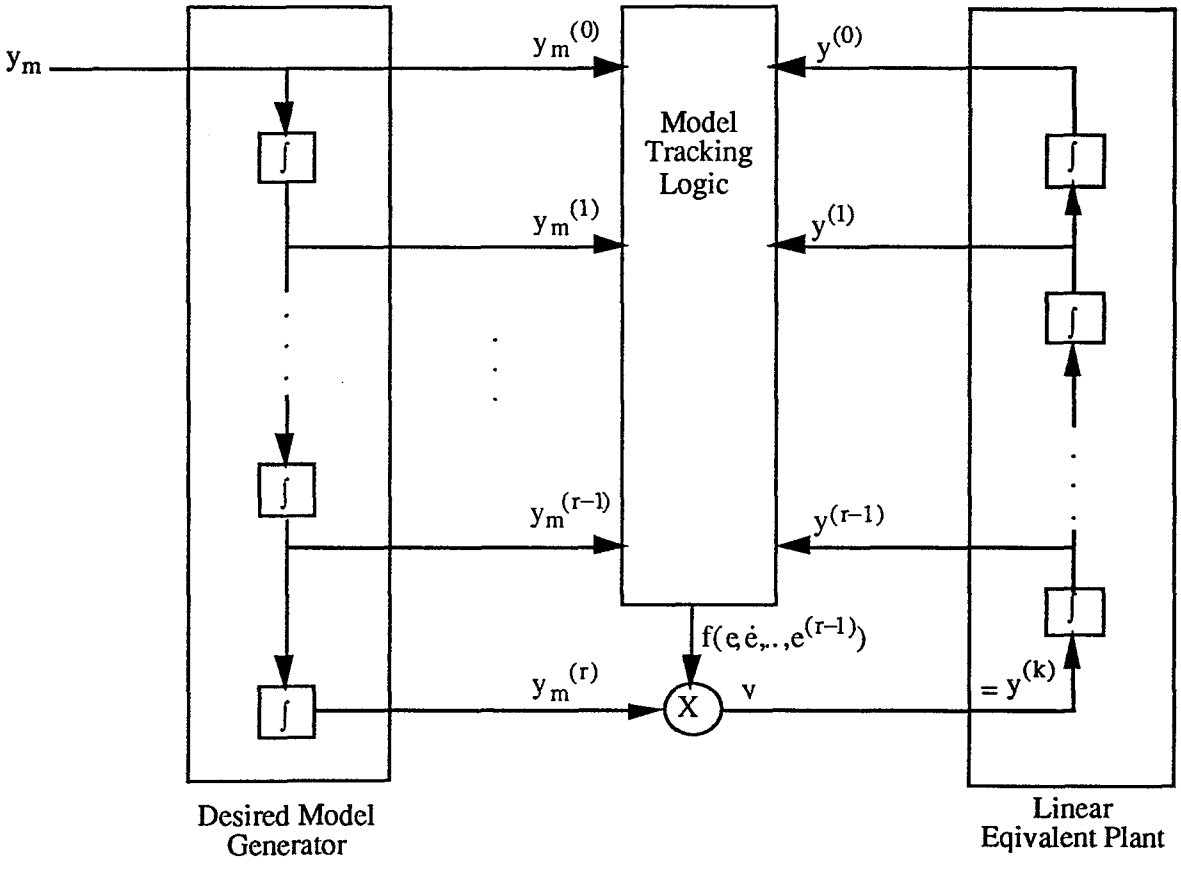

Figure 5-3 Actuator dynamics modelling and system augmentation

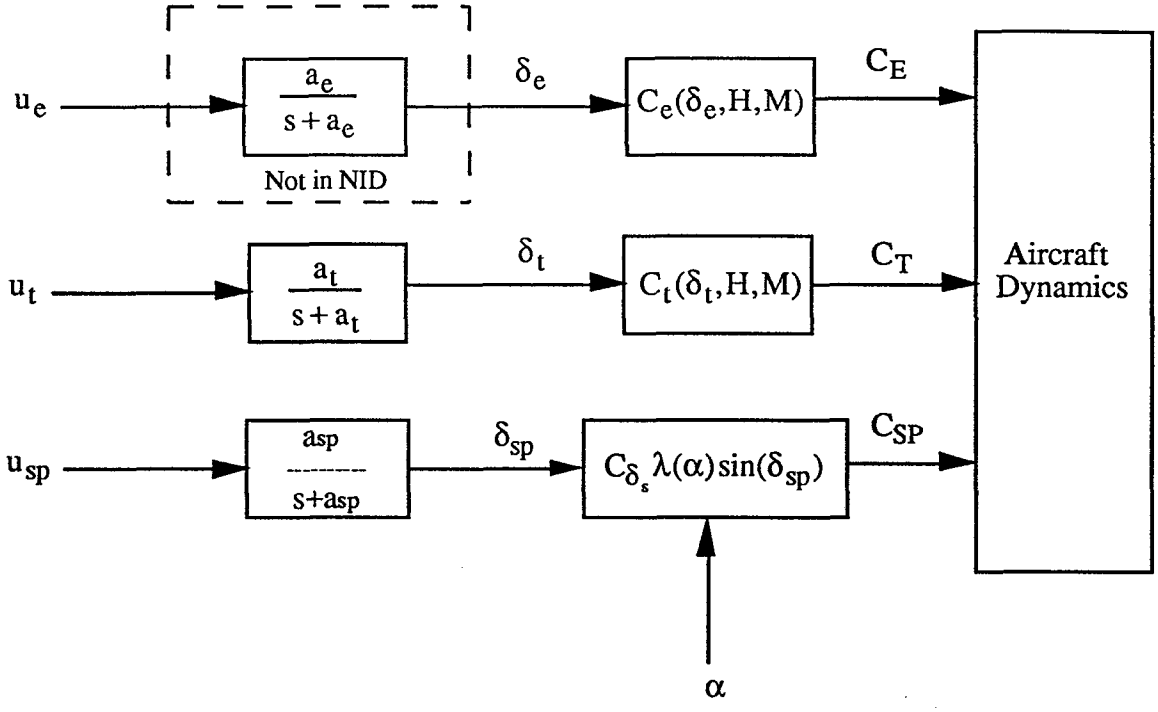

Figure 5-4 LIDFCS configuration

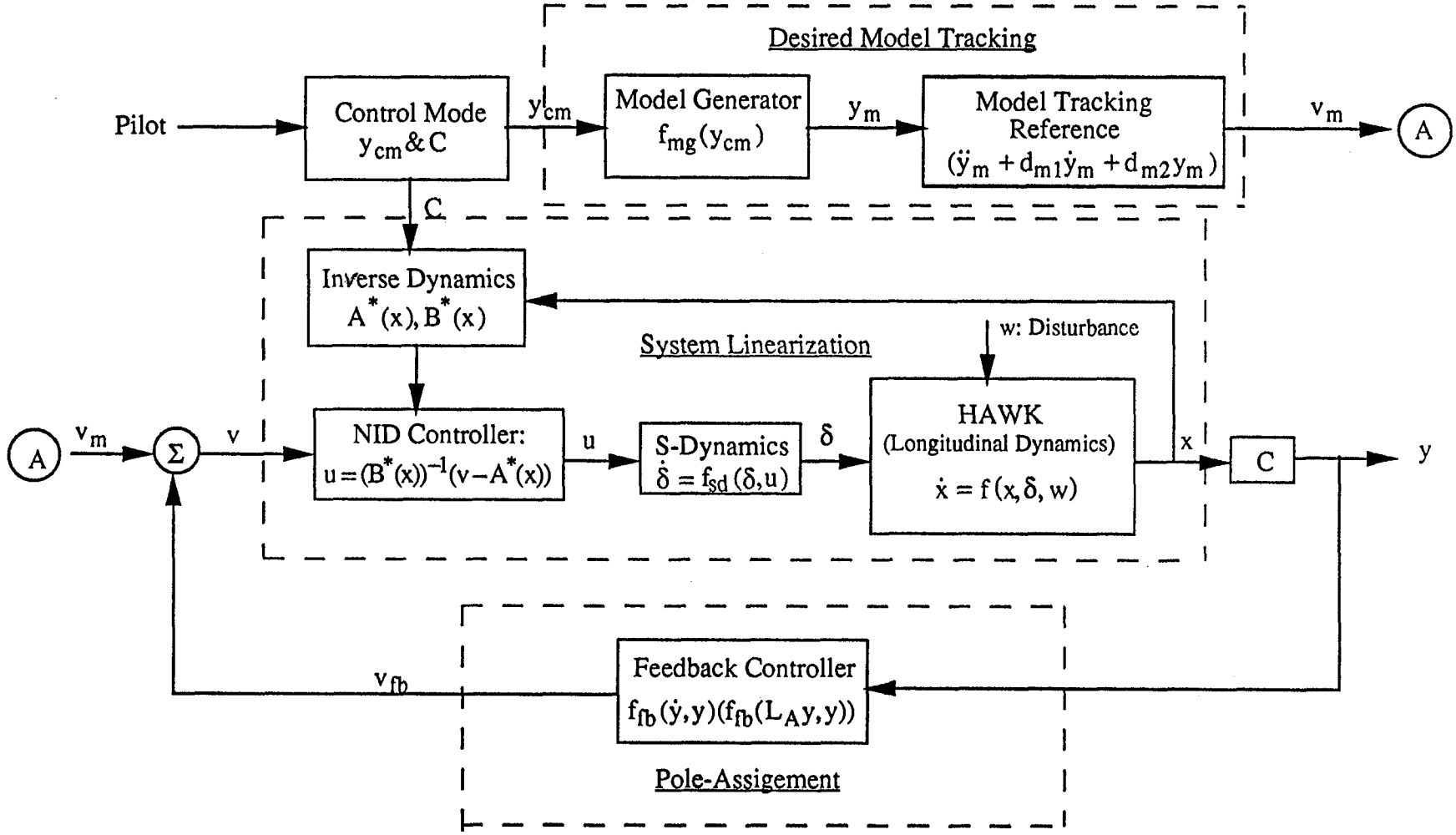

Figure 5-5 Flow chart of program 'IDMFCT'

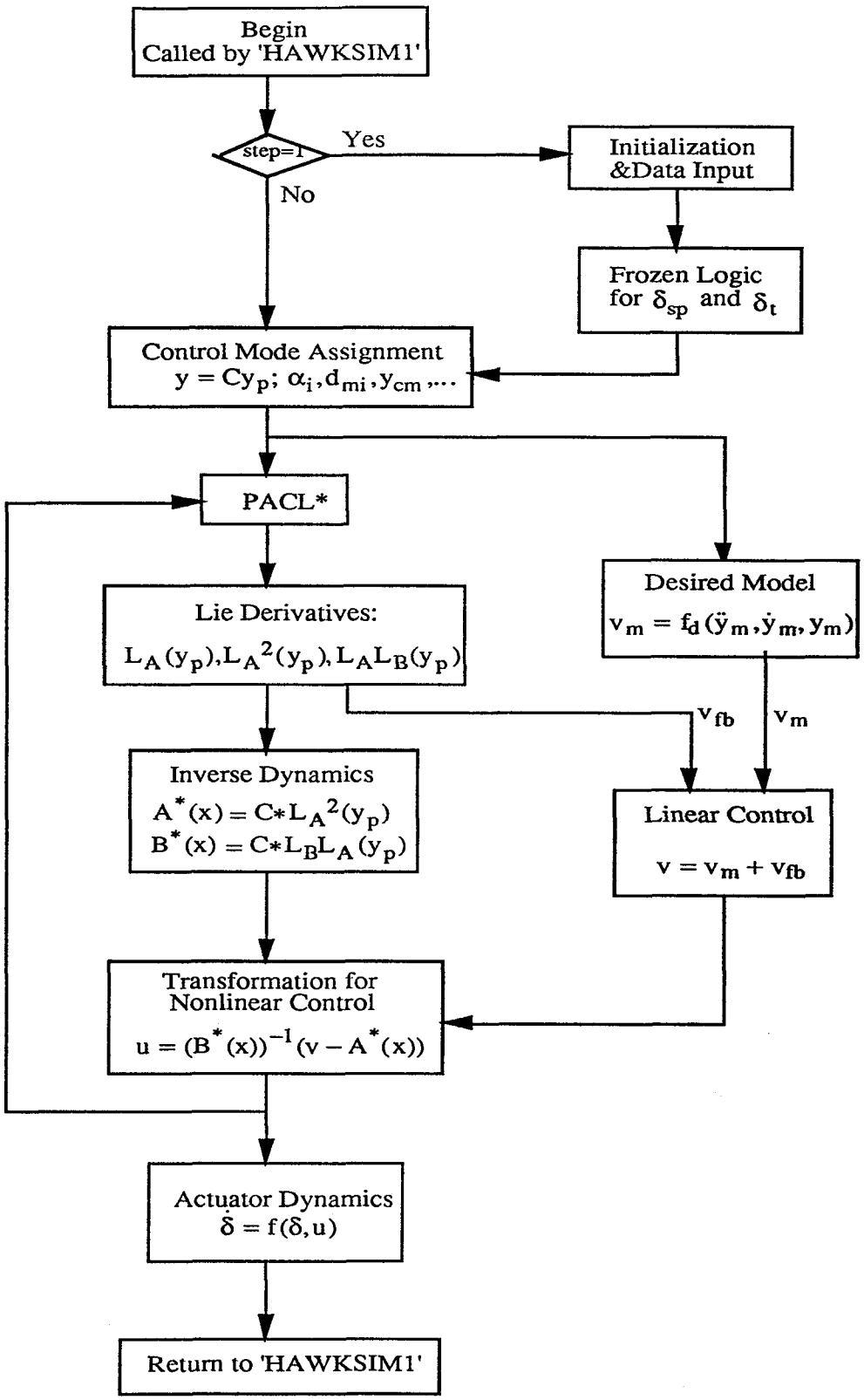

* Parameter Adaptive Control Logic (see **Chapter Seven**)

Chapter Six

AIRCRAFT PERFORMANCE ENHANCEMENT USING SPOILER CONTROL

6.1 General Remarks

The theme of this chapter is on the application studies of spoiler control to the enhancement of aircraft performance.

The development of the LIDFCS in **Chapter Five** provides the basis for active control of aircraft using spoilers. The studies in this chapter were made on some typical flight control applications which explore the spoiler control potential and its significant role in ACT. These have included: (1) decoupled attitude and trajectory control for superior manoeuvre of aircraft, which utilises the unique control effect of spoilers on the flight path angle; (2) fast deceleration control, which takes advantages of significant spoiler drag; and (3) control augmentation for gust/turbulence and microburst alleviation, which benefit from the spoiler feature of rapid force adjustment.

The procedures involved in the application studies of spoiler control can be summarized as:

1) Define control tasks which are within the beneficial usage region of spoilers, for conventional spoilers, that is normally characterized by rapid and effective control in positive drag and negative lift directions.

2) Find appropriate groups of the output control variables corresponding to the mission objectives of interest and then match these with the control modes (controllers) in the LIDFCS.

3) Perform control law programming, simulations and evaluations. In most of the augmentation control cases, adaptive adjustments in the spoiler off-setting balance angle and the system parameters are required for full use of spoiler control effectiveness.

Combined with the spoiler control applications, this Chapter also initiates the new control concepts of the programmed mode-shifting flight control and the microburst penetrating flight control, and deals with the problems in conjunction with the flight control simulations. Detailed simulation results are given.

6.2 Summary of Longitudinal Flight Control Modes

The concept of **control mode** is closely connected with a multi-controllers system and refers to the control state where a controller is adopted for some mission objective. For a NID flight control system, the control modes are defined by, and connected with, the choices of the groups of the output control variables and the controllers as described in **Chapter 5**. According to these, **Table 6-1** summarizes some major control modes designed for the longitudinal flight control of the HAWK, with the class A for the conventional control and class B for the unconventional control. The modes A1 and A2 are designed for the conventional control augmentation in aircraft velocity and attitude while B1 ~ B4 are the control modes utilising the spoiler control for some unconventional control purposes. The mission objectives for which a control mode is expected to be applicable are listed in the right hand column of the Table.

For the implementation of the control system on a Fly-by-Wire system, these control modes will be constructed through different data bases and program routines so they are flexibly switched from one to another according to different flight mission objectives and system performance requirements.

Table 6-1 Summary of Longitudinal Control Modes

Control Mode	Output Control Variables	Mission Objectives
A (conventional)		
A1 (Controller 4*)	[V θ]	Cruising
A2 (Controller 5)	[V α]	Conventional Trajectory Manoeuvring
B(unconventional)		
B1 (Controller 6)	[θ γ]	Unconventional Level-flight Decelerating.
B2 (Controller 1)	[V γ θ]	Decoupled V, γ, θ Manoeuvring (take-off & landing)
B3 (Controller 2)	[V γ α]	Decoupled V, γ, α Manoeuvring
B4 (Controller 3)	[V α θ]	Decoupled V, θ, α Manoeuvring

* : as defined in **Chapter Five.**

6.3 Spoiler Control Application --- Case One: Decoupled Flight Attitude and Trajectory Control

6.3.1 General remarks

From the view point of decoupled flight control, the introduction of spoilers provides an extra control freedom for aircraft. The advantages of the extra freedom can be seen through the flexibility it offers in sophisticated control synthesis, the possibility of back-up system re-constitution for conventional control, and, in particular, the unique and unconventional decoupled control abilities it can import to aircraft.

These features have become even more significant when the spoiler control is combined with the LIDFCS for control augmentation of HAWK, where an extra decoupled output control variable can therefore be made available. Based on the increased dimension of the output control variables, some unconventional controls ,such as separated angular variable (θ, γ or α) manoeuvres, can be realized.

6.3.2 Programming of decoupling control

To further illustrate the decoupled control abilities, a special longitudinal flight control mission was designed for the HAWK aircraft flying along a trajectory containing both the conventional and unconventional manoeuvres. The trajectory, shown in **Fig. 6-1**, involves the successive motions of climb, fuselage pointing (pure pitch control with flight trajectory fixed), and level-attitude descent.

The control programming was made by matching the control mission with the longitudinal control modes shown in **Table 6-1**. According to the mission, three of the modes: the conventional V-α manoeuvring (control mode A2), the decoupled V-γ-θ manoeuvring (control mode B2) and the V-α-θ manoeuvring (control mode B4), were selected and then linked successively by the LIDFCS to form the required mode-shifting control.

During the control, the spoiler was modelled as the nonlinear **Spoiler Model One** (given by (2-31), (2-32) and (2-33)). The coefficients of the desired model generators were made the same as that of the close-loop pole polynomials shown in **Table 5-1.**

6.3.3 Simulation of the flight control and trajectory

The flight trajectory generated by the programmed control is shown in **Fig. 6-1(a)**. It can be divided into the following three manoeuvre segments relating to the selected control modes:

Segment 1 (t: 0~10s) is a fixed rate of climb from the conventional control A2, with the output control variables V and α being controlled from the balanced flight state (H_0=500m, V_0=189m/s, α=0°) to the objective state (H_0=710m, V_1=199m/s, α=1°). The manoeuvre shows the conventional coupling relation between the attitude (pitch angle θ) and the trajectory (path angle γ).

Segment 2 (t: 10s~30s) is the level-off fuselage pointing generated by employing the unconventional control mode B2, with the output control variables as V, γ and θ. During the process, the flight was firstly switched from the climb-up to a constant height keeping (H=710m) by shifting the control from the mode A2 to B2 and defining the objective output variables V=189m/s, γ=0° and θ=4.0°. Then a separate pitch angle control was performed by the mode B2 to change θ from 4.0° to 8.0° while augmenting the flight trajectory vector as constant (V=189m/s, γ=0°).

Segment 3 (t: 30s~53s) is the level-attitude descent with different rates. It involved a shift from the control mode B2 to the control mode B4 with the objective output variables V=189 (m/s), α=6° and θ=0°. Then the descent rate was halved by separately controlling the incidence α from 6° to 3°, while augmenting the other output variables as constant. The simulation continued until the aircraft reached the height of 400 meters.

Table 6-2 contains a detailed summary of the flight simulation broken down into 10s manoeuvre blocks.

Table 6-2 Simulation Summary

Seg.No.	Time (s)	C. Mode	Output Variables				
			V(m/s),	γ(°),	α(°),	θ(°),	H
1	0~10	A2	189 ~ 199	0 ~ 11.8	0 ~ 1	0 ~ 12.8	500 ~ 710
2	10~20	B2	199 ~ 189	11.8 ~ 0	1 ~ 4	12.8 ~ 4	710
	20~30	B2	189	0	4 ~ 8	4 ~ 8	710
3	30~40	B4	189	0 ~ -6	0 ~ 6	8 ~ 0	710 ~ 530
	40~53	B4	189	0 ~ -3	0 ~ 3	0	530 ~ 400

The time histories of the three angular variables γ, θ, α during the whole controlled manoeuvring are presented together in **Fig. 6-1(b)**, which clearly shows the progress of the control shifting and the resulted angular decoupling effects. **Fig. 6-1(c)** gives the simulation result of the path velocity V. **Fig. 6-1(d)** and **(e)** show the variation patterns of the three control variables, δ_e and δ_t, and δ_{sp}, respectively.

6.3.4 Analysis and summary

It can be seen from the simulations that following the programmed mode-shifting control, the LIDFCS commanded the logical deflections and changes of the control variables (**Fig. 6-1(d), (e)**) and gave out the precisely decoupled controls on the output variables of interest (**Fig. 6-1(a), (b)**). Due to the engine dynamics delay in the thrust response, which was modelled as the first-order lag element in **Chapter Five**, and the constraints on both the δ_{tmax} and $\dot{\delta}_{tmax}$ (**Appendix A.5**), the flight path velocity was controlled and augmented in a slow mode and was occasionally affected by the violent spoiler controls (**Fig. 6-1(c), (d)**).

Considering the fast acting feature of spoilers, it is apparent from the simulations that while working within their control authority, spoilers are able to provide effective and separate control on the path angle γ. Combining this with the separate velocity and attitude controls using the conventional control devices provides aircraft the unique decoupling control ability and, therefore, enhanced manoeuvrability.

It is considered that the fuselage pointing manoeuvre will enhance the air-superiority of a fighter during combat, or will improve the attitude handling and augmentation during the landing. While the direct force manoeuvre (flight trajectory control with fixed attitude), as shown in the **segment 3**, will considerably improve the manoeuvrability of a modern aircraft and be used for the flight missions such as air-refueling, formation, taking off/landing and air-superiority.

While used for these manoeuvres, spoiler control effectiveness is mainly decided by its lift coefficient C_{LSP}. It can be seen from the simulation (**Fig. 6-1(b), (e)**) that for the nonlinear spoiler model with the gain K_I= -0.46 and an upper deflection limitation of 90^o, in a balanced flight at a Mach number of 0.6, up to 8^o of separate α (or γ) control can be gained.

Furthermore, to gain a quantitative evaluation of the angular decoupling control using spoilers, a series of the decoupling control simulations were carried out. The analysis was based on the nonlinear spoiler model described above with the test flight conditions ranging from low Mach number (low altitude) to high Mach number (high altitude). The simulations centred on the measurement of the balanced separate path angle (γ) control from the spoilers, with the pitch angle (θ) being controlled by the elevator to a constant (e.g. =0). Due to the angular relation in the longitudinal dynamics: $\alpha = \theta - \gamma$, a more convenient and explicit way used to show the decoupling ability was the relation between the separately controlled incidence (α_c) and spoiler deflection (δ_{sp}).

In **Fig. 6-2**, three $\alpha_c(\delta_{sp})$ curves are given which correspond to the flight conditions of M=0.4 (H=100m), M=0.6 (H=1000m) and M=0.8 (H=6000m), respectively.

It can be concluded from the analysis that (1): due to the nonlinearity in C_{LSP} (2-31), the relation between α_c and δ_{sp} is generally nonlinear, with decreased control effectiveness at the higher deflection angles, (2): the spoiler control effectiveness varies with the flight conditions, increasing as the Mach number increases, with the maximum α_c around 11^o.

In addition, **Fig. 6-2** provides a way of defining the pre-set deflection angles of spoilers in some control applications, as shown in late studies.

6.4 Spoiler Control Application --- Case Two: Fast Deceleration Control

The spoiler effectiveness in providing drag enhancement is mainly determined by its drag coefficient C_{DSP}, from its design and configuration on a wing, and has been demonstrated in the previous modelling and simulations. Generally speaking, when spoilers on wing surfaces are fully deployed (e.g. 90^o upwards), a substantial drag can be expected..

The task here is to use this feature effectively, through the LIDFCS system, for the fast deceleration control demanded by some mission objectives. Examples are superior deceleration manoeuvre for advantageous positioning, and distance shortening of a landing approach. In this study, the control mode B1 was used for commanding a highly decoupled γ-θ manoeuvre, giving large deflection of spoilers, so that high drag can be acquired for fast deceleration along the flight trajectory. During the progress, the thrust was separately set or controlled to specified values.

Based on the HAWK flight simulator, simulations were carried out for the evaluation of the spoiler control and to compare it with the conventional thrust control in the aircraft deceleration. A typical example was shown in **Fig. 6-3** where the control mission was to decelerate the HAWK in level-off flight (H_0=400m) in the quickest way and using the possible extreme control means. The time duration was 20sec..

Four control cases are presented:

Case A: used the conventional thrust shutting-off with a dynamic lag of $\frac{0.5}{s+0.5}$ and the constraints $\delta_{tmax} \geq 0$ and $|\dot{\delta}_{tmax}| \leq 0.2$. (**Fig. 6-3** Case A)

Case B: was the fast deceleration control using the NID control mode B1, with the **Spoiler Model One** ((2-31), (2-32) and (2-33)) and the drag gain coefficient of K_d=-0.05. The balanced spoiler deflection was -50°, gained by commanding the output control variables γ and θ to 0° and 8°, respectively. (**Fig. 6-3** Case B).

In principle, a manoeuvre like this can make full use of both the large spoiler drag and the nonlinear lift-induced drag of the aircraft, while keeping the trajectory direction constant.

Case C: was similar to Case B but doubling the gain K_d to -0.1. (**Fig. 6-3** Case C), resulting in the balanced deflection of δ_{sp}=-42°.

Case D: was similar to Case B but using the **Spoiler Model Three** (linear models (2-35), (2-36) and (2-37)) and the derivative $C_{d\delta_s}$=-0.05, giving the balance deflection angle δ_{sp}=-48° (**Fig. 6-3** Case D)

In the B, C and D cases, the thrust control was programmed to be the same as the Case A.

Remarks: comparing **Case A** with **Case B**, it can be seen that the use of the nonlinear spoiler gains nearly double the deceleration of the pure thrust control (with the average deceleration -2.3 (m/s^2) vs the thrust deceleration -1.26 (m/s^2)). This in turn brings a flight distance shortened by about 220 meters in 20 seconds.

As expected, the decelerating capacity is dominated by the spoiler drag coefficient. As shown in **Case C**, the increase of the drag coefficient enhances the deceleration with the average deceleration raising to -3.1(m/s^2). However, the best deceleration control comes from the use of the linear spoiler (**Case D**) where the maximum deceleration is reached as -3.32 (m/s^2). Considering the drag gain in this case was only half of that in **Case C** and the same as **Case B**, the unexpected incidence effect, as modelled in (2-25), on the spoiler drag coefficient, seems great.

So conclusions can be drawn as: (1) under appropriate controls, spoilers are able to provide substantial drag for enhancing the deceleration control of aircraft, thus improve the performance levels. (2) the deceleration control of spoilers is mainly dependant on the drag coefficient C_{DSP} and can be heavily influenced by the incidence-induced nonlinearity. In this sense, the increase of the drag coefficient and the reduction of the incidence effect seem the two major ways of enhancing the deceleration effectiveness of spoilers.

6.5 Spoiler Control Application --- Case Three: Gust/Turbulence Alleviation for Improving Safety and Ride Quality of Aircraft.

6.5.1 General remarks

Apart from the applications for manoeuvre enhancement, spoiler control can also be very useful for the control augmentation of aircraft flying into a strong disturbance atmosphere. According to the objectives, two kinds of augmentation cases regarding the use of spoilers can be defined, namely Gust/Turbulence Alleviation and Microburst Alleviation, respectively.

The atmosphere through which an aircraft flies is constantly in turbulent motion. The velocity field within the atmosphere varies in both space and time in a random manner. The winds and wind gusts created by the movement of atmospheric air masses can degrade the performance and flying qualities of an aircraft, they may also cause damage to the aircraft structure subject to the continuous changes in loads from the gusts. Another important effect of gust/turbulence is on the ride quality of an aircraft. Turbulent motions result in accelerations which are experienced by passengers and crews as unpleasant effects.

The effect of vertical gusts on an aircraft, for example, can be seen through the transformation of the gust velocity onto the body axes, so a gust-induced incidence is formed as:

$$\alpha_g=\tan^{-1}(-W_g/U_0) \qquad (6\text{-}1)$$

Here W_g is the vertical gust velocity along the positive body axis, U_0 is the equivalent flight velocity along the body axis. Due to the gust-induced incidence, (also $\dot{\alpha}_g = -q_g$, if the length of the aircraft is taken into account), the whole force and moment equations, hence the motion, of the aircraft are affected.

To alleviate the influence of turbulence is to effectively counter both the force and moment changes exited by the gust. The general principle of gust/turbulence alleviation control (GTAC) can be described as: a number of specially located sensors give the effect measurement to a controller. The controller commands appropriate deflections of control devices to effectively, and almost simultaneously, generate additional aerodynamic forces and moments to cancel the acceleration caused by the gusts.

However, one of the fundamental problems with most GTAC systems using conventional control techniques is that, when a gust has been sensored, the system cannot take action instantly until it is too late to achieve much effect, or sometimes the delayed action may lead to even an adverse effect during a sudden change in the gust direction. Clearly, to avoid those defects demands innovative control designs and, more important, the adoption of fast and direct force control devices, such as spoilers.

Here, combined with the LIDFCS, a controller utilising spoilers for gust/turbulence alleviation was designed and its effect was evaluated by the simulations of the control of the HAWK aircraft approaching an airfield before landing and encountering a low-altitude turbulence.

6.5.2 Turbulence model

In the turbulence simulation, a non-**Gaussian** vertical atmospheric turbulence model (REEVES et al, 1971) was used. The model consists of the addition of Gaussian and modified Bessel processes, and hence has a more realistic turbulence spectrum and contains more large gusts and longer relatively quiet periods. **Fig. 6-4** shows a simulation structure of the turbulence model used by PESMAJOGLOU (1989).

The turbulence used in the simulations is shown in **Fig. 6-5(a)**, with the parameters σ_W=2.0 (m/s), L_W=100(m), R=1.0 and the distribution on the distance scale the same as used in the simulation. According to the specification in **Mil-F-8785c**, this is equivalent to a low-altitude moderate turbulence case.

The turbulence model was introduced into the HAWK flight simulator through the link of the package 'HAWKSIM1' with the package for the turbulence generation 'TURBUL'. The vertical gusts V_{WG} generated by TURBUL were directly input as a disturbance into the simulations through the following relation:

$$V_D(t)=V_{KD}(t)-V_{WG}(t) \qquad (6\text{-}2)$$

where the 'frozen turbulence' assumption was used so that a space/time transformation was taken for the gust velocity $V_{WG}(X)$, V_D is the vertical velocity of the aircraft relative to the air and V_{KD} is the vertical velocity relative to the earth.

The in-turbulence flight performance was evaluated by the following time-average error derivative index:

$$J_{Ey_i} = \frac{1}{T_a} \sum_{k=k_1}^{k_2} (y_i(kT) - y_{di}(kT))^2 \qquad (6\text{-}3)$$

where y_i is an output variable, which was chosen from the output control variables of interest, including the normal acceleration A_{nz} as a measure of aircraft ride quality, y_{di} is the desired trajectory of the variable, T is the time step, T_a is the evaluation time duration ($T_a=(k_2-k_1)T$).

6.5.3 Controller design

The design was based on the LIDFCS. For augmenting the longitudinal flight in turbulence, the trajectory and attitude are among the most important variables to be stabilised, so the output control variables of the most interest were defined as V, γ and θ. Consequently, the mode B2 was chosen as the principal control mode.

An important measure concerning the increase of spoiler control authority is the off-set of its balanced deflection before entering a turbulent field, for effectively countering the gusts from both directions. The pre-set can be decided by estimation of the possible maximum gust and is constrained by the deflection scope. In this study, a way of defining the off-set angle was:

1) Estimate the possible maximum gust incidence $|\alpha_{gmax}|$, by (6-1) from the peak gust velocity.

2) From **Fig. 6-2**, find the balanced spoiler deflection angle corresponding to the incidence.

3) Set the off-set angle δ_{spo} to approximately that angle by commanding $\alpha_c=|\alpha_{gmax}|$ prior to the turbulence encountering. Clearly, for countering the gusts from both directions, δ_{spo} should be constrained by half the maximum spoiler control effectiveness. So when $-90^o \le \delta_{sp} \le 0^o$, for the

linear spoilers, there is $-45^o \le \delta_{spo} \le 0^o$, while for the nonlinear (sine function) spoilers, there is $-30^o \le \delta_{spo} \le 0^o$.

According to the method, for the turbulence shown in **Fig. 6-5(a)** with the maximum gust $|V_{WGmax}| < 6$m/s, an appropriate off-set angle, based on U_0=100m/s and W_{gmax}= 6m/s, was determined as δ_{spo}=-25°, corresponding to a command α_c of 4°.

6.5.4 Simulation of in-turbulence flight

The simulations for the in-turbulence flight and control, mostly at low altitudes and low-speeds simulating the approaches before landing, were carried out. The example shown next is the simulation of HAWK aircraft flying at a super-low altitude of H=100m with a low airspeed of 100m/s (360km/h) and encountering a turbulence as shown in **Fig. 6-5(a)**. The simulation was programmed as the following:

Starting from a balanced flight at H_0=100m, V_0=185 (m/s), the aircraft was firstly controlled, using the mode B1, to perform a fast level-off deceleration flight till reaching a desired approaching airspeed of V=100(m/s), and then it began a level-off flight at the designed low-speed, with an incidence of α_0=4°, for balancing the lift. This plus the extra incidence α_c=4° for the off-set of the spoiler decided the desired output control variables as γ_d=0°, θ_d=8° and V_d=100 (m/s), for the control mode B2. **Fig. 6-5(b)** shows the desired trajectory.

The whole simulation time was T_{total} =120s. The turbulence was introduced into the flight from t=50s and the in-turbulence flight duration $T_{tur}(=T_a)$= 60s.

Three cases of control and augmentation were applied to the in-turbulence flight and their effects were compared to each other. The three cases are:

Case A: programmed flight without control augmentation, with the control inputs pre-set.

Case B: integrated pitch and velocity control augmentation (IPVCA) , using the control mode A1.

Case C: integrated pitch and trajectory control augmentation (IPTCA), using the control mode B2.

Evaluation: **Table 6-3** summarizes the evaluation results using formula (6-2), for the three control cases in the interesting output variables V, γ, θ and Anz. The comparisons of the time histories of $\gamma(t)$ and V(t) are shown in **Fig. 6-5(c)** and **(d)**, respectively. The trajectory derivations are compared in **Fig. 6-5(e)**. The spoiler control output is presented in **Fig. 6-5(f)**.

Table 6-3 Gust/Turbulence Alleviation Comparisons

Case Type	J_{EV}	$J_{E\gamma}$	$J_{E\theta}$	J_{EAnz}
A	100	100	100	100
B	9.6	300	0.42	178
C	10.4	8.2	0.42	30

(T_a=60.0s, in ratio form%)

6.5.5 Analysis and summary

It can be concluded from the above evaluation that the use of spoilers is very beneficial for turbulence/gust alleviation during landing approach or low altitude flight. From this particular test when the aircraft flies into a vertical turbulence with the maximum gust speed up to 6(m/s) (medium turbulent strength), using the nonlinear spoiler control gives a nearly perfect augmentation in both the trajectory (V, γ) and the pitch attitude (θ). These in turn enhance the ride quality reflected in the J_{EAnz} evaluation (by an average of 70% improvement over the non augmentation case) and the flight safety shown in the height deviation (see **Fig. 6-5(e)**, $|\Delta H_{cp\text{-}p}|$<3m, compared with $|\Delta H_{ap\text{-}pmax}|$=20m and $|\Delta H_{bp\text{-}pmax}|$=17m), thus considerably improving the low-altitude flight performance of the aircraft.

From the spoiler control shown in **Fig. 6-5(f)**, it can be seen that the off-set angle of the spoiler enabled the spoiler to work within an increased control authority and therefore to effectively counter the modelled gusts. Further investigation in this aspect showed that while the off-set angle was made at half the maximum projection height position ($\sin(\delta_{spo})$=0.5, δ_{spo}=30°), maximum force cancellation, hence an improved alleviation, could be achieved.

Also, the simulation shows that the conventional IPVCA has actually caused a deterioration in the γ and A_{nz} deviations, and therefore is not ideal for turbulence/gust alleviation. This adverse effect is mainly due to the delay in the force variation from the conventional moment control using the elevator. In addition, from the Case C control using the spoiler, it can be observed that the derivations in γ and H were mainly caused

by the maximum negative gusts at t=73.5s (X=9000m), where although the spoiler deflection appeared working within its control authority, the delay in the spoiler actuator dynamics (modelled as $\frac{40}{s+40}$) had actually made the cost. This plus the spoiler control pattern in **Fig. 6-5(f)** make it clear that in order to keep the control up with the random and fast gust changes, very powerful and fast (with negligible time-delay) servo dynamics for spoiler control are demanded.

6.6 Spoiler Control Application --- Case Four: Low-Altitude Windshear/ Microburst Alleviation for Improving Landing/Take-Off Safety

6.6.1 General remarks

Different from atmospheric turbulence which constantly occurs within a considerable large region of space and time, and includes relatively small gust scales, wind shear is defined as local, transient change in the wind vector which brings a rapid and highly influential change in the airflow over the aerodynamic surface of an aircraft.

A form of wind shear which is of particular concern to flight safety is the microburst, in which a large mass of air is propelled downwards in a jet form, from some convective fields and/or a rapid build-up of small weather cells (see **Fig. 6-6**). An intense microburst can produce about 70m/s (150mph) horizontal winds as well as 20m/s (48mph) down flows at tree top levels. Such a violent and invisible change in wind velocity presents the greatest danger to aircraft flying at low altitudes and at low speeds. It is believed to be the real cause of many aircraft accidents during landing and take-off phases, e.g. the crash of a Boeing 727 at JFK airport in NewYork in June 1975 (McLEAN 1991).

Following the effective gust/turbulence alleviation using spoilers, a special spoiler control for control augmentation and microburst alleviation, for aircraft penetrating a severe microburst during approach to landing, was designed and evaluated by simulation. The control programming is characterized by direct countering of the microburst impacts using the fast and direct force control from spoilers, and differs from most of the prior studies concerning microbursts where emphases were put on avoidance and escape procedures. (MELO, 1991)

6.6.2 Modelling of low-altitude microbursts

A series of microburst models and simulations were presented at the NASA Workshop on Wind Shear/Turbulence Inputs to Flight Simulation and System

Certification (BOWLES & FORST (Eds.), NASA CP2474, 1984), including a further developed analytical microburst model addressed in detail by BRAY. A three-dimensional analytic microburst model ,based on boundary stagnation flow analyses, was proposed by OSEGUERA and BOWLES in 1988. A similar but simplified two-dimensional microburst model was studied by MELO & HANSMAN (1991) and applied to their simulations on the lateral control manoeuvres of aircraft for microburst avoidance.

The two-dimensional microburst model was used in this study. The data of the maximum intensity horizontal and vertical velocity profiles referred to the Andrews Air Force Base event in 1983, which was believed to represent a worst case with the maximum horizontal velocity V_{umax}= 27m/s and the maximum vertical velocity V_{wmax} 20m/s. **Fig. 6-7(a)** shows the model and its distribution on the distance scale for the simulation.

6.6.3 Controller design

The control design and simulations were based on the LIDFCS and the HAWK simulator. The nonlinear spoiler model for HAWK, **Spoiler Model One**, was used. As in the turbulence cases, the control mode B1 was firstly used for the deceleration control prior to the landing approach and for an off-set of the spoiler angle.

As distinct from the turbulence cases, the off-set angle δ_{spo} for microburst alleviation is purely decided by the worst negative incidence α_{gmax} which may result from a microburst. This arises from the special velocity profiles of the microburst model shown in **Fig. 6-7(a)**, where the most influential and dangerous impacts to aircraft result from the wind-shear induced α_{gmax}. In the case of the balanced flight path velocity V_0=120 (m/s), from (6-1) the worst incidence resulting from the microburst in **Fig. 6-7(a)** could be approximately estimated as:

$$\alpha_{g\,max} = -\tan^{-1}\left(\frac{V_{w\,max.}}{V_0 - V_{u\,max}}\right) = -\tan^{-1}\left(\frac{20}{120-27}\right) = -12.1^{o}$$

So to effectively counter the microburst while stabilising the attitude at the same time, an equal valued positive incidence control should be made by the spoiler control, i.e. α_c=-α_{gmax}. However, referring to the $\alpha_c(\delta_{sp})$ curves in **Fig. 6-2**, this α_c is actually beyond the maximum control which the spoiler is able to offer. Also, it is considered not practical in real flight to set up such a high incidence prior to the microburst which, plus the possible balanced incidence α_0, may easily cause flow separation and flutter. By

trade-off, in the simulations, α_c was chosen as 7.5°, corresponding to the off-set δ_{spo}=-70°.

6.6.4 Simulation of microburst penetrating flight

The simulations of the penetrating flight through the microburst were programmed as the following:

Stage 1: starting from a low altitude balanced flight of the HAWK at H_0=1000m, V_0=193m/s.
Stage 2: decelerating the flight from V_0 to the desired descent speed V_d=120m/s.
Stage 3: performing the landing approach following the desired gliding trajectory with the output variables as: V_d=120m/s (268 knots) and γ_d=-3°, which correspond to a descent rate of $\dot{H}_d$=6.3m/s.

The desired trajectory is shown in **Fig. 6-7(b)**. The microburst was introduced to the approach process through the variables $V_{wg}(X)$ and $V_{ug}(X)$, with the microburst centre located at X=8900m from the start point of the simulations. The whole simulation duration was 100 seconds, with the deceleration time automatically set by the reach of the desired approaching speed (V_d=120m/s, t=22s). The desired terminal height was H_{dt}=500m.

Similar to the turbulence alleviations, the three control cases described in **6.5.4** were applied to the simulation **stage 3**, respectively. This allows the comparison of the microburst effects and alleviations.

Evaluation: **Table 6-4** summarizes the maximum deviations from the desired trajectory, in the principal state variables of H, X, V and γ, in the three microburst-penetration flights. While **Fig. 6-9(b)**, **(c)** and **(d)** present the comparisons of the trajectory H(X), the path velocity V(t) and angle γ(t) between the three cases, respectively. **Fig. 6-7(e)** shows the time history of spoiler control output.

Table 6.4 Max. Deviation Comparison

	Case A	Case B	Case C
$\|dH\|_{max}$ (m)	Impact (t=94s)	150	30
$\|dX\|_{max}$ (m)	Impact	2470	610
$\|dV_{max}\|$ (m/s)	Divergence	1.3	2.6
$\|d\gamma_{max}\|$ (°)	24	9.5	3.5

6.6.5 Analysis and summary

From the simulations and evaluation, it can be seen that severe microbursts are indeed a great threat to aircraft flying at low altitudes and low speeds, e.g. take-off and landing phases. Even for the aircraft like HAWK which has a very desirable natural stability at low altitudes (see **Chapter 3**), without augmentation and precaution measures, the worst microburst as simulated may still result in more than 500 meters loss in the height from the desired flight trajectory halfway to the touchdown and the large divergences in the major variables. This is the state concerning both the height and stability losses therefore there is no doubt it is one of the highest dangers to both commercial and military aircraft.

Although the conventional augmentation control using the elevator and thrust brought considerable improvement in the stability of the penetrating flight, the most beneficial control augmentation came from the introduction of the spoiler, attributing to its unique control effects on the direct suppression of the force impacts of the microburst and on precise trajectory keeping. By appropriately choosing the control mode and off-setting the spoiler deflection angle (-70^{o} in this case), use of the spoiler control gave a good and almost deviation free augmentation in H, V and γ, and substantially improved results over the conventional control, therefore improving the safety and performance levels of aircraft.

The evaluation of the spoiler control output **Fig. 6-7(e)** suggests the further off-setting of the spoiler may bring an even better augmentation result. However, due to the deceleration process in aircraft landing which normally has already resulted in some incidence for balancing the lift loss (considering $L=1/2\rho V^2 S C_L(M, \alpha, \delta_{sp})$), further off-set of the spoiler will meet the constraints of both the wing stall and the control effectiveness of spoilers due to the nonlinearity. The situation may be improved while using a linear spoiler (as **Spoiler Model Three**), combined with auxiliary lift devices, such as flaps, to set up an ideal off-set angle of the spoilers prior to microburst encounters.

6.7 Concluding Remarks

It is considered that the ultimate aim of this spoiler study is for the active control of modern aircraft in order to enhance performance levels. From this view point, effort has been devoted to the investigation of the flight control applications where spoilers may be practically useful. The applications mentioned above range from the use of spoilers for manoeuvre enhancement (by providing the unique decoupling control abilities) to fast

deceleration control (by the special combination control), and to the alleviation of some severe atmospheric disturbance (making use of the effective trajectory control augmentation). These are believed to be only part of the possible spoiler control applications, however they clearly demonstrate the effectiveness and potential of spoiler control for present and future aircraft.

All these applications rely on the fact that spoilers can rapidly provide large effects on lift and drag force. This gives the use of spoilers a big advantage over the other conventional flap-style control surfaces such as the leading and trailing flaps, especially for the alleviation of disturbance caused by gusts or microbursts.

However, use of spoiler control also brings demands for special control designs and measures, due to the spoiler's unique properties and geometrical features, aimed at making the most use of its control potential. It has been demonstrated by various applications that the NID control and LIDFCS provide a flexible and effective frame for the use of spoilers for different control missions. As far as the deflection angle constraint is concerned, the study proposed a method for the setting of the off-set angle of spoilers according to the curves relating separately controlled incidence and the spoiler deflection angle. The technique has been proven efficient and successful, at the cost of a partial loss of the thrust.

It is important that, for most applications, the spoilers are driven by very powerful and fast servos. According to the simulation, the spoiler angular velocity in the gust alleviation case might reach 700°/s or greater. Doubtless in practice the use of such high-bandwidth servo mechanisms will bring some unexpected problems to the system. In this aspect, further studies are needed.

Figure 6-1(a) Flight trajectory in H-X plane

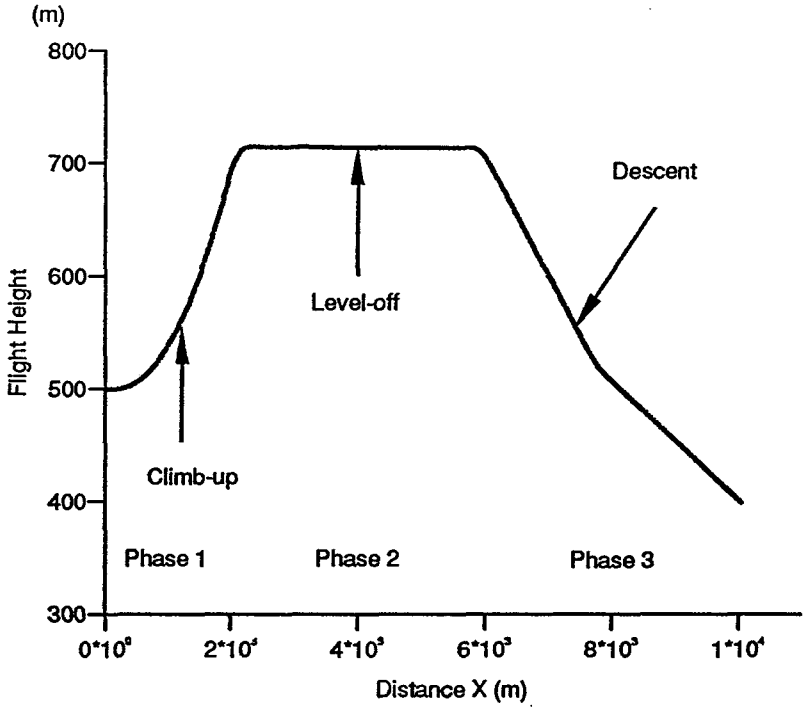

Figure 6-1(b) Decoupled control of angular variables

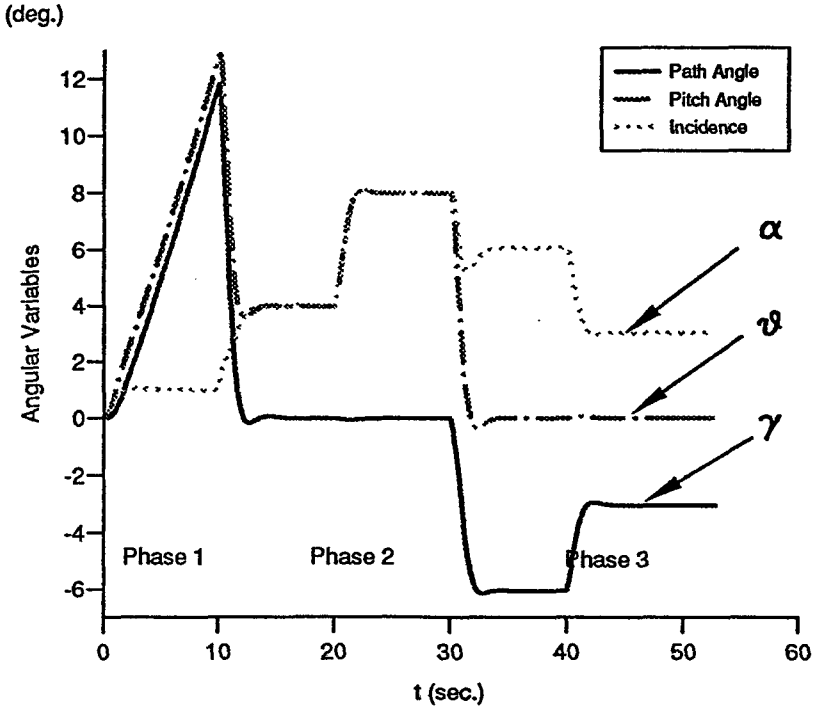

Figure 6-1(c) Control of flight path velocity

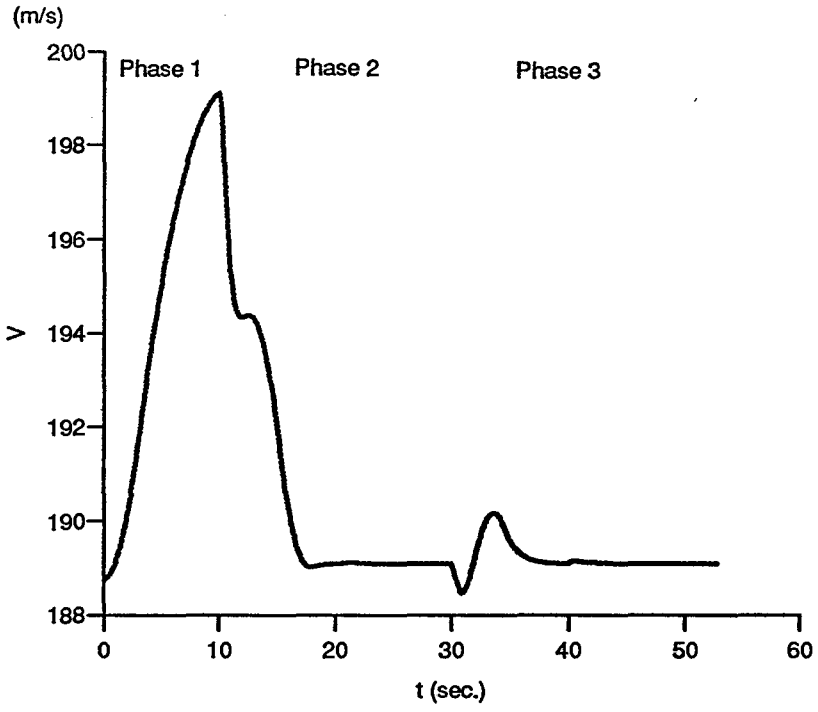

Figure 6-1(d) Elevator & Thrust control outputs

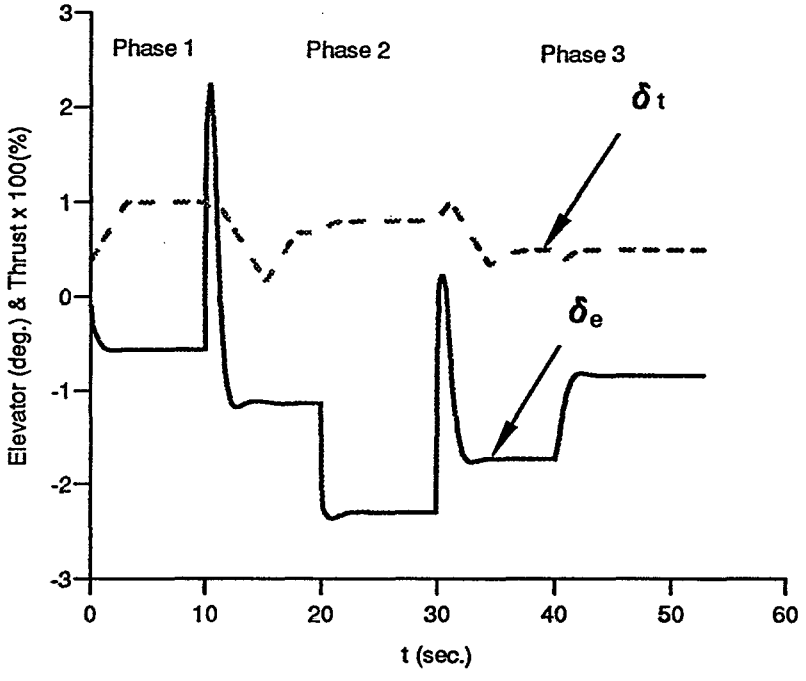

Figure 6-1(e) Spoiler control output

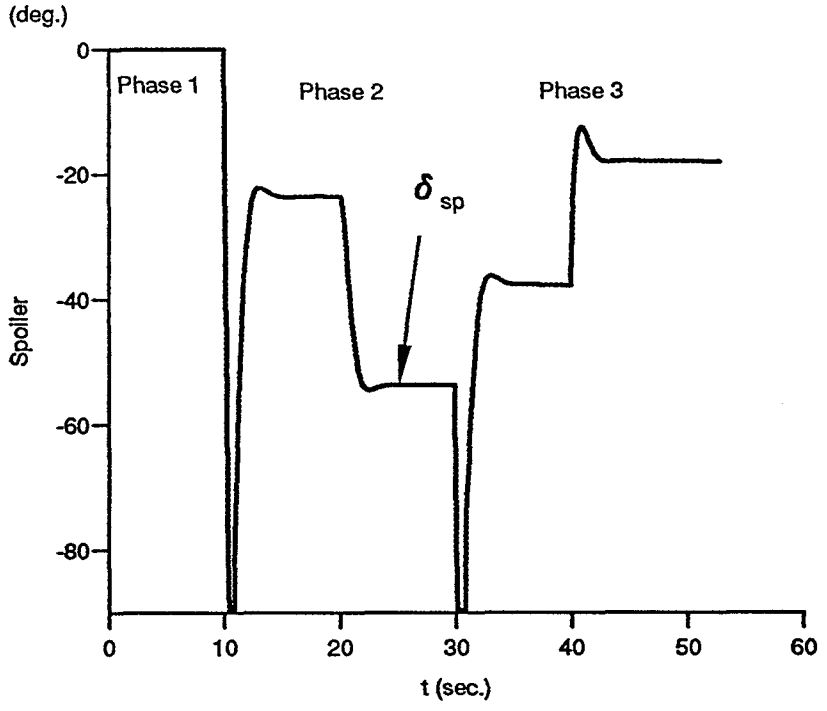

Figure 6-2 Spoiler control effectiveness curves
(separately controlled incidence vs spoiler deflection)

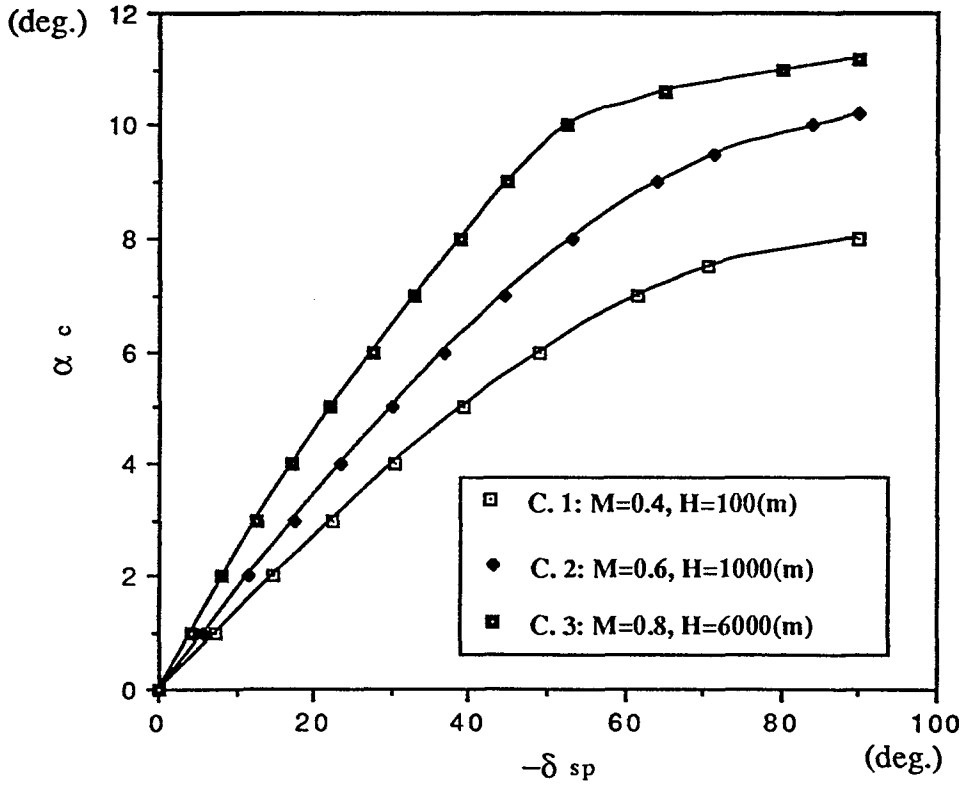

Figure 6-3(a) Deceleration: comparison of velocity responses

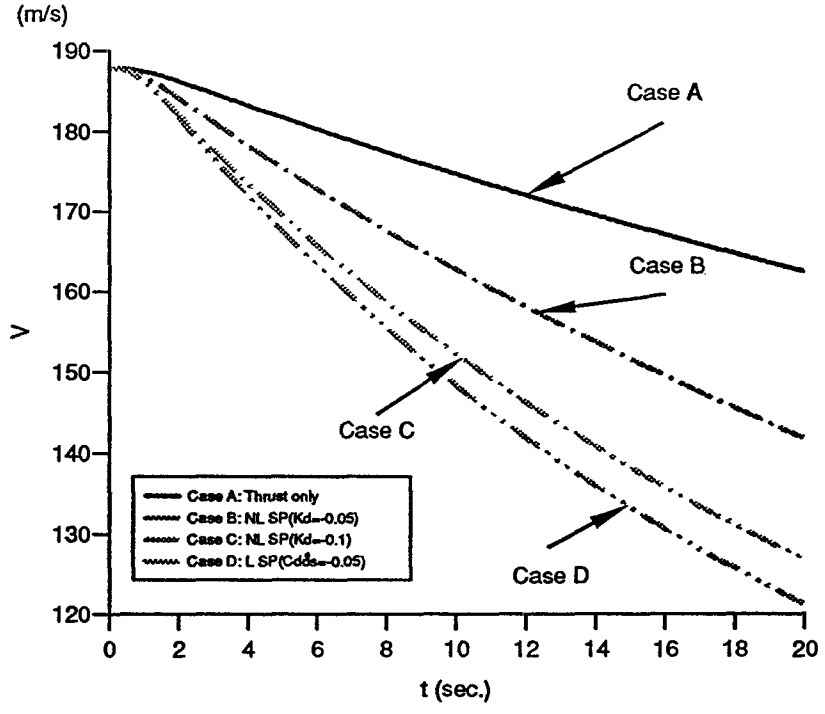

Figure 6-3(b) Deceleration: comparison of flight distances

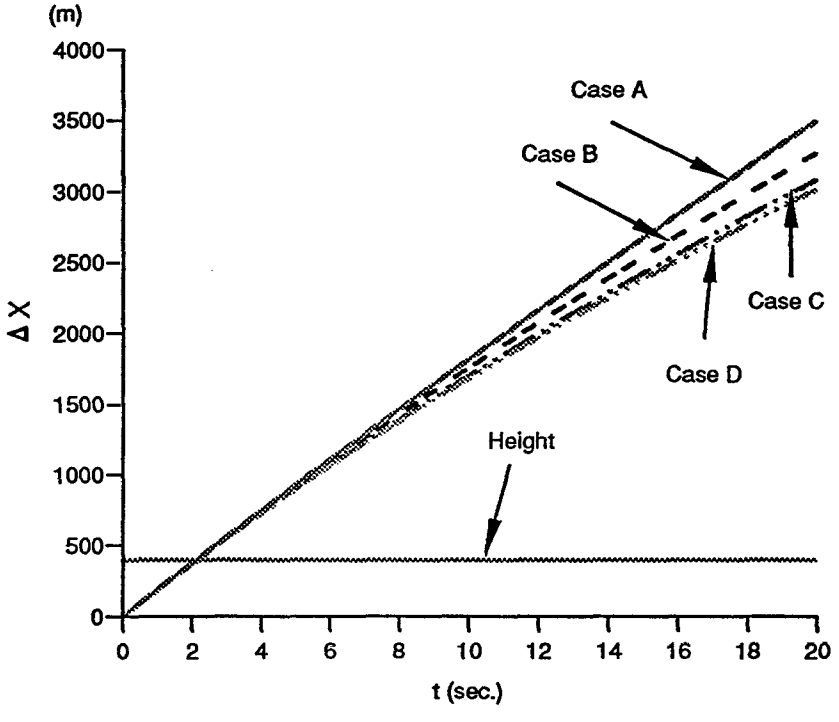

Figure 6-4 Simulation structure of a non-Gaussian atmospheric turbulence model (PESMAJOGLOU, 1989)

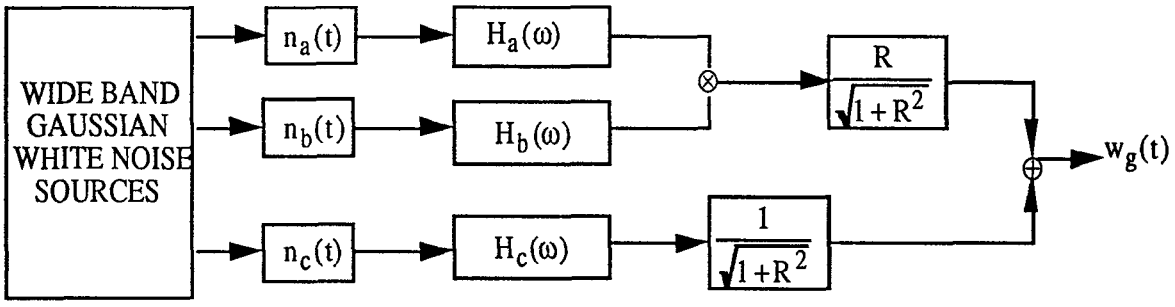

where the filter functions H_a, H_b and H_c are so chosen that they give the desired output spectrum. R is a parameter for modifying the contours of the output turbulence. For the vertical turbulence, there are:

Vertical Model Constants

	H_a	H_b	H_c
a	$\frac{V}{2L_w}$	$\frac{V}{2L_w}$	$\frac{V}{L_w}$
b	$\frac{1}{4}\sigma_w\sqrt{128}$	0	$\sigma_w(\frac{V}{L_w})^{3/2}$
c	$\frac{1}{2}\sigma_w\sqrt{128}\frac{V}{L_w}$	$\frac{1}{4}(\frac{V}{L_w})^2$	$\sigma_w(\frac{3V}{L_w})^{1/2}$

where V is the mean airspeed, L_w is the integral scale length, σ_w is the standard deviation of the gust velocities, and $H(\omega) = \frac{c+ds}{(a+s)^2}$.

Figure 6-5(a) Turbulence model and distribution

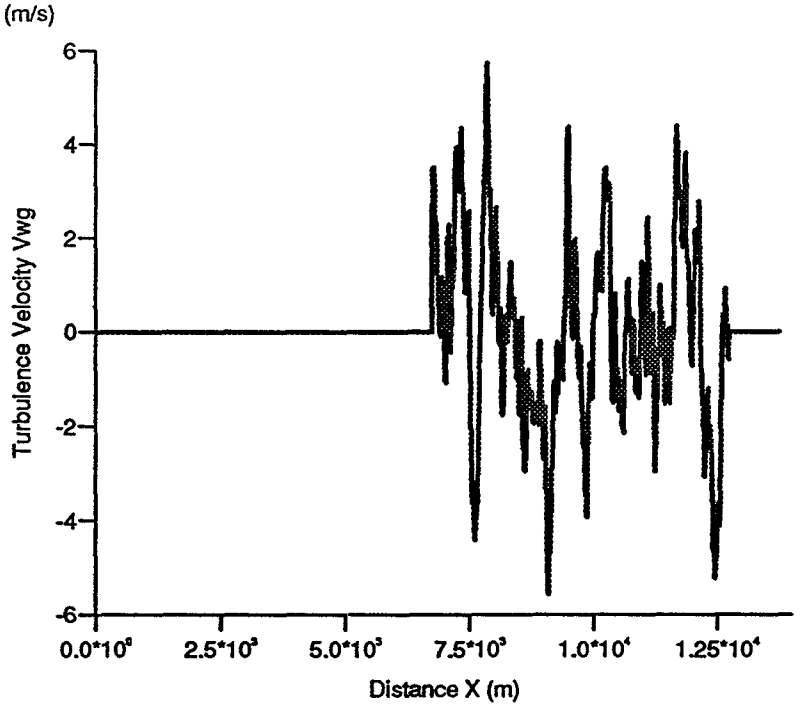

Figure 6-5(b) Desired flight trajectory

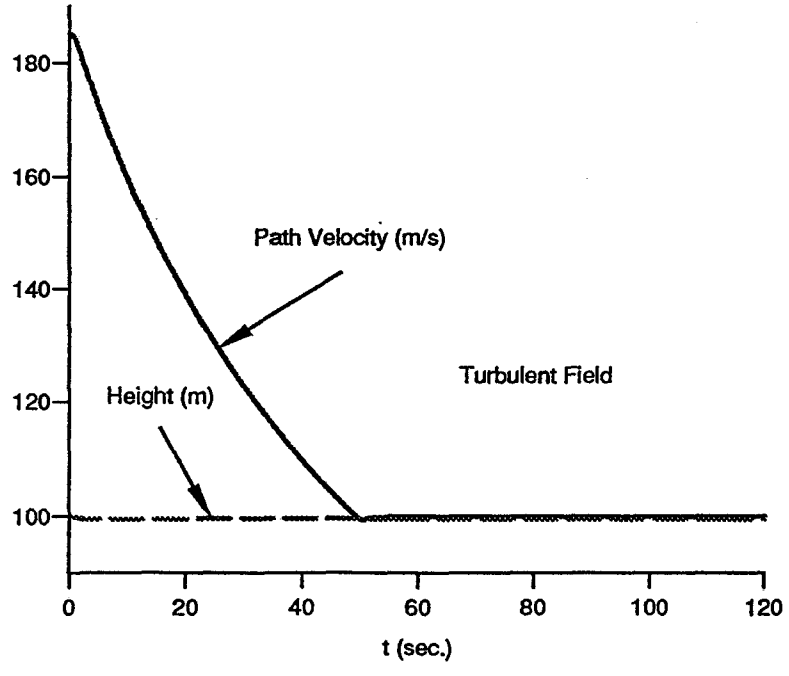

Figure 6-5(c) Comparison of path angle responses to the turbulence

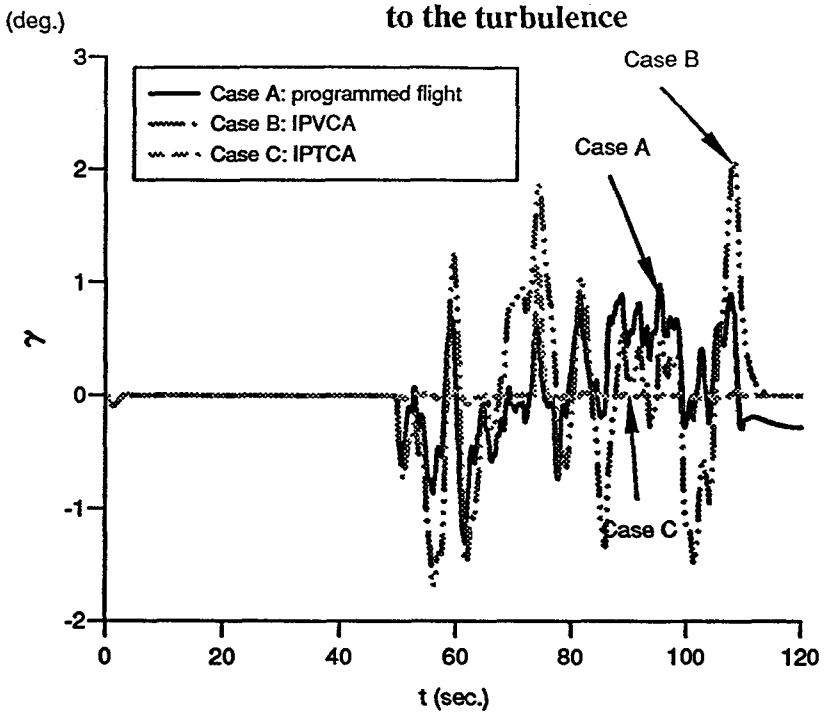

Figure 6-5(d) Comparison of path velocity responses (in the turbulence field)

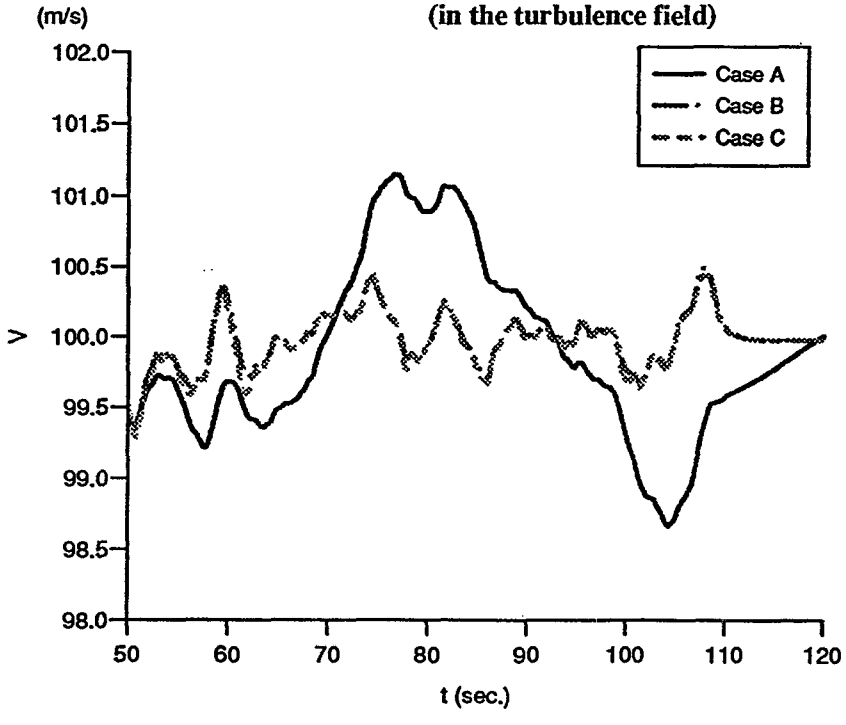

Figure 6-5(e) Comparison of flight trajectories in H-X plane

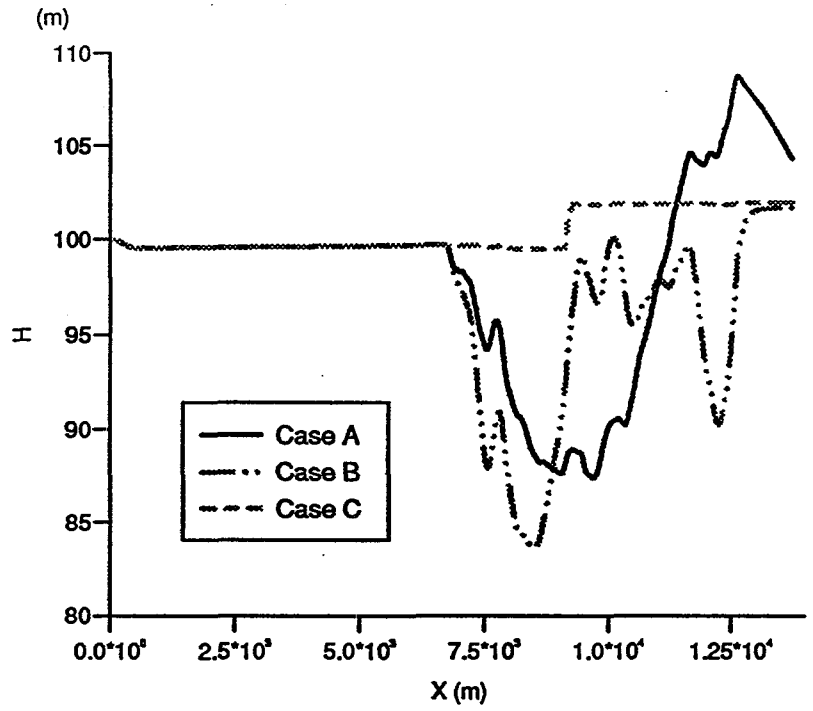

Figure 6-5(f) Spoiler control output

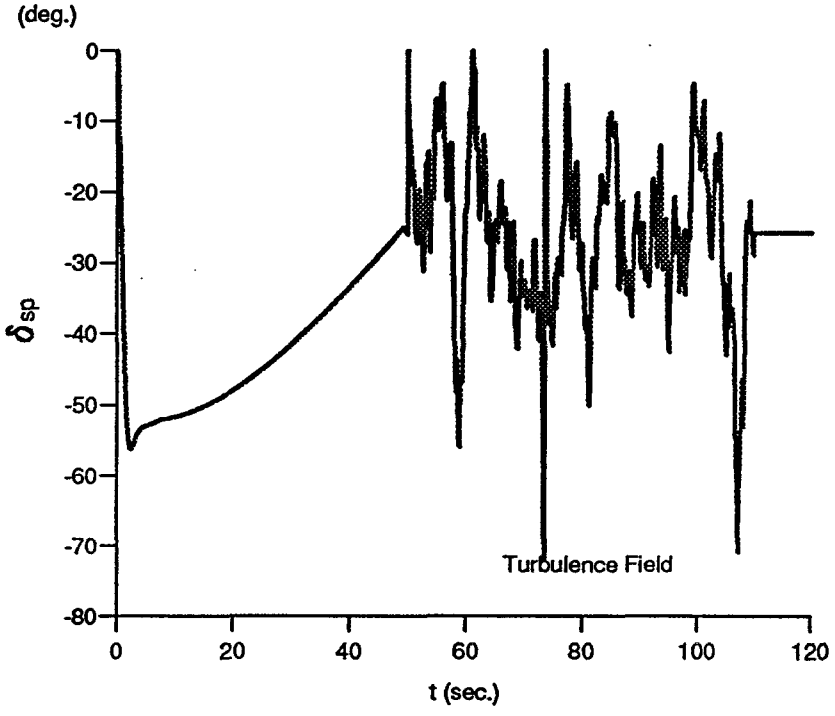

Figure 6-6 Phenomena of low-altitude microbursts
(McCARTHY, NASA CP 2474, 1984)

Figure 6-7(a) Microburst model and distribution

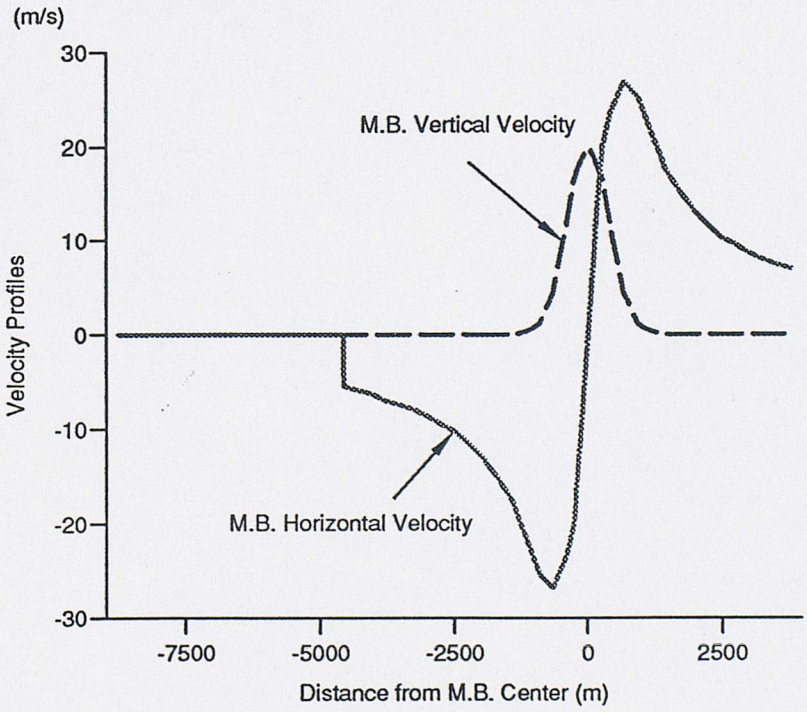

Figure 6-7(b) Comparison of flight trajectories in the microburst penetration

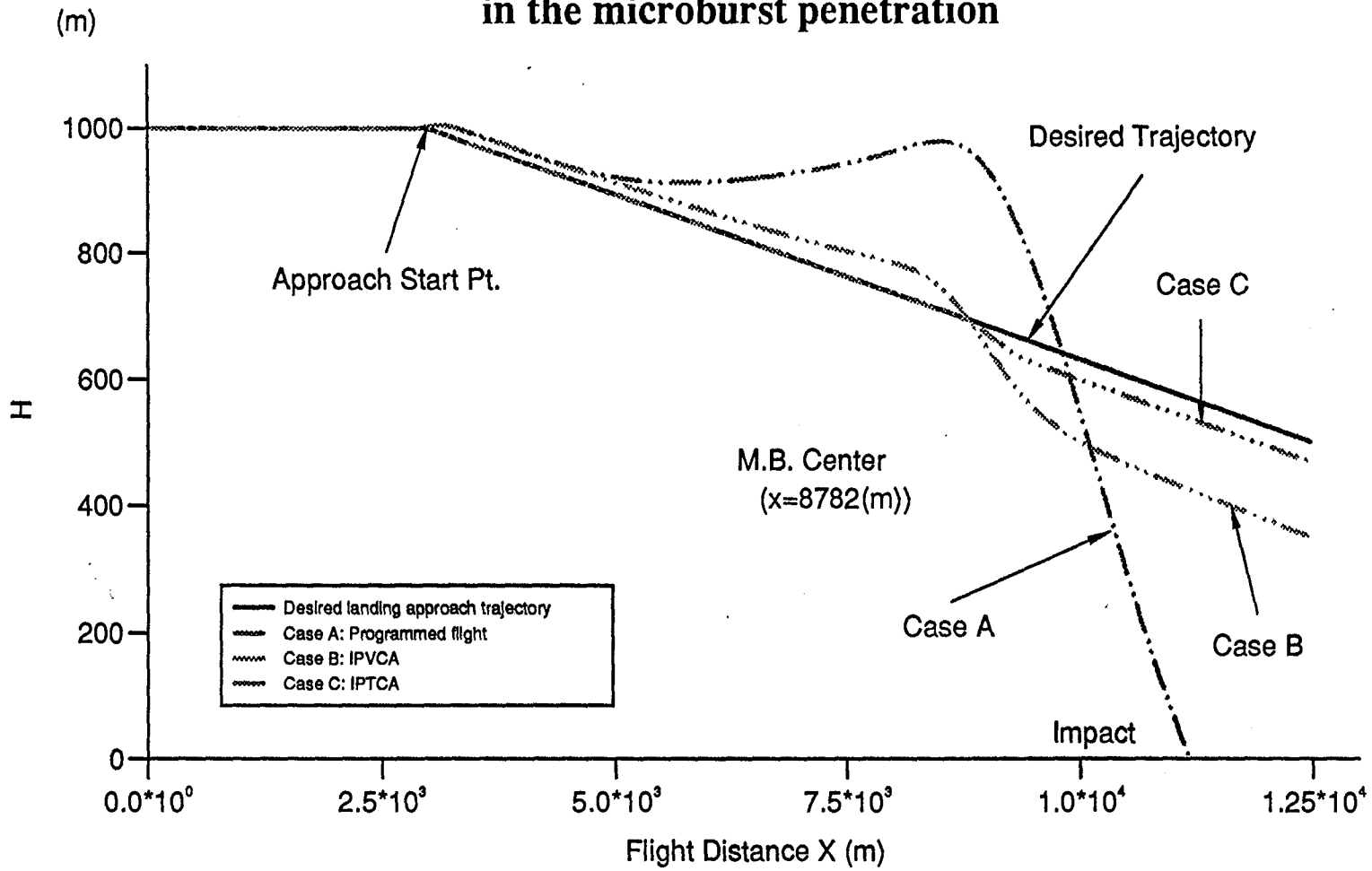

Figure 6-7(c) Comparison of path velocity responses

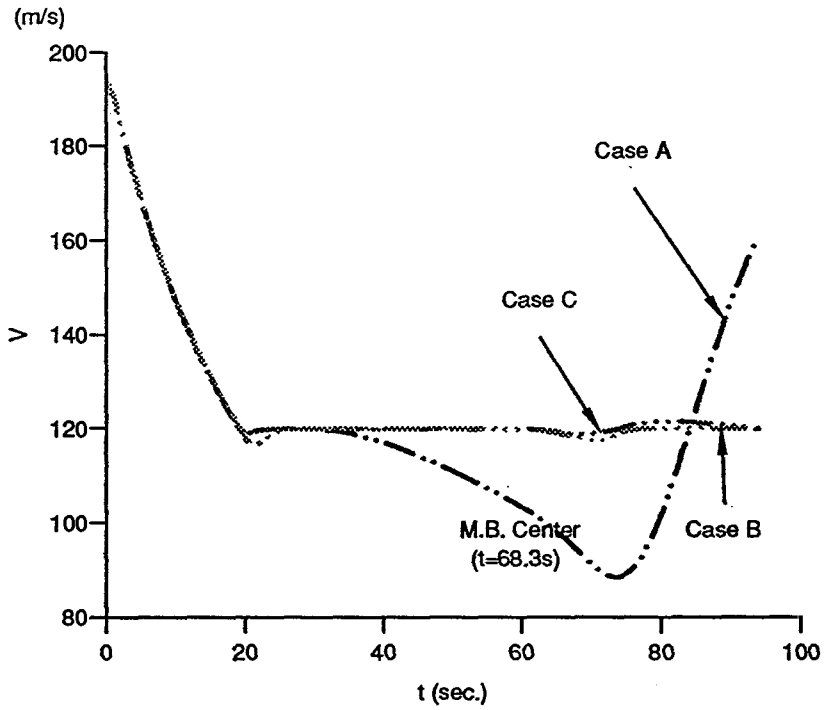

Figure 6-7(d) Comparison of path angle responses

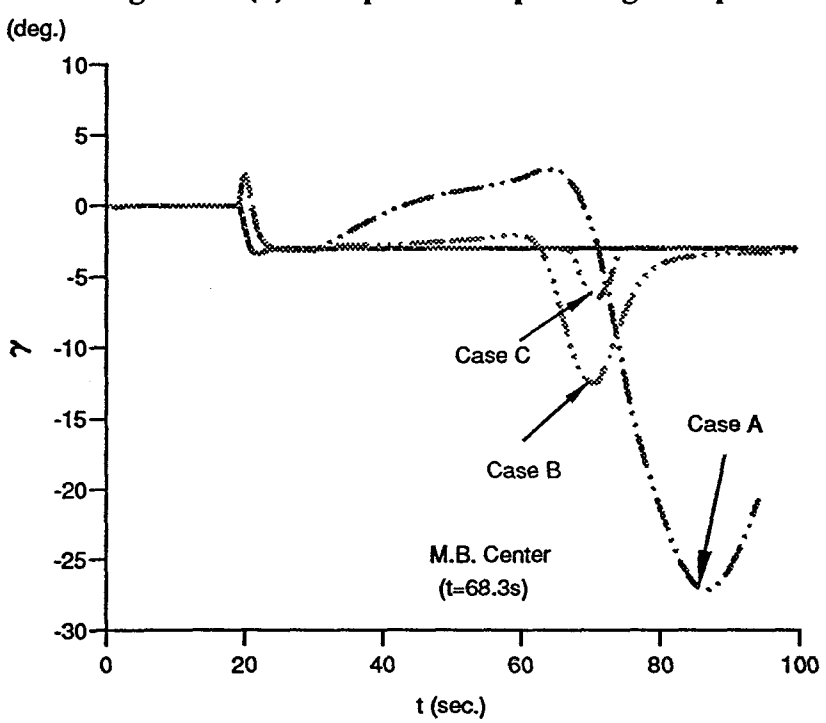

Figure 6-7(e) Spoiler control output

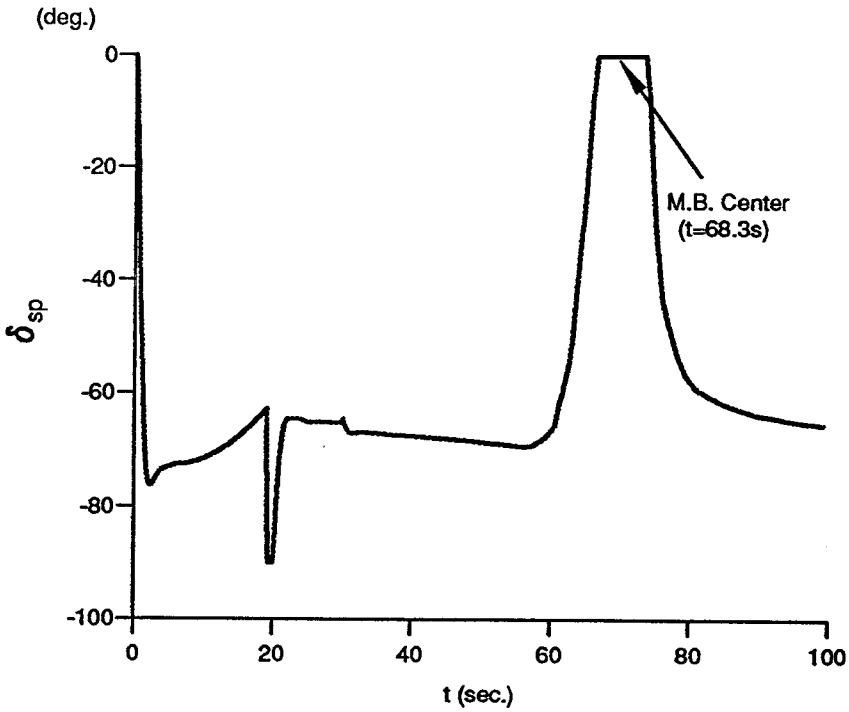

Chapter Seven

ADAPTIVE CONTROL OF NONLINEAR AIRCRAFT SYSTEMS

7.1 General Remarks

The work of this chapter concerns the robustness enhancement of the control of nonlinear aircraft systems. Based on the simulation investigations on the aircraft responses to the disturbances resulting from the system modelling errors, an approach using a parameter adaptive control logic (PACL) for the robustness of the designed longitudinal inverse dynamics flight control system was studied.

The importance of the adaptive control is a consequence of the following two facts. First, the effectiveness of the desired NID control is heavily dependent on the modelling accuracy of the dynamic systems to be controlled. This means that an exact cancellation of all nonlinear terms concerned should be obtained for the implementation of exactly linear control laws and system decouplings. Therefore if there is any uncertainty or errors in the modelling process, and hence in the inverse dynamics formulation, the cancellation would not be exact and so the resulting control might not meet the design specifications. The second fact is that it has been increasingly difficult to model precisely a modern aircraft with increased dynamic ranges and flight envelopes, nonlinearities and complex aerodynamics.

Moreover, the issue could become even crucial in some worst cases where a stable model based NID is applied to the controlled aircraft which is naturally unstable (as for the relaxed static stability cases), as later shown.

Upon the analysis of the key stability factors in aircraft longitudinal modelling, a parameter adaptive control algorithm for the robustness of HAWK control under the parameter error-induced disturbance was developed. It referred to the newly developed adaptive control theory for a class of linearizable control systems (SASTRY &ISIDORI, 1989) and was combined with the LIDFCS design. Simulations of flight controls under some worst modelling cases of the aircraft dynamics are presented, showing the effectiveness of the adaptive control in the enhancement of aircraft control and stability.

7.2 Adaptive Control Based on NID Design --- Recent Theory Review

The NID-based adaptive control aims to solve the following problem: suppose a

nonlinear system described as (5-1) has the system dynamic matrix A(x) and the control matrix B(x) as:

$$A(x) = \sum_{i=1}^{n_1} \theta_{A_i} A_i(x) \tag{7-1}$$

and

$$B(x) = \sum_{i=1}^{n_2} \theta_{B_j} B_j(x) \tag{7-2}$$

where θ_{A_i}, i=1,..., n_1; θ_{B_j}, j=1,..., n_2 are unknown parameters and the $A_i(x)$ and $B_j(x)$ are known functions. And at time t, we have the estimates of $\hat{A}(x)$ and $\hat{B}(x)$ which take the forms:

$$\hat{A}(x) = \sum_{i=1}^{n_1} \hat{\theta}_{A_i} A_i(x) \tag{7-3}$$

and

$$\hat{B}(x) = \sum_{i=1}^{n_2} \hat{\theta}_{B_j} B_j(x) \tag{7-4}$$

Here $\hat{\theta}_{A_i}$ and $\hat{\theta}_{B_j}$ stand for the estimates of θ_{A_i} and θ_{B_j}.

For a **SISO** system with the relative order r, ideally there is:

$$L_B C = L_B L_A C = \cdots = L_B L_A{}^{r-2} C = 0; \quad L_B L_A{}^{r-1} C \neq 0 \tag{7-5}$$

and, according to (5-5) and (5-7), the state feedback control can be written as:

$$u = \frac{(-L_A{}^r C + v)}{L_B L_A{}^{r-1} C} \tag{7-6}$$

where the control law v for model-tracking is, from (5-12),

$$v = y_m{}^r + \alpha_r (y_m{}^{r-1} - y^{r-1}) + \cdots + \alpha_1 (y_m - y) \tag{7-7}$$

On the other hand, the feedback control based on the inaccurate model (7-3) and (7-4) yields:

$$\hat{u} = \frac{(-\hat{L}_A{}^r C + \hat{v})}{\hat{L}_B \hat{L}_A{}^{r-1} C} \qquad (7\text{-}8)$$

and the implementation of the tracking law $\hat{v}$:

$$\hat{v} = y_m{}^r + \alpha_r[y_m{}^{r-1} - (\hat{L}_A{}^{r-1}C)] + \cdots + \alpha_1(y_m - y) \qquad (7\text{-}9)$$

where $\hat{L}_A{}^i C$ and $\hat{L}_B \hat{L}_A{}^{r-1}$ denote the estimates of $L_A{}^i C$ and $L_B L_A{}^{r-1}$, resulting from (7-3) and (7-4),

$$\hat{L}_A{}^i C := L_{\hat{A}}{}^i C \qquad i=1,\ldots,r \qquad (7\text{-}10)$$

$$\hat{L}_B \hat{L}_A{}^{r-1} C = L_{\hat{B}} L_{\hat{A}}{}^{r-1} C \qquad (7\text{-}11)$$

Some examples are as:

$$r=1: \quad L_{\hat{A}} C = \sum_{i=1}^{n_1} \hat{\theta}_{A_i} L_{A_i} C \qquad L_{\hat{b}} C = \sum_{j=1}^{n_2} \hat{\theta}_{B_j} L_{B_j} C$$

$$r=2: \quad L_{\hat{A}}{}^2 C = \sum_{i=1}^{n_1} \sum_{j=1}^{n_1} \frac{\partial}{\partial x}\left(\frac{\partial C}{\partial x} A_j\right) A_i \hat{\theta}_{A_i} \hat{\theta}_{A_j}$$

$$L_{\hat{B}} L_{\hat{A}} C = \sum_{i=1}^{n_2} \sum_{j=1}^{n_1} \frac{\partial}{\partial x}\left(\frac{\partial C}{\partial x} A_j\right) B_i \hat{\theta}_{B_i} \hat{\theta}_{A_j}$$

and so on. The development of the preceding section could easily be repeated if we define each of the parameter products to be a new parameter.

Define $\Theta \in \Re^k$ as the K (generally K is large!) component vector of parameters $\theta_{A_i}, \theta_{A_i}\theta_{A_j}, \theta_{A_i}\theta_{A_j}\theta_{A_k}, \underbrace{\ldots\ldots, \theta_{A_i}\ldots\theta_{A_j}}_{r}, \underbrace{\theta_{A_i}\ldots\theta_{A_j}}_{r-1}\theta_{B_i}$. Thus, for example, if r=3, the Θ contains $\theta_{A_i}\binom{1}{n_1}, \theta_{A_i}\theta_{A_j}\binom{2}{n_1}, \theta_{A_i}\theta_{A_j}\theta_{A_k}\binom{3}{n_1}, \theta_{A_i}\theta_{A_j}\theta_{b_i}\binom{2}{n_1}\binom{1}{n_2}$, where $\binom{m}{n}$ denotes $\frac{n!}{(n-m)!m!}$. Define $\hat{\Theta}(t)$ as the estimate of Θ.

Due to the inaccuracies in the modelling ((7-3), (7-4)), there will not be an explicit linear relation between y^r and v (y^r=v in accurate modelling cases), rather it is replaced by the following relation as far as (5-2) and (7-8) are concerned:

$$y^r = L_A{}^r C + L_B L_A{}^{r-1} C\hat{u}$$

$$= L_A{}^r + \frac{L_B L_A{}^{r-1} C}{\hat{L}_B \hat{L}_A{}^{r-1} C}\left(-\hat{L}_A{}^r C + \hat{v}\right) \qquad (7\text{-}12)$$

Based on (7-7) and (7-12), the tracking error equation for $e=y-y_m$ in the existence of parameter uncertainty becomes:

$$e^r + \alpha_1 e^{r-1} + \ldots\ldots + \alpha_r e$$
$$= L_A{}^r C + \frac{L_B L_A{}^{r-1} C}{L_{\hat{B}} L_{\hat{A}}{}^{r-1} C}\left(-L_{\hat{A}}{}^r C + \hat{v}\right) - v$$
$$= (L_A{}^r C - L_{\hat{A}}{}^r C) + (L_B L_A{}^{r-1} C - L_{\hat{B}} L_{\hat{A}}{}^{r-1} C)\frac{\left(-L_{\hat{A}}{}^r C + \hat{v}\right)}{L_{\hat{B}} L_{\hat{A}}{}^{r-1} C} + \hat{v} - v$$
$$:= \Phi' W_1 + \Phi' W_2 = \Phi' W \qquad (7\text{-}13)$$

where $\Phi := \hat{\Theta}(t) - \Theta, W = [W_1 + W_2]$, W_1 comes from the mismatch between the ideal linearizing law and the actual linearizing law and W_2 is from the mismatch between the ideal model following control v and the actual tracking control $\hat{v}$.

So the effect of parameter uncertainty in system modelling is explicitly expressed by the introduction of the stimulating item $\Phi' W$ into the tracking error equation. The adaptive control logic for SISO systems is based on the following theorem.

Theorem (basic tracking theorem for **SISO** systems with relative degree greater than 1; SASTRY and ISIDORI, 1989):

Consider the control law of (7-8) and (7-9) applied to an exponentially minimum-phase nonlinear system with parameter uncertainty as given in (7-1) and (7-2).

If $y_m, \dot{y}_m, \cdots, y_m{}^{(r-1)}$ are bounded, $\hat{L}_B \hat{L}_A{}^{(r-1)} C$ is bounded away from zero, A, B, C, $L_A{}^k C$ are Lipschitz continuous functions of x, and $W(x,\hat{\Theta})$ has bounded derivatives in x, $\hat{\Theta}$, then the parameter update law

$$\dot{\Phi} = \frac{-e\zeta}{1+\zeta'\zeta} \qquad (7\text{-}14)$$

with

$$\zeta = L^{-1}(s)W = M(s)W \qquad (7\text{-}15)$$

yields bounded tracking (i.e. x is bounded and $y \to y_m$ as $t \to \infty$).

Here: $L^{-1}(s) = M(s) = \dfrac{1}{s^r + \alpha_1 s^{r-1} + \cdots + \alpha_r}$ with the stable poles defined by α_i and W is as defined in (7-10).

Parameter update procedure

Based on the theorem above, a parameter update procedure was developed and applied to the parameter adaptive control in the LIDFCS. The major steps of the procedure are summarised as:

1) Define a proper polynomial $L(s) = S^r + a_1 S^{r-1} + \ldots\ldots + a_r$, so $M(s) = L^{-1}(s)$ is strictly proper and stable. In many cases, $a_{i\ (i=1\ldots r)}$ can refer to $\alpha_{i\ (i=1\ldots r)}$ in (5-15) for the desirable pole assignment.

2) Define the error equation (7-13) (key step!) according to specified parameter adaptations.

3) From the error equation, get the mismatch regressor W and then the intermediate variable $\xi = M(s)W$.

4) From the measurement $e = y_m - y$, use of the normalized gradient-type algorithm (7-14) gives the update law:

$$\dot{\Phi} = \frac{-e\xi}{1 + \xi'\xi}$$

5) In the case of θ being constant or its variation being negligible in the updating process, we have:

$$\dot{\hat{\theta}} = \dot{\Phi}$$

so an update computation of $\hat{\theta}$ can be made through:

$$\hat{\theta}_{k+1} = \hat{\theta}_k + \dot{\Phi}T$$

6) Go back to step (3) for the iteration.

7.3 Effects of Modelling Uncertainty on Flight Control and Stability

Combined with the LIDFCS, some worst effects from the system modelling were studied by simulations.

7.3.1 Modelling errors in the longitudinal moment equation

As the pitch attitude dynamics of an aircraft are directly connected with the moment equation of the longitudinal dynamics, special attention was drawn to the modelling errors in this equation, which, in this study, has the form as:

$$\dot{q} = \frac{1}{2I_{yy}}\rho V^2 S\bar{c}(C_{m0}(M) + C_{m\alpha}(M)\alpha + C_{m\delta_e}(M)\delta_e + C_{MSP}(\alpha,\delta_{sp}) + \frac{1}{4I_{yy}}\rho V S\bar{c}^2(C_{mq}(M)q + C_{m\dot{\alpha}}(M)\dot{\alpha}) \quad (7\text{-}16)$$

The importance of the equation and its influence on aircraft dynamics and stability can be recognised by the following:

1. In conventional aircraft and flight, equation (7-16) governs the highly influential short period mode of the aircraft's longitudinal dynamics, hence its change could affect the stability and control of an aircraft in a fast and considerable way. Analysis in the longitudinal approximations (NELSON, 1989) has shown that the stability derivatives C_{mq} and $C_{m\dot{\alpha}}$ have direct effects on the damping of short-period motion while $C_{m\alpha}$, the change in the pitching moment coefficient with incidence angle, is directly connected with aircraft static stability and the frequency of the short-period mode. While in many studies these coefficients are ideally treated as constant (or nearly constant), in practice they are in constant variation with flight conditions.

2. The modern active control of an aircraft may well adopt the RSS function (**Chapter One**) to gain higher lift/drag ratio. This can be achieved by reducing the static stability margin of the aircraft and hence may result in a naturally (statically) unstable ($C_{m\alpha} \geq 0$) aircraft.

7.3.2 Effects of the modelling errors --- flight simulations

Simulations were carried out to study the effects of modelling errors owing to inaccurate moment equation parameters for the HAWK. It was revealed, from both the theoretical analysis and simulations, that the longitudinal static stability derivative $C_{m\alpha}$ could be one of the most influential coefficients for longitudinal flight.

Fig. 7-1(a) shows an angular tracking control for the pitch angle θ and path angle γ, with the aircraft model being accurately estimated but varying with different static stability. The control mode used here was B2 from LIDFCS to control the aircraft performing a decoupling manoeuvre. The three selected stability states of the aircraft were $C_{m\alpha}$= -0.18 (nominal, stable), $C_{m\alpha}$=0 (neutral) and $C_{m\alpha}$=0.18 (unstable).

While **Fig. 7-1(b)** presents the three elevator controls corresponding to the three stability cases.

Comments: Of all the three cases where accurate aircraft models were used for the NID computations (7-8), (7-9), LIDFCS brought precise tracking controls to both the attitude and trajectory. The effects from the difference in the static stability of the aircraft can be clearly observed by comparison of the elevator control profiles for these three cases. The trimming deflection tends to vary from negative to positive corresponding to the change of the aircraft static stability (ACSS) varying from the stable to unstable. The changes also brought some variation in the overshoot for the three cases (see $\theta(t)$ in **Fig. 7-1(a)**), with the worst relating to the unstable case.

An extreme yet most dangerous case from the modelling inaccuracy point of view in (7-16) was proposed and simulated where the aircraft was assumed to be made statically unstable through RSS, with the coefficient $C_{m\alpha}$=0.185, while the NID control applied to the aircraft was still based on the nominal stable coefficient $C_{m\alpha}$=-0.185. Simulation of applying the NID control to the aircraft using the control mode A1 gives the divergence results shown in **Fig. 7-2.**

Comment: Owing to the large error in the estimation of the key coefficient in the moment equation, the LIDFCS failed to augment the aircraft using the designed feedback control and model-tracking, and hence resulted in loss of both control and stability.

7.4 Development of Adaptive Control for LIDFCS

In order to try to enhance the robustness of the NID control to modelling inaccuracies, an parameter adaptive control logic (PACL) based on the theory in **7.2** and the longitudinal dynamics of HAWK was designed and applied to the control augmentation of the aircraft in conjunction with the LIDFCS.

At a first case, a **SISO** problem was formulated for the aircraft system with the input u chosen as the elevator and the output y as the pitch attitude (θ). It can be

described by: suppose the aircraft dynamics have the parameter composition form of (7-1) and (7-2), with some unknown parameters θ_{A_i} and θ_{B_i} in the model; find a parameter adaptive logic (in the form of (7-15)) for the parameters which ensures bounded tracking using the NID control, i.e. x is bounded and $y \to y_m$ as $t \to \infty$.

7.4.1 PACL for parameter uncertainty in A(x)

First, consider the case of parameter uncertainty only in the dynamic matrix A(x) which takes the form:

$$A(x)=\theta_{A_1} A_1(x)+\theta_{A_2} A_2(x) \qquad (7\text{-}17)$$

So (5-1) becomes:

$$\dot{x} = \theta_{A_1} A_1(x) + \theta_{A_2} A_2(x) + B(x)u \quad , \quad y = Cx \qquad (7\text{-}18)$$

Suppose that θ_{A_2} is inaccurate, thus the estimated aircraft model on which the NID control based is:

$$\dot{x} = \theta_{A_1} A_1(x) + \hat{\theta}_{A_2} A_2(x) + B(x)u \quad , \quad y = Cx \qquad (7\text{-}19)$$

Here, $\theta_{A_2} A_2(x)$ can be defined to be any interesting part in the aircraft model. When it is chosen as part of the moment equation, referring to the HAWK model (**Appendix**), we have:

$$\begin{aligned} A_1(x)&=[a_1(x),\ a_2(x),\ a_3(x),\ a_{41}(x),\ a_5(x),\ a_6(x)]';\\ A_2(x)&=[\ 0\ ,\ 0\ ,\ 0\ ,\ a_{42}(x),\ 0\ ,\ 0\ ]';\\ B(x)&=[\ 0\ ,\ 0\ ,\ 0\ ,\ b_e(x),\ 0\ ,\ 0\ ]',\\ C&=[\ 0\ ,\ 1\ ,\ 1\ ,\ 0\ ,\ 0\ ,\ 0\ ]'. \end{aligned} \qquad (7\text{-}20)$$

where $x=[V, \gamma, \alpha, q, \delta_t, \delta_{sp}]$, $u=\delta_e$, $y=\theta$.

PACL development:

Since r=2, it follows from (7-9) that

$$\hat{v} = \ddot{e} + \alpha_1 \dot{e} + \alpha_2 e + \ddot{y} + \alpha_1 (\dot{y} - \hat{L}_A C) \qquad (7\text{-}21)$$

From the actual model (7-18), we have:

$$\dot{y} = \hat{L}_A C = C[\theta_{A_1} A_1(x)] \tag{7-22}$$

$$\ddot{y} = C(\theta_{A_1})^2 \frac{\partial A_1(x)}{\partial x} A_1(x) + C\theta_{A_1}\theta_{A_2}(\frac{\partial A_1(x)}{\partial x})A_2(x) + C\theta_{A_1}(\frac{\partial A_1(x)}{\partial x})B(x)u \tag{7-23}$$

From (7-8), the control based on the inaccurate model is

$$\hat{u} = \frac{(-\hat{L}_A{}^2 C + \hat{v})}{\hat{L}_B \hat{L}_A C} \tag{7-24}$$

where

$$\hat{L}_A{}^2 C = C(\theta_{A_1})^2 \frac{\partial A_1(x)}{\partial x} A_1(x) + C\theta_{A_1}\hat{\theta}_{A_2}(\frac{\partial A_1(x)}{\partial x})A_2(x), \tag{7-25}$$

$$\hat{L}_B \hat{L}_A C = C\theta_{A_1}(\frac{\partial A_1(x)}{\partial x})B(x). \tag{7-26}$$

Substitute $\ddot{y}$, $\dot{y}$ and $\hat{L}_A C$ in (7-21) for (7-22) through (7-26), to give the error equation in the form of (7-13):

$$\ddot{e} + \alpha_1 \dot{e} + \alpha_2 e = \Phi W \tag{7-27}$$

where $\Phi = \hat{\theta}_{A_2} - \theta_{A_2}$ and $W = C\theta_{A_1} \frac{\partial A_1(x)}{\partial x} A_2(x)$.

7.4.2 PACL for parameter uncertainty in A(x) and B(x)

In this case, the actual aircraft dynamics is supposed to be

$$\dot{x} = \theta_{A_1} A_1(x) + \theta_{A_2} A_2(x) + \theta_B B(x)u \quad , \quad y = Cx \tag{7-28}$$

while the NID control refers to the following estimated model:

$$\dot{x} = \theta_{A_1} A_1(x) + \hat{\theta}_{A_2} A_2(x) + \hat{\theta}_B B(x)u \quad , \quad y = Cx \tag{7-29}$$

where $\hat{\theta}_{A_2}$ and $\hat{\theta}_B$ are the uncertain parameters and $A_1(x)$, $A_2(x)$ and $B(x)$ take the same form as (7-20).

As in **7.4.1**, define the output as θ and the input δ_e. Then we have (7-22), (7-24), (7-25) and

$$\ddot{y} = C(\theta_{A_1})^2 \frac{\partial A_1(x)}{\partial x} A_1(x) + C\theta_{A_1}\theta_{A_2}(\frac{\partial A_1(x)}{\partial x})A_2(x) + C\theta_{A_1}\theta_B(\frac{\partial A_1(x)}{\partial x})B(x)u \tag{7-30}$$

$$\hat{L}_B\hat{L}_A C = C\theta_{A_1}\hat{\theta}_B(\frac{\partial A_1(x)}{\partial x})B(x). \tag{7-31}$$

So from (7-21), the error equation for this case is:

$$\ddot{e} + \alpha_1\dot{e} + \alpha_2 e = \hat{v} - \ddot{y} = \begin{bmatrix}\Phi_{A_2} & \Phi_B\end{bmatrix}\begin{bmatrix}W_A \\ W_B\end{bmatrix} \tag{7-32}$$

where $\Phi_{A_2} = \hat{\theta}_{A_2} - \theta_{A_2}$, $\Phi_B = \hat{\theta}_B - \theta_B$;

$$W_A = C\theta_{A_1}(\frac{\partial A_1(x)}{\partial x})A_2(x),$$

$$W_B = C\theta_{A_1}(\frac{\partial A_1(x)}{\partial x})B(x)\frac{(-\hat{L}_A^{(2)}C + \hat{v})}{\hat{L}_B\hat{L}_A C} = C\theta_{A_1}(\frac{\partial A_1(x)}{\partial x})B(x)\hat{u}.$$

7.5 Adaptive Control of HAWK Aircraft with Uncertain Static Stability

The adaptive control of the HAWK with uncertain static stability owing to parameter errors can be seen as a particular application of the PACL described above by which its effectiveness in the enhancement of the robustness of the NID control is shown.

7.5.1 PACL design for the HAWK

As pointed in **7.3.1**, the static stability of an aircraft can be decided by the moment coefficient $C_{m\alpha}$. Suppose this key coefficient is uncertain, the PACL development for the aircraft with uncertain static stability can be made as the following:

PACL for uncertain $C_{m\alpha}$ and the known B(x)

According to (7-18) and (7-20), define: $\theta_{A_1} = 1.0$, $\theta_{A_2} = C_{m\alpha}$.

Since $\dot{\gamma} = a_2(x)$ and $\dot{\alpha} = a_3(x)$, there is:

$$C\theta_{A_1}(\frac{\partial A_1(x)}{\partial x}) = 1$$

So the right side of the error equation (7-27) becomes:

$\Phi = \hat{C}_{m\alpha} - C_{m\alpha}$, W= $a_{42}(x)$, where $a_{42}(x) = (\rho V^2 S\bar{c}\alpha) / 2I_{yy}$.

PACL for uncertain $C_{m\alpha}$ and B(x)

According to (7-28) and (7-20), choose: $\theta_{A_1} = 1.0$, $\theta_{A_2} = C_{m\alpha}$, $\theta_B = C_{m\delta_e}$.

The right side of the error equation (7-32) becomes:

$$\Phi = \begin{bmatrix} \Phi_{A_2} & \Phi_B \end{bmatrix}; \quad \Phi_{A_2} = \hat{C}_{m\alpha} - C_{m\alpha}, \Phi_B = \hat{C}_{m\delta_e} - C_{m\delta_e}.$$

$$W = \begin{bmatrix} W_A \\ W_B \end{bmatrix}; \quad W_A = a_{42}(x), W_B = b(x)\left(\frac{-\hat{L}_A^{(2)}C + \hat{v}}{\hat{L}_A\hat{L}_B C}\right) = b(x)\hat{u}_e$$

where $b(x) = (\rho V^2 S\bar{c}\delta_e) / 2I_{yy}$.

Once Φ and W are decided, the parameter update procedure in **7.2** can be programmed and performed. In the HAWK cases, the PACL was incorporated with the package 'HAWKSIM1'. For $y=\theta$, L(s) was taken the same as the pole polynomial for θ in **Table 5-1**.

7.5.2 Adaptive control simulations

Based on the PACL design, further simulations were conducted on the evaluation of its effectiveness in the enhancement of the NID robustness.

Fig. 7-3 shows the application of the NID control augmented with PACL to the HAWK with uncertain static stability. Here the initial estimate of $C_{m\alpha}$ and the control objective were the same as that shown in **Fig. 7-2**. However, due to the introduction of the PACL, the system becomes stable and follows well the control objective, after a short period of initial and much reduced oscillation.

Fig. 7-4 presents a comparison between the system performances using PACL and that without using PACL. Here the actual aircraft was supposed to be neutrally stable

with the stability coefficients $C_{m\alpha}$=0.0 and $C_{m\delta e}$= -0.475, while the initial estimated aircraft model for the NID control employed the nominal data $\hat{C}_{m\alpha}$=-0.185 and the reduced estimate $\hat{C}_{m\delta e}$= -0.2.

From the simulation without using PACL, the LIDFCS, using the control mode A1, failed to control both θ (**Fig. 7-4(a)**) and V (**Fig. 7-4(b)**) tracking the desired trajectories and caused several deterioration in the stability (in a violent oscillation) and handling of the aircraft. In sharp contrast, by applying PACL to the system, the stability of the aircraft was immediately restored after a short period of 'stimulating process' for the parameter updating and θ and V tracked the desired trajectories.

Fig. 7-5 shows the case where the control mode B2 (with the spoiler control) was applied. By comparison between the cases with and without the use of PACL, it can be seen that even in the presence of the extra control input (spoilers) which may stimulate the original oscillation, the designed adaptive control logic still works properly and brings an improved, robust, NID control to the aircraft.

The update trend for the key coefficient $\hat{C}_{m\alpha}$ is shown in **Fig. 7-6.** It can be seen that at the time of gaining stability and control, the PACL also brings a desirable coefficient update towards the real data. It should be remembered, however, that according to the bounded tracking theory, matching between the model parameters and the real parameters during the transient period is not guaranteed, although most simulations in this aspect did suggest that the matching took place.

7.6 Concluding Remarks

This chapter summarizes the final phase of the study on the application of NID-based adaptive control to the LIDFCS of the HAWK, in order to enhance the robustness of NID control. This work is somewhat preliminary yet the results have proven encouraging.

A design procedure for PACL was developed and was applied to NID control of the HAWK. By simulating some of the worst modelling errors in the aircraft dynamics, the need for employing an accurately estimated system model for NID control was revealed. However, this demand could become less important if we combine the PACL with the normal NID control and gain improved robustness in stability and control. This is the benefit of the use of PACL. Further, from design experience, it seems that the

adaptive control logic can be conveniently implemented along with the normal NID control computations.

Although the emphasis here has been on SISO theory and applications, it has been shown that in some particular cases, such as for the uncertainty in the aircraft moment equation only, the PACL is applicable to the adaptive control of nonlinear MIMO systems. However, it is clear that for more sophisticated and multi-functional adaptive control of aircraft, further study of the adaptive control of nonlinear MIMO systems for aircraft is needed.

Figure 7-1(a) Angular trackings at different ACSS
(with accurate modelling of AC)

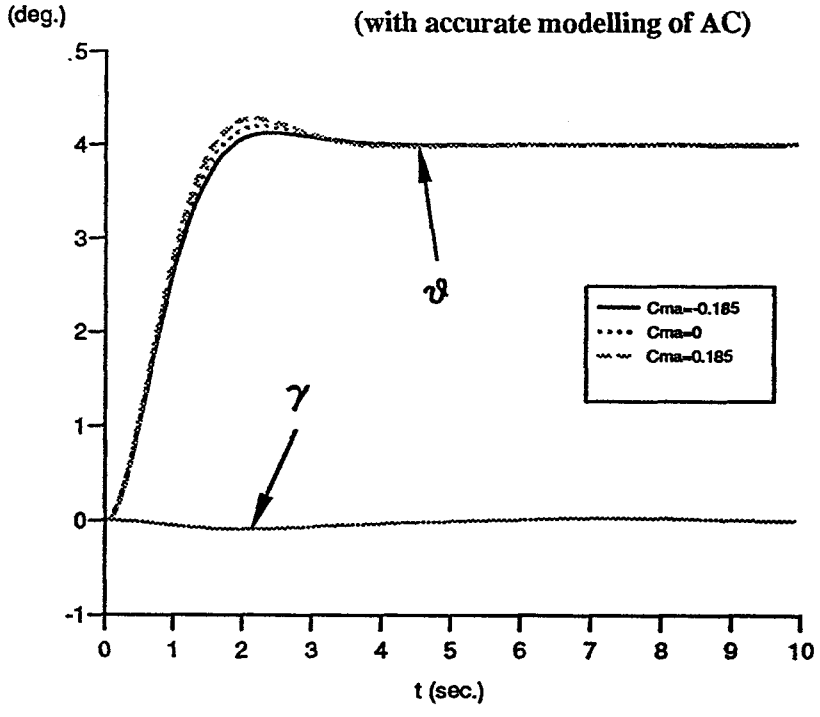

Figure 7-1(b) Time-histories of elevator controls at different ACSS

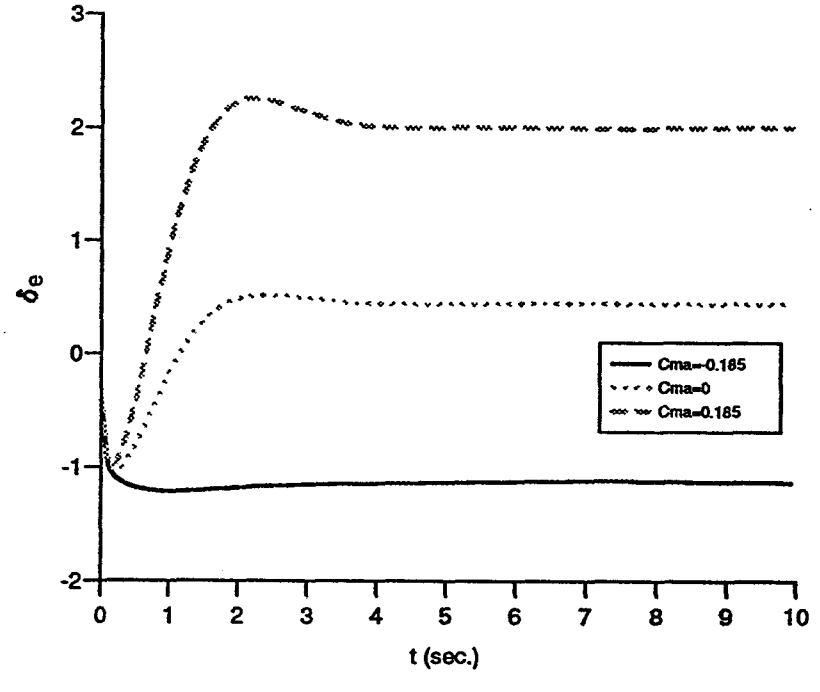

Figure 7-2(a) Angular trackings at unstable ACSS (inaccurate AC model: $C_{m\alpha}$=0.185, $\hat{C}_{m\alpha}$= -0.185)

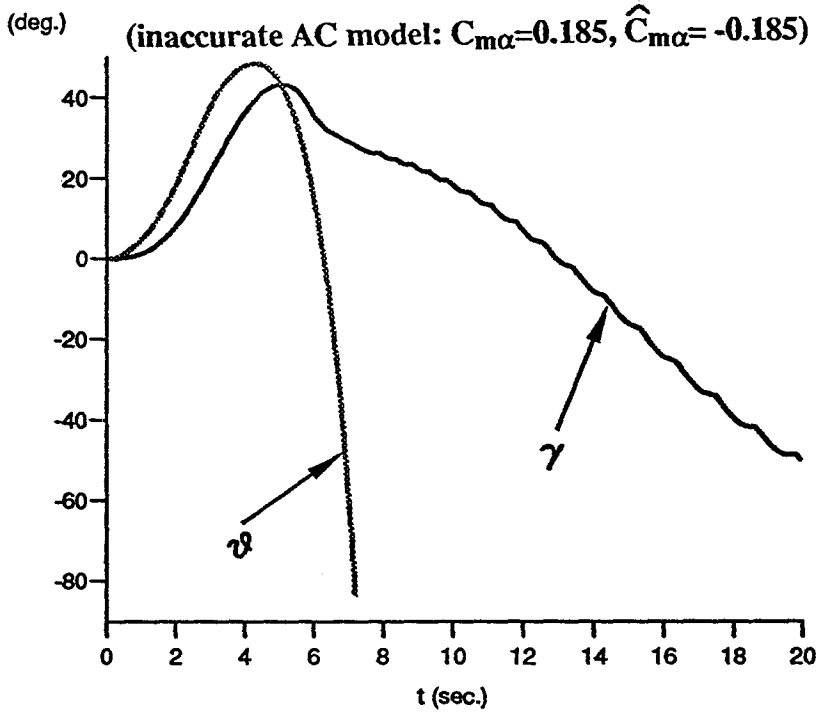

Figure 7-2(b) Response of path velocity

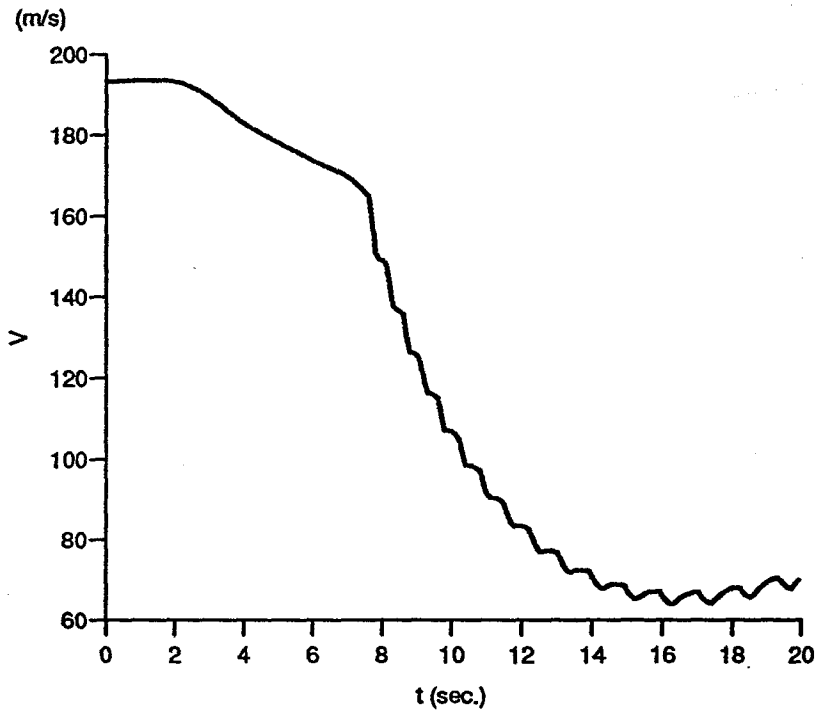

Figure 7-3(a) Angular trackings at unstable ACSS
(with PACL: $C_{m\alpha}$=0.185, $\hat{C}_{m\alpha}$= -0.185)

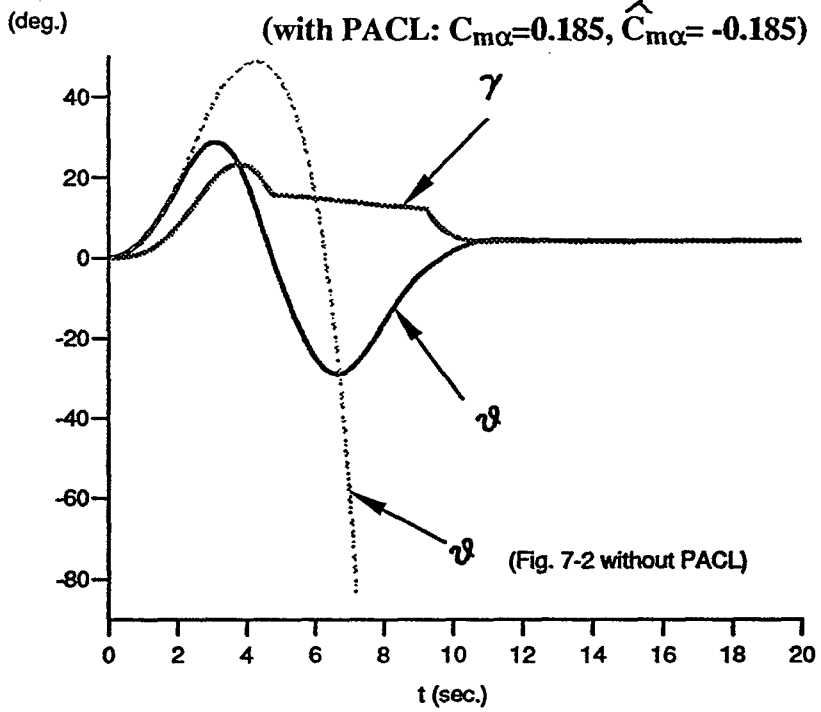

Figure 7-3(b) Improvement in V tracking using PACL

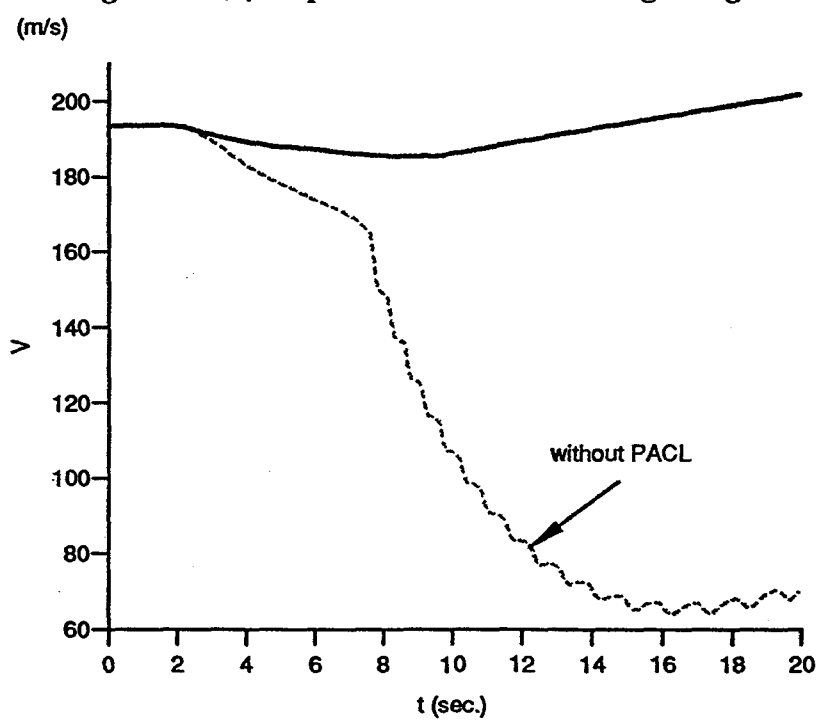

Figure 7-4(a) Comparison of pitch angle trackings
($C_{m\alpha}$=0, $C_{m\delta e}$= -0.475; $\hat{C}_{m\alpha}$= -0.185, $\hat{C}_{m\delta e}$= -0.2)

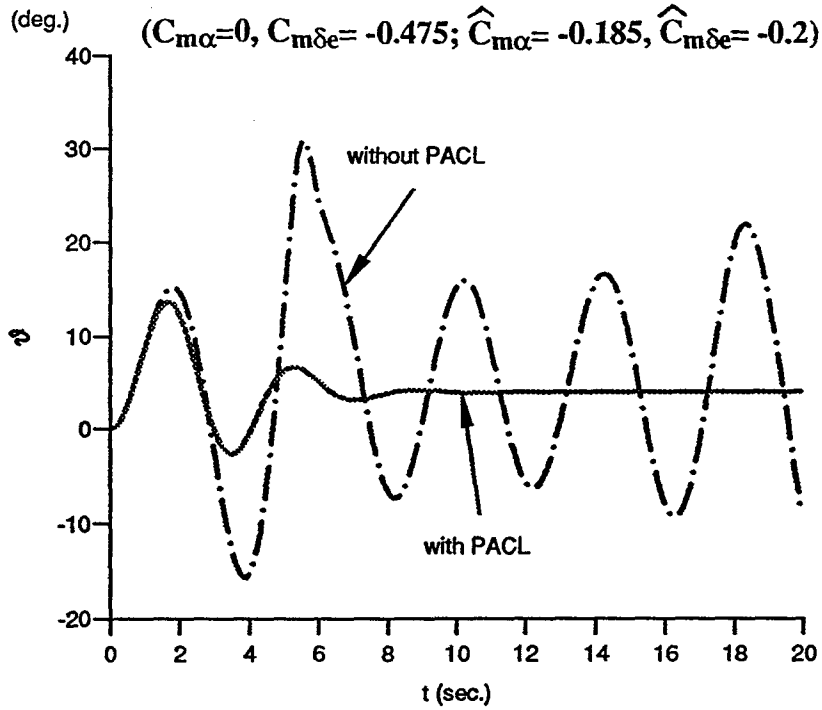

Figure 7-4(b) Comparison of velocity trackings

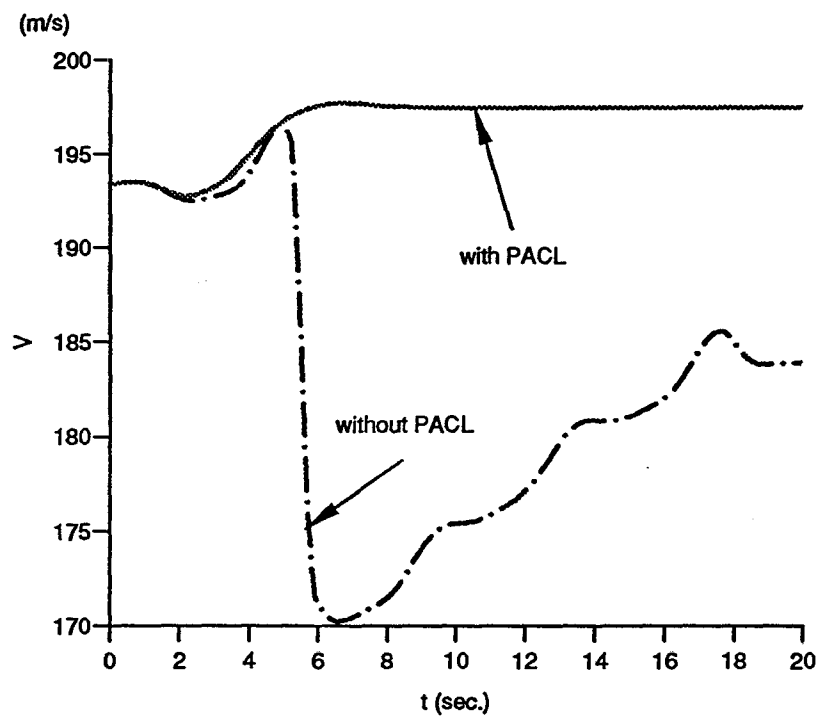

Figure 7-5 Comparison of pitch angle trackings (in the existence of spoiler control)

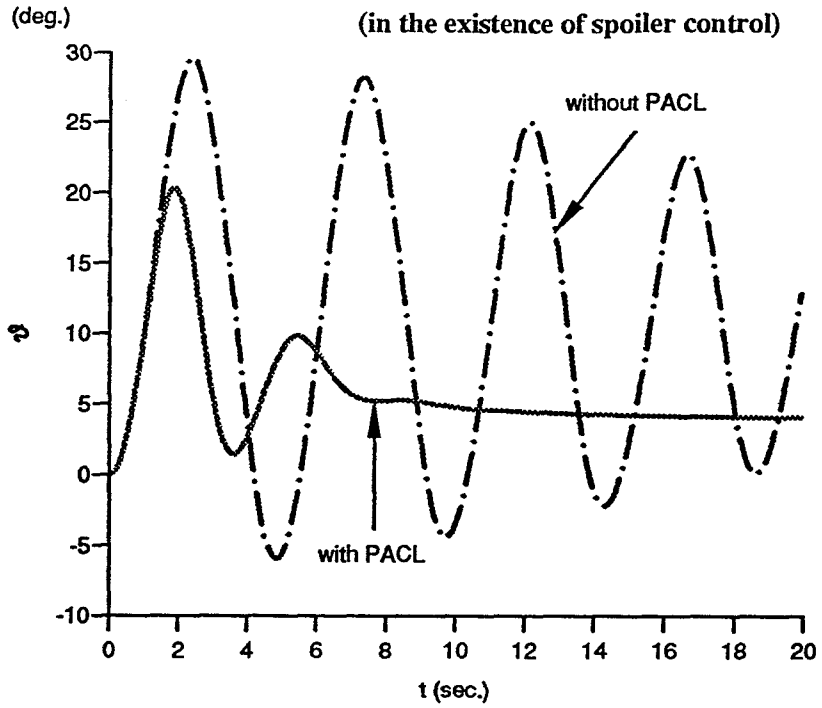

Figure 7-6 Time-histories of Cma updating using PACL

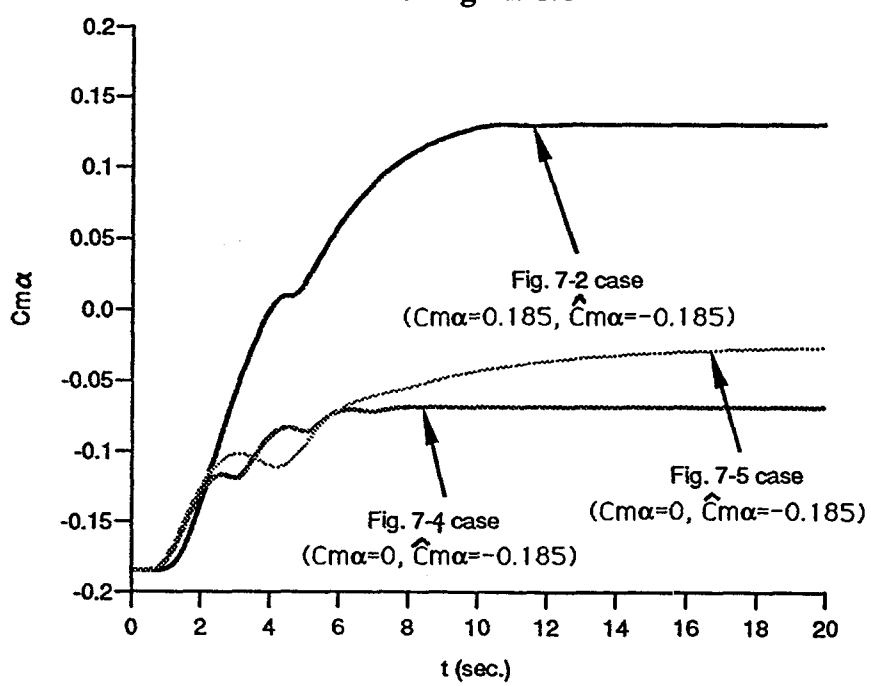

Chapter Eight

CONCLUSIONS AND FUTURE WORK

The theme of this research has been spoilers and their application to the active control of modern aircraft. A series of studies, concerning the modelling, control configuration and active use of spoilers in flight control, have been carried out. These have involved a systematic analysis of spoiler control and have clearly demonstrated that spoilers can be more useful than might have been expected for conventional aircraft and their role in the active control of future aircraft seems promising.

There is no doubt that advanced control comes from sophisticated control law design and effective system development. Combined with the spoiler control issues, this thesis has studied and employed a number of advanced methodologies for control design and system development, including the range space method for linear optimal control, the Haniltonian minimization principle for the nonlinear two-point boundary-value optimal control, and the newly-developed differential geometric control theory for the design and development of the global model-tracking nonlinear control and its robustness. Although the particular emphasis was on the flight control applications of the methodologies, various successful routines and design procedures used in the work should certainly stimulate and benefit many other control studies.

8.1 Conclusions

8.1.1 On spoiler control modelling

The work reported here seems to be the first attempt at generating a generic control model for most conventional aft-mounted spoilers. It yielded expressions for the coefficients of C_{LSP}, C_{DSP} and C_{MSP}, in both linear and nonlinear forms, directly from the experimental data.

The work has shown that the generic model proposed does indeed provide a logical, practical and yet also flexible way for representing the major control features of spoilers. The model can be used easily in different flight control studies and system developments.

As far as the modelling aspect is concerned, the model has incorporated the two most influential factors: the spoiler deflection angle δ_{sp} and the wing incidence α. A notable discovery is that the force effectiveness of spoilers, regardless of the

wing/aerofoil types, is almost proportional to their projected heights. This discovery not only suggested the 10% WC normalized spoiler but also led to the more accurate modelling using the sine form. The effect of the spoiler location on the moment coefficient has been shown to be significant.

It is concluded that in the use of spoilers for active control of aircraft, the lift coefficient C_{LSP} and the drag coefficient C_{DSP} are most decisive. The moment coefficient C_{MSP} has some unexpected and negative effects on the control effectiveness, and should be confined as a minimum (e.g. by properly shifting the spoiler hinge line towards to the middle wing chord position).

HAWK control simulations have shown that there are significant differences between the use of the linear model (**Spoiler Model Three**) and the nonlinear model (**Spoiler Model One**). It is therefore suggested that the nonlinear model be used whenever possible in order to obtain more realistic analysis of spoiler control. And accordingly, the effective deflection range of the spoiler is from 0 to 90^0.

8.1.2 On spoiler control effectiveness and applications

The conventional use of spoilers is for steady braking or lift dumping, this study has centred on the use of spoilers for fast control of aircraft dynamics, using their unique ability for generating quick direct force variations. Control effectiveness has been demonstrated in the analysis using range space theory, in open-loop optimal control studies and in a wide-range of flight simulations.

The work has shown that spoilers are best at controlling the flight path angle γ and the path velocity V. Since these variables are closely connected to the trajectory of an aircraft in the longitudinal profile, it is therefore concluded that spoilers can be very effective at achieving changes in flight trajectory.

Various different control application studies were carried out concerning the use of spoilers for the enhancement of the HAWK's performance levels, combined with the development of the longitudinal inverse dynamics flight control system. The studies were concerned with the important active control issues such as manoeuvrability enhancement, fast deceleration and gust/microburst alleviation, leading to the following conclusions regarding spoiler active control:

1. Spoilers are able to augment stability and enhance trajectory control of aircraft, and may well be applied to the achievement of mission objectives for some demanding

superior manoeuvres, e.g. for decoupled trajectory/attitude control, and/or for precise trajectory augmentation control.

2. Owing to the complexity in both the spoiler model and the nonlinear aircraft dynamics, advanced and sophisticated nonlinear control and the accompanying system development are required.

3. Special measures, such as the pre-set of the spoiler 'neutral' angle, normally varying from $0^o \sim -45^o$ for linearly-behaved spoilers and $0^o \sim -30^o$ for the nonlinearly-behaved spoilers, should be taken to exploit fully their control potential. In this thesis, a way of defining the neutral angle according to the relation between the spoiler deflection angle and the separately controlled incidence angle was proposed and has been proven successful.

4. It is important to note that making the best use of spoilers requires the employment of fast and powerful actuators in the spoiler control channel (characterised by high bandwidth and negligible delay and nonlinear effects).

8.1.3 On NID control and applications

A systematic study of the NID control scheme and its applications to nonlinear aircraft control were carried out. This yielded a sophisticated system on which various control mission objectives could be realized. The experience gained in the use of the methodology leads to the following conclusions:

1. System development using inverse dynamics is an effective method for synthesizing nonlinear controllers and generating a decoupled, multi-mode control system for a modern aircraft.

2. A new design procedure was found to be an efficient design routine for the applications of NID control and may well be used for other similar system developments. The procedure was based on the use of a set of principal output control variables and an uniform relative degree for all the control modes of interest, and involved the introduction of flight quality specifications directly into the controller syntheses.

3. The design process suggested that the system parameters should be made changeable to adapt to changes in both the flight conditions and the mission objectives, e.g. the parameters of the desired models should be made adjustable to compensate for nonlinearities resulted from control constraints.

8.1.4 On nonlinear adaptive flight control

It is concluded that the use of the NID based parameter adaptive control logic is important and can be very beneficial to the stability augmentation of aircraft and for the robustness enhancement of the NID control, especially in the cases where significant errors occur in the modelling of the controlled plant. The design procedure has also shown the flexibility of combining the PACL with the NID control. Although the emphasis was on the SISO control in this study, the simulation suggested that in some particular cases in flight control, PACL used can be applicable to MIMO cases including that both spoiler and thrust controls are used.

8.2 Future Work

1. On spoiler control modelling. This study has presented a systematic modelling procedure for a range of conventional spoilers. However, it has been realized during the modelling process that there is not enough spoiler aerodynamic data to enable the development of spoiler control model which can be confidently considered practical and reliable. Hence further studies on the spoiler aerodynamics are needed, with emphasis on the systematic and accurate measurement of all the control coefficients associated with a spoiler. Particular attention should be paid to the effects of spoiler moment coefficient, three-dimensional flow and flight conditions (e.g. Mach no. and flight height), on spoiler effectiveness. Moreover, owing to increased interest in the unsteady aerodynamics of spoilers, with which the innovative 'adverse lift' is connected, there is a challenge to investigate the modelling and control issues for unsteady spoilers.

2. On NID control and applications. Further work is needed on the applications of NID design to flight control, with emphasis on the analysis of the effects of parameters in the desired models, of the pole polynomials on model tracking, and on the application of parameter adaptation to the models for the alleviation of the nonlinear effects from control constraints. Additional future work in this area should focus on robustness of NID control, nonlinear MIMO adaptive control and the NID based H-infinity control, and their applications to aircraft.

3. On flight control systems. Design and development of a full 6-degrees of freedom flight control system with spoilers as an active control device should be done to further explore the use of the spoilers on a larger scale for both longitudinal and lateral control. The realization of NID controllers using digital fly-by-wire control systems should also be studied.

REFERENCE

Abed, E.H., "Nonlinear Stability Control of High Angle of Attack Flight Dynamics," *AIAA Paper*, No. 89-3487-CP, 1989.

Akhrif, O. and G. L. Blankenship, "Using Computer Algebra for design of Nonlinear Control systems," *Thesis Report* M.S. 87-2, University of Maryland, 1987.

Akhrif, O. and G.L. Blankenship, "Robust Stabilization of Feedback linearizable Systems," *Proc. of the 27th CDC*, pp. 1714-1719, 1988.

Asseo, S.J. "Decoupling of a Class of Nonlinear Systems and Its Application to an Aircraft Control Problem," *AIAA J. Aircraft*, no. 10, pp. 739-747, 1973.

Atherton, D.P., *Nonlinear Control Engineering*, Van Nostrand Reinhold Ltd, London, 1975.

Ayoub, A., S. Bodapati, K. Karamchet and H.C. Seetharam, "Unsteady Flow Patterns Associated with Spoiler Control Device," *AIAA Paper* No. 82-0217, 1982.

Barnes, C.S., "A Developed Theory of Spoilers on Airfoils", *British ARC* CP887, 1965.

Baumann, W.T. and W.J. Rugh, "Feedback Control of Nonlinear Systems by Extended Linearization," *IEEE Trans. on Automatic Control*, Vol. AC-31, no. 1, pp. 40-46, 1986.

Bodapati, S., M.D. Mack and K. Karamcheti , "Basic Studies of the Flow Fields of Aerofoil-Flap-Spoiler System," *AIAA Paper* No. 82-0173, 1982.

Bowles, R.L. and W. Forst, "Wind-Shear/Turbulence Inputs to Flight Simulation and Systems Certification," *NASA* CP-2474,1987.

Brockett, R.W., *Finite Dimensional Linear Systems*, John Wiley & Sons, 1970.

Bryson, E., Jr. and Y.C. Ho, *Applied Optimal Control* (Revised Printing), Halsted Press, John Wiley & Sons Inc., New York, 1975.

Bugajski, D.J., D.F. Enns and M. Elgersma, "A Dynamic Inversion Based Control Law with Application to the High Angle-of-Attack Research Vehicle," *AIAA Paper* No. 90-3407-CP, 1990.

Chen, C.T., *Linear System Theory and Design*, Holt, Rinchart and Winston, New York, 1970,

Consigny, H., A. Gravelle and R. Molinaro, "Aerodynamic Characteristics of a Two-Dimensional Moving Spoiler in Subsonic and Transonic Flow," *AIAA J. Aircraft*, Vol. 21, no. 9, 1984.

Corless, M.J. and G. Leitmann, "Continuous State Feedback Guaranteeing Uniform Ultimate Boundedness for Uncertain Dynamic Systems," *IEEE Trans. on Automatic control*, Vol. AC-26, pp. 1139-1144, 1981.

Costes, H., A. Gravelle and J.J. Philippe, "Investigation of Unsteady Subsonic Spoiler And Flap Aerodynamics," *AIAA J. Aircraft*, Vol. 24, no. 9, 1987.9.

Dystuynder, R., "Multi-Control System In Unsteady Aerodynamics Using Spoilers," *AIAA Paper* No. 87-0855, 1987.

Enns, D., "Robustness of Dynamic Inversion vs μ-Synthesis: Lateral-Directional Flight Control Example," *AIAA Paper* No. 90-3338-CP, 1990.

Etkin, B., *Dynamics of Atmospheric Flight*, John Wiley, New York, 1972.

Fab, P.L. and W.A. Wolovich, "Decoupling in the Design and Synthesis of Multivariable Control Systems," *IEEE Trans. on Automatic control*, Vol. AC-12, pp. 651-659, 1967.

Francis, M.S., J.E. Keesee, F.J. Seiler, J.D. Lang and G.W. Sparks, Jr., " Aerodynamic Characteristics of an Unsteady Separated Flow," *AIAA Paper* No. 79-0283, 1979.

Franks, R., "The application of a Simplified Lifting-Surface Theory to the prediction of the Rolling Effectiveness of Plain Spoiler Ailerons at Subsonic Speeds," *NACA* RM-A54H26a, 1954.

Freund, E., "Decoupling and Pole Assignment in Nonlinear Systems," *Electro. Lett.*, no. 9, pp. 373-374, 1973.

Freund, E., "The Structure of Decoupled Nonlinear systems," *Int. J. Control*, no. 21, pp. 443-450, 1975.

Gallaway, C.R. and R.F. Osborn, "Aerodynamics Perspective of Supermaneuverability," *AIAA Paper* No. 85-4068, 1985.

Garrard, W., D.F. Enns and S.A. Snell, "Nonlinear Longitudinal Control of A Supermaneuverable Aircraft," *Proc. 1989 American Control Conference*, 1989.

Gilbert, E. and I.J. Ha, "An Approach to Nonlinear Feedback Control with Applications to Robotics," *IEEE Trans. on System, Man, Cybern.*, Vol. SMC-14, pp. 879-884, 1984.

Golub and Vanloan, *Matrix Computations*, 2nd Ed, Johns Hopkins, 1989.

Gutman, S., "Uncertain Dynamic Systems --- A Lyapunov Min-max Approach," *IEEE Trans. on Automatic Control*, Vol. AC-24, pp. 437-443, 1979.

Ha, I.J. and E.G. Gilbert, "Robust Tracking in Nonlinear Systems," *IEEE Trans. on Automatic control*, Vol. AC-32, pp. 763-771, 1987.

Hauser, J., S. Sastry and G. Meyer, "On the Design of Nonlinear Controllers for Flight Control Systems," *AIAA Paper* No. 89-3489-CP, 1989.

Herbst, W.B., "Future Fighter Technologies," *J. Aircraft*, Vol. 7, no. 8, pp. 561-566, 1980.

Herdric, J.K. and S. Gopalswamy, "Nonlinear Flight Control Design via Sliding Methods," *J. Guidance*, Vol 13, No 5, pp. 850~858, 1989.

Henderson, M.L., "A Solution to the 2-D Separated Wake Modelling Problem and Its Use to Predict Clmax of Arbitrary Aerofoil Sections," *AIAA Paper* No. 78-159, 1978.

Herd, J., "Digital Simulation Techniques for a Fixed-Wing Aircraft," 3rd Year Report, Dept. of Aeronautics, Imperial College, London, 1985.

Huang, C.Y. and G.J. Knowles, "Application of Nonlinear Control Strategies to Aircraft at High Angle of Attack," *Proc. of the 29th IEEE Conference on Decision and Control*, WA 8, Dec. 1990.

Huang, C.Y. and R.F. Stengel, "Restructurable Control Using Proportional-Integral Implicit Model-Following," *AIAA Guidance, Navigation and Control Conference*, AIAA Paper 87-2312, Aug. 1987.

Huang, C.Y., "Application of Robust Model-Following Concepts to Aircraft Control," *Proc. of the 1990 American Control Conference*, May 1990.

Hunt, L.R. and R. Su, "Control of Nonlinear Time-varying Systems," *Proc. of the 20th CDC*, pp. 558-563, 1981.

Hunt, L.R., R. Su and G. Meyer, "Global Transformations of Nonlinear Systems," *IEEE Trans. on Automatic Control*, Vol. AC-28, p. 24, 1983.

Innocenti, M., "High Gain Flight Controllers for Nonlinear Systems," *AIAA Paper* No. 89-3488-CP, 1989.

Isidori, A, A.J. Krener, C.G. Giorgi and S. Monaco, " Nonlinear Decoupling via Feedback: a Differential Geometric Approach," *IEEE Trans. on Automatic Control*, Vol. AC-26, pp. 331-345, 1981.

Isidori, A. and C.H. Moog, "On the Nonlinear Equivalent of the Notion of Transmission Zeros," *Modelling and Adaptive control*, C. Byrnes and A. Kurszanski (Eds.), Springer-Verlag, 1987.

Isidori, A., *Nonlinear Control Systems*, Springer Verlag, 1990.

Kalkanis, P., "Numerical Simulation of Spoiler Flows," Ph.D. Thesis, Dept. of Aeronautics, Imperial College, 1988.

Kalligas, K. and D.L. Birdsall, "A Comparative Assessment of Different Types of Rapidly Moving Spoilers at Low Airspeed," Technical Rpt., Dept. of Aerospace Engineering, University of Bristol, 1987.

Khoo, H. and J.M.R. Graham, "Stall Control of Wind Turbine Blades," Technical Rpt., Dept. of Aeronautics, Imperial College, 1989.

Kravaris, C. and C.B. Chung, "Nonlinear State Feedback Synthesis by Global Input/ Output Linearization," J. AICHE, Vol. 33, p. 592, 1987.

Kravaris, C. and S. Palanki, "A Lyapunov Approach for Robust Nonlinear State Feedback Synthesis," *IEEE Trans. on Automatic Control*, Vol. AC-33, pp. 1188-1191, 1988.

Lane, S.H. and R.F. Stengel, "Flight Control Design Using Nonlinear Inverse Dynamics," *Automatica*, Vol. 24, no. 4, pp. 471-483, 1988.

Lane, S.H. and R.F. Stengel, "Nonlinear Inverse Dynamics Control Laws - A Sampled Data Approach," *Proc. 1987 American Control Conference*, pp. 1224-1226, 1987.

Lang, J.D. and Francis, M.S., "Unsteady Aerodynamics and Dynamic aircraft Maneuver -ability," AGARD-CP-386, Paper no. 29, Gottingen, Germany, May 1985.

Lee, C.S. and S. Bodapati, "A Comparison Between Theoretical and Experimental Flow Field of an Airfoil with Deflected Spoiler," *AIAA Paper* No. 85-0269, 1985.

Lewis, F.L., *Optimal Control*, John Wiley & Sons, 1986.

Mabey, D.G., B.L. Welsh, G. Stott and B.E. Cripps, "The Dynamic Characteristics of Rapidly Moving Spoilers at Subsonic and Transonic Speeds," *RAE Tech. Rpt.* no. 82109, 1982.

Mack, M.D., H.C. Seetharam, W.G. Kuhn and J.T. Bright, "Aerodynamics of Spoiler Control Devices," *AIAA Paper* 79-1843, 1979.

Marino, R. "High Gain Feedback in Nonlinear Control Systems," *Int. J. Control*, Vol 42, pp 1369~1385, 1985.

McLachlan, B.G., K. Karamcheti, A. Ayoub and G. Hadjidakis, "A Study of the Unsteady Flow Field of an Airfoil with Deflected Spoiler," *AIAA Paper* No. 83-2131, 1983.

McLean, D., *Automatic Flight Control Systems*, Prentice-Hall, Cambridge, 1990.

McMahom, D.H., J.K. Herdrick and S.E. Shladover, "Vehicle Modelling and Control for Automated Highway Systems," *Proc. 1990 American Control Conference.*

Melo, D.A. and R.J. Hansman Jr., "Analysis of Aircraft Performance During Lateral Maneuvring for Microburst Avoidance," *AIAA J. Aircraft*, Vol. 18, no. 12, 1991.

Menon, P.K.A., M.E. Badgett and R.A. Walker, "Nonlinear Flight Test Trajectory Controllers for Aircraft," *AIAA Paper* No. 85-1890-CP, 1985.

Meyer, G. and L. Cicolani, "Application of Nonlinear System Inverses to Automatic Flight Control Design --- System Concepts and Flight Evaluations," AGARDograph 251 on Theory and Applications of Optimal Control in Aerospace Systems, Paper no. 10, 1981.

Meyer, G. and L. Cicolani, "A Formal Structure for Advanced Automatic Flight Control Systems," *NASA* TN-D-7940, May, 1975.

Meyer, G., R. Su and L.R. Hunt, "Application of Nonlinear Transformations to Automatic Flight Control," *Automatica*, Vol. 20, no. 1, pp. 103-107, 1984.

Mabey, D.G., "On the Prospects for Increasing Dynamic Lift," *Aeronautical Journal*, March 1988.

Moorhouse, D.J. and R.J. Woodcock, "Background Information and User Guide for MIL-F-8785c Military Specification --- Flying Qualities of Piloted Airplanes," *AFWAL* TR-81-3109, 1982.

Myers, P.G. and D.L. Birdsall, "An Experimental Study of the Static and Dynamic Properties of a Wing with a Spoiler at an Arbitrary Position," Technical Rpt. Dept. of Aerospace Engineering, University of Bristol, 1989.

Nam, K. and A. Arapostathis, "A Model Reference Adaptive Control Scheme for Pure Feedback Nonlinear Systems," Preprint, University of Texas, Austin, 1986.

Nelson, R.C., *Flight Stability and Automatic Control,* McGraw-Hall Inc., 1989.

Nguyen, L.T., R.D. Whipple, and J.M. Brandon, "Recent Experiments of Unsteady Aerodynamic Effects on Aircraft Flight Dynamics at High Angle of Attack," AGARD-CP-386, Paper no. 28, Gottingen, Germany, May 1985.

Nicosia, S and P. Tomei, "Model Reference Adaptive Control for Rigid Robots," *Automatica*, Vol. 20, pp. 635-644, 1984.

Oseguera, R.M. and R.L. Bowles, "A Simple Analytic 3-Dimensional Downburst Model Based on Boundary Layer Stegnation Flow," NASA TM-100632, July, 1988.

Parkinson, G.V. and W. Yeung, "A Wake Source Model For Aerofoils With Separated Flow," *J. Fluid Mech.*, Vol. 179, pp. 41-57, 1987.

Parkinson, G.V., G.P. Brown and T. Jandali, "The Aerodynamics of Two-Dimensional Airfoils with Spoilers," *AGARD* CP-143, 1974.

Pesmajoglou, S., "Applications of Control Theory to the Simulation of a Digital Gust Alleviation Flight Control System," MSc Thesis, Dept. of Aeronautics, Imperial College, London, 1989.

Reeves, P.M., G.S. Campbell, V.M. Ganzer and R.G. Joppa, "Development and Application of A Non-Gaussian Atmospheric Turbulence Model for Use in Flight Simulations," *NASA* CR-2451, 1974.

Polak, E., *Computational Methods in Optimization: A Unified Approach,* Academic Press, New York, 1971.

Rugh, W.J., "Design of Nonlinear Compensators for Nonlinear Systems by an Extended Linearization Technique," *Proc. of the 23th IEEE Conference on Decision and Control*, pp. 9-13, 1984.

Sastry, S. and M. Bodson, *Adaptive Control,* Prentice-Hall, Englewood Cliffs, New Jersey, 1989.

Sastry, S. and A. Isidori, "Adaptive Control of Linearizable Systems," *IEEE Trans. on Automatic Control*, Vol. AC-34, pp. 1123-1131, 1989.

Seetharam, H.C. and W.H. Wentz, Jr., "A Low Speed Two-Dimensional Study of Flow Separation on the GA(w)-1 Airfoil with 30-Percent Chord Fowler Flap," *NASA* CA-2844, 1977.

Siddalingappa, S.R. and G.J. Hancock, "Some Qualitative Experiments on the Local Flow about Spoilers in Unsteady Motions at Low Speeds," Technical Rpt. EP-1036, Queen Mary College, 1980.

Singh, S.N. and A.A.R. Coelho, "Nonlinear Control of Mismatched Uncertain Linear Systems and Application to Control of Aircraft," *AIAA J. Dynamics Syst. Means. Control*, Vol. 106, pp. 203-210, 1984.

Singh, S.N. and A. Schy, "Output Feedback Nonlinear Decoupled Control Synthesis and Observer Design for Maneuvering aircraft," *Int. J. Control*, No. 31, pp. 781-806, 1980.

Singh, S.N. and W.J. Rugh, "Decoupling in a Class of Nonlinear Systems by State Variable Feedback," *AIAA J. Dynamics Syst. Means. Control*, pp. 323-329, 1972.

Singh, S.N., "Asymptotically Decoupled Discontinuous Control of Systems and Nonlinear Aircraft Maneuver," *IEEE Trans. on Aerospace and Electronic Systems*, Vol. 25, no. 3, pp. 380-391, May 1989.

Slotine, J. -J.E. and W.P. Li, *Applied Nonlinear Control*, Prentice Hall, Englewood Cliffs, New Jersey, 1991.

Smith, G.A. and G. Meyer, "Applications of the Concept of Dynamic Trim Control to Automatic Landing of Carrier Aircraft," *NASA* TP-1512, 1980.

Staford, H., "On Robust Control of Wing Rock Using Nonlinear Control," *Proc. 1987 American Control Conference*, pp. 1890-1899, 1987.

Sun, X.D. and J.C. Allwright, "Turbulence/Gust Alleviation Using Spoiler Control," *Proc. 1992 American Control Conference*, June 1992.

Sun, X.D., J.C. Allwright, J.M.R. Graham and D.J. Doorly, "A Nonlinear Inverse-Dynamics Flight Control System," *Proc. 6th IMA Conference on Control: Modelling, Computation, Information*; Sept. 1992.

Su, R., " On the Linear Equivalents of Nonlinear Systems," *System & Control Letter* , no. 2, p. 48, 1982.

Su, R., G. Meyer and L.R. Hunt, "Transformation of Nonhomogenrous Nonlinear systems," *Proc. of the 19th Allerton Conference on Communication, Control and Computing*, p. 462, 1981.

Su. R., G. Meyer and L.R. Hunt, "Robustness in Nonlinear Control," *Differential Geometric Control Theory* Brockett et al (Eds.), Birkhauser, 1983.

Taylor, D., P. Kokotovic and R. Marino, "Nonlinear Adaptive Control with Unmodelled Dynamics," preprint, University of Illinois, Dec. 1987.

Tou, H.B. and G.J. Hancock, "An Inviscid Model for the Low Speed Flow Past an Airfoil-Spoiler-Flap Configuration," Technical Rpt. EP-1067, Queen Mary College, 1985.

Tou, H.B. and G.J. Hancock, "Supplement to an Inviscid Model Prediction of Steady Two-Dimensional Aerofoil-Spoiler Characteristics at Low Speeds," Technical Rpt. EP-1056, Queen Mary College, 1983.

Utkin, V.I., "Variable Structure Systems with Sliding Mode: A Survey," *IEEE Trans. on Automatic Control*, Vol. AC-22, no. 2, 1977.

Wang, J. and W.J. Rugh, "Linearized Model Matching for Single-Input Nonlinear Systems," *IEEE Trans. on Automatic control*, Vol. AC-33, no. 8, pp793-796, 1988.

Wang, J. and W.J. Rugh, "Parametrized Linear systems and Linearization Families for Nonlinear Systems," *IEEE Trans. on Circuits and Systems*, Vol. CAS-34, no. 6, pp. 650-657, 1987.

Wehrend, W.R., Jr and G. Meyer, "Flight Tests of the Total Automatic Flight Control System (TAFCOS) Concept on a DHC-6 Twin Otter Aircraft," *NASA* TP-1513, 1980.

Weick, F.E. and J.A. Short, "Wind Tunnel Research Comparing Lateral Control Devices, Particularly at High Angles of Attack Spoiuler and Ailerons on Rectangular Wings," *NACA* Rpt. 439, 1932.

Wentz, W.H., Jr., "Wind Tunnel Tests of the GA(w)-2 Airfoil with 20% Aileron, 25% Slotted Flap and 10% Slot Lip Spoiler," *NASA* CA-145139, 1977.

Wentz, W.H., Jr., C. Ostowari and H.C. Seetharam, " Effects of Design Variables on Spoiler Control Effectiveness, Hinge Moments and Wake Turbulence," *AIAA Paper* No. 81-0072, 1981.

Whitford, R., "Four Decades of Transonic Fighter Design," *J. Aircraft* , Vol. 28, No. 12, 1991.

Woods, L.C., "Theory of Airfoil Spoilers," *Aero. Res. Council* R&M 2969, 1956.

Yoerger, D.R., J.B. Newman and J.-J.E. Slotine, "Supervisory Control System for the JASON ROV," *IEEE J. Oceanic Eng.* OE-11, No. 3, 1986.

Appendix One

AIRCRAFT MODELLING

A.1 A 12-state nonlinear aircraft model

When adopting a hybrid coordinate system consisting of combined wind and body axes, a nonlinear aircraft model with 12 states can be generated (ETKIN, 1972):

$$\dot{V} = -\frac{D}{m} - g\sin\gamma$$
$$\dot{\alpha} = q - q_w \sec\beta - (p\cos\alpha + r\sin\alpha)\tan\beta$$
$$\dot{\beta} = r_w + p\sin\alpha - r\cos\alpha$$

$$\dot{\gamma} = q_w\cos\varphi - r_w\sin\varphi$$
$$\dot{\varphi} = p_w + (q_w\sin\varphi + r_w\cos\varphi)\tan\gamma$$
$$\dot{\psi} = (q_w\sin\varphi + r_w\cos\varphi)\sec\gamma$$

$$\dot{q} = \frac{1}{I_{yy}}[M + I_{xz}(r^2 - p^2) + (I_{zz} - I_{xx})rp]$$
$$\begin{bmatrix}\dot{p}\\ \dot{r}\end{bmatrix} = \begin{bmatrix} I_{xx} & -I_{xz}\\ -I_{xz} & I_{zz}\end{bmatrix}^{-1}\begin{bmatrix}(L + I_{xz}pq + (I_{yy} - I_{zz})qr\\ (N - I_{xz}qr + (I_{xx} - I_{yy})pq\end{bmatrix}$$

$$q_w = \frac{1}{mV}(L - mg\cos\gamma\cos\varphi)$$
$$r_w = \frac{1}{mV}(-S + mg\cos\gamma\sin\varphi)$$
$$p_w = p\cos\alpha\cos\beta + (q - \dot{\alpha})\sin\beta + r\sin\alpha\cos\beta$$

(a-1)

where V is the flight path velocity, α is the incidence (angle of attack); β is the side-slip angle; γ, φ, ψ are the wind-axis Euler angles; q, p, r are the body-axis angular rates; q_w, p_w, r_w are the wind-axis angular rates; D, L, S are the drag, lift and side forces; *M*, *L*, *N* are the pitching, rolling and yawing moments. For the reference frames and transformations, refer to Chapter 4 of ETKIN's 'Dynamics of Atmospheric Flight'.

A.2 A general longitudinal aircraft model

A general nonlinear aircraft model for longitudinal flight can be obtained by assigning the lateral-related variables in (a-1) as zero, giving:

$$\dot{V} = -\frac{D}{m} - g\sin\gamma$$
$$\dot{\gamma} = q_w = \frac{1}{mV}(L - mg\cos\gamma)$$
$$\dot{\alpha} = q - q_w = q - \frac{1}{mV}(L - mg\cos\gamma)$$
$$\dot{q} = \frac{M}{I_{yy}}$$
$$\dot{\theta} = q$$

(a-2)

where θ is the pitch angle and γ is the flight path (or clibing) angle. As seen from **Fig. A-1** there is $\theta=\alpha+\gamma$ in the longitudinal profile.

Figure A-1 Reference frames for aircraft longitudinal modelling

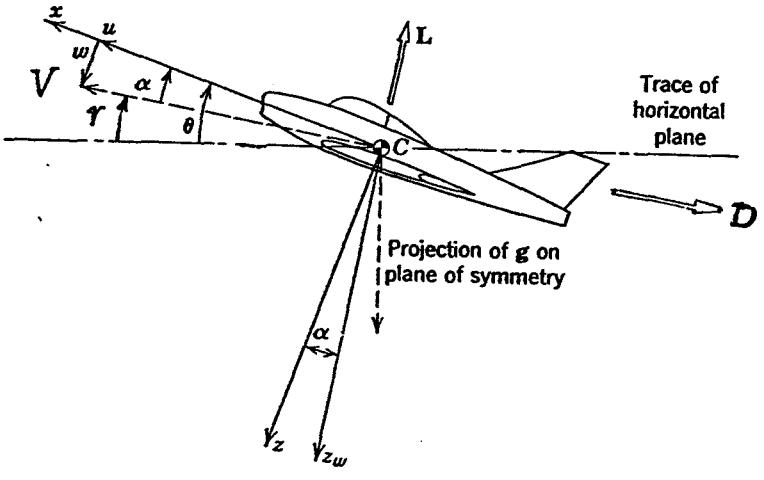

A.3 Aircraft model for open-loop optimal control synthesis

The aircraft model used in this study for the open-loop optimal control synthesis (**Chapter Four**) is as the following:

General Form ((4-1)):

$$\dot{x} = f(x,u,t)$$

where the state variables $x=[V, \gamma, \alpha, q, \theta, H]'$, the control variables $u=[\delta_e, \delta_t, \delta_{sp}]'$ and

$$f(x,u,t)=\begin{bmatrix} -\frac{D}{m}-g\sin\gamma \\ \frac{1}{mV}(L-mg\cos\gamma) \\ q-\frac{1}{mV}(L-mg\cos\gamma) \\ \frac{M}{I_{yy}} \\ q \\ V\sin\gamma \end{bmatrix} \qquad \text{(a-3)}$$

This is the model on which a numerical method was based (LEWIS, 1986) for the computation of the Jacobians $\frac{\partial f}{\partial x}$ and $\frac{\partial f}{\partial u}$.

For HAWK aircraft, the drag, lift and pitching moment can be expressed as:

Lift and Drag:

$$L=\frac{1}{2}\rho V^2 S C_L + C_{LT} \qquad \text{(a-4)}$$

$$D=\frac{1}{2}\rho V^2 S C_D + C_{DT} \qquad \text{(a-5)}$$

where

$$C_L = C_{L0}(M)+C_{L\alpha}(M)\alpha + C_{LSP}(\alpha,\delta_{sp})$$
$$= C_{L\alpha}+C_{LSP}(\alpha,\delta_{sp}) \qquad \text{(a-6)}$$

$$C_D = C_{D0}(M)+GK1(M)C_L{}^2 + C_{DSP}(\alpha,\delta_{sp})$$
$$= C_{DL}+C_{DSP}(\alpha,\delta_{sp})$$
$$\text{when } C_L \le C_{LC}(M) \qquad \text{(a-7)}$$

or

$$C_D = C_{D0}(M)+GK2(M)C_L{}^2 + (GK1(M)-GK2(M))C_{LC}{}^2(M) + C_{DSP}(\alpha,\delta_{sp})$$
$$= C_{DL}+C_{DSP}(\alpha,\delta_{sp})$$
$$\text{when } C_L > C_{LC}(M) \qquad \text{(a-8)}$$

$$C_{LT} = C_{t\,max}(H,M)\delta_t \sin\alpha \qquad \text{(a-9)}$$

$$C_{DT} = -C_{t\,max}(H,M)\delta_t \cos\alpha \qquad \text{(a-10)}$$

and M is Mach number, C_{tmax} is the maximum power of the jet engine which is decided by interpolating a $C_{tmax}(H,M)$ table. $C_{L0}(M)$, $C_{D0}(M)$, $C_{LC}(M)$, GK1(M) and GK2(M) are M-dependant tabular functions. (for HAWK they can be found in the report of HERD(1987).

Moment:

$$
\begin{aligned}
M &= \frac{1}{2}\rho V^2 S\bar{c}(C_{m0}(M) + C_{m\alpha}(M)\alpha + C_{m\delta_e}(M)\delta_e + C_{MSP}(\alpha,\delta_{sp}) \\
&\quad +\rho VS(\frac{\bar{c}}{2})^2(C_{mq}(M)q + C_{m\dot{\alpha}}(M)\dot{\alpha}) \\
&= \frac{1}{2}\rho V^2 S\bar{c}(C_{m0}(M) + C_{m\alpha}(M)\alpha + C_{m\delta_e}(M)\delta_e + C_{MSP}(\alpha,\delta_{sp}) \\
&\quad +\rho VS(\frac{\bar{c}}{2})^2(C_{mq}(M)q + C_{m\dot{\alpha}}(M)q + \frac{g\cos\gamma}{V}C_{m\dot{\alpha}}(M) - \frac{\rho VS}{2m}C_{L\alpha} \\
&\quad -\frac{\rho VS}{2m}C_{LSP}(\alpha,\delta_{sp}) - \frac{1}{mV}C_{LT}) \\
&= M_A + \frac{1}{2}\rho V^2 S\bar{c}C_{m\delta_e}(M)\delta_e + \frac{1}{2}\rho V^2 S\bar{c}C_{MSP}(\alpha,\delta_{sp}) \\
&\quad -\frac{(\rho VS\bar{c})^2}{8m}C_{LSP}(\alpha,\delta_{sp}) - \frac{\rho VS\bar{c}^2}{4mV}C_{LT} \qquad \text{(a-11)}
\end{aligned}
$$

A set of values for the longitudinal stability derivatives C_{m0}, $C_{m\alpha}$, $C_{m\delta_e}$, C_{mq} and $C_{m\dot{\alpha}}$ was given in HERD's report.

When the spoiler model takes the form of (2-32), (2-33) and (2-34). We can approximately model the aircraft in the nonlinear form (4-10), i.e.

$$\dot{x} = A(x) + B(x)u$$

where

$$
A(x) = \begin{bmatrix}
-\frac{\rho V^2 S}{2m}C_{LD} - g\sin\gamma \\
\frac{\rho VS}{2m}C_{L\alpha} - \frac{g\cos\gamma}{V} \\
q - \frac{\rho VS}{2m}C_{L\alpha} + \frac{g\cos\gamma}{V} \\
\frac{M_A}{I_{yy}} \\
q \\
V\sin\gamma
\end{bmatrix};
$$

$$B(x) =$$

$$\begin{bmatrix} 0 & \frac{\cos\alpha}{m}C_{t\,max}(H,M) & -\frac{\rho V^2 S\lambda_D(\alpha)}{2m}C_{d\delta_s} \\ 0 & \frac{\sin\alpha}{mV}C_{t\,max}(H,M) & \frac{\rho VS\lambda_L(\alpha)}{2m}C_{l\delta_s} \\ 0 & -\frac{\sin\alpha}{mV}C_{t\,max}(H,M) & -\frac{\rho VS\lambda_L(\alpha)}{2m}C_{l\delta_s} \\ \frac{\rho V^2 S\bar{c}}{2I_{yy}}C_{m\delta_e}(M) & -\frac{\rho VS\bar{c}^2\sin\alpha}{4mVI_{yy}}C_{t\,max}(H,M) & (\frac{\rho V^2 S\bar{c}\lambda_M(\alpha)}{2I_{yy}}C_{m\delta_s} - \frac{(\rho VS\bar{c})^2\lambda_L(\alpha)}{8mI_{yy}}C_{l\delta_s}) \\ 0 & 0 & 0 \\ 0 & 0 & 0 \end{bmatrix}$$

(a-12)

This is the model on which an explicit derivation of the Jacobians ((4-11), (4-12)) was based.

A.4 Aircraft model for NID control design

The aircraft model on which the NID control design has based is:

$$\dot{x} = A(x) + B(x)u$$

where $x=[V, \gamma, \alpha, q, \delta_t, \delta_{sp}]'$, $u=[u_e, u_t, u_{sp}]'$,

$$A(x) = \begin{bmatrix} -\frac{D}{m} - g\sin\gamma \\ \frac{1}{mV}(L - mg\cos\gamma) \\ q - \frac{1}{mV}(L - mg\cos\gamma) \\ \frac{M}{I_{yy}} \\ -a_t\delta_t \\ -a_{sp}\delta_{sp} \end{bmatrix}, \quad B(x) = \begin{bmatrix} 0 & & \\ 0 & & \\ 0 & & \\ b_q(x) & & \\ & a_t & \\ & & a_{sp} \end{bmatrix},$$

(a-13)

and $b_q(x) = \frac{\rho V^2 S\bar{c}}{2I_{yy}}C_{m\delta_e}(M)$.

For (5-17), there are

$$A_1(x)=\begin{bmatrix} -\frac{D}{m}-g\sin\gamma \\ \frac{1}{mV}(L-mg\cos\gamma) \\ q-\frac{1}{mV}(L-mg\cos\gamma) \end{bmatrix},\quad A_2(x)=\begin{bmatrix} \frac{M}{I_{yy}} \\ -a_t \\ -a_{sp} \end{bmatrix} \text{ and } B_2(x)=\begin{bmatrix} b_q(x) & & \\ & a_t & \\ & & a_{sp} \end{bmatrix}.$$

A.5 Actuator dynamics and saturation constraints of the HAWK

In longitudinal control, the actuator dynamics and saturation constraints of the control devices: elevator, thrust and spoiler, of the HAWK are as the following:

Elevator:

$$\dot{\delta}_e=-a_e\delta_e+a_eu_e \qquad \text{(a-14)}$$

with the deflection rate limitation: $\dot{\delta}_{e\max}\le 40^o$ / sec. and the deflection angle limitation: $-15^o\le\delta_e\le 6^o$. a_e is chosen by referring to the elevator servo dynamics and is given as 20.0 (T_e=0.05s).

Thrust:

$$\dot{\delta}_t=-a_t\delta_t+a_tu_t \qquad \text{(a-15)}$$

with the throttle changing limitation: $\dot{\delta}_{t\max}\le 20\%$ / sec. and the throttle control limitation : $0\le\delta_t\le 1$. a_t is given as 0.5 (T_t=2.0s).

Spoiler(artificially modelled):

$$\dot{\delta}_{sp}=-a_{sp}\delta_{sp}+a_{sp}u_{sp} \qquad \text{(a-16)}$$

with only the deflection limitation of $-90^o\le\delta_{sp}\le 0^o$. a_{sp} is given as 10.0 (T_{sp}=0.1s).